UBIQUITIN DEPENDENT DEGRADATION OF ENDOPLASMIC RETICULUM MEMBRANE-BOUND SUBSTRATES - MECHANISMS AND REQUIREMENTS

Von der Fakultät Energie-, Verfahrens- und Biotechnik der Universität Stuttgart zur Erlangung der Würde eines Doktors der Naturwissenschaften (Dr. rer. nat.) genehmigte Abhandlung

Vorgelegt von
M.Sc. Nicole Zabel
geb. Berner aus Böblingen

Hauptberichter:	Prof. Dr. Dieter H. Wolf
Mitberichter:	Prof. Dr. Stephan Nussberger
Tag der mündlichen Prüfung:	26. November 2020

Institut für Biochemie und Technische Biochemie Abteilung Biochemie
der Universität Stuttgart
2021

TABLE OF CONTENT

ABBREVIATIONS

(ΔCS)	truncated version of the cytosolic sequence
(CS)	cytosolic sequence
(v/v)	volume fraction
(w/v)	mass fraction
*P	probability value
%	persent
°C	degree Celsius
ΔA_{410nm}	absorbance of a sample measured at a wavelength of 410 nm
∅	diameter
~	approximately, tilde
19S	regulatory particle
20S	core particle
26S proteasome	yeast proteasome
A	alanine
AAA	ATPases associated with diverse cellular activities
AAA+	AAA domain
AG	joint stock company
AgeI-HF	restriction enzyme
approx.	approximately
APS	ammonium persulfate
Asi	amino acid sensor-independent 1
Asn	asparagine
ATP	adenosine triphosphate
ATPase	enzyme that catalyzes the hydrolysis of ATP
Bit	basic unit of information
Blm	bleomycin resistance
BP	binding protein
Bp	base pair
BRcat	benign-catalytic
BTpNA	*N*-benzoyl-L-tirosine *p*-nitroanilide
C	cysteine
C*	mutated Form of carboxypeptidase Y
CD4	T-cell surface glycoprotein
Cdc	cell division cycle
CFTR	cystic fibrosis transmembrane conductance regulator
C_{in}	C-terminal part is located intracellular
Cne1	calnexin and calreticulin homolog
CPY	carboxypeptidase Y
CPY*	mutated form of the carboxypeptidase Y
Cre	causes recombination

cryo-EM	cryogenic electron microscopy
CTE	C-terminal element
CUE	coupling of ubiquitin conjugation to ER degradation
$CuSO_4$	copper sulfate
ddH_2O	double-destilled water
Der	degradation in the endoplasmic reticulum
Dfm	Der1-like family member
DMSO	dimethyl sulfoxide
DNA	desoxyribonucleic acid
dNTP	nucleoside triphosphate
Doa	degradation of α 2
DpnI	restriction enzyme
Dsk2	abbreviation is not determined
DTT	dithiothreitol
DUB	deubiquitinating enzyme
E. coli	*Escherichia coli*
e.g.	for example
E1	ubiquitin-activating enzyme
E2	ubiquitin-conjugating enzyme
E3	ubiquitin ligase
EcoRI-HF	restriction enzyme
EDTA	ethylendiaminetetraacetic acid
ε -NH_2	amino group
ER	endoplasmic reticulum
ERAD	ER-associated degradation
et al.	*et alii*
EtOH	ethanol
F	phenylalanine
G	gravity of earth
G	glycine
GFP	green fluorescent protein
GFP_{fast}	superfast-folding green fluorescent protein variant
Glc	glucose
$GlcNAc_2$	*N*-acetylglucosamine
Gls	glucosidase
Gly	glycine
GmbH	private limited company
GmbH & Co. KG	limited partnership business entity
H	hour
H_2O	water
HA	hemagglutinin
HCl	hydrogen chloride

HECT	homologous to E6AP C-terminus
HEPES	4-(2-hydroxyethyl)-1piperazineethanesulfonic acid
HF	high fidelity
HindIII-HF	restriction enzyme
His	histidine
Hmg	3-hydroxy-3-methylglutaryl-coenzyme A reductase
Hrd	HMG-coA reductase degradation
HRP	horseradish peroxidase
Hsp	heat schock protein
Htm	homologous to mannosidase I
Hul	HECT ubiquitin ligase
I	isoleucine
IgG $_{\kappa}$	immunoglobulin G light chain kappa
in vitro	in the glass
in vivo	within the living
Inc.	incorporation
INM	inner nuclear membrane
IP	immunoprecipitation
Jem1	dnaJ-like protein of the ER membrane
K	lysine
kan^{r}	kanamycin resistance
Kar	karyogamy
Kb	kilo base pairs
Kbp	kilo base pairs
KCl	potassium chloride
kDa	kilo dalton
KGaA	german corporate " Kommanditgesellschaft auf Aktien"
KpnI-HF	restriction enzyme
kV	kilovolt
L	leucine
LB	lysogeny broth
Leu2	leucine biosynthesis
loxP	locus of X-over P1
Ltd.	private company limited by shares
Lys	lysine
M	molar
mA	milli ampere
Man	mannose
mg	milligram
$MgCl_2$	magnesium chloride
$MgSO_4$	magnesium sulfate
min	minute

ml	milliliter
mM	millimolar
mm	millimeter
Mnl	mannosidase-like protein
Mns	mannosidase
ms	millisecond
Myc	myelocytomatosis
N	asparagine
N	number of observations
n.a.	not necessary to analyze
Na_2CO_3	sodium carbonate
Na_2HPO_4	disodium phosphate
NaCl	sodium chloride
NAD^+	nicotinamide adenine dinucleotide
NaF	sodium fluoride
NaH_2PO_4	monosodium phosphate
NaN_3	sodium azide
NaOAc	sodium acetate
natB	N-terminal acetyltransferase B complex
Nedd8	neural precursor cell expressed, developmentally down-regulated
ng	nanogram
NH_4Ac	ammonium acetate
NheI-HF	restriction enzyme
Ni	nickel
nm	nanometer
NotI-HF	restriction enzyme
N_{out}	N-terminal part is located extracellular
NP-40	nonyl phenoxypolyethoxylethanol
Npl4	nuclear protein localization
NTA	aminopolycarboxylic acid
OD_{600}	absorbance of a sample measured at a wavelength of 600 nm
OST	oligosaccharyltransferase complex
Otu	ovarian tumor
P	pellet or proline as indicated
p97	abbreviation is not determined
PA	proteasome activator
PacI	restricion enzyme
PBS-T	phosphate-buffered saline containing triton X-100
PCR	polymerase chain reaction
Pdi	protein disulfide isomerase

Pdr	pleiotropic drug resistance
Pdr5*	mutated form of Pdr5
PEG	polyethylene glycol
PGK	phosphoglycerate kinase
pH	decimal logarithm of the reciprocal hydrogen ion activity
PhD	Doctor of Philosophy
PMSF	phenylmethylsulfonyl fluoride
Pmt	protein O-mannosyltransferase
PNK	polynuclotide 5'-hydroxyl-kinase
P_{PRC1}	*PRC1* promoter
PRC	proteinase C
PTM	posttranslational modification
R	arginine
Rad	radiation sensitive
RBR	RING-in-between-RING
Rcat	required-for-catalysis
Rer	retention in the ER
RING	really interesting new gene
RNA	ribonucleic acid
RNase	ribonuclease
rpm	revolutions per minute
Rpn	regulatory particle non-ATPase
Rpt	regulatory particle triple-A protein
RT	room temperature
Rub	related to ubiquitin
S	Svedberg unit
S	serine
Sbh	Sec61 beta homolog
S. cerevisiae	*Sacchaormyces cerevisiae*
Scj	*S. cerevisiae* dnaJ
SDS	sodium dodecyl sulfate
SDS-PAGE	sodium dodecyl sulfate-polyacrylamide gel electrophoresis
sec	second
Sec	secretory
SEM	standard error of the mean
Ser	serine
SHP box	small heterodimer partner
Sis	Sit4 suppressor
Smt	suppressor of Mif two
SN	supernatant
SOC	super optimal broth medium with catabolite repression
SpeI-HF	restriction enzyme

SPR	signal recognition particle
SRH	second region of homology
Ssa	stress-seventy subfamily A
Ssh	sec sixty-one homolog
Sss	sec sixty-one suppressor
St.	Saint
Ste	sterile
SUMO	small ubiquitin-like modifier
t	point in time
$t_{\frac{1}{2}}$	half-life
TA	tail-anchored
TAE	tris base, acetic acid, EDTA
Taq	thermostable
TCA	trichloroacetic acid
TDH	triose-phosphate dehydrogenase
TE	tris base, EDTA
TEMED	tetramethylethylenediamine
Thr	threonine
tilde	approximately
™	trademark symbol
TMD	transmembrane domain
T_{Pdr5}	last transmembrane helix of Pdr5
T_{PRC1}	*PRC1* terminator
TRIS	tris(hydroxymethyl)aminomethane
ts	temperature-sensitive allele
Tul	transmembrane ubiquitin ligase
T_{Wsc1}	transmembrane domain of Wsc1
U	unit
U.S.	united states
Ub	ubiquitin
UBA	ubiquitin-associated domain
Ubc	ubiquitin-conjugating enzyme
UBL	ubiquitin-like
UBP	ubiquitin-specific protease
Ubr1	abbreviation is not determined
Ubx	ubiquitin regulatory X
Ub_X	polyubiquitin chains
Ufd	ubiquitin fusion degradation protein
UK	United Kingdom
UPOM	unfolded protein *O*-mannosylation
UPR	unfolded protein response

UPS	ubiquitin-proteasome system
Usa	U1-Snp1 associating
V	volt
V	valin
V_{max}	at full speed
Vms1	VCP/Cdc48-associated mitochondrial stress-responsive
W	tryptophane
WB	Western blot
Wsc1	cell wall integrity and stress response component
×	times/copies
Y	tyrosine
Ydj	yeast dna Y
YidC	abbreviation is not determined
Yos	yeast OS-9 homolog
µg	microgram
µl	microliter
µM	micromolar

LIST OF FIGURES

LIST OF TABLES

SUMMARY

Quality control mechanisms maintain the cellular function by protecting the proteome from misfolding. In case the recognition and subsequent elimination of aberrant proteins fails, the formation of aggregates is promoted. Aggregates disturb the cellular protein homeostasis, which leads to diabetes and cancer but also to neurodegenerative diseases, such as Alzheimer's disease, Creutzfeldt-Jakob disease, Huntington's disease or Parkinson's disease.

In the endoplasmic reticulum, the entry gate of proteins into the secretory pathway, a multicomponent system, called endoplasmic reticulum associated degradation (ERAD), mediates the elimination of aberrant secretory proteins. Thereby, the location of the lesion within the protein determines the elimination process. ER proteins containing aberrant lumenal, membrane or cytosolic parts are degraded by the respective ERAD-L, ERAD-M or ERAD-C mechanisms. In this work numerous artificially misfolded ER membrane proteins were generated. With these ERAD substrates the mechanisms how ERAD-L and ERAD-M substrates are degraded were shown in more detail. Up to now the ER membrane protein Der1 was shown to be a central player exclusively required for elimination of ERAD-L substrates. In this work direct evidence was provided that Der1 is also required for degradation of proteins with a misfolded ER lumenal domain and an aberrant membrane part as long as lysine residues are lacking in their cytosolic parts. Presence of lysine residues in the cytosolic part of these proteins lead to degradation, which is independent of Der1. Furthermore, it was shown that these lysine-containing ERAD-M substrates are ubiquitinated and finally eliminated by the ER membrane embedded ubiquitin ligases Hrd1 as well as the nuclear Asi complex, in collaboration with the ubiquitin-conjugating enzyme Ubc7. In comparison, proteins with a misfolded ER lumenal domain and an aberrant membrane part, containing serine residues, instead of lysine, in their cytosolic part absolutely require Der1 for degradation and are ubiquitinated by Hrd1 together with Ubc1, Ubc6 and Ubc7. Most fascinating was that proteins containing lesions in their ER lumenal as well as membrane parts are not degraded at all, when they are lacking any amino acid, which can be ubiquitinated, in their cytosolic part. These nondegradable proteins are still ubiquitinated exclusively by the ubiquitin ligase Hrd1. Since only the ER lumenal parts of these proteins contain amino acids for ubiquitination, it implies that the ER

lumenal part loops-out in some way, but final retrotranslocation is prevented. Detailed analysis of the ERAD-L degradation mechanism unveiled that Der1 is required for degradation of proteins with ER lumenal misfolded domains and properly folded membrane parts, lacking lysine residues in their cytosolic part. Ubiquitination of these ERAD-L substrates is mediated by Hrd1 together with Ubc1, Ubc6 and Ubc7. In case these substrates contain lysine residues in their cytosolic part, the ERAD-L as well as the ERAD-M degradation mechanisms are involved in degradation of these lysine-containing proteins, thus, they are called ERAD-L/M substrates. Ubiquitination of these ERAD-L/M substrates is achieved by Hrd1 as well as the Asi complex, however, only the Hrd1 mediated ubiquitination leads to degradation. Only Ubc1 and Ubc7 participate in ubiquitination of ERAD-L/M substrates. For membrane extraction of all degradable substrates the AAA ATPase Cdc48 is required. In summary, it was shown that the cytosolic part of ER membrane proteins has an extraordinary role for their degradation.

ZUSAMMENFASSUNG

Zelluläre Qualitätskontrollsysteme verhindern die Entfaltung von Proteinen und gewährleisten somit die Funktionalität der Zelle. Fehlgefaltete Proteine, welche den Kontrollsystemen entgehen, können stabile Aggregate bilden. Diese lösen Krebs und Diabetes aber auch eine Gruppe von Proteinfaltungserkrankungen aus. Fehlgefaltete Proteine des sekretorischen Wegs werden im endoplasmatischen Retikulum (ER) erkannt, zurückgehalten, retrograd ins Zytosol transportiert und dort schlussendlich abgebaut. Dieser Prozess wird als ER-assoziierte Degradation (ERAD) bezeichnet. Abhängig von der Lage der Fehlfaltung in den verschiedenen Domänen der Proteine, werden diese Proteine über unterschiedliche Mechanismen abgebaut. Fehlgefaltete ER lumenale Domänen führen zum ERAD-L Abbau, gestörte Membrandomänen führen zu einem ERAD-M Abbau und fehlgefaltete zytosolische Domänen zu einem ERAD-C Abbau.

In dieser Arbeit wurden zahlreiche künstlich fehlgefaltete Membranproteine des endoplasmatischen Retikulums hergestellt, um feine Unterschiede des ERAD-L und ERAD-M Abbaus zu untersuchen.

Bisher hat man angenommen, dass das ER Membranprotein Der1 ausschließlich für den Abbau von Proteinen mit einer fehlgefalteten ER lumenalen Domäne benötigt wird. In dieser Arbeit wurde gezeigt, dass Der1 auch für den Abbau von Proteinen benötigt wird, die nicht nur eine fehlgefaltete ER lumenale Domäne, sondern auch eine fehlgefaltete Membrandomäne tragen, wenn Lysin-Reste in ihrer zytosolischen Domäne fehlen. Für das Anhängen von Ubiquitinketten wird sowohl die Ubiquitinligase Hrd1 des endoplasmatischen Retikulums als auch der Asi Komplex, der in der inneren Kernmembran liegt, benötigt. Dabei arbeiten die genannten Ubiquitinligasen mit dem Ubiquitin-konjugierenden Enzym Ubc7 zusammen. Im Gegensatz dazu wird das Protein Der1 für den Abbau von Proteinen mit ER lumenaler fehlgefalteter Domäne, fehlgefalteter Membrandomäne und Serinresten anstatt Lysinen, benötigt. An der Ubiquitinierung dieser Proteine ist nur die Ubiquitinligase Hrd1 beteiligt, welche mit den Ubiquitin-konjugierenden Enzymen Ubc1, Ubc6 und Ubc7 zusammenarbeitet. Sehr interessant war die Erkenntnis, dass Proteine mit fehlgefalteten ER lumenalen Domänen und fehlgefalteten Membrandomänen nicht mehr abgebaut werden, wenn sie in der zytosolischen Domäne keine Aminosäure tragen, an welcher eine Ubiquitinierung stattfinden kann. Erstaunlicherweise werden diese nicht-abbaubaren

Proteine weiterhin mit Ubiquitinketten, welche ausschließlich durch die Ubiquitinligase Hrd1 katalysiert werden, ausgestattet. Da nur die ER lumenale Domäne dieser nicht abbaubaren Proteine, Aminoäuren an welchen ubiquitiniert werden kann, trägt, kann davon ausgegangen werden, dass diese Domäne in irgendeiner Form ins Zytosol gelangt, dort ubiquitiniert wird, aber die komplette Retrotranslokation des gesamten fehlgefalteten Proteins ausbleibt.

Eine genaue Untersuchung des ERAD-L Abbaumechanismus zeigte, dass Der1 für den Abbau von Membranproteinen mit fehlgefalteter ER lumenaler Domäne und intakter Membrandomäne benötigt wird, wenn diese keine Lysinreste in ihrer zytosolischen Domäne tragen. Für die Markierung dieser Proteine mit Ubiquitinketten, werden die Ubiquitinligase Hrd1 und die Ubiquitin-konjugierenden Enzyme Ubc1, Ubc6 und Ubc7 benötigt. Enthalten diese Proteine jedoch Lysinreste in ihrer zytosolischen Domäne, ist nicht nur der ERAD-L Weg am Abbau beteiligt, sondern auch der ERAD-M Weg. Denn für die Markierung dieser sogenannten ERAD-L/M Proteine mit Ubiquitinketten, wird nicht nur Hrd1 sondern auch der Asi Komplex benötigt, wobei hier gezeigt wurde, dass nur die Ubiquitinketten, angehängt durch Hrd1, als Abbausignal dienen. Zusätzlich werden nur die Ubiquitin-konjugierenden Enzyme Ubc1 und Ubc7 benötigt.

Schlussendlich ist die AAA ATPase Cdc48 für die Membranextraktion aller abbaubaren Proteine verantwortlich.

Zusammenfassend konnte in dieser Arbeit gezeigt werden, dass der zytosolische Teil von Membranproteinen des endoplasmatischen Retikulums eine große Rolle spielt, obwohl diese fehlgefaltete ER lumenale Domänen und intakte oder fehlgefaltete Membrandomänen tragen. Außerdem dirigiert die Art der zytosolischen Domäne den Weg des Abbaus dieser Proteine.

1. INTRODUCTION

The unique structure of every protein in the cell is very sensitive to alterations in its amino acid sequence. There are various causes for alterations, such as DNA damage, age-related errors or exposure to environmental stress conditions. These mistakes can lead to misfolded proteins, which are finally prone to aggregation. Incorrect posttranslational modifications (PTM's) also influence the folding status of the proteins. Aggregates perturb the protein homeostasis in cells. In humans this leads to severe diseases. These diseases comprise, for instance, neurodegenerative diseases, such as Alzheimer's disease, Creutzfeldt-Jakob disease, Huntington's disease or Parkinson's disease but for instance also diabetes and cancer [1–5]. It is therefore of utmost importance that the quality control systems of the cell are prepared to guarantee the full integrity of protein homeostasis. The function of these quality control systems is the recognition and removal of aberrant proteins in nearly each cellular compartment.

Basic discoveries in protein quality control and protein degradation have been made using the eukaryotic microorganism yeast *Saccharomyces cerevisiae* as a model [6–8]. It serves as a blueprint for similar processes in higher eukaryotes. Recently, it was shown that almost half of the essential yeast genes could be replaced by their human orthologs [9].

1.1 Protein quality control in the ER and endoplasmic reticulum-associated degradation (ERAD)

Protein synthesis starts at ribosomes in the cytosol. 20 – 40% of the proteome are secretory proteins [10–12]. These are equipped with motifs targeting them for import into the endoplasmic reticulum (ER). These hydrophobic stretches of amino acids are recognized and the respective proteins are able to enter the ER. There are various ways into the ER either by a signal recognition particle (SRP) dependent or independent mechanism, also called co- or posttranslational import, respectively. All import pathways merge at the translocon, which is embedded in the ER membrane.

This heterotrimeric complex is formed by Sec61, the protein conducting channel, and its complex partners Sbh1 and Sss1 [13]. Crystal and cryogenic electron microscopy (cryo-EM) structures showed protein translocation as well as lateral membrane insertion conducted by Sec61 [14]. In yeast, an alternative translocon exists, it is composed of the pore-forming Ssh1 and its complex partners Sbh2 and Sss1 [15]. It is supposed, that the alternative translocon functions as a back-up system, which can substitute in case of Sec61 overload [16].

After the nascent polypeptide chain emerges in the ER lumen, it is immediately occupied by the Hsp70 chaperone Kar2. This prohibits the backward movement of the polypeptide chain and leads to a forward movement of the peptide into the ER lumen [17,18]. There, Kar2 prevents aggregation of the polypeptide and possibly supports its folding [19].

In the ER lumen, the polypeptide is further processed. The targeting motif is cleaved off by the signal peptidase complex and is further degraded by the signal peptide peptidase [20,21].

In the oxidative environment of the ER lumen, disulfide bridge formation is catalyzed by protein disulfide isomerases (Pdi1) [22].

Another posttranslational modification (PTM) in the ER is the attachment of single mannose moieties on hydroxyl groups of serine or threonine residues within the protein. There is no consensus sequence for this so-called *O*-mannosylation. It is catalyzed by the Pmt1/Pmt2 complex and can be further processed within the Golgi apparatus [23–25]. *O*-mannosylation is also found to mark terminal misfolded proteins for degradation. This degradation pathway is called unfolded protein *O*-mannosylation (UPOM). It is not part of the classical ER-associated degradation (ERAD) pathway [26,27].

If the newly emerging polypeptide possesses a consensus sequence (Asn-X-Ser/Thr; Asn, asparagine; X can be any amino acid except proline; Ser, serine; Thr, threonine) for *N*-glycosylation, a preassembled core $Glc_3Man_9GlcNAc_2$ glycan (Glc, glucose; Man, mannose; $GlcNAc_2$, *N*-acetylglucosamine), the so-called core *N*-glycan, is transferred by the oligosaccharyl transferase (OST) complex. *N*-glycosylation is achieved during ER import, before folding of the protein [23,28].

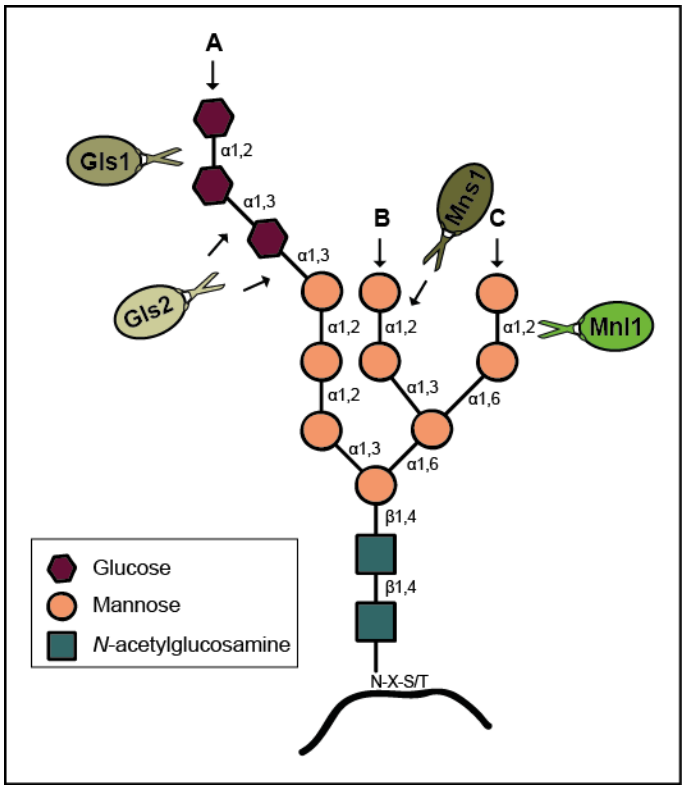

Figure 1: Core *N*-glycan structure attached on a consensus sequence of a secretory protein
In the ER lumen, proteins become *N*-glycosylated on special asparagine residues within a consensus sequence (shown as black line). The core *N*-glycan consists of two *N*-acetylglucosamine residues (turquoise squares), nine mannose residues (orange circles) and three glucose residues (red hexagons). The residues are linked as indicated. During quality control steps in the ER trimming of the core *N*-glycan occur on the different glycan branches (indicated as A, B and C) via glucosidase I (Gls1), glucosidase II (Gls2), mannosidase I (Mns1) and the exomannosidase (Mnl1 alias Htm1). (Figure adapted form Berner *et al.* 2018)

To guarantee that only mature proteins leave the ER, the folding as well as the modification status of the secretory proteins are monitored. One part of this surveillance system is a glycan trimming cycle (Figure 1). In a first step, glucosidase I (Gls1) removes the terminal glucose residue of the A branch of the core *N*-glycan. The following glucose residue is cleaved off by glucosidase II (Gls2). Cne1, a lectin with chaperone activity, binds to monoglucosylated core *N*-glycan and is further involved in protein folding [29]. The remaining glucose residue is removed by glucosidase II.

The α-1,2-mannosidase I (Mns1) recognizes $Man_9GlcNAc_2$ and takes off the terminal mannose residue of the B branch, leading to $Man_8GlcNAc_2$ [30,31]. In yeast, trimming of the core *N*-glycan by Gls1, Gls2 and Mns1 determines the length of time a glycoprotein spends in the ER. Especially the removal of the mannose residue by Mns1 is very slow, in yeast it takes about 10 minutes [23–25]. In case a protein failed to fold in this

timeframe it is eliminated. The incorrectly folded protein possesses the $Man_8GlcNAc_2$ glycan, which is recognized by Pdi1. The protein disulfide isomerase is in complex with the α-1,2-specific exomannosidase (Mnl1 alias Htm1) [23,32–36]. Finally, the terminal mannose of the C branch is cleaved off by Mnl1 (Figure 1). The remaining $Man_7GlcNAc_2$ glycan is a determinant for elimination by the ER-associated degradation (ERAD) pathway [23,37–39].

Causes of misfolding are not only incorrect PTM's, but also environmental stress such as exposure to heavy metals, which leads to mutations, or to temperature changes, which induces denaturation, and also genetic alterations. Without recognition by quality control systems and their final elimination, these unfolded proteins would form stable aggregates, which then disturb the cellular functions.

Elimination of all aberrant proteins of the ER is achieved by a multi-component system, called ERAD [6,8,40]. The ER is a tubular membrane system associated with the nuclear membrane. There, proteins with various topologies occur, such as soluble ER lumenal proteins or membrane proteins with domains inside and outside of the ER. Degradation of these different proteins is dependent on their specific topologies. ERAD-L, -M and -C are the degradation pathways to eliminate ER lumenal misfolded proteins, as well as proteins with aberrant membrane domain and membrane proteins with lesions in their cytosolic domain [41,42].

Since no degradation system exists within the ER, all ERAD substrates undergo retrograde transport back to the cytosol, where they are marked with ubiquitin chains and are finally degraded by the 26S proteasome ([43] , republished in [44]).

Thus, each pathway consists of the same order: recognition of the misfolded protein, retrotranslocation into the cytosol, ubiquitination as mark for degradation, membrane extraction and finally degradation (for review see [6]). These steps are further explained in the following chapters.

1.2 Recognition of misfolded proteins

Recognition is a prerequisite for the removal of aberrant proteins by the ubiquitin proteasome system. It has to be tightly controlled, otherwise inefficient recognition leads to protein accumulation, which disturbs the cellular functions. Thus, recognition of misfolded proteins must be finely balanced. On the one hand all aberrant proteins have to be captured but on the other hand an overreactive ERAD has to be prevented. Location of the folding lesion determines the degradation pathway. Thus, the three ERAD pathways are most divergent in recognition. Therefore, they are discussed separately.

Recognition of ERAD-L substrates:

Proteins of the ERAD-L substrate family can either be soluble or membrane-bound. Since the aberrant domain is located in the ER lumen, the carbohydrate modification plays an important role in recognition of ERAD-L substrates.

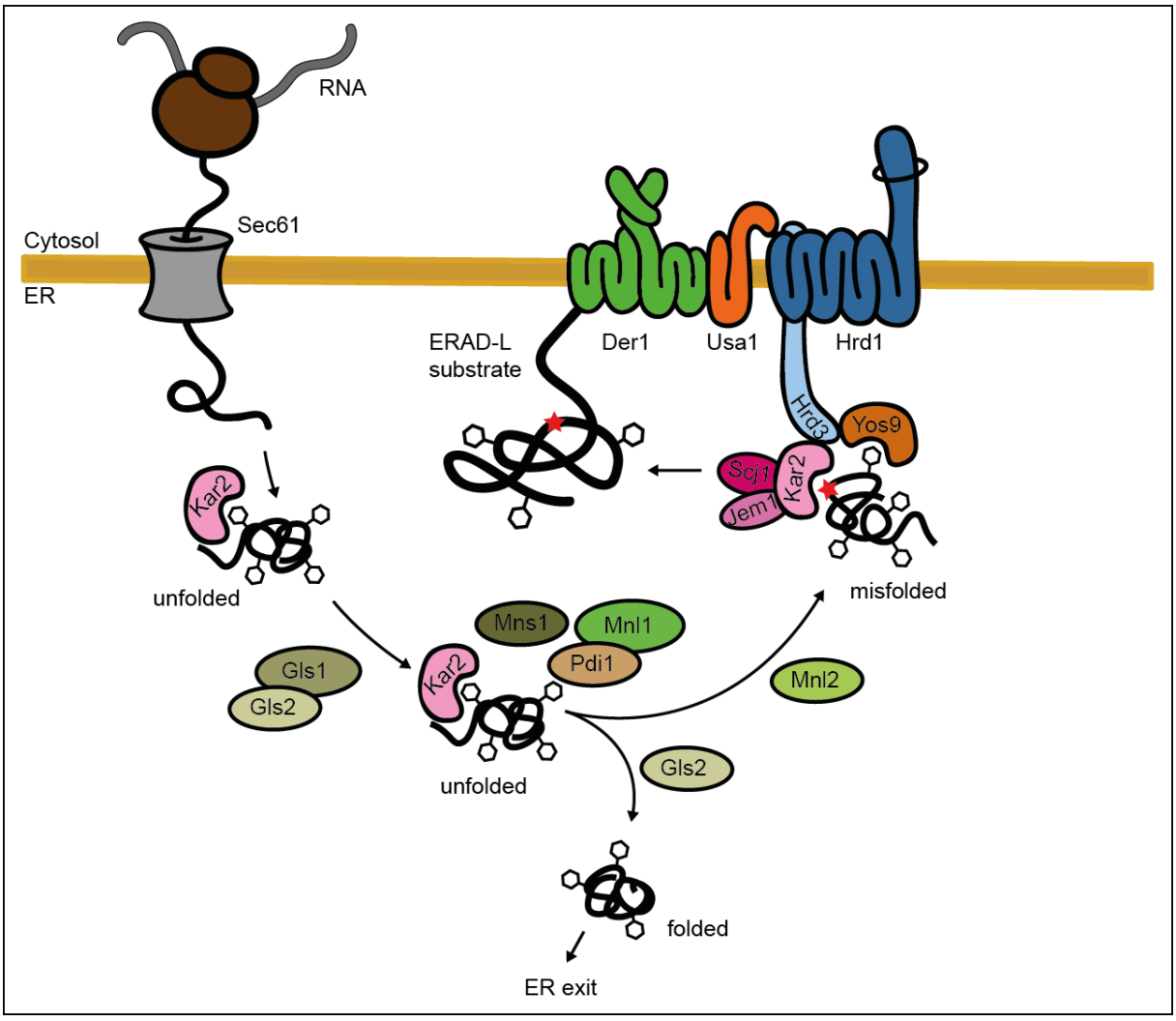

Figure 2: Components necessary for recognition of ERAD-L substrates.
Secretory proteins enter the ER via the Sec61 translocon. During ER import, they are glycosylated. The core *N*-glycan is trimmed by glucosidase I (Gls1) and glucosidase II (Gls2). After removal of the glucose residues, several mannose moieties are cleaved off by α-1,2-mannosidase I (Mns1) and the α-1,2-specific exomannosidase (Mnl1 alias Htm1). This provides time for protein folding. In case the folding failed, the α-1,6-linked mannose moiety is exposed, further mannose residues are removed by α-1,2-mannose (Mnl2) and recognized by the lectin Yos9. The Hsp70/Hsp40 chaperone complex (Kar2, Scj1 and Jem1), as well as Yos9 bind to Hrd3, which is in complex with the ubiquitin ligase Hrd1 (alias Der3). Der1 also recognizes misfolded proteins and is recruited to the *HRD* ligase complex via Usa1. (Figure adapted form Berner *et al.* 2018)

In case the trimmed core *N*-glycan (Figure 1) exposes a α-1,6-linked mannose, it is recognized by the lectin Yos9 [32–34,45–48]. The α-1,2-mannosidase (Mnl2) is found to remove further mannose residues. The resulting $Man_6GlcNAc_2$ and $Man_5GlcNAc_2$ glycans are preferentially bound by Yos9 [34].

Yos9, together with the Hsp70 chaperone Kar2 and its complex partners the Hsp40 chaperones Scj1 and Jem1 are able to bind misfolded as well as proteins with incorrect

PTM's. By binding to the misfolding sensor Hrd3 the proteins are delivered to the degradation machinery [49–51]. Hrd3 is an integral ER membrane protein with a large ER lumenal domain. Hrd3 itself is able to bind misfolded proteins [52,53], but it also binds Kar2 and Yos9 [42,54–58] (Figure 2). Thus, Hrd3 provides an interface between ERAD-L substrate recognition and degradation.

Hrd3 is in complex with the ubiquitin ligase Hrd1 (alias Der3), which mediates the attachment of ubiquitin to substrate proteins [42,53,54,57,59,60]. Interaction between Hrd1 and Hrd3 is mediated by their transmembrane helices, they form the so-called *HRD* ligase complex [59,61]. The inactive rhomboid Der1, which is essential for the removal of ERAD-L substrates, is recruited to the *HRD* ligase complex by Usa1 [60] in an oligomeric stage [41,60–62]. Usa1 is embedded in the ER membrane and exposes its N- and C-termini to the cytosol. Via its N-terminal ubiquitin-like (UBL) domain it binds the C-terminus of Hrd1. Der1 is bound to the C-terminus of Usa1 [60]. In this complex Der1 participates on the recognition of ERAD-L substrates and, furthermore, introduces them into the ER membrane ([61,62] and reviewed in [6,40]). This *HRD*-Der1 complex is suggested to participate also in retrotranslocation [61,63]. Retrotranslocation and ubiquitination will be explained in the following chapters.

Recognition of ERAD-M substrates:

ER- and inner nuclear membrane-embedded proteins with a disordered membrane domain are members of the ERAD-M substrate family. Transmembrane helices are usually 12-35 amino acids long. They share unifying sequence features, vary widely in hydrophobicity and helical propensity [64]. Little is known about their recognition. But it seems that the ubiquitin ligases themselves are responsible for recognition of ERAD-M substrates.

In a systematic analysis of the ubiquitin ligase Hrd1 (alias Der3), various *hrd1* mutants were found with impaired ERAD-M substrate degradation [65]. Residues specific for the recognition of aberrant membrane domains are located in the transmembrane domain of Hrd1. It is hypothesized, that recognition is induced by the interaction of normally buried hydrophilic residues of the substrate membrane domain with hydrophilic residues of the ligase [41,65].

Doa10, a ubiquitin ligase of the ER and the inner nuclear membrane (INM), was shown to recognize degrons within the membrane part of tail-anchored (TA) proteins. This was shown using Sbh2. In its native environment, Sbh2 is in complex with Ssh1 and Sss1. This complex forms the alternative translocon. In case its binding partner Ssh1 is lacking, Sbh2 exposes polar residues. These residues are recognized by Doa10 and lead to fast degradation of Sbh2. Thus, orphan Sbh2 is a native ERAD-M substrate [66].

Previously, it was also found that a ubiquitin ligase, located in the inner nuclear membrane is responsible for ubiquitination of incorrectly localized ERAD-M substrates. This ligase complex is composed of Asi1 and Asi3. It is further postulated that this ligase complex itself recognizes aberrant membrane parts of proteins [67,68].

Recognition of ERAD-C substrates:

Cytosolic, misfolded, soluble proteins as well as membrane proteins of the ER and the inner nuclear membrane (INM) with lesions in the cytosolic and nucleoplasmic part, respectively, are members of the ERAD-C substrate family [69].

Prior to attachment of ubiquitin, ERAD-C substrates are recognized by the ER and INM membrane-embedded ubiquitin ligase Doa10 [70–72].
In addition, the cytosolic Hsp70/Hsp40 machinery participates in Doa10 substrate recruitment [73–76]. The Hsp70 chaperones of the Ssa family cooperate with the cytosolic Hsp40 chaperones Ydj1 and Sis1 [40,69,73,77]. Thereby, the Hsp40 chaperones recognize specific degrons and thus increase the substrate specificity of Doa10.
Doa10 contains at its cytosolic C-terminus a C-terminal element (CTE). The CTE is conserved from yeast to men and is a stretch of 16 amino acids. It forms an interface for substrate recognition, assisted by the cytosolic Hsp40 chaperones [72].

1.3 Retrotranslocation: A way back to the cytosol

There is no degradation system within the ER, thus, the ER membrane serves as physical barrier between protein folding in the ER and protein degradation in the cytosol. Proteins recognized by the ER quality control as misfolded have to be removed by degradation. Therefore, they need to undergo retrograde transport back to the cytosol ([43], republished in [44]).
The retrotranslocation process is an area of highly active research (reviewed in [6,40,63,78]).

At the moment, two prime candidates exist to form a retrotranslocon for the retrograde transport of ERAD-L and ERAD-M substrates.

As a first nominee Sec61 was predicted. Sec61 forms the protein-conducting pore of a trimeric complex, responsible for ER import, also called the translocon [13]. In cell free experiments it was demonstrated that Sec61 allows bilateral transport [79]. Furthermore, retrotranslocation of small peptides by Sec61 was observed [80–82].
Co-immunoprecipitation experiments revealed an association of Sec61 with various ERAD substrates. Moreover, degradation of a large number of ERAD substrates is disturbed in cells containing different Sec61 mutations (reviewed in [78]). One of these mutants is *sec61S353C*, which is competent in protein import but shows impaired export [83,84]. This is in accordance with its reduced affinity to bind the 19S regulatory particle of the proteasome [83].
Interaction between Sec61 and the ubiquitin ligases Hrd1 (alias Der3) and Doa10 as well as the AAA ATPase Cdc48 and the proteasome, corroborate the assumption of Sec61 as retrotranslocon [83,85–88]. Finally, Sec61 was found to be involved in ERAD independent degradation of pro-α - factor [89,90].
This huge amount of data leads to the assumption that Sec61 participates in retrotranslocation. But there is also data suggesting that Hrd1 instead of Sec61 is involved in retrotranslocation of misfolded ER proteins [91–93].

More recent evidence proposes that the ubiquitin ligase Hrd1 might form the retrotranslocon.

It was uncovered that Hrd1 is composed of 8 transmembrane segments [59] instead of the predicted 6 transmembrane helices [94]. Moreover, it builds oligomers [60,95] and associates with various ERAD substrates by its transmembrane helices [65,95,96]. Furthermore, it was shown that Hrd1 associates with distinct ERAD substrates in the early retrotranslocation stage [60,95].

Reconstitution experiments with proteoliposomes containing only Hrd1 showed that a membrane-bound ERAD substrate is retrotranslocated, dependent on the autoubiquitination of the ligase Hrd1 [97].

Finally, cryo-EM structure of a tetramer, which is composed of two symmetry-related molecules of Hrd1 and Hrd3, showed that five of the 8 transmembrane helices of Hrd1 form a funnel across the ER membrane. The first transmembrane helix of Hrd1 seals the funnel of the neighboring Hrd1 molecule. The two Hrd3 molecules form an arch with their ER lumenal moieties [59]. Additionally, an aqueous cavity was found [59]. It is reminiscent of the cavity found in Sec61 and the prokaryotic homolog SecY. This allows transport in opposite directions [98,99].

This proofs that Hrd1 provides conditions that allow ERAD substrate retrograde transfer back to the cytosol. Nevertheless, there are still open questions because in the absence of Hrd1 a fusion substrate, which is composed of Hmg1 and the Hrd1 RING domain, undergoes retrotranslocation [91].

A cryo-EM structure was solved for Hrd1 in complex with Hrd3, which is required for elimination of ERAD-M substrates. Deep cytosolic invaginations were found, which are also found in the bacterial YidC protein and its homologs in plant and mitochondria [100,101]. Related to their function it is proposed that these invaginations allow ERAD-M substrates to laterally enter the retrotranslocon [102].

The following results imply that Hrd1 might form the retrotranslocon for ERAD-L as well as for ERAD-M substrates.

Degradation of ERAD-L substrates is dependent on oligomeric Der1 [41,60–62], which is recruited by Usa1 [60] to the *HRD* ligase complex formed by Hrd1 and Hrd3 [42,53,54,57,59,60]. Thereby, Der1 conducts the membrane insertion of ERAD-L substrates ([61,62] and reviewed in [6,40]) but it is dispensable for degradation of ERAD-M substrates [41,42]. Thus, it is proposed that Der1 might replace one of the Hrd3 molecules to gain access to the lateral gate of Hrd1 [102]. Further cryo-EM structures of Hrd1 in complex with Hrd3, Der1 and Usa1 as well as in complex with distinct ERAD substrates might shed more light

into the proposed Hrd1 function.

It was shown that the ubiquitin ligase Hrd1 interacts with various ERAD-M substrates. Thereby, residues located in the transmembrane domain (TMD) of Hrd1 are responsible for the interaction with distinct ERAD-M substrates [40,65].

Furthermore, it was shown that the AAA ATPase Cdc48 provides the power to extract ERAD-M substrates out of the ER membrane [103–105]. The ER membrane protein Dfm1 is able to recruit Cdc48 to the ER membrane independently of the Cdc48 membrane anchor protein Ubx2 [86,106]. The interaction is mediated by the C-terminal SHP box of Dfm1 [86,107,108]. In cells lacking Dfm1 or in the absence of the SHP box, retrotranslocation of the *bona fide* ERAD-M substrate Hmg2 is impaired [106]. Furthermore, it was shown that in the absence of its complex partner Hrd3, Hrd1 is rapidly degraded [53,54] in a process dependent on Dfm1 [106]. But, in case of strong overexpression of ERAD-M substrates, cells lacking Dfm1 undergo rapid suppression, which requires Hrd1 [106].

It is completely unclear whether a retrotranslocation channel for ERAD-C substrates exists or whether these substrates are directly extracted out of the ER membrane by the power machine Cdc48 [69,109]. The ubiquitin ligase Doa10 is also discussed to form a retrotranslocon, since its TMD is composed of 14 helices [40,69,109].

In general, during retrotranslocation the core *N*-glycan is removed [110,111]. In addition, the breakdown of disulfide bonds increases the retrotranslocation efficiency [112].

In mammals it was shown that the formation of lipid droplets eliminates some macromolecules and viruses out of the ER [113]. However, in yeast this model is dispensable for ERAD [114].

In summary, the retrotranslocation process of misfolded secretory proteins seems to be highly dynamic and it might be that there are several ways out of the ER.

1.4 Ubiquitination: Targeting ERAD substrates for elimination

ERAD substrates are recognized and finally proteolytically eliminated. They are selectively marked with ubiquitin, which targets them to the proteasome.

Ubiquitin is a polypeptide, highly conserved from yeast to man. The orthologs differ only in 3 of their 76 amino acids. Ubiquitin is highly stable and as a β-grasp family member it is compactly folded, and it contains a flexible six-residue C-terminal tail [115]. Typically, ubiquitin is covalently bound to the ε-NH_2 group of lysine residues of the selected proteins, forming an isopeptide bond with the carboxyl group of its C-terminal glycine residue (Gly76). It can also form oxyester and thioester bonds, in case it is attached to non-*canonical* amino acids such as serine, threonine and cysteine, respectively [116,117].

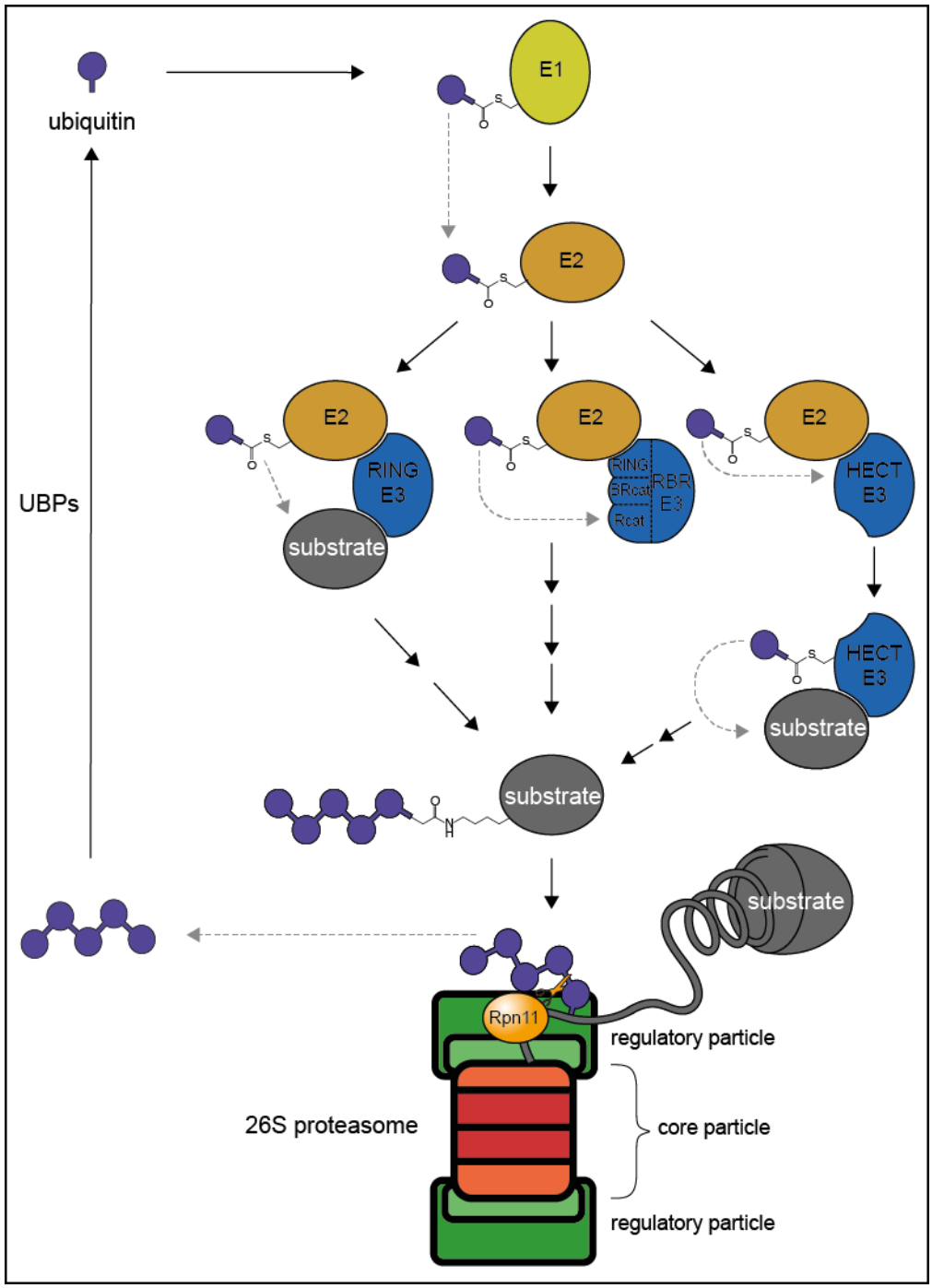

Figure 3: Attachment of ubiquitin is mediated by an enzymatic cascade, composed of E1, E2 and E3 enzymes.

First a thioester bond is formed between the carboxy-terminus of ubiquitin and the active site cysteine of the ubiquitin-activating enzyme (E1). By transesterification ubiquitin is attached to the active site cysteine residue of a ubiquitin-conjugating enzyme (E2). Finally, an isopeptide bond between ubiquitin and either lysine, serine, cysteine or threonine residues of substrate proteins is catalyzed by ubiquitin ligases (E3). Ubiquitin chains are formed by several cycles of the enzymatic cascade. Chains of four ubiquitin moieties are sufficient to be efficiently recognized by the 26S proteasome. The proteasome-associated metalloprotease Rpn11 cleaves the ubiquitin chain prior to final destruction of the substrate, leading to recycling of ubiquitin. Isopeptide bonds between ubiquitin moieties in chains are hydrolyzed by specific ubiquitin proteases (UBPs). (Figure adapted form Berner *et al.* 2018)

Ubiquitin is catalytically attached to the protein to be degraded by a cascade of three enzymes E1-E2-E3 (Figure 3). First, it is bound with its carboxy-terminus to a cysteine residue at the active site of the ubiquitin-activating enzyme (E1). This consumes ATP and thereby a ubiquitin-adenylate intermediate is formed. After release of AMP and pyrophosphate, ubiquitin is activated by an energy-rich thioester bond. In a next step, ubiquitin is transferred to the active site cysteine of a ubiquitin-conjugating enzyme (E2) by a transesterification reaction. Finally, a ubiquitin ligase (E3) facilitates the transfer of activated ubiquitin to the substrate protein (reviewed in [70]).

Substrates modified with single ubiquitin moieties can be also accepted by the 26S proteasome [118] but essentially the proteasome recognizes ubiquitin chains most efficiently that contain at least four ubiquitin moieties [119].

Ubiquitin contains 7 internal lysine residues (Lys) at position Lys6, Lys11, Lys 27, Lys29, Lys33, Lys48, Lys63 that function as potential covalent ubiquitination sites. By head to tail formation, the carboxy-terminus of the distal ubiquitin moiety can bind to an internal lysine residue or the amino-terminus of the proximal ubiquitin unit. Thus, substrates can also be polyubiquitinated [120–122]. Polyubiquitin chains are formed by successive rounds of the catalytic ubiquitination cascade. Depending on the internal lysine residues of ubiquitin used for linkage, homogenous, heterogenous, linear or branched polyubiquitin chains can arise.

All possible linkages are observed (reviewed in [123]). Lys27-, Lys29- and Lys33-linked ubiquitin chains are detected on few substrates. Their function is poorly understood [124,125]. Common chains are polyLys48-linked chains which are the *canonical* signal for final degradation by the 26S proteasome [120]. Lys6-linked chains are involved in autophagy [126,127]. Besides marking proteins for degradation [125], ubiquitination plays also a role in non-proteolytic processes. Lys11-linked chains participate in the regulation of mitosis [128], hypoxia response [129] and mitophagy [126]. Lys63-linked ubiquitin chains prevent proteins from binding to the proteasome [70]. They drive proteins to specific signaling complexes [130] and are involved in DNA repair [131]. Heterotypic Lys11-/Lys48-linked ubiquitin chains are found to signal proteasome-mediated degradation.

Linkage formation in ubiquitin chains is directed depending on either the ubiquitin-conjugating enzyme or the ubiquitin ligase.

In a particular case, it was reported that bacterial pathogens are also able to ubiquitinate human proteins independently of the E1 and E2 enzymes [132].

In yeast a single ubiquitin-conjugating enzyme (E1) exists, which is an essential protein. There are 13 ubiquitin-conjugating enzymes (E2) in yeast, but only 11 of them are involved in ubiquitin transfer. Of the remaining two, Ubc9 is involved in the transfer of Smt3, which is a ubiquitin-like protein and homologous to the mammalian SUMO, while Ubc12 is associated with the Nedd8 homolog, Rub1 [133,134].

There are 60-100 known yeast ubiquitin ligases (E3) in yeast, which belong to RING (really interesting new gene), HECT (homologous to E6AP C-terminus) and RBR (RING-in-between-RING) classes of ubiquitin ligases.

A common feature of RING ligases is to equally bind substrate and E2~Ub conjugate. Then, the ligase sets the stage for the orientation of both and thus supports ubiquitin transfer. Since the ligase is able to recognize its substrate proteins, ubiquitin chain formation is conducted at preferred positions but can also occur randomly [135]. The E2 transfers preassembled short ubiquitin chains containing a favored linkage [136–138] or an initiating E2 cooperates with a specific chain-elongating E2 ([139] and reviewed in [140]). Thus, it is assumed that the linkage specificity is determined by the E2 and not by the RING ligase [141].

The catalytic domain of HECT ubiquitin ligases contains an N-terminal and a C-terminal lobe. The N-terminal lobe binds the E2~Ub conjugate. Then a thioester bond is formed between ubiquitin and a catalytic cysteine in the C-terminal lobe of the ubiquitin ligase [142,143]. The acceptor lysine of the substrate attacks the thioester and ubiquitin is transferred to the substrate. Therefore, the HECT ligase has to position the substrate as well as the ubiquitin. This leads to the assumption that the linkage specificity is determined by the HECT ligase and not by the E2 enzyme (reviewed in [140]).

A special group of ligases are the RBR ubiquitin ligases, which act as RING/HECT hybrids. They contain a RING domain, a BRcat (benign-catalytic) domain and a Rcat (required-for-catalysis) domain. A common feature of RBR ligases is their autoinhibition of the Rcat domain. The RING domain recruits the E2~Ub conjugate, which leads to rearrangement of the domains and promotes the transfer of ubiquitin to a cysteine in the Rcat domain [144,145]. Finally, ubiquitin is transferred to the substrate protein. During ubiquitin transfer from E2 via E3 to the substrate, the ligase undergoes several rearrangement steps. Thus, it is predicted that the linkage specificity is determined by the RBR ubiquitin ligase (reviewed in [140]).

The RING ubiquitin ligases Hrd1 (alias Der3), Doa10, Asi complex and Ubr1 as well as the HECT ubiquitin ligase Hul5 are involved in elimination of ERAD substrates.

In a genetic screen several *DER* (degradation of ER) genes were identified. When mutated they all confer impaired degradation of the ERAD substrate CPY*, which is a mutant version of the vacuolar carboxypeptidase Y [43,62,146,147]. At the same time another genetic screen using the ERAD substrate 3-hydroxy-3methylglutaryl-CoA reductase isoenzyme 2 (HMG2) identified the *HRD* genes (HMG-CoA reductase degradation) [52]. Later it was shown, that *DER3* and *HRD1* are identical genes coding for the ubiquitin ligase Hrd1 (alias Der3) [94,148,149]. In this work, the Hrd1/Der3 ubiquitin ligase is designated as Hrd1.

Hrd1 cooperates with the ubiquitin-conjugating enzyme Ubc7 in degradation of misfolded ER lumenal proteins (ERAD-L) [43,150]. The cytosolic, soluble Ubc7 is recruited to the ER by the membrane anchor protein Cue1. The CUE domain has an activating effect on Ubc7 activity. It stabilizes and accelerates the growth of the ubiquitin chain [151–153]. The ubiquitin-conjugating enzymes Ubc1 and Ubc6 are also involved [43,149,154].

Hrd1 together with Ubc7 [65,149] is also involved in recognition and ubiquitination of ER proteins with an aberrant membrane part (ERAD-M) [65]. Whereas oligomerization of Hrd1 is a prerequisite for ubiquitination of ERAD-M substrates, but it is dispensable for ubiquitination of ERAD-L substrates [60].

Membrane proteins with cytosolic parts smaller than 60 kDa can move to the inner nuclear membrane via lateral diffusion [155,156]. These incorrectly localized proteins are recognized, ubiquitinated and finally destructed. In this process, the membrane-embedded ubiquitin ligases Doa10 and the Asi complex cooperate with the ubiquitin-conjugating enzymes Ubc6 and Ubc7 [66–68,155,157].

Doa10 is also the key ubiquitin ligase in ubiquitination of ER proteins exposing a misfolded cytosolic domain (ERAD-C substrates) [69,139,158]. In 2016, Weber and colleagues published a sequential mechanism for ubiquitination of a certain ERAD-C substrate [139], containing priming and elongation. For the priming, Ubc6 mediates monoubiquitination at either lysine, serine or threonine residues of the substrate protein. Then lysine 48-linked ubiquitin chain elongation is achieved by Ubc7 together with its membrane anchor protein Cue1. The substrate is stabilized in cells lacking either Doa10 or Ubc6 or Ubc7. No ubiquitination is observed in *doa10*Δ and *ubc6*Δ cells. There is residual ubiquitination, an accumulation of monoubiquitinated variants,

in cells depleted of Ubc7. This can be explained by the fact that in the absence of Ubc7, Doa10 and Ubc6 are able to ubiquitinate the substrate, but this ubiquitination mark is not sufficient to be recognized as degradation signal [139].

Since ERAD-C substrates contain lesions in their cytosolic part, the cytosolic ubiquitin ligase Ubr1 can resume ubiquitination of these substrates in case the *canonical* ER ubiquitin ligases Doa10 and Hrd1 are lacking [159]. Thereby, Ubr1 cooperates with the ubiquitin-conjugating enzyme Ubc2 [159].

1.5 Membrane extraction by the Cdc48 motor

The cytosolic AAA ATPase Cdc48 (cell division cycle) provides the engine to pull ubiquitinated proteins out of the ER membrane. It is highly conserved from yeast (Cdc48) to man (p97) and is in complex with various cofactors (reviewed in [6,160–164]).
Besides its function in ERAD, it is involved in many cellular processes such as transcriptional and metabolic regulation, DNA damage, chromatin remodeling, selective autophagy, cell cycle progression and cell death [165–170], where it separates ubiquitinated targets from binding partners or membranes.
The Cdc48 motor is recruited to the ER membrane by different membrane-embedded proteins. Ubx2 (ubiquitin regulatory x) bridges Cdc48 to the *canonical* ERAD ubiquitin ligases Hrd1 and Doa10. In cells lacking Ubx2, degradation of ERAD substrates with lesions in the ER lumen and the membrane domain is impaired [171,172]. Additionally, Dfm1 recruits Cdc48 to the ER membrane in a Ubx2 independent way [107,108]. Like Ubx2, Dfm1 is in complex with Hrd1 and Doa10 [86].

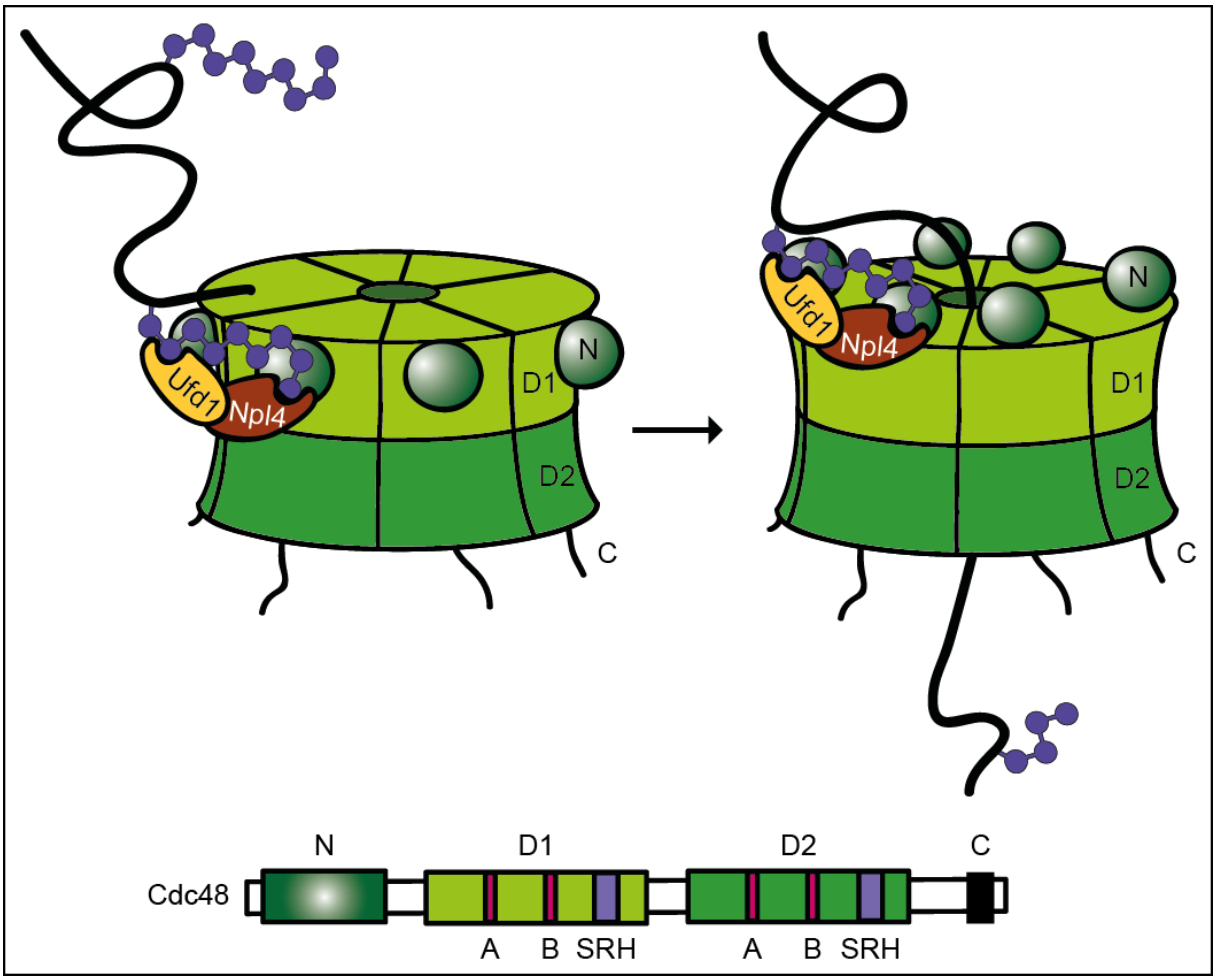

Figure 4: The AAA ATPase complex Cdc48-Npl4-Ufd1 is required for the extraction of proteins from the ER membrane.

Six Cdc48 protomers form a stacked double ring-shaped complex. Each monomer contains a mobile N domain, two ATPase domains (D1 and D2) and a flexible C-terminal tail. The Cdc48 cofactors Npl4 and Ufd1 are ubiquitin receptors. Conformational changes of the variable N domain as well as ATP hydrolysis leads to unfolding of ubiquitinated proteins and entire translocation through the central pore of Cdc48. (Figure adapted form Berner *et al.* 2018)

Each Cdc48 protomer is composed of two ATPase domains (D1 and D2), flanked by a mobile N domain and a disordered C-terminal tail. Six protomers form a double ring-shaped complex containing a central pore. The D1 domains build the *cis* side ring and the D2 the *trans* side ring, respectively. Both domains contain the highly conserved Walker A and Walker B motifs and a second region of homology (SRH). The nucleotide binding side is formed by the Walker A motif. The Walker B motif is responsible for ATP hydrolysis, which is assisted by the SRH domain (Figure 4; lower part).

The question is whether the substrates are able to pass the central pore or take an alternative route through Cdc48 [173,174]. Current cryo-EM structures propose that the substrates translocate through the central pore of Cdc48 [175,176].

Substrate recruitment is mediated by the Cdc48 cofactors Ufd1 and Npl4, which bind ubiquitin [105]. A single Ufd1-Npl4 heterodimer associates with the N domains of Cdc48 [105,177–179]. In an ATP-bound state the N domains are in an up-conformation (Figure 4; right side) [174,180–182]. Polyubiquitin chain binding affects ATP hydrolysis. It decreases at the D1 domain and increases at the D2 domain. Several cycles of ATP hydrolysis at D2 provide the energy to entirely pull the substrate through the central pore, by which it is simultaneously unfolded [175,176]. Substrate release requires the action of a deubiquitinating enzyme (DUB) and ATP hydrolysis at D1 [176]. The DUB Otu1 binds to the same binding site of the N domains as Ubx2 [96,171]. Thus, it is speculated that the Cdc48 complex dissociates from the ER membrane after complete extraction of the substrate [96]. Otu1 trims some but not all ubiquitin moieties of the substrates [183]. Thus, the remaining ubiquitin as well as the substrate translocate through the central pore of Cdc48 [184–186]. ATP hydrolysis at the D1 domain causes conformational changes, the N domains in a down conformation prevent further binding of DUB and allow recruitment to the ER membrane (Figure 4; left side). Degradation of ERAD substrates is not disturbed in cells lacking Otu1 [96]. This indicates that an alternative DUB might be associated with the Cdc48 motor [96].

Degradation of distinct ERAD-L and ERAD-C substrates is impaired in cells lacking the Cdc48 cofactor Ubx4. Since the ER membrane anchor protein Ubx2 and the cytosolic Ubx4 were not found at the same Cdc48 complex, it is suggested that Ubx4 participates at Cdc48 substrate release [187]. Vms1 depleted cells stabilize ERAD-L substrates to the same extent than cells depleted of Ubx4 [187,188].

Although there are still open questions concerning the exact mechanism of membrane extraction and substrate release (discussed in [6,102,163]) by Cdc48, the ATP motor is essential for the extraction of all three types of ERAD substrates containing lesions in the ER lumenal domain [103,105,158,164,189–194], the membrane part [190,195,196] and the cytosolic domain [158,195], prior to final destruction by the 26S proteasome.

1.6 Degradation by the 26S proteasome

Downstream of Cdc48-conducted membrane extraction, the ubiquitinated ERAD substrates are shuttled to the 26S proteasome by the adaptor proteins Dsk2 and Rad23. The ubiquitin moieties are bound by the UBA domains of the ubiquitin receptors. Via their ubiquitin-like (UBL) domains, Dsk2 and Rad23 are able to associate with the proteasome [189,193,197].

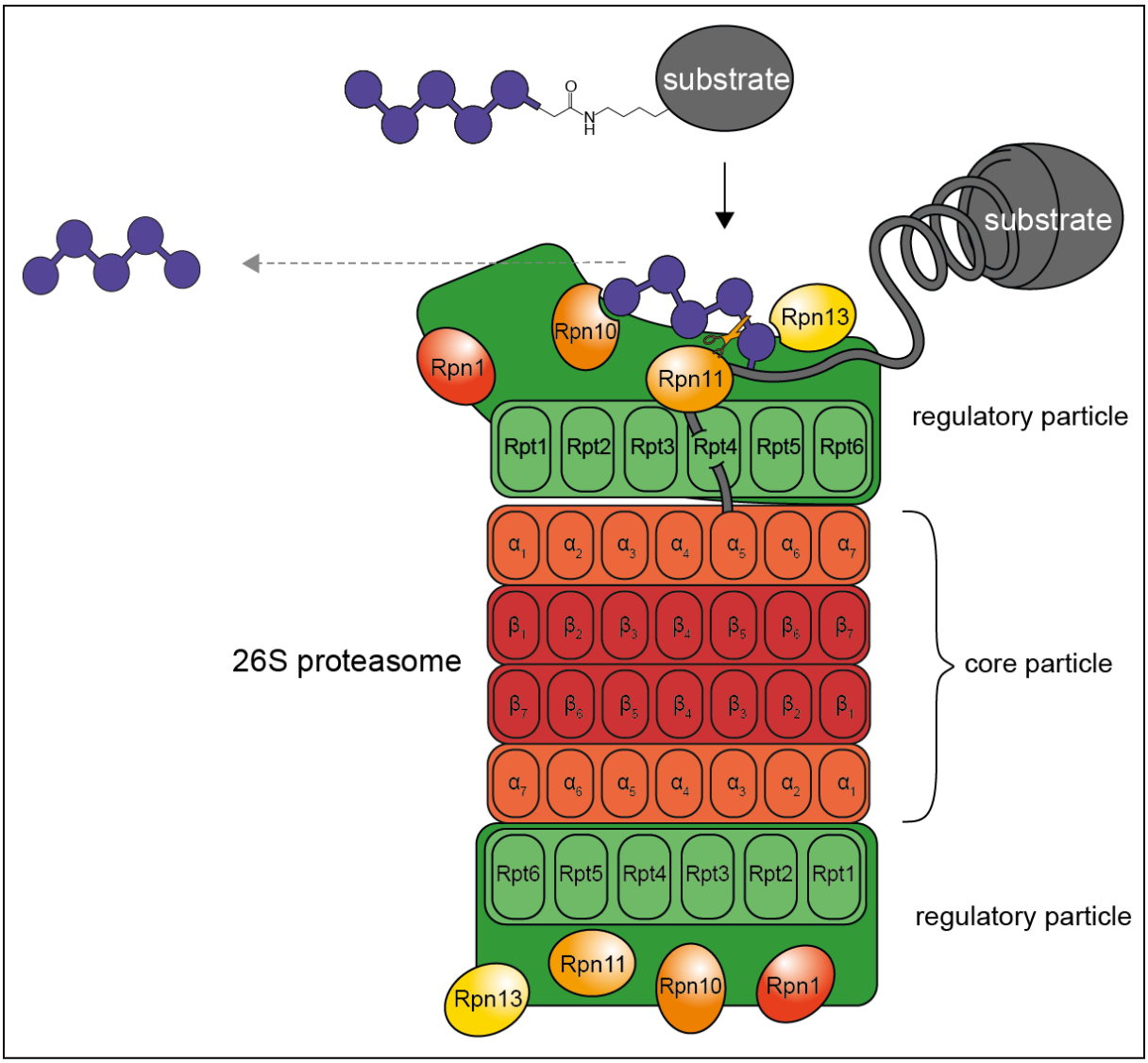

Figure 5: The 26S proteasome in association with a ubiquitinated substrate.
The 26S proteasome consists of the core particle and one or two regulatory particles. The regulatory particle is shown in green, highlighted are the intrinsic ubiquitin receptors (Rpn1, Rpn10 and Rpn13), the deubiquitinase Rpn11 and the ring-shaped heterohexameric AAA ATPases (Rpt1-6), which provides the engine to unfold the non-ubiquitinated substrate and channels it into the core particle. The proteolytically active barrel-shaped core particle (highlighted in variations of red) is formed by four stacked heteroheptameric rings. (Figure adapted form Berner *et al.* 2018)

The proteasome is the major protease in eukaryotic cells responsible for the breakdown of proteins into peptides. It is located in the nucleus and the cytosol of cells and consists of a barrel-shaped 20S core particle, flanked on each side by a 19S regulatory particle (Figure 5; reviewed in [70,198–202]).

The regulatory particle is formed by two subcomplexes, the lid and the base [203,204]. Both are hold together by the ubiquitin receptor Rpn10 [205,206].

The base includes three non-ATPases and 6 ATPases. The non-ATPases Rpn1 and Rpn2 are binding sites for ubiquitin and extrinsic ubiquitin receptors. The third non-ATPase is the intrinsic ubiquitin receptor Rpn13, which is a binding partner of Rpn2 [202,207–209]. The extrinsic ubiquitin receptors Dsk2 and Rad23 prefer binding to Rpn1 as well as Rpn13 [210]. By binding at additional extrinsic ubiquitin receptors, the substrate specificity of the proteasome increases.

The 6 AAA ATPases (Rpt1 to Rpt6) form a ring-shaped heterohexameric motor. The AAA+ domains bind ATP and mediate ATP hydrolysis. Thereby, chemical energy is converted into mechanical work, which conducts protein unfolding and introduction of the substrate into the catalytically active 20S core particle [211–215].

Prior to final degradation, the substrate-attached ubiquitin chains are cleaved off by Rpn11, which is a Zn^{2+} dependent deubiquitinase (DUB). This metalloprotease, together with 8 scaffold proteins, build the lid of the regulatory particle. This is necessary because ubiquitin must be recycled and the substrate is then able to enter the ATPase ring of the base [216–218].

The 20S core particle is formed by four stacked heteroheptameric rings, which assemble into an $\alpha 7\,\beta 7\,\beta 7\,\alpha 7$ structure. The outer α rings regulate substrate access into the proteolytic chamber, which is formed by the β subunits [201,219]. Three out of 7 β subunits (β_5, β_2 and β_1) are proteolytically active. They belong to the threonine class of proteases and cut after hydrophobic, basic and acidic residues, respectively [201,219–221].

The free 20S core particle of the proteasome is closed by the N-terminal tails of the α subunits. 19S regulatory binding opens the proteolytic chamber of the core particle. There are a set of factors that compete with the regulatory particle, including PA28 $\alpha\ \beta$, PA28 γ, Blm10 and Cdc48 [200,222]. These factors are not able to recognize ubiquitin but by binding to the α subunits, they open the proteolytically active 20S core

particle. Thus, they are involved in ubiquitin independent protein degradation [200,222].

1.7 Overview of the various ERAD pathways and the aim of this work

In the endoplasmic reticulum (ER), which is the ignition point of the secretory pathway, an elaborated mechanism has been evolved, which is responsible for the recognition and degradation of terminally damaged proteins. This multi-step pathway was called ER-associated degradation (ERAD) [6,8,40]. The consecutive steps to degrade an ERAD substrate comprise: substrate recognition, retrograde translocation, ubiquitination, membrane extraction and finally elimination in the cytosol.

Depending on their final location and function, secretory proteins exist with different topologies in the ER: soluble ER lumenal proteins and ER membrane-bound proteins. Alterations within these proteins lead to misfolding, which can finally be localized in different domains of these ER proteins. Misfolding can occur in the ER lumenal domain, the membrane domain and in the cytosolic domain of ER membrane-bound proteins facing the cytosol. Depending on the location of the aberrant domain, the degradation pathways and the specific components necessary for degradation were grouped into ERAD-L, ERAD-M or ERAD-C type of pathways, respectively. Since the late 1990's researchers around the world adhered to these pathways. It could be shown that ERAD-L and ERAD-M pathways differ in distinct parts, especially in the processes of substrate recognition and membrane passage [41,42]. The retrotranslocation event is controversy discussed and no final explanation could be tracked down yet [6,63,78]. It is established that the AAA ATPase Cdc48 and its cofactors pull all ERAD-substrates out of the ER membrane [103,105,158,164,189–194]. In all ERAD pathways the final elimination of aberrant proteins is executed by the 26S proteasome ([43], republished in [44]).

In order to search for new components, and to further differentiate the elimination pathways, various artificially misfolded ERAD substrates were designed, in such manner that each belongs to one single ERAD pathway.

Classification of the ERAD components into distinct pathways was made based on the criteria established by Vashist and Ng 2004 [41] as well as Carvalho *et al.* 2006 [42]. Vashist and Ng designed new fusion substrates to distinguish differences between ERAD-L and ERAD-C degradation pathways. To obtain the membrane-bound ERAD-

L substrate KWW [41], they substituted the extracellular domain of Wsc1, a plasma membrane protein, for the *bona fide* soluble ERAD-L substrate KHN (simian virus 5 HA-Neuraminidase ectodomain combined with Kar2 signal sequence) [41]. KWW consists of a misfolded ER lumenal domain, a native membrane domain and a native cytosolic domain, which contains multiple serine and lysine residues. Degradation of KWW is affected in cells lacking either the ubiquitin ligase Hrd1 or the ER membrane protein Der1 and not affected in cells lacking the ubiquitin ligase Doa10. This is not surprising, since Doa10 is the key ubiquitin ligase in ERAD-C substrate ubiquitination. To receive an ERAD-C substrate, they replaced the native cytosolic domain of KWW with the misfolded cytosolic domain of Ste6*, resulting in the KSS substrate [41]. It was shown that degradation of KSS depends on the ubiquitin ligase Doa10 but is independent of Hrd1 and Der1, which are components of the ERAD-L pathway. Based on their results, they postulated a sequential checkpoint mechanism. As a primary checkpoint, the folding status of cytosolic domains is monitored. Recognition of an unfolded cytosolic domain leads to elimination of the whole protein without proving the ER lumenal domain. The second checkpoint is in the ER lumen. There, misfolded lumenal domains are recognized and delivered to the ERAD machinery. For the first time, Vashist and Ng introduced the terms of ERAD-L and ERAD-C and postulated the existence of an ERAD-M degradation pathway [41] (an overview is given in Table 1).
Carvalho and colleagues focused on components of the ERAD-M and ERAD-L degradation pathway, respectively. Therefore, they operated with *bona fide* substrates, such as the ERAD-L substrates CPY*, KHN and KWW, as well as the ERAD-M substrates Sec61-2, HMG2, Pdr5* and CD4.

Taken all data together the different mechanisms how ERAD substrates are eliminated is explained in the following.
The fundamental steps in degradation of proteins containing a misfolded ER lumenal domain (ERAD-L substrates) were found by using a mutated form of carboxypeptidase yscY (CPY*) [223] and some membrane-bound CPY* derivatives. Recognition of ERAD-L substrates occurs with the support of the protein disulfide isomerase Pdi1 together with the exomannosidase Mnl1 [23,32–36], the ER lumenal chaperone Kar2 [49–51], the lectin Yos9 [224,225], the Pmt1/Pmt2 Dol-P:*O*-mannosyltransferase complex [26,27,226], and the membrane-bound Hrd3 [42,53–58] (for more details see chapter 1.2).

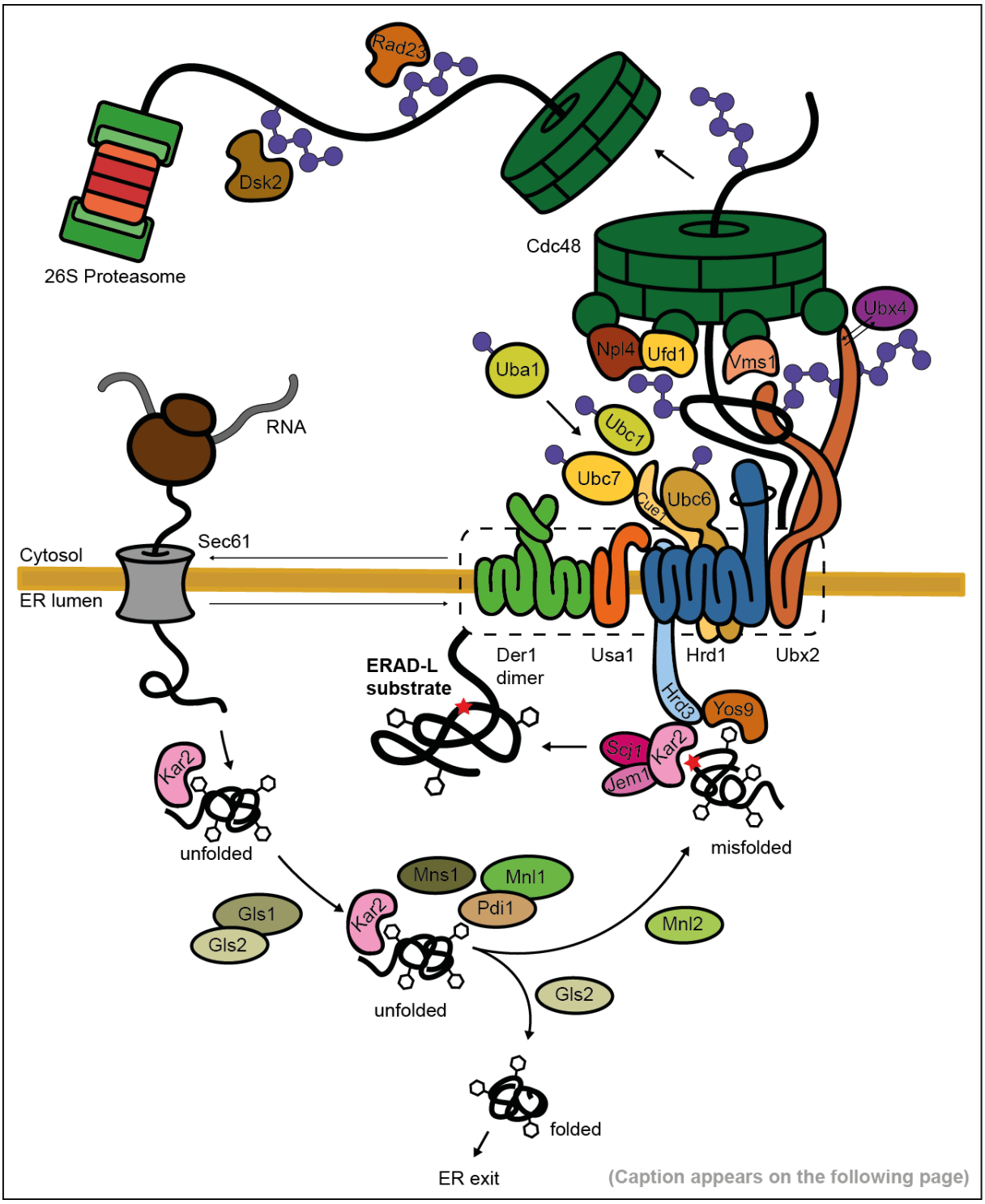
Rad23
Dsk2
26S Proteasome
Cdc48
Ubx4
Npl4
Ufd1
Vms1
Uba1
Ubc1
Ubc7
Cue1
Ubc6
RNA
Sec61
Cytosol
ER lumen
Der1
Usa1
Hrd1
Ubx2
ERAD-L
substrate
dimer
Hrd3
Yos9
Scj1
Jem1
Kar2
misfolded
unfolded
Mns1
Mnl1
Pdi1
Gls1
Gls2
Mnl2
unfolded
Gls2
folded
ER exit
(Caption appears on the following page)

Figure 6: Components required to degrade proteins containing lesions in their ER lumenal parts.

Proteins of the secretory pathway enter the ER through the Sec61 translocon. In the ER lumen, a core *N*-glycan is attached to the nascent peptide. Folding status is monitored during trimming of the glycan structure by glucosidase I (Gls1) and glucosidase II (Gls2). Successful folding of the protein leads to ER exit. When it fails to fold, further trimming of the *N*-glycan structure by the mannosidases Mns1, Mnl1 (alias Htm1) and Mnl2 is initiated. The Hsp70 chaperone Kar2 together with its Hsp40 cochaperones Scj1 and Jem1 deliver the misfolded protein to the misfolding receptor Hrd3. The lectin Yos9 binds the trimmed glycan and escorts the misfolded protein to Hrd3. Hrd3 is in complex with the ubiquitin ligase Hrd1. The pseudorhomboid Der1 is recruited to the *HRD* ligase by Usa1 and is required to introduce the ERAD-L substrate into the membrane-embedded complex which possibly forms the retrotranslocon. In the cytosol the protein is ubiquitinated by the ubiquitin ligase Hrd1 together with the ubiquitin-conjugating enzymes Ubc1, Ubc6 and the Cue1-bound Ubc7. The Ubx2 membrane anchor protein recruits the Cdc48-Npl4-Ufd1 complex to the ER membrane to extract the ubiquitinated substrate out of the ER membrane. Release of the substrate is mediated by Ubx4 and Vms1 and it is delivered to the 26S proteasome by the ubiquitin receptors Dsk2 and Rad23 for final destruction. (Figure adapted form Berner *et al.* 2018)

Then, the recognized proteins are delivered to an oligomeric complex, the *HRD*-Der1 complex [6]. It consists of the membrane embedded ubiquitin ligase Hrd1 [94,148,149], which forms dimers with Hrd3 and is called the *HRD* ligase complex [42,53,54,57,59,60] and the oligomeric Der1 proteins [41,60–62], which are recruited to the *HRD* ligase complex by Usa1 [60]. In this *HRD*-Der1 complex the misfolded proteins are introduced into the ER membrane by Der1. However, the complex mediates also retrotransloctaion of some ERAD-L substrates. Immediately after they occur at the cytosol, they are accessible to be ubiquitinated by the Hrd1 ligase with the help of the ubiquitin-conjugating enzymes Ubc1, Ubc6 and Ubc7 [43,149,150,154]. The ubiquitinated proteins are extracted out of the ER membrane. This process is facilitated by the Cdc48-Npl4-Ufd1 complex [103,105,164,189–193]. Rad23 and Dsk2 serve as shuttling proteins, which deliver the misfolded proteins to the 26S proteasome for final elimination [189,193,197] (an overview of ERAD-L is shown in Figure 6).

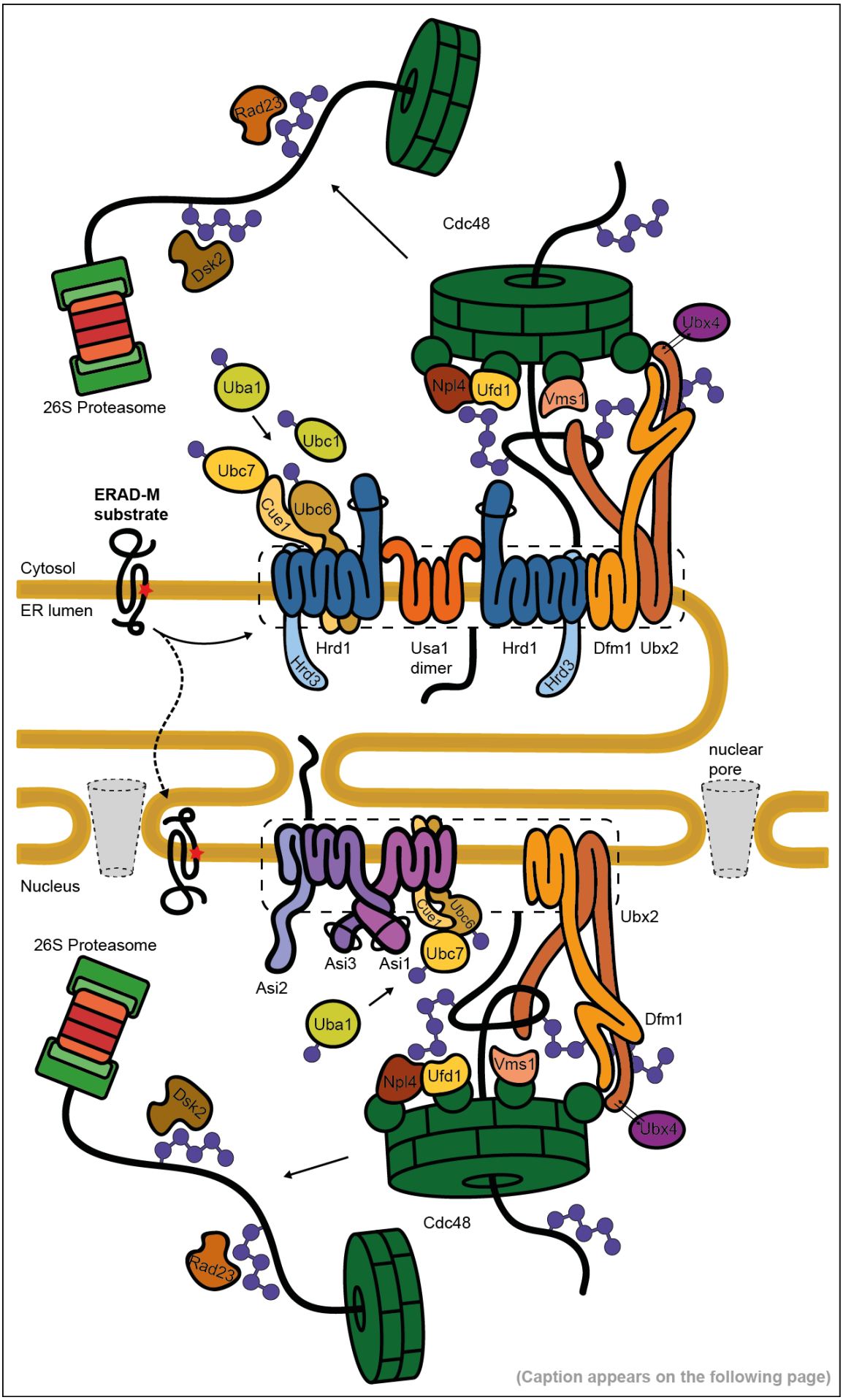

(Caption appears on the following page)

Figure 7: Elimination of secretory proteins containing aberrant membrane domains.
Aberrant membrane domains are recognized by ubiquitin ligases: The Asi complex embedded in the INM, the ubiquitin ligase Hrd1 localized in the ER membrane, or Doa10, which was found in the INM and the ER. As indicated, together with the ubiquitin-conjugating enzymes Ubc1, Ubc6 and Ubc7 the ERAD-M substrates are polyubiquitinated. Cdc48 is recruited to the nuclear or ER membrane either by Dfm1 or by Ubx2 and extracts the ERAD-C substrates out of the ER membrane for final elimination by the 26S proteasome. (Figure adapted form Berner *et al.* 2018)

In contrast to ER lumenal misfolded proteins, ERAD-M substrates carry impaired membrane domains. The ERAD-M pathway was analyzed using the HMG-CoA reductase isoenzyme 2 [52,146], a temperature sensitive mutated form of the Sec61 translocon (Sec61-2) [68,227] and the mutated multidrug transporter Pdr5* [227].

The Hrd1 ubiquitin ligase, a member of the *HRD* ligase complex, itself is able to recognize and ubiquitinate ERAD-M substrates [65], without the help of Der1 [41,42,60]. Proteins, with a cytosolic domain smaller than 60 kDa can move to the inner nuclear membrane [155,156]. There, they are ubiquitinated by the Asi complex, which is a RING ubiquitin ligase, formed by Asi1 and Asi3 [67,68]. The AAA ATPase Cdc48 pulls the ERAD-M substrates out of the INM as well as ER membrane [190,195,196] for final destruction by the 26S proteasome (an overview of ERAD-M is shown in Figure 7).

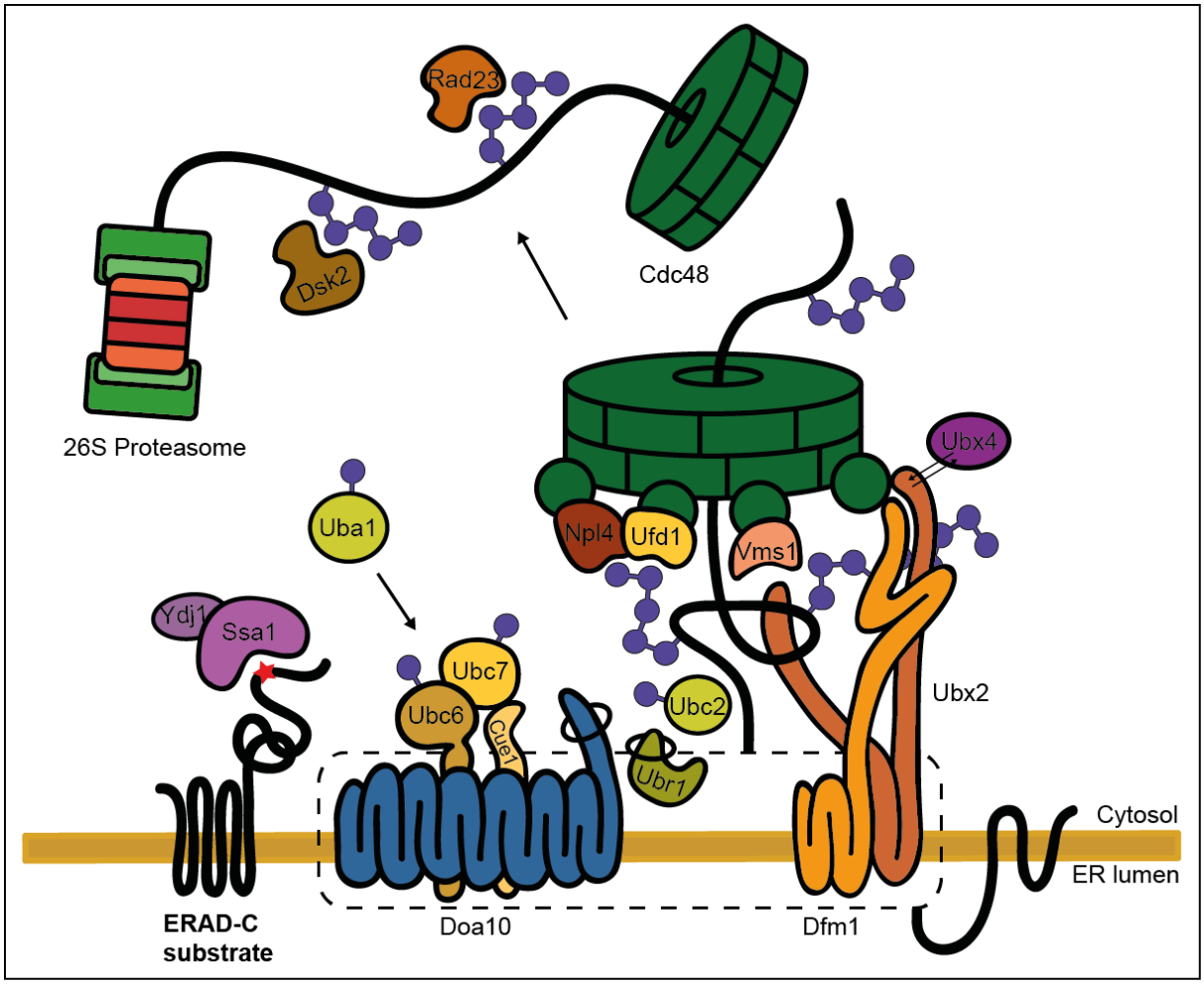

Figure 8: Degradation of proteins containing an aberrant cytosolic domain.
Lesions in the cytosolic part of ER proteins are recognized by the cytosolic Hsp70 chaperone Ssa1 together with its cochaperonesYdj1 and by the ER-membrane-embedded ubiquitin ligase Doa10 itself. Ubiquitination is conducted by Dao10 together with the ubiquitin-conjugating enzymes Ubc6 and the Cue1-bound Ubc7. In some cases, the cytosolic ubiquitin ligase Ubr1 together with Ubc2 leads to ubiquitination of ERAD-C substrates. Membrane extraction is mediated by the cytosolic AAA ATPase Cdc48 together with its cofactors Npl4 and Ufd1. The ubiquitin receptors Dsk2 and Rad23 escort the substrates to the 26S proteasome. (Figure adapted form Berner *et al.* 2018)

For ERAD-C pathway analysis, artificially misfolded ER proteins containing lesions in their cytosolic domain were used, such as the truncated ATP binding cassette transporter Ste6* [159] and the cystic fibrosis conductance regulator CFTRΔF508 [159,228]. In this pathway the cytosolic Hsp70/Hsp40 chaperons are required for degradation [76,158,229] , they recognize the ERAD-C substrates und shuttle them to the ubiquitin ligase Doa10 [73–76]. The ligase itself might also be able to recognize the substrates [70–72]. Together with the ubiquitin-conjugating enzymes Ubc6 and Ubc7, Doa10 mediates ubiquitination [69,139,155,158]. Under stress conditions and in case of the canonical ER ubiquitin ligases Doa10 and Hrd1 are lacking, the cytosolic ubiquitin ligase Ubr1 is able

to ubiquitinate Doa10 client proteins [159]. Dfm1, the yeast Der1 homolog [147], recruits Cdc48 to the ER membrane [107,108] and is important for the ERAD-C substrate degradation [86]. Cdc48 pulls the ubiquitinated proteins out of the ER membrane [158]. In the cytosol they are eliminated by the 26S proteasome (an overview of ERAD-C is shown in Figure 8).

It has become clear that there are key components in each of the ERAD branches. Der1 is a main player in ERAD-L degradation. Doa10 is mainly restricted to the ERAD-C degradation pathway, whereas Hrd1 plays a central role in ERAD-L as well as ERAD-M degradation (an overview is given in Table 1).

Table 1: Classification of ERAD substrates into the ERAD-L, ERAD-M and ERAD-C group of substrates established by Vashist and Ng 2004 as well as Carvalho *et al.* 2006

A green check mark indicates requirment for degradation; a red cross symbol means dispensable for degradation; n.a. stands for not analyzed. The ERAD components Der1, a membrane protein, and the ubiquitin ligases Hrd1 and Doa10 are central players in the different degradation pathways.

		Der1	Hrd1	Doa10
ERAD-L	Soluble, ER lumenal misfolded (KHW; CPY*)	✓	✓	✗
ERAD-L	Membrane-bound, ER lumenal misfolded (KWW)	✓	✓	✗
ERAD-M	Membrane-bound, ER lumenal misfolded (Sec61-2; Hmg2; Pdr5*)	✗	✓	n.a.
ERAD-C	Membrane-bound, cytosolically misfolded (Ste6*, KSS, KWS)	✗	✗	✓

According to the current classification [41,42], it was assumed that all ERAD-L substrates are degraded in a Der1 dependent manner: e.g. CPY*, which is a soluble ER lumenal protein, is completely stabilized in *der1*Δ cells [196]. However, in some specific cases, for instance the substrates KHN and KWW [41], ERAD-L substrate degradation is only slightly impaired in cells lacking Der1 [41,230]. This incongruency poses a question to the ERAD-L classification.

A discrepancy can be also found in the degradation of the CPY* derivatives CTL* (new

name C*T_{Pdr5}(CS)Leu2) and CTG* (new name C*T_{Pdr5}(CS)GFP). Both contain a single transmembrane helix. As a cytosolic domain they possess either the β-isopropylmalate dehydrogenase (Leu2) or the green fluorescent protein (GFP), respectively. Both domains were shown to be functional and properly folded [45,194,196,197,231]. Although they contain the same modular structure – membrane-embedded, properly folded cytosolic domain and misfolded ER lumenal CPY* moiety – Der1 was shown to be indispensable for C*T_{Pdr5}(CS)Leu2 degradation (Data published in PhD thesis Stefanie Besser [232]) but dispensable for C*T_{Pdr5}(CS)GFP degradation [196].

In summary, at the moment Der1 is the main requirement in the ERAD-L degradation pathway [41,42]. However, there are substrates, which all contain an ER lumenal misfolded domain, the hallmark of ERAD-L substrates, but do not require Der1 (C*T_{Pdr5}(CS)GFP) or just to a certain extent (KHN and KWW).

The aim of this thesis was to determine under which circumstances Der1 is required for ERAD, which leads to a more detailed picture about the mechanisms leading to degradation of proteins of the different ERAD classes. Furthermore, the detailed requirements of amino acids within a substrate to render it prone for degradation were elucidated. Therefore, an appropriate set of ERAD substrates with related modular structure was established and characterized. Finally, it was analyzed which ubiquitin ligases and ubiquitin-conjugating enzymes as well as Cdc48 are necessary to degrade the generated representatives of the ERAD pathways.

2. MATERIALS AND METHODS

2.1 Material, instruments and enzymes

2.1.1 Chemicals

Table 2: List of all chemicals used in this work.

Chemical	Manufacturer
Acetic acid	Carl Roth GmbH & Co. KG; Karlsruhe; Germany
Acetone	VWR International; Radnor; Pennsylvania; U.S.
Adenine hemisulfate salt	Sigma-Aldrich; St. Louis; Missouri; U.S.
Adenosine 5'-Triphosphate	New England Biolabs® Inc.; Ipswich; Massachusetts; U.S.
Agarose LE	Genaxxon bioscience GmbH; Ulm; Germany
Albumin Fraction V	Carl Roth GmbH & Co. KG; Karlsruhe; Germany
Ammonium acetate	Carl Roth GmbH & Co. KG; Karlsruhe; Germany
Ammonium peroxidesulphate	Carl Roth GmbH & Co. KG; Karlsruhe; Germany
Ampicillin sodium salt	Carl Roth GmbH & Co. KG; Karlsruhe; Germany
Bacto™ Agar	Becton Dickinson; Franklin Lakes; New Jersey; U.S.
Bacto™ Peptone	Becton Dickinson; Franklin Lakes; New Jersey; U.S.
Bacto™ Tryptone	Becton Dickinson; Franklin Lakes; New Jersey; U.S.
Bacto™ Yeast Extract	Becton Dickinson; Franklin Lakes; New Jersey; U.S.
β -glycerophosphate disodium salt	Illinois Tool Works Inc.; Chicago, Illinois; U.S.
Bromophenol blue sodium salt	Carl Roth GmbH & Co. KG; Karlsruhe; Germany
cOmplete™ Protease inhibitor cocktail	Roche; Basel; Switzerland
Copper(II) sulfate	Sigma-Aldrich; St. Louis; Missouri; U.S.
Cycloheximide	Sigma-Aldrich; St. Louis; Missouri; U.S.
D(+)-galactose	Carl Roth GmbH & Co. KG; Karlsruhe; Germany
D(+)-glucose monohydrate	Carl Roth GmbH & Co. KG; Karlsruhe; Germany
Difco™ Yeast Nitrogen Base w/o Amino Acids	Becton Dickinson; Franklin Lakes; New Jersey; U.S.
Digitonin	Merck KGaA, Darmstadt; Germany
Dimethylformamide	Thermo Fisher Scientific; Waltham; Massachusetts; U.S.
di-sodium hydrogen phosphate	Carl Roth GmbH & Co. KG; Karlsruhe; Germany

1,4-dithiothreitol	Carl Roth GmbH & Co. KG; Karlsruhe; Germany
DMSO	Thermo Fisher Scientific; Waltham; Massachusetts; U.S.
D-sorbitol	Carl Roth GmbH & Co. KG; Karlsruhe; Germany
Ethanol absolute	VWR International; Radnor; Pennsylvania; U.S.
Ethylenediamine tetraacetic acid disodium salt dihydrate	Carl Roth GmbH & Co. KG; Karlsruhe; Germany
G-418 solution	Roche; Basel; Switzerland
GelRed®	Genaxxon bioscience GmbH; Ulm; Germany
Glass beads (∅ 0.25 – 0.5 mm)	Carl Roth GmbH & Co. KG; Karlsruhe; Germany
Glycerol	Carl Roth GmbH & Co. KG; Karlsruhe; Germany
Glycine	Carl Roth GmbH & Co. KG; Karlsruhe; Germany
Glycine	Sigma-Aldrich; St. Louis; Missouri; U.S.
Guanidine Hydrochloride	Carl Roth GmbH & Co. KG; Karlsruhe; Germany
HEPES	Carl Roth GmbH & Co. KG; Karlsruhe; Germany
5 × HF buffer	Thermo Fisher Scientific; Waltham; Massachusetts; U.S.
Hydrochloric acid fuming	Carl Roth GmbH & Co. KG; Karlsruhe; Germany
Imidazole	Carl Roth GmbH & Co. KG; Karlsruhe; Germany
L-alanine	Sigma-Aldrich; St. Louis; Missouri; U.S.
L-arginine	Sigma-Aldrich; St. Louis; Missouri; U.S.
L-asparagine monohydrate	Sigma-Aldrich; St. Louis; Missouri; U.S.
L-aspartic acid	Sigma-Aldrich; St. Louis; Missouri; U.S.
L-cysteine	Sigma-Aldrich; St. Louis; Missouri; U.S.
L-glutamic acid	Sigma-Aldrich; St. Louis; Missouri; U.S.
L-glutamine	Sigma-Aldrich; St. Louis; Missouri; U.S.
L-histidine monohydrochloride monohydrate	Sigma-Aldrich; St. Louis; Missouri; U.S.
Lithium acetate dihydrate	Sigma-Aldrich; St. Louis; Missouri; U.S.
L-isoleucine	Sigma-Aldrich; St. Louis; Missouri; U.S.
L-leucine	Sigma-Aldrich; St. Louis; Missouri; U.S.
L-lysine	Sigma-Aldrich; St. Louis; Missouri; U.S.
L-methionine	Sigma-Aldrich; St. Louis; Missouri; U.S.
L-phenylalanine	Sigma-Aldrich; St. Louis; Missouri; U.S.
L-proline	Sigma-Aldrich; St. Louis; Missouri; U.S.
L-serine	Sigma-Aldrich; St. Louis; Missouri; U.S.
L-threonine	Sigma-Aldrich; St. Louis; Missouri; U.S.
L-tryptophan	Sigma-Aldrich; St. Louis; Missouri; U.S.
L-tyrosine	Sigma-Aldrich; St. Louis; Missouri; U.S.

L-valine	Sigma-Aldrich; St. Louis; Missouri; U.S.
Magnesium chloride hexahydrate	Carl Roth GmbH & Co. KG; Karlsruhe; Germany
Magnesium sulfate hydrate	Carl Roth GmbH & Co. KG; Karlsruhe; Germany
2-mercaptoethanol	Sigma-Aldrich; St. Louis; Missouri; U.S.
Methanol	VWR International; Radnor; Pennsylvania; U.S.
Milk powder	Carl Roth GmbH & Co. KG; Karlsruhe; Germany
Milli-Q ultrapure water	Merck KGaA, Darmstadt; Germany
Myo-inositol	Sigma-Aldrich; St. Louis; Missouri; U.S.
NAD^+	Carl Roth GmbH & Co. KG; Karlsruhe; Germany
N-benzoyl-L-tyrosine *p*-nitroanilide	Sigma-Aldrich; St. Louis; Missouri; U.S.
Ni-NTA Agarose	QIAGEN; Venlo; Netherlands
Nonidet™ P 40 Substitute	Sigma-Aldrich; St. Louis; Missouri; U.S.
Nucleotide solution	New England Biolabs® Inc.; Ipswich; Massachusetts; U.S.
Para-aminobenzoic acid	Sigma-Aldrich; St. Louis; Missouri; U.S.
Pepstantin A	Sigma-Aldrich; St. Louis; Missouri; U.S.
Phenol:chlorophorm:Isoamyl Alcohol 25:24:1	Sigma-Aldrich; St. Louis; Missouri; U.S.
Phenylmethylsulfonyl fluoride	Carl Roth GmbH & Co. KG; Karlsruhe; Germany
Poly(ethylene glycol) BioUltra 3,350	Sigma-Aldrich; St. Louis; Missouri; U.S.
Potassium acetate	Merck KGaA, Darmstadt; Germany
Potassium chloride	Carl Roth GmbH & Co. KG; Karlsruhe; Germany
Promega Herring Sperm DNA	Promega Corporation; Madison; Wisconsin; U.S.
2-Propanol	VWR International; Radnor; Pennsylvania; U.S.
Protein A Sepharose™	GE Healthcare; Chicago; Illinois; U.S.
Rotiphorese® Gel 30 (37.5:1)	Carl Roth GmbH & Co. KG; Karlsruhe; Germany
Rotiphorese® Gel 40 (29:1)	Carl Roth GmbH & Co. KG; Karlsruhe; Germany
SDS pellets	Carl Roth GmbH & Co. KG; Karlsruhe; Germany
Sodium acetate anhydrous	Carl Roth GmbH & Co. KG; Karlsruhe; Germany
Sodium azide	Carl Roth GmbH & Co. KG; Karlsruhe; Germany
Sodium carbonate anhydrous	Sigma-Aldrich; St. Louis; Missouri; U.S.
Sodium chloride	Carl Roth GmbH & Co. KG; Karlsruhe; Germany
Sodium dihydrogen phosphate Monohydrate	Sigma-Aldrich; St. Louis; Missouri; U.S.
Sodium fluoride	Sigma-Aldrich; St. Louis; Missouri; U.S.
Sodium hydroxide	Carl Roth GmbH & Co. KG; Karlsruhe; Germany
TEMED	Carl Roth GmbH & Co. KG; Karlsruhe; Germany
Trichloroacetic acid	Carl Roth GmbH & Co. KG; Karlsruhe; Germany
Tricine	AppliChem GmbH; Darmstadt; Germany
TRIS	Carl Roth GmbH & Co. KG; Karlsruhe; Germany

Triton X-100	Carl Roth GmbH & Co. KG; Karlsruhe; Germany
Tween® 20	Carl Roth GmbH & Co. KG; Karlsruhe; Germany
Uracil	Sigma-Aldrich; St. Louis; Missouri; U.S.
Urea	Carl Roth GmbH & Co. KG; Karlsruhe; Germany

2.1.2 Instruments and software

Table 3: List of all instruments and software used in this work.

Instruments / Software	Description	Manufacturer
Adobe CS6	Software	Adobe Inc.; San Jose; California; U.S.
CLIQS version 1.2.044	Quantification software	TotalLAb Ltd.; Newcastle upon Tyrne; UK
Disruptor Genie™ Cell Disruptor	Cell disruptor	Scientific Industries, Inc.; Bohemia; New York; U.S.
Disruptor Genie™ Digital Cell Disruptor	Cell disruptor	Scientific Industries, Inc.; Bohemia; New York; U.S.
EnSpire Multimode Plate Reader	Plate reader	PerkinElmer, Inc.; Waltham; Massachusetts; U.S.
Eppendorf 5415D Centrifuge	Centrifuge	Eppendorf; Hamburg; Germany
Eppendorf 5417C Centrifuge	Centrifuge	Eppendorf; Hamburg; Germany
Eppendorf 5804R Centrifuge	Centrifuge	Eppendorf; Hamburg; Germany
Eppendorf Rotor A-4-44	Rotor	Eppendorf; Hamburg; Germany
EPSON PERFECTION V700 PHOTO	Scanner	Seiko Epson Corporation; Suwa; Nagano Prefecture; Japan
Heraeus B6120 incubator	Incubator	Thermo Fisher Scientific; Waltham; Massachusetts; U.S.
Heraeus B6200 incubator	Incubator	Thermo Fisher Scientific; Waltham; Massachusetts; U.S.
Heraeus™ Pico™ 21 Microcentrifuge	Centrifuge	Thermo Fisher Scientific; Waltham; Massachusetts; U.S.
Herasafe™ KS	Safety Cabinet	Thermo Fisher Scientific; Waltham; Massachusetts; U.S.
Hettich Rotor 1617	Rotor	Andreas Hettich GmbH & Co. KG; Tuttlingen; Germany
Lab pH meter inoLab® pH7110	pH meter	Xylem Inc.; Rye Brook; New York; U.S.

Membrane vacuum pump	Vacuum pump	Analytik Jena AG; Jena; Germany
Medeley Desktop Version 1.19.4	Reference manager software	Mendeley Ltd.; London; UK
MicroPulser™ Electroporation Apparatus	Electroporation apparatus	Bio-Rad Laboratories, Inc.; Hercules; California; U.S.
Milli-Q® Advantage A10® System	Ultrapure water	Merck KGaA, Darmstadt; Germany
Mini-PROTEAN Handcast System	Gel casting apparatus	Bio-Rad Laboratories, Inc.; Hercules; California; U.S.
Mini-PROTEAN Tetra Vertical Electrophoresis Cell	Electrophoresis cell	Bio-Rad Laboratories, Inc.; Hercules; California; U.S.
Mini-Sub Cell GT System	Electrophoresis cell	Bio-Rad Laboratories, Inc.; Hercules; California; U.S.
Mini Trans-Blot Cell chamber	Electrophoresis cell	Bio-Rad Laboratories, Inc.; Hercules; California; U.S.
MS Office Version 2016	Software	Microsoft Corporation; Redmond; Washington; U.S.
Multitron	Incubator	Infors HT; Bottmingen; Basel-Country; Switzerland
NanoDrop 1000 Spectrophotometer	Spectrophotometer	Thermo Fisher Scientific; Waltham; Massachusetts; U.S.
NOVASPEC II UV/VIS-Spectrometer	UV/VIS-Spectrophotometer	GE Healthcare; Chicago; Illinois; U.S.
Optima™ TLX-CE Preparative Ultracentrifuge	Ultracentrifuge	Beckman Coulter Inc.; Brea; California; U.S.
OptiMax X-ray Processor	X-ray film processor	PROTEC GmbH & Co. KG; Oberstenfeld; Germany
Power Pac 300 Electrophoresis Power Supply	Power supply	Bio-Rad Laboratories, Inc.; Hercules; California; U.S.
Power Supply Model 200/2.0	Power supply	Bio-Rad Laboratories, Inc.; Hercules; California; U.S.
Precision balance 572	Precision balance	KERN; Balingen; Germany
Quantum ST5	Gel documentation system	Vilber Lourmat Sté; Collégien; France
Quintix 124-1S analytical lab balance	Balance	Sartorius; Göttingen; Germany
RCT basic	Stirring hot plate	IKA®-Werke GmbH & Co. KG; Staufen; Germany
Rotixa 50 RS Refrigerated	Centrifuge	Andreas Hettich GmbH & Co.

Centrifuge		KG; Tuttlingen; Germany
Roto-Shake Genie, SI-1102	Rocking platform	Scientific Industries, Inc.; Bohemia; New York; U.S.
Scotsman AF 103 Ice Flaker	Ice machine	Scotsman; Vernon; Illinois; U.S.
Super Bright transilluminator TFX-20 MX	Transilluminator	Vilber Lourmat Sté; Collégien; France
Tabletop High-Speed Micro Centrifuge CT15RE	Centrifuge	Koki Holdings Co., Ltd.; Tokyo; Japan
TGradient	PCR thermocycler	Analytik Jena AG; Jena; Germany
Thermomixer pro	Thermomixer	Cellmedia GmbH & Co. KG; Elsteraue; Germany
TLA-110 Fixed-Angle Rotor	Rotor	Beckman Coulter Inc.; Brea; California; U.S.
Tpersonal	PCR thermocycler	Analytik Jena AG; Jena; Germany
T1 Thermocycler	PCR thermocycler	Analytik Jena AG; Jena; Germany
Universal 320	Centrifuge	Andreas Hettich GmbH & Co. KG; Tuttlingen; Germany
Wide Mini-Sub Cell GT System	Electrophoresis cell	Bio-Rad Laboratories, Inc.; Hercules; California; U.S.
Vortex Genie 2	Vortexer	Scientific Industries, Inc.; Bohemia; New York; U.S.

2.1.3 Antibodies and binding proteins

Table 4: List of all antibodies and binding proteins used in this work.
WB, Western blot; IP, immuno precipitation

Antibody / binding protein	Host	Used dilution	Reference	Application
Anti-CPY antibody; monoclonal	mouse	1 : 5,000	Abcam; Cambridge; UK	WB
Anti-Cue1; polyclonal	rabbit	1 : 1,000	Provided by Thomas Sommer; Max-Delbrück Center for Molecular Medicine; Berlin; Germany	WB
Anti-Dfm1; polyclonal	rabbit	1 : 5,000	Stolz *et al.* 2011 [86]	WB

Anti-GFP; monoclonal	mouse	1 : 2,000	Sigma-Aldrich; St. Louis; Missouri; U.S.	WB
Anti-HA.11 (16B12); monoclonal	mouse	1 : 5,000	BioLegend; San Diego; California; U.S.	WB
Anti-Kar2; polyclonal	rabbit	1 : 10,000	Provided by Alexander Varshavsky; California Institute of Technology; Pasadena; California; U.S.	WB
Anti-mouse IgG	goat	1 : 10,000	Jackson ImmunoResearch; West Grove; Pennsylvania; U.S.	WB
Anti-rabbit IgG	goat	1 : 10,000	Sigma-Aldrich; St. Louis; Missouri; U.S.	WB
Anti-Sec61; polyclonal	rabbit	1 : 7,500	Provided by Thomas Sommer; Max-Delbrück Center for Molecular Medicine; Berlin; Germany	WB
c-Myc (9E10): sc-40; monoclonal	mouse	1 : 5,000	Santa Cruz Biotechnology, Inc.; Dallas; Texas; U.S.	WB
HA-probe (F7): sc-7392; monoclonal	mouse	1 : 5,000	Santa Cruz Biotechnology, Inc.; Dallas; Texas; U.S.	IP
His-probe (AD1.1.10): sc-53073; monoclonal	mouse	1 : 2,000	Santa Cruz Biotechnology, Inc.; Dallas; Texas; U.S.	WB
m-IgG κ BP-HRP:sc-516102		1 : 10,000	Santa Cruz Biotechnology, Inc.; Dallas; Texas; U.S.	WB
Phosphoglycerate kinase antibody; monoclonal	mouse	1 : 10,000	Thermo Fisher Scientific; Waltham; Massachusetts; U.S.	WB
V5 Tag antibody (E10/V4RR); monoclonal	mouse	1 : 5,000	Thermo Fisher Scientific; Waltham; Massachusetts; U.S.	WB; IP

2.1.4 Enzymes

Table 5: List of all enzymes used in this work.

Name	Reference
AgeI-HF	New England Biolabs® Inc.; Ipswich; Massachusetts; U.S.
DpnI	New England Biolabs® Inc.; Ipswich; Massachusetts; U.S.
EcoRI-HF	New England Biolabs® Inc.; Ipswich; Massachusetts; U.S.
HindIII-HF	New England Biolabs® Inc.; Ipswich; Massachusetts; U.S.
KpnI-HF	New England Biolabs® Inc.; Ipswich; Massachusetts; U.S.
NheI-HF	New England Biolabs® Inc.; Ipswich; Massachusetts; U.S.
NotI-HF	New England Biolabs® Inc.; Ipswich; Massachusetts; U.S.
PacI	New England Biolabs® Inc.; Ipswich; Massachusetts; U.S.
Phusion High Fidelity DNA Polymerase	Thermo Fisher Scientific; Waltham; Massachusetts; U.S.
Proteinase K	Thermo Fisher Scientific; Waltham; Massachusetts; U.S.
Ribonuclease A	Serva Electrophoresis GmbH; Heidelberg; Germany
Shrimp Alkaline Phosphatase	Fermentas; Waltham; Massachusetts; U.S.
SpeI-HF	New England Biolabs® Inc.; Ipswich; Massachusetts; U.S.
T4 polynucleotide kinase	New England Biolabs® Inc.; Ipswich; Massachusetts; U.S.
Taq DNA Ligase	New England Biolabs® Inc.; Ipswich; Massachusetts; U.S.
Zymolyase 20T	Seikagaku Corporation; Tokyo; Japan
Zymolyase 100T	Seikagaku Corporation; Tokyo; Japan

2.1.5 Molecular-weight size marker

DNA ladder:

1 kbp DNA-Ladder; Carl Roth GmbH & Co. KG; Germany

Protein ladder:

PageRuler™ Plus Prestained Protein Ladder, 10 to 250 kDa; Thermo Fisher Scientific; Waltham, Massachusetts; U.S.

Spectra™ Multicolor Low Range Protein Ladder; Thermo Fisher Scientific; Waltham, Massachusetts; U.S.

2.1.6 Commercial kits

Table 6: List of all commercial kits used in this work.

Application	Name	Reference
An enhanced chemiluminescent substrate for detection of HRP	Pierce® ECL Western Blotting Substrate	Thermo Fisher Scientific; Waltham; Massachusetts; U.S.
An enhanced chemiluminescent substrate for detection of HRP	Western Lightning® Plus-ECL	PerkinElmer, Inc.; Waltham; Massachusetts; U.S.
DNA clean-up; Extraction of DNA fragments out of agarose gels	NucleoSpin® Gel and PCR clean-up	MACHEREY-NAGEL GmbH & Co. KG; Düren; Germany
Isolation of plasmid DNA out of *E. coli*	NucleoSpin® Plasmid	MACHEREY-NAGEL GmbH & Co. KG; Düren; Germany
Ligation of DNA fragments	Rapid DNA Ligation Kit	Thermo Fisher Scientific; Waltham; Massachusetts; U.S.

2.2 Cultivation media and microbial strains

All cultivation media and buffers, used in this work, were prepared with Milli-Q ultrapure water.

Prior to inoculating yeast and *E. coli* cultures, all media and consumables were autoclaved at 121°C for 30 min.

2.2.1 Cultivation media for *E. coli*

LB broth:

0.5% (w/v)	Bacto™ yeast extract
1% (w/v)	Bacto™ Tryptone
0.5% (w/v)	NaCl
adjusted to pH 7.5	

100 µg/ml of ampicillin were added to *E. coli* cultures containing a plasmid, encoding for an ampicillin resistance gene.

Solid LB broth media additionally contained 2% (w/v) Bacto™ agar.

SOC:

0.5 (w/v)	Bacto™ yeast extract
2% (w/v)	Bacto™ Tryptone
0.4% (w/v)	D-glucose
10 mM	NaCl
10 mM	$MgCl_2$
10 mM	$MgSO_4$
2.5 mM	KCl
adjusted to pH 7.4	

2.2.2 Cultivation media for *S. cerevisiae*

Rich media (YPD):

1% (w/v)	Bacto™ yeast extract
2% (w/v)	Bacto™ Peptone
2% (w/v)	D-glucose

adjusted to pH 5.5

Complete minimal media (CM):

0.67% (w/v)	Difco™ yeast nitrogen base w/o amino acids
2% (w/v)	D-glucose
0.0117% (w/v)	L-alanine
0.0117% (w/v)	L-arginine
0.0117% (w/v)	L-asparagine
0.0117% (w/v)	L-aspartic acid
0.0117% (w/v)	L-cysteine
0.0117% (w/v)	L-glutamine
0.0117% (w/v)	L-glutamic acid
0.0117% (w/v)	glycine
0.0117% (w/v)	L-isoleucine
0.0117% (w/v)	L-methionine
0.0117% (w/v)	L-phenylalanine
0.0117% (w/v)	L-proline
0.0117% (w/v)	L-serine
0.0117% (w/v)	L-threonine
0.0117% (w/v)	L-tyrosine
0.0117% (w/v)	L-valine
0.00117% (w/v)	para-aminobenzoic acid
0.0117% (w/v)	myo-inositol

adjusted to pH 5.6

The following amino acids have to be added depending on the selected auxotrophy marker:

0.3 mM	L-histidine HCl H_2O
1.7 mM	L-leucine
1 mM	L-lysine
0.4 mM	L-tryptophan
0.3 mM	Adenine hemisulfate salt
0.2 mM	Uracil

Solid media additionally contained 2% (w/v) Bacto™ agar.

200 µg/ml of Geniticin G-418 was added to yeast cultures, containing a heterologous *kan*^{r} marker, which confers resistance to the antibiotic.
To induce the *GAL1* promoter, 2% (w/v) D-galactose, instead of D-glucose, was added to the yeast cultivation media.

2.2.3 *E. coli* strains

Table 7: List of all *E. coli* strains used in this work.

Strain	Genotype	Reference
DH5 α	*F$^-$endA1 glnV44 thi-1 recA1 relA1 gyrA96 deoR nupG purB20 ϕ80dlacZΔM15 Δ(lacZY-argF)U169, hsdR17(r_K-m_{K+}), λ^-*	Hanahan, 1983 [233]

2.2.4 *S. cerevisiae* strains

Table 8: List of all *S. cerevisiae* strains used in this work.
Strains in black were used for experiments. Strains in gray were used to generate new yeast strains.

YWO number	Strain designation	Genotype	Reference
YWO 0340	*pra1Δ prb1Δ prc1Δ*	*MAT**a** ura3-1 his3-11,15 leu2-3,112 trp1-1ade2-1ocre can1-100 pep4Δ::HIS3 prb1Δ::hisG prc1Δ::hisG*	Wilcox *et al.* 1992 [234]
YWO 0343	*prc1-1*	*MATα ura3-1 his3-11,15 leu2-3,112 trp1-1ade2-1ocre can1-100 prc1-1*	Knop *et al.* 1996 [62]
YWO 0349	*prc1-1 ubc6Δ*	*MATα ura3-1 his3-11,15 leu2-3,112 trp1-1ade2-*	Hiller *et al.* 1996 [43]

		1ocre can1-100 *prc1-1 ubc6Δ::LEU2*	
YWO 0636	*prc1Δ*	*MAT α* *ura3-1 his3-11,15 leu2-3,112 trp1-1ade2-1ocre can1-100* *prc1Δ::LEU2*	Plemper *et al.* 1999 [235]
YWO 0713	*prc1-1 dfm1Δ*	*MAT α* *ura3-1 his3-11,15 leu2-3,112 trp1-1ade2-1ocre can1-100* *prc1-1 dfm1Δ::His3MX6*	Hitt & Wolf 2004 [147]
YWO 1220	*prc1-1 cue1Δ*	*MAT**a*** *ura3-1 his3-11,15 leu2-3,112 trp1-1ade2-1ocre can1-100* *prc1-1 cue1Δ::LEU2*	Plemper *et al.* 1999 [53]
YWO 1320	*prc1Δ hul5Δ*	*MAT α* *ura3-1 his3-11,15 leu2-3,112 trp1-1ade2-1ocre can1-100* *prc1Δ::LEU2 hul5Δ::HIS3*	Kohlmann *et al.* 2008 [194]
YWO 1343	*prc1Δ hrd1Δ*	*MAT α* *ura3-1 his3-11,15 leu2-3,112 trp1-1ade2-1ocre can1-100* *prc1Δ::LEU2 hrd1Δ::HIS3*	Kohlmann *et al.* 2008 [194]
YWO 1526	*prc1Δ doa10Δ*	*MAT**a*** *ura3-1 his3-11,15 leu2-3,112 trp1-1ade2-1ocre can1-100* *prc1Δ::LEU2 doa10Δ::kanMX*	Benitez *et al.* 2011 [224]
YWO 1528	*prc1Δ hrd1Δ* *doa10Δ*	*MAT α* *ura3-1 his3-11,15 leu2-3,112 trp1-1ade2-1ocre can1-100* *prc1Δ::LEU2 hrd1Δ::HIS doa10Δ::kanMX*	Stolz *et al.* 2013 [159]
YWO 1529	*prc1-1 hrd1Δ*	*MAT α* *ura3-1 his3-11,15 leu2-3,112 trp1-1ade2-1ocre can1-100* *prc1-1 hrd1Δ::HIS*	provided by Alexandra Stolz
YWO 1644	*prc1Δ der1Δ*	*MAT α* *ura3-1 his3-11,15 leu2-3,112 trp1-1ade2-1ocre can1-100* *prc1Δ::LEU2 der1Δ::His5+*	provided by Stefanie Besser [232]
YWO 1711	*prc1Δ cdc48^{ts}*	*MAT α* *ura3-1 his3-11,15 leu2-3,112 trp1-1ade2-1ocre can1-100* *prc1Δ::LEU2 cdc48^{T413R}*	provided by Stefanie Besser [232]
YWO 1774	*prc1-1 ubc1Δ*	*MAT α* *ura3-1 his3-11,15 leu2-3,112 trp1-1ade2-1ocre can1-100* *prc1-1 ubc1Δ::HIS3*	Friedlander *et al.* 2000 [154]
YWO 1775	*prc1-1 ubc7Δ*	*MAT α* *ura3-1 his3-11,15 leu2-3,112 trp1-1ade2-1ocre can1-100* *prc1-1 ubc7Δ::LEU2*	Friedlander *et al.* 2000 [154]
YWO 2093	*prc1Δ der1Δ* *dfm1Δ*	*MAT α* *ura3-1 his3-11,15 leu2-3,112 trp1-1ade2-1ocre can1-100* *prc1Δ::loxP der1Δ::LEU2 dfm1Δ::His3MX6*	This work
YWO 2103	*prc1Δ dfm1Δ*	*MAT α* *ura3-1 his3-11,15 leu2-3,112 trp1-1ade2-1ocre can1-100*	This work

		prc1Δ::URA3 dfm1Δ::His3MX6	
YWO 2106	*prc1Δ dfm1Δ*	*MAT α* *ura3-1 his3-11,15 leu2-3,112 trp1-1ade2-1ocre can1-100* *prc1Δ::loxP dfm1Δ::His3MX6*	This work
YWO 2145	*prc1Δ asi1Δ*	*MAT α* *ura3-1 his3-11,15 leu2-3,112 trp1-1ade2-1ocre can1-100* *prc1Δ::LEU2 asi1Δ::URA3*	This work
YWO 2146	*prc1Δ hrd1Δ asi1Δ*	*MAT α* *ura3-1 his3-11,15 leu2-3,112 trp1-1ade2-1ocre can1-100* *prc1Δ::LEU2 hrd1Δ::HIS asi1Δ::URA3*	This work
YWO 2147	*prc1Δ ubc7Δ*	*MAT α* *ura3-1 his3-11,15 leu2-3,112 trp1-1ade2-1ocre can1-100* *prc1Δ::LEU2 ubc7Δ::His5+*	This work
YWO 2150	*prc1Δ doa10Δ ubc7Δ*	*MAT α* *ura3-1 his3-11,15 leu2-3,112 trp1-1ade2-1ocre can1-100* *prc1Δ::LEU2 doa10Δ::kanMX* *ubc7Δ::His5+*	This work
YWO 2151	*prc1Δ asi3Δ*	*MAT α* *ura3-1 his3-11,15 leu2-3,112 trp1-1ade2-1ocre can1-100* *prc1Δ::LEU2 asi3Δ::URA3*	This work
YWO 2153	*prc1Δ hrd1Δ asi3Δ*	*MAT α* *ura3-1 his3-11,15 leu2-3,112 trp1-1ade2-1ocre can1-100* *prc1Δ::LEU2 hrd1Δ::HIS3 asi3Δ::URA3*	This work
YWO 2154	*prc1Δ doa10Δ ubc6Δ*	*MAT α* *ura3-1 his3-11,15 leu2-3,112 trp1-1ade2-1ocre can1-100* *prc1Δ::LEU2 doa10Δ::kanMX* *ubc6Δ::His5+*	This work
YWO 2156	*prc1Δ asi1Δ*	*MAT α* *ura3-1 his3-11,15 leu2-3,112 trp1-1ade2-1ocre can1-100* *prc1Δ::LEU2 asi1Δ::loxP*	This work
YWO 2157	*prc1Δ asi3Δ*	*MAT α* *ura3-1 his3-11,15 leu2-3,112 trp1-1ade2-1ocre can1-100* *prc1Δ::LEU2 asi3Δ::loxP*	This work
YWO 2159	*prc1Δ hrd1Δ asi3Δ*	*MAT α* *ura3-1 his3-11,15 leu2-3,112 trp1-1ade2-1ocre can1-100* *prc1Δ::LEU2 hrd1Δ::HIS3 asi3Δ::loxP*	This work
YWO 2160	*prc1Δ ubc6Δ*	*MAT α* *ura3-1 his3-11,15 leu2-3,112 trp1-1ade2-1ocre can1-100* *prc1Δ::LEU2 ubc6Δ::His5+*	This work
YWO 2163	*prc1Δ hrd1Δ asi1Δ*	*MAT α* *ura3-1 his3-11,15 leu2-3,112 trp1-1ade2-1ocre can1-100* *prc1Δ::LEU2 hrd1Δ::HIS asi1Δ::loxP*	This work

2.2.5 Oligonucleotides

Table 9: List of all oligonucleotides used in this work.
Letters, which are underlined, indicate alterations to the template DNA sequence. Capital letter represent the template DNA sequence.

Name	Sequence 5' -> 3'	Reference
Asi1delfor	CTGGGTTTTTTTCTTCTTTTTACAAAGAAACTATGCTAAGA ATCAGCTGAAGCTTCGTACGC	Microsynth AG; Balgach; Switzerland
Asi1delrev	CCAAACGAAAAACCTCTTTTAGATACCATGCAAAAGTTCTT AAACTAGCATAGGCCACTAGTGGATCTG	Microsynth AG; Balgach; Switzerland
Asi3delfor	GTCAGGAACAGTCATTACGTAGGGATTTTCAAAAGTTTGA CTGCAGCTGAAGCTTCGTACGC	Microsynth AG; Balgach; Switzerland
Asi3delrev	CCTATGATGTCTTAAATACGTATACCTAATAAAATAATTGC ATAGGCCACTAGTGGATCTG	Microsynth AG; Balgach; Switzerland
CPYTERfor	GTGTGTGAATTCAGCGTGTATGTGTAGGC	Eurofins; Luxembourg
CPYTERrev	ACACACACTAGTGAATTTAGTTCTTCCTCCCC	Eurofins; Luxembourg
CT for	TGACTGAAGCTTTTCCGTATATGATGATACATATGTTAGG	Eurofins; Luxembourg
CT rev	GACTGAAAGCTTTTATTTCTTGGAGAGTTTACCGT	Eurofins; Luxembourg
delUBC6for	CCGCATTCGCAAATTGCAAACAAAGTACGTACAATAGTAC AGCTGAAGCTTCGTACGC	Microsynth AG; Balgach; Switzerland
delUBC6rev	CTGTGTTGTCAAAATTTATCTAAAGTTTAGTTCATTTAATGG CTGCATAGGCCACTAGTGGATCTG	Microsynth AG; Balgach; Switzerland
delUBC7for	CTAAAAGGAACTTCCCTAGTAATAGTGTAATTTGGAAGGG CATAGCCAGCTGAAGCTTCGTACGC	Microsynth AG; Balgach; Switzerland
delUBC7rev	CAGTTAAAAGGAAGACCAAATGATCATTAACCTGCTACCT GCTTGCATAGGCCACTAGTGGATCTG	Microsynth AG; Balgach; Switzerland
DER1delfor	CAGAGATTTCGTCACCAACAGAAGAAAAGCTAAAGCCCAA	Eurofins;

	GCAATCAGCTGAAGCTTCGTACGC	Luxembourg
DER1delrev	TTCACTTTTGTTATTGGTTTTTGGTAAATAAAAACGGCCTTTCCTGCATAGGCCACTAGTGGATCTG	Eurofins; Luxembourg
eGFPfor	GAGAGATTAATTAAAAGTAAAGGAGAAGAACTTTTCACTGGAGTT	Eurofins; Luxembourg
eGFPrev	TCTCTCGCTAGCTTACAATTCGTCGTGTTTGTATAGTTCATCCAT	Eurofins; Luxembourg
MutCPY	CAAGGGCCAAGATTTCCACATCGCTGGGGAATCCTACGCCGGCCATTACATC	Microsynth AG; Balgach; Switzerland
MutCT1	5'PHO-CTTTTTCTACTGGTTAGCAAGAGTGCCTTAAAAGCTTTCAGTCGATATCGAATTC	Microsynth AG; Balgach; Switzerland
MutCT3	CTACTGGTTAGCAAGAGTGCCTGCAGCGAACGGTGCACTCTCCGCGGCATAAAAGCTTTCAGTCGATAT	Eurofins; Luxembourg
MutCT4	CTACTGGTTAGCAAGAGTGCCTGCAGCGAACGGTGCACTCGCCGCGGCATAAAAGCTTTCAGTCGATAT	Eurofins; Luxembourg
MutCT5	CTGGTTAGCAAGAGTGCCTAAATAAAAGCTTTCAGTCGATATC	Eurofins; Luxembourg
MutCT6	GTTAGCAAGAGTGCCTGCATAAAAGCTTTCAGTCGATATC	Eurofins; Luxembourg
MutCT7	GTTAGCAAGAGTGCCTGCAGCGAACGGTAAATAAAAGCTTTCAGTCGATATCGAATTCCTG	Eurofins; Luxembourg
MutCT11	5'PHO-GTATCTTCATCTGTTATATTGCATTCAATAAAATCGCTGGTGTCTTTTTCTACTGGTTAG	Microsynth AG; Balgach; Switzerland
MutCT12	CTTTCTACAGTGAGAGATGGAGAAATAAAGGTATCTTCATCTGTTATATTGCATTCA	Microsynth AG; Balgach; Switzerland
MutCT13	GAGAAATTATGGTATCTTCATCTGTAAAATTGCATTCAATTATATCGCTGGTGTC	Microsynth AG; Balgach; Switzerland
MutCT14	ATCGCTGGTGTCTTTTTCAAATGGTTAGCAAGAGTGCCTTAAAAG	Microsynth AG; Balgach; Switzerland
MutCT15	CTTTCTACAGTGAGAGATGGAGAAATTCTGGTATCTTCATCTGTTATATTGCATTCA	Microsynth AG; Balgach; Switzerland
MutCT16	ATCGCTGGTGTCTTTTTCTCTTGGTTAGCAAGAGTGCCTTA	Microsynth AG;

	AAAG	Balgach; Switzerland
MutCT17	GTATCTTCATCTGTTATATTGCATTCAATTCTATCGCTGGTGTCTTTTTCTACTGGTTAG	Microsynth AG; Balgach; Switzerland
MutCT18	GAGAAATTATGGTATCTTCATCTGTTCTATTGCATTCAATTATATCGCTGGTGTC	Microsynth AG; Balgach; Switzerland
MutCT29	CTGACACCTGTAGTTTCTGTCAAATAAAAACAACCAATGATTACTTAGCTAATG	Microsynth AG; Balgach; Switzerland
MutCT30	CTTAGCTAATGTCAATTCTTTCTACAAAGAGAGATGGAGAAATTATGGTATC	Microsynth AG; Balgach; Switzerland
MutCT33	CTGGTTAGCAAGAGTGCCTTCTTAAAAGCTTTCAGTCGATATC	Microsynth AG; Balgach; Switzerland
MutCT34	CTACTGGTTAGCAAGAGTGCCTTCTGCATAAAACTTTCAGTCGATATCGAATTCAGCGTG	Microsynth AG; Balgach; Switzerland
MutCT35	AGTGCCTAAAAAGAACGGTAAACTCAAAAAGAAATAAAAGCTTGATATCGAAT	Microsynth AG; Balgach; Switzerland
MutCT36	AGTGCCTAAAAAGAACGGTAAACTCGCAAAGAAATAAAAGCTTGATATCGAAT	Microsynth AG; Balgach; Switzerland
MutCT41	CCTTACTCGAGGATGAAAATGCCACTTATCCATATGATGTTCCAGATTATGCTGACACCTGTAGTTTCTGTCAAATA	Microsynth AG; Balgach; Switzerland
MutCT42	CGAGGATGAAAATGCCACTGGTAAACCAATTCCAAATCCATTGTTGGGTTTGGATTCAACTGACACCTGTAGTTTCTGTC	Microsynth AG; Balgach; Switzerland
MutCTLHA	CGAAGAAGTTAAGAAAATCCTTGCTTATCCATATGATGTTCCAGATTATGCTTAAAAAGATTCTCTTTTTTTATGATAT	Microsynth AG; Balgach; Switzerland
Mutfast	5'PHO-CATGGCATGGATGAACTATACAAATAAGCTAGCGGCGCGCCACTTCTAAATAAG	Eurofins; Luxembourg
MutLys	5'PHO-	Eurofins;

	GTAAACTCTCCAAGAAATTAATTAAAAGTAAAGGAGAAGAACTTTTCACTG	Luxembourg
MutWSC1	TCAATTCTTTCTACAGTGAGAGATGGAGAATTGTAGGCGGCGTTGTAGGTTATATTGCATTCAATTATATCGCTGGTGTC	Microsynth AG; Balgach; Switzerland
MutWSC2	GAGATGGAGAATTGTAGGCGGCGTTGTAGGTGGTGTAGTGGGAGCCGTAGCCGGTGTCTTTTTCTACTGGTTAGCA	Microsynth AG; Balgach; Switzerland
MutWSC3	TAGGTGGTGTAGTGGGAGCCGTAGCCATTGCTCTTTGTATCTTGTTGAGAGTGCCTAAAAAGAACGGTAAAC	Microsynth AG; Balgach; Switzerland
MutWSC5	CTCTTTGTATCTTGTTGAGAGTGCCTAAATAAAAGCTTGATATCGAATTCAGC	Microsynth AG; Balgach; Switzerland
MutWSC6	CTCTTTGTATCTTGTTGAGAGTGCCTGCATAAAAGCTTGATATCGAATTCAGC	Microsynth AG; Balgach; Switzerland
MutWSC7	CTCTTTGTATCTTGTTGAGAGTGCCTTCTTAAAAGCTTGATATCGAATTCAGC	Microsynth AG; Balgach; Switzerland
PRC1delfor	CTAGAGATTGTTTCTTTTCTACTCAACTTAAAGTATACATACGCTCAGCTGAAGCTTCGTACGC	Eurofins; Luxembourg
PRC1delrev	CGATCGTAGCTGATAATAAAAACGGTATGCCTACACATACACGCTGCATAGGCCACTAGTGGATCTG	Eurofins; Luxembourg Eurofins; Luxembourg
TDH3forNheI	TATATAGCTAGCGGCGCGCCACTTCTAAATAAGC	Eurofins; Luxembourg
TDH3revEcoRI	TCTCTCGAATTCGCTCGTTTAAACTGGATGGCGG	Eurofins; Luxembourg
TRPmutHindIII	5'PHO-GGTTGGAAGGCAAGAGAGCCCCGAAAGTTTACATTTTATGTTAGCTGGTGGACTGACGC	Eurofins; Luxembourg

2.2.6 Plasmids

Table 10: List of all plasmids used in this work.

Plasmids used for cloning are indicated in grey. Plasmids used for experiments are highlighted in black. Promoters are indicated with P, terminators with T, respectively.

Name	Insert designation	Description/Genotype	Backbone	Reference
pBM8	C*T_{Pdr5}(CS)Leu2	[P_{PRC1} – C*T_{Pdr5}(CS)LEU2]	pRS316	Medicherla *et al.* 2004 [197]
pCT67	C*T_{Pdr5}(CS)	[P_{TDH3}::*prc1-1*::$pdr5_{4332-4532}$]	pRS316	Taxis *et al.* 2003 [196]
pMA1	C*T_{Pdr5}(CS)GFP^{K604N}	[P_{TDH3}::*prc1-1*::$pdr5_{4332-4532}$::*GFP*]	pRS316	Taxis *et al.* 2003 [196]
pRS314			pRS314	Sikorski & Hieter 1989 [236]
pRS316			pRS316	Sikorski & Hieter 1989 [236]
pRS424			pRS424	Sikorski & Hieter 1989 [236]
pSH63		*GAL1-cre, TRP1*		Gueldener et al. 2002 [237]
pSK007	C*T_{Pdr5}(CS)$Leu2^{myc}$	[P_{GAL4} – C*T_{Pdr5}(CS)$LEU2^{myc}$]	pRS316	Kohlmann *et al.* 2008 [194]
pUG27		*loxP-His5+-loxP*		Gueldener et al. 2002 [237]
pUG72		*loxP-URA3-loxP*		Gueldener et al. 2002 [237]
pUG73		*loxP-LEU2-loxP*		Gueldener et al. 2002 [237]
pWO1265		[P_{CUP1} – His_6-UB – T_{CYC1}]]	YEplac195	Diploma Thesis Derrick Norell [238]
pWO1414	C*T_{Pdr5}(CS)	[P_{PRC1} – C*T_{Pdr5}(CS)]	pRS316	This work
pWO1456	C*T_{Pdr5}(CS)$GFP_{fast;HDEL}$	[P_{PRC1} – C*T_{Pdr5}(CS)$GFP_{fast;HDEL}$ –T_{TDH3}]	pRS316	This work
pWO1476	C*T_{Pdr5}(CS)GFP	[P_{PRC1} – C*T_{Pdr5}(CS)GFP]	pRS316	This work
pWO1477	C*T_{Pdr5}(CS)GFP_{fast}	[P_{PRC1} –	pRS316	This work

		C^*T_{Pdr5}(CS)GFP_{fast} – T_{TDH3}]		
pWO1479	pRS424$^{-hindII}$	HindIII restriction site within the auxotrophy marker is mutated: 5'-AAGTTT-3'	pRS424	This work
pWO1481	His_6-Ub	[P_{CUP} – His_6-Ub]	pRS424$^{-hindIII}$	This work
pWO1486	$C^*T_{Pdr5}(CS^{K->A})$	[P_{PRC1}– $C^*T_{Pdr5}(CS^{K->A})$]	pRS316	This work
pWO1487	C^*T_{Pdr5}(ΔCS)AANGK	[P_{PRC1} – C^*T_{Pdr5}(ΔCS)AANGK)]	pRS316	This work
pWO1496	C^*T_{Pdr5}(CS)	[P_{PRC1} – C^*T_{Pdr5}(CS) – T_{PRC1}]	pRS316	This work
pWO1497	$C^*T_{Pdr5}(CS^{K/S->A})$	[P_{PRC1} – $C^*T_{Pdr5}(CS^{K/S->A})$]	pRS316	This work
pWO1499	$C^*T_{Pdr5}(CS^{K->A})$	[P_{PRC1} – $C^*T_{Pdr5}(CS^{K->A})$ – T_{PRC1}]	pRS316	This work
pWO1500	C^*T_{Pdr5}(ΔCS)AANGK	[P_{PRC1} – C^*T_{Pdr5}(ΔCS)AANGK) – T_{PRC1}]	pRS316	This work
pWO1502	$C^*T_{Pdr5}(CS^{K/S->A})$	[P_{PRC1} – $C^*T_{Pdr5}(CS^{K/S->A})$ – T_{PRC1}]	pRS316	This work
pWO1503	C^*T_{Pdr5}(ΔCS)K	[P_{PRC1} – C^*T_{Pdr5}(ΔCS)K – T_{PRC1}]	pRS316	This work
pWO1504	C^*T_{Pdr5}(ΔCS)A	[P_{PRC1} – C^*T_{Pdr5}(ΔCS)A – T_{PRC1}]	pRS316	This work
pWO1507	C^*T_{Pdr5}(ΔCS)	[P_{PRC1} – C^*T_{Pdr5}(ΔCS) – T_{PRC1}]	pRS316	This work
pWO1512	$C^*T_{Pdr5}^{Y1\rightarrow K}$(ΔCS)	[P_{PRC1} –	pRS316	This work

		$C^{*}T_{Pdr5}^{Y1\rightarrow K}(\Delta CS)$– $\top_{PRC1}$]		
pWO1513	$C^{*}T_{Pdr5}^{Y2\rightarrow K}(\Delta CS)$	[P_{PRC1} – $C^{*}T_{Pdr5}^{Y2\rightarrow K}(\Delta CS)$– $\top_{PRC1}$]	pRS316	This work
pWO1514	$C^{*}T_{Pdr5}^{Y3\rightarrow K}(\Delta CS)$	[P_{PRC1} – $C^{*}T_{Pdr5}^{Y3\rightarrow K}(\Delta CS)$– $\top_{PRC1}$]	pRS316	This work
pWO1515	$C^{*}T_{Pdr5}^{Y4\rightarrow K}(\Delta CS)$	[P_{PRC1} – $C^{*}T_{Pdr5}^{Y4\rightarrow K}(\Delta CS)$– $\top_{PRC1}$]	pRS316	This work
pWO1516	$C^{*}T_{Pdr5}^{Y1\rightarrow S}(\Delta CS)$	[P_{PRC1} – $C^{*}T_{Pdr5}^{Y1\rightarrow S}(\Delta CS)$– $\top_{PRC1}$]	pRS316	This work
pWO1517	$C^{*}T_{Pdr5}^{Y2\rightarrow S}(\Delta CS)$	[P_{PRC1} – $C^{*}T_{Pdr5}^{Y2\rightarrow S}(\Delta CS)$– $\top_{PRC1}$]	pRS316	This work
pWO1518	$C^{*}T_{Pdr5}^{Y3\rightarrow S}(\Delta CS)$	[P_{PRC1} – $C^{*}T_{Pdr5}^{Y3\rightarrow S}(\Delta CS)$– $\top_{PRC1}$]	pRS316	This work
pWO1519	$C^{*}T_{Pdr5}^{Y4\rightarrow S}(\Delta CS)$	[P_{PRC1} – $C^{*}T_{Pdr5}^{Y4\rightarrow S}(\Delta CS)$– $\top_{PRC1}$]	pRS316	This work
pWO1520	$C^{*}T_{Wsc1\Delta\Delta}(CS)$	[P_{PRC1} – $C^{*}T_{Wsc1\Delta\Delta}(CS)$ – $\top_{PRC1}$]	pRS316	This work
pWO1521	$C^{*}T_{Wsc1\Delta}(CS)$	[P_{PRC1} – $C^{*}T_{Wsc1\Delta}(CS)$ – $\top_{PRC1}$]	pRS316	This work
pWO1522	$C^{*}T_{Wsc1}(CS)$	[P_{PRC1} – $C^{*}T_{Wsc1}(CS)$ – $\top_{PRC1}$]	pRS316	This work
pWO1523	$C^{*}T_{Pdr5}(\Delta CS)S$	[P_{PRC1} – $C^{*}T_{Pdr5}(\Delta CS)S$ – $\top_{PRC1}$]	pRS316	This work
pWO1524	$C^{*S548K}T_{Pdr5}(\Delta CS)$	[P_{PRC1} – $C^{*S548K}T_{Pdr5}(\Delta CS)$ – $\top_{PRC1}$]	pRS316	This work

pWO1526	C*^{S562K}T$_{Pdr5}$(ΔCS)	[P$_{PRC1}$ – C*^{S562K}T$_{Pdr5}$(ΔCS) – T$_{PRC1}$]	pRS316	This work
pWO1528	C*T$_{Pdr5}$(CS)Leu2^{HA}	[P$_{PRC1}$ – C*T$_{Pdr5}$(CS)LEU2^{HA}]	pRS316	This work
pWO1529	C*T$_{Pdr5}$(CS)Leu2^{myc}	[P$_{PRC1}$ – C*T$_{Pdr5}$(CS)LEU2^{myc}]	pRS316	This work
pWO1534	C*T$_{Wsc1}$(ΔCS)	[P$_{PRC1}$ – C*T$_{Wsc1}$(ΔCS) – T$_{PRC1}$]	pRS316	In collaboration with Dorothea Mandlmeir [239]
pWO1538	C*T$_{Pdr5}$(ΔCS)SA	[P$_{PRC1}$ – C*T$_{Pdr5}$(ΔCS)SA – T$_{PRC1}$]	pRS316	This work
pWO1551	C*T$_{Pdr5}$(CS$^{S->K}$)	[P$_{PRC1}$ – C*T$_{Pdr5}$(CS $^{S->K}$) – T$_{PRC1}$]	pRS316	This work
pWO1552	C*T$_{Pdr5}$(CS$^{S->A}$)	[P$_{PRC1}$ – C*T$_{Pdr5}$(CS $^{S->A}$) – T$_{PRC1}$]	pRS316	This work
pWO1553	C*T$_{Wsc1}$(ΔCS)A	[P$_{PRC1}$ – C*T$_{Wsc1}$(ΔCS)A – T$_{PRC1}$]	pRS316	This work
pWO1554	C*T$_{Wsc1}$(ΔCS)S	[P$_{PRC1}$ – C*T$_{Wsc1}$(ΔCS)S – T$_{PRC1}$]	pRS316	This work
pWO1555	C*T$_{Wsc1}$(ΔCS)K	[P$_{PRC1}$ – C*T$_{Wsc1}$(ΔCS)K – T$_{PRC1}$]	pRS316	This work
pWO1591	C*^{HA}T$_{Pdr5}$(ΔCS)	[P$_{PRC1}$ – C*^{HA}T$_{Pdr5}$(ΔCS) – T$_{PRC1}$]	pRS316	This work
pWO1593	C*^{HA}T$_{Wsc1}$(ΔCS)	[P$_{PRC1}$ – C*^{HA}T$_{Wsc1}$(ΔCS) – T$_{PRC1}$]	pRS316	This work
pWO1595	C*^{HA}T$_{Wsc1}$(ΔCS)	[P$_{PRC1}$ – C*^{HA}T$_{Wsc1}$(ΔCS) – T$_{PRC1}$]	pRS314	This work

pWO1596	$C^{*HA}T_{Pdr5}(\Delta CS)$	$[P_{PRC1} - C^{*HA}T_{Pdr5}(\Delta CS) - T_{PRC1}]$	pRS314	This work
pWO1602	$C^{*V5}T_{Pdr5}(\Delta CS)$	$[P_{PRC1} - C^{*V5}T_{Pdr5}(\Delta CS) - T_{PRC1}]$	pRS316	This work
pWO1603	$C^{*V5}T_{Wsc1}(\Delta CS)$	$[P_{PRC1} - C^{*V5}T_{Wsc1}(\Delta CS) - T_{PRC1}]$	pRS316	This work
pWO1604	$CT_{Pdr5}(CS)$	$[P_{PRC1} - CT_{Pdr5}(CS) - T_{PRC1}]$	pRS316	This work
pWO1605	$CT_{Pdr5}(CS^{K->A})$	$[P_{PRC1} - CT_{Pdr5}(CS^{K->A}) - T_{PRC1}]$	pRS316	This work
pWO1606	$CT_{Pdr5}(\Delta CS)$	$[P_{PRC1} - CT_{Pdr5}(\Delta CS) - T_{PRC1}]$	pRS316	This work
pWO1607	$CT_{Wsc1}(\Delta CS)A$	$[P_{PRC1} - CT_{Wsc1}(\Delta CS)A - T_{PRC1}]$	pRS316	This work
pWO1608	$CT_{Wsc1}(\Delta CS)S$	$[P_{PRC1} - CT_{Wsc1}(\Delta CS)S - T_{PRC1}]$	pRS316	This work
pWO1609	$CT_{Wsc1}(\Delta CS)K$	$[P_{PRC1} - CT_{Wsc1}(\Delta CS)K - T_{PRC1}]$	pRS316	This work
pWO1610	$CT_{Pdr5}(CS^{K/S->A})$	$[P_{PRC1} - CT_{Pdr5}(CS^{K/S->A}) - T_{PRC1}]$	pRS316	This work
pWX204	ER-GFP_{fast}	$[P_{TDH3} - kar23.2\text{-}GFP_{fast} - T_{Actin}]$	pRS316	Xu *et al.* 2013 [27]

2.3 Cell culture and cell-biological methods

Ideal supply of nutrients and optimal growth conditions were achieved, using flasks with a volume, which is five times larger than the volume of the culture. Flasks, containing liquid cultures, were incubated in a shaker at 200 rpm.

2.3.1 Growth conditions for *E. coli* cultures

Liquid as well as solid *E. coli* cultures were incubated at 37°C and shaking at 200 rpm for 16 hours.

2.3.2 Measurement of cell growth

To monitor the growth of yeast cells, photometric measurement at 600 nm (OD_{600}) was applied. Yeast cells growing in logarithmic growth phase have an OD_{600} value in range between 0.7 ad 2.0. An OD_{600} value of 1.0 corresponds to a cell density of 2×10^7 cells per ml. As reference the appropriate media was used. Cultures were diluted 1:10 with the appropriate media prior to the measurement.

2.3.3 Growth conditions for *S. cerevisiae* cultures

Yeast 5 ml precultures were inoculated with single colonies derived from agar plates and grown in a shaker at 200 rpm at 30°C for 18-20 hours. Main cultures, volume depended on the kind of experiment, were inoculated by diluting the precultures. Main cultures were grown in a shaker at 200 rpm at 30°C for 18-20 hours, until the growth of corresponding cells reached the logarithmic growth phase.

2.3.4 Glycerol stocks of *E. coli* and *S. cerevisiae* cells

Long-time storage of yeast strains:

First, a single yeast colony was spread on a new agarose plate and grown at 30°C overnight. Then, all cells were transferred into 15% (w/v) glycerol and immediately frozen and stored at -80°C.

Long-time storage of *E. coli* cultures:

Liquid media was inoculated with a single *E. coli* colony and incubated at 37°C for 16 hours. Then, equal amounts of culture and 60% glycerol were mixed, immediately frozen and stored at -80°C.

2.3.5 Fluorescence microscopy

Live cell imaging was performed using LSM 710 Zeiss confocal microscope equipped with a Plan-Apochromat 63x/1.40 Oil DIC M27 objective and a XL-LSM 710 S1 incubation chamber for temperature and CO_2 control. For microscopy, yeast cells in logarithmic growth phase were used.

2.4 Molecular biological methods

2.4.1 Isolation of genomic DNA from *S. cerevisiae*

Breaking buffer:

2% (v/v)	Triton X-100
1% (w/v)	SDS
100 mM	NaCl
10 mM	Tris-HCl pH 8.0
1 mM	EDTA pH 8.0

Precultures were prepared as described in chapter 2.3.3. All cells were harvested and transferred in a safe-lock reaction tube. The cell pellet was resuspended in 200 µl of breaking buffer. 300 µl of glass beads (∅ 0.25 – 0.5 mm) and 200 µl of phenol/chloroform were added followed by 4 rounds of each 1 min vortexing and 1 min resting on ice. After centrifugation at V_{max} in a table centrifuge for 10 min, the supernatant was transferred to a new safe-lock reaction tube. 100 µl of phenol/chlorophorm was added, the suspension was vortexed for 30 sec and again centrifugated at V_{max} for 10 min. In order to precipitate the nucleic acids, the supernatant fraction was transferred to a reaction tube containing ice-cold 100% EtOH the mixture was incubated at -80°C for 20 minutes. Afterwards, the EtOH was removed (V_{max} at 4°C for 10 min) and nucleic acids were dried at RT. The pellet was rehydrated in 400 µl of ddH_2O, containing 3 µl of RNase (10 mg/ml) and incubated at 37°C for 10 minutes. RNA digestion was stopped with 10 µl of NH_4Ac (5 M) and 1 ml of EtOH. DNA was precipitated at -80°C for 15 minutes. EtOH was removed (V_{max} at 4°C for 10 min) and the pellet, containing DNA, was washed once with 1 ml of 70% EtOH (V_{max} at 4°C for 10 min). Subsequently, the pellet was dried at RT and finally the DNA was rehydrated in 40 µl of ddH_2O. The DNA was directly used for downstream experiments or stored at -20°C.

2.4.2 DNA precipitation

Prior to DNA precipitation, the volume of the DNA-containing solution was determined. Then, three times of the sample volume of ice-cold EtOH and 1/10th of the sample volume of a 3 M NaOAc were added to the sample and carefully mixed. DNA was precipitated at -80°C for 20 minutes. EtOH was removed (V_{max} at 4°C for 15 min) and the pellet, containing DNA, was washed once with 1 ml of 70% EtOH (V_{max} at 4°C for 10 min). The pellet, containing DNA, was dried at RT and finally the DNA was rehydrated in the appropriate amount of ddH_2O. The DNA was directly used for downstream experiments or stored at -20°C.

2.4.3 Isolation of plasmid DNA from *E. coli*

For the isolation of plasmid DNA the NucleoSpin® Plasmid Kit (MACHAREY-NAGEL) was used. Plasmid DNA was isolated from *E. coli* cells according to the instructions recommended in the manual of the manufacturer.
Isolated plasmid DNA was checked by digestion with appropriate restriction enzymes and finally sequenced.

2.4.4 5'- Phosphorylation of oligonucleotides

5' Phosphorylation of oligonucleotides was catalyzed by the T4 polynucleotide kinase. The PCR primer used for mutagenesis PCR (chapter 2.4.5) was 5'-phosphorylated before, using the T4 PNK (New England BioLabs®) according to the instructions recommended in the manual of the manufacturer.

2.4.5 Polymerase chain reaction

Exponential amplification of DNA fragments was performed with polymerase chain reaction (PCR).
After initial DNA denaturation, a temperature program was running for 30 – 40 cycles. Each cycle consisted of DNA denaturation, primer annealing and elongation. Finally, a last elongation step was performed. Temperature of primer annealing was specific

for the pair of primers. Denaturation temperature was dependent on the template DNA and elongation temperature was dependent on the polymerase. Elongation time was dependent on the length of the DNA fragment to be amplified.
In this work all PCR's were performed, using the Phusion High Fidelity DNA polymerase (Thermo Fisher Scientific).

The PCR program, as recommended in the manual of the manufacturer, was optimized individually for different applications:

Standard DNA fragment amplification

PCR-mix:

32.5 µl	ddH_2O
1 µl	Template DNA (~ 50 ng/µl)
2.5 µl	Primer forward (10 µM)
2.5 µl	Primer reverse (10 µM)
10 µl	5 × HF buffer
1 µl	dNTP mix (10 mM)
0.5 µl	Phusion High Fidelity DNA Polymerase

PCR-program:

	Temperature [°C]	Time	
Initial denaturation	98	30 sec	
Denaturation	98	8 sec	
Annealing	Specific for pair of primer	20 sec	× 40
Elongation	72	30 sec/kb	
Final elongation	72	7 min	

Amplification of disruption cassettes

PCR-mix:

135 µl	ddH_2O
1 µl	DMSO
8 µl	Template DNA (~ 50 ng/µl)
5 µl	Primer forward (10 µM)
5 µl	Primer reverse (10 µM)
40 µl	5 × HF buffer
4 µl	dNTP mix (10 mM)
2 µl	Phusion High Fidelity DNA Polymerase

PCR-program:

	Temperature [°C]	Time	
Initial denaturation	98	2 min	
Denaturation	98	10 sec	× 35
Annealing	Specific for pair of primer	30 sec	
Elongation	72	30 sec/kb	
Final elongation	72	5 min	

Colony PCR – Screen for positive plasmids after cloning

PCR-mix:

16.25 µl	ddH_2O
0.5 µl	single *E. coli* colony resuspended in 10 µl ddH_2O
1.25 µl	Primer forward (10 µM)
1.25 µl	Primer reverse (10 µM)
5 µl	5 × HF buffer
0.5 µl	dNTP mix (10 mM)
0.25 µl	Phusion High Fidelity DNA Polymerase

PCR-program:

	Temperature [°C]	Time
Initial denaturation	98	30 sec
Denaturation	98	8 sec
Annealing	Specific for pair of primer	20 sec
Elongation	72	30 sec/kb
Final elongation	72	7 min

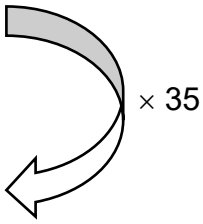

In order to check whether the PCR generated the correct amplicon, agarose gel electrophoresis was performed (for more details see chapter 2.4.6).

Mutagenesis - PCR – Insertion, deletion or exchange of nucleotides within DNA fragments

In the mutagenesis PCR circular DNA to be modified served as template DNA. The additional heat-stable DNA ligase in the PCR mixture mediated the recircularization of the newly synthesized linear DNA strand containing the desired modifications, which were determined by the 5'-phosphorylated primer.

Mutagenesis-mix:

23.5 µl	ddH_2O
1 µl	Template DNA (~ 50 ng/µl)
1 µl	Primer (10 µM, 5'-phosphorylated)
10 µl	NAD^+ (5 mM)
10 µl	5 × HF buffer
2.5 µl	dNTP mix (10 mM)
1 µl	Phusion High Fidelity DNA Polymerase
1 µl	*Taq* DNA Ligase

PCR-program:

	Temperature [°C]	Time
Initial denaturation	95	1 min
Denaturation	95	1 min
Annealing	55	1 min
Elongation	65	4 min

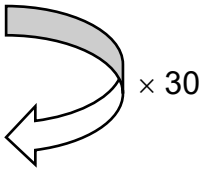

Subsequent restriction digestion of template DNA with DpnI (New England BioLabs®), followed by DNA purification with the NucleoSpin® Gel and PCR clean-up Kit (MACHAREY-NAGEL), guaranteed that only newly generated DNA, containing the desired modifications, was introduced into *E. coli* cells via transformation.

2.4.6 Agarose gel electrophoresis

1 × TAE buffer:

40 mM	Tris
20 mM	Acetic acid
1 mM	EDTA pH 8.0

6 × Loading buffer:

40 mM	Tris
20 mM	Acetic acid
1 mM	EDTA pH 8.0
30% (v/v)	Glycerol
0.25% (w/v)	Bromophenol blue

Agarose gel electrophoresis is a method to separate charged biomolecules like DNA in an agarose matrix. DNA is separated by applying an electric field to move the negatively charged DNA fragments to the anode. Migration of DNA through the pores of the agarose matrix is size dependent. Small DNA molecules migrate faster than larger ones.

Prior to loading of the DNA samples on the agarose gels, the samples were mixed with 1 × loading buffer. 1 × TAE buffer was used for preparation of the agarose gels and served as running buffer. As DNA migration standard, a 1 kbp DNA-ladder (Carl Roth) was used. DNA-staining was achieved by using the fluorescent nucleic acid dye GelRed® (Genaxxon). The electrophoresis was run at constant voltage (120 V) for 1 hour in a Mini-Sub Cell GT System or Wide Mini-Sub Cell GT System (Bio-RAD). The separated DNA molecules were visualized using the Quantum ST5 gel documentation system with a 16-bit USB2 camera with 2.0/7.6 megapixel Sony ICX-CCD sensor (Vilber Lourmat).

2.4.7 Extraction of DNA molecules from agarose gels

For the extraction of DNA molecules from agarose gels the NucleoSpin® Gel and PCR clean-up Kit (MACHAREY-NAGEL) was used. DNA molecules were isolated according to the instructions recommended in the manual of the manufacturer.
Isolated DNA was used for cloning.

2.4.8 Restriction digest of plasmid DNA

All restriction enzymes, used in this work, were ordered from New England BioLabs® and are listed in Table 5. Digestion of plasmid DNA used for cloning was performed according to the instructions recommended in the manual of the manufacturer.

2.4.9 Ligation of DNA fragments

To prevent self-ligation of the digested plasmid DNA used for cloning, the DNA fragments were dephosphorylated at their 5’ termini using the shrimp alkaline phosphatase (fermentas) prior to ligation. Dephosphorylation was performed according to the instructions recommended in the manual of the manufacturer.
Then, the dephosphorylated DNA fragments were purified using the NucleoSpin® Gel and PCR clean-up Kit (MACHAREY-NAGEL).
Ligation of DNA fragments was done using the Rapid DNA Ligation Kit (Thermo Fisher Scientific) according to the instructions recommended in the manual of the

manufacturer.
Prior to transformation, the ligation mixture was purified using the NucleoSpin® Gel and PCR clean-up Kit (MACHAREY-NAGEL).

2.4.10 Preparation of competent *E. coli* cells

Preparation of electrocompetent cells:

First, 50 ml of LB medium was inoculated with a single colony of *E. coli* DH5 α derived from an LB agar plate and grown in a shaker at 200 rpm at 37°C for 16-18 h. Cells were diluted with fresh media to start an OD_{600} of approximately 0.5. Then, the culture was chilled on ice for 15 min. After harvesting the cells at 2,000 $\times$ g at 4°C for 15 min, the cells were washed two times with 400 ml of pre-cold, sterile water. After washing the cells in sterile, pre-cold 10% glycerol, the cells were resuspended in equal amount of sterile, pre-cold 10% glycerol, snap-freezed in 40 µl aliquots in liquid nitrogen and finally stored at -80°C.

Preparation of chemically competent cells:

Chemically competent cells were exactly prepared according to the protocol published in Inoue *et al.* 1990 ([240] republished in [241]).

2.4.11 Transformation of *E. coli* cells

As part of the cloning procedure, e.g. newly generated plasmids containing antibiotic resistance genes are introduced into competent *E. coli* cells, a process called transformation. Competent cells were prepared according to the procedures described in the previous chapters.

Transformation by electroporation:

40 µl of electrocompetent *E. coli* DH5α cells were gently mixed with DNA to be transformed (either 5 µl of purified ligation mix or 1 ng of plasmid DNA) and transferred into an electroporation cuvette. Electroporation was performed at constant voltage of 1.8 kV for 4 ms. Cells were immediately transferred into prewarmed SOC media and incubated at 37°C for 45 min. Finally, they were plated out on solid selective media. Plates were incubated at 37°C for 16 hours.

Transformation by heat-shock:

Chemically competent *E. coli* DH5α cells were thawed on ice. Then, 100 µl of competent cells were gently mixed with DNA (either 5 µl of purified ligation mix or 1 ng of plasmid DNA) and chilled on ice for 30 min. Afterwards, the cells were incubated at 42°C (heat shock) for 30 sec and immediately chilled on ice for 2 min. Cells were transferred into prewarmed SOC media and incubated at 37°C for 45 min. Finally, they were plated out on solid selective media. Plates were incubated at 37°C for at least 16 hours.

2.4.12 Transformation of *S. cerevisiae* cells

LiOAc/TE/H_2O:

10 mM	Tris
1 mM	EDTA pH 8.0
100 mM	LiOAc pH 7.5

Transformation of *S. cerevisiae* cells was performed similar to the protocol published in Guldener *et al.* 1996 [242]. Briefly, a 5 ml preculture of yeast strain to be transformed was grown in a shaker at 200 rpm at 30°C for 18-20 hours. Then, the 5 ml culture was diluted with fresh media in a total volume of 50 ml and further grown at 30°C for 3 hours. Cells were harvested (2,000 $\times$ g; 3 min) and washed with 10 ml of sterile ddH_2O, again with 1 ml of sterile ddH_2O and finally with 1 ml of sterile LiOAc/TE/H_2O. Cells were resuspended in 200 µl of sterile LiOAc/TE/H_2O (ratio 1:1:8). The competent yeast

cells were aliquoted in 50 µl and subsequently frozen at -80°C or further processed.
For transformation with either plasmid DNA or double stranded linear DNA (disruption cassettes), the DNA to be transformed, 300 µl of sterile LiOAc/TE/PEG (ratio 1:1:8) and 50 µl of competent yeast cells were incubated with 5 µl of pre-boiled and chilled ssDNA (10 mg/ml) at 30°C for 30 min. Afterwards, heat shock was performed at 42°C for 15 min. Finally, 800 µl of sterile ddH_2O was added to the transformation mixture and the cells were spread on solid selective media. The plates were incubated at 30°C for 3 days.

2.4.13 Sequencing of plasmid DNA

In order to check DNA sequences or monitor a cloning process, DNA samples were sent for Sanger sequencing to Microsynth AG. The DNA samples were prepared as described in the sample preparation guide found on the Microsynth homepage.

2.4.14 Construction of *S. cerevisiae* strains

All yeast strains used in this work are listed in Table 8. Oligonucleotides as well as all plasmids used to generate the yeast strains are listed in Table 9 and Table 10, respectively.
Yeast strains used in this work were generated according to the instructions recommended by Gueldener *et al.* 2002 [237].
Deletion of the genes *PRC1*, *DER1*, *ASI1*, *ASI3*, *UBC6* and *UBC7* was performed via PCR-based amplification of disruption cassettes and subsequent gene-specific homologous recombination. The disruption cassettes were PCR-amplified using the plasmids pUG27, pUG72 or pUG73 as template DNA and a primer pair specific to both the template plasmid and the flanking regions of the target gene.
The amplified disruption cassettes finally consist of an auxotrophic marker determined by the choice of the template plasmid flanked by up- and downstream sequences of the gene to be deleted.
The double stranded disruption cassettes were finally introduced in competent yeast cells. The disruption cassettes were genomically integrated by homologous recombination at the targeted DNA loci, whereas the endogenous genes were deleted.

The auxotrophic marker genes were flanked by *loxP* sites. Using the Cre/*loxP* technology, the auxotrophic marker genes were often removed by expressing the plasmid-encoded Cre recombinase in the cells.

The gene *PRC1* was deleted by homologous recombination of the *loxP-URA3-loxP* gene disruption cassette in YWO 713 (MATα ura3-1 his3-11,15 leu2-3,112 trp1-1ade2-1ocre can1-100 prc1-1 dfm1Δ::His3MX6). The cassette was generated using the pair of primers PRC1delfor / PRC1delrev, as well as pUG72 as template DNA. This led to the strain YWO 2103 (*MATα ura3-1 his3-11,15 leu2-3,112 trp1-1ade2-1ocre can1-100 prc1Δ::URA3 dfm1Δ::His3MX6*). Removal of the URA3 auxotrophy marker was achieved by the expression of the Cre recombinase, which was introduced by the plasmid pSH63 and led to the strain YWO 2106 (*MATα ura3-1 his3-11,15 leu2-3,112 trp1-1ade2-1ocre can1-100 prc1Δ::loxP dfm1Δ::His3MX6*).

The strain YWO 2093 (*MATα ura3-1 his3-11,15 leu2-3,112 trp1-1ade2-1ocre can1-100 prc1Δ::loxP der1Δ::LEU2 dfm1Δ::His3MX6*) was generated by deleting *DER1* in YWO 2106. Therefore, a *loxP-LEU2-loxP* gene disruption cassette was amplified using the pair of primers DER1delfor / DER1delrev as well as pUG73 as template DNA.

ASI1 deletion was introduced in YWO 636 (*MATα ura3-1 his3-11,15 leu2-3,112 trp1-1ade2-1ocre can1-100 prc1Δ::LEU2*) and YWO 1343 (*MATα ura3-1 his3-11,15 leu2-3,112 trp1-1ade2-1ocre can1-100 prc1Δ::LEU2 hrd1Δ::HIS*) to achieve the strains YWO 2145 (*MATα ura3-1 his3-11,15 leu2-3,112 trp1-1ade2-1ocre can1-100 prc1Δ::LEU2 asi1Δ::URA3*) and YWO 2146 (*MATα ura3-1 his3-11,15 leu2-3,112 trp1-1ade2-1ocre can1-100 prc1Δ::LEU2 hrd1Δ::HIS asi1Δ::URA3*), respectively. Therefore, the gene disruption cassette *loxP-URA3-loxP* was amplified using the pair of primers Asi1delfor / Asi1delrev as well as pUG72 as template DNA. Removal of the *URA3* auxotrophy marker was achieved by the expression of the Cre recombinase, which was introduced by the plasmid pSH63 and led to the strains YWO 2156 (*MATα ura3-1 his3-11,15 leu2-3,112 trp1-1ade2-1ocre can1-100 prc1Δ::LEU2 asi1Δ::loxP*) and YWO 2163 (*MATα ura3-1 his3-11,15 leu2-3,112 trp1-1ade2-1ocre can1-100 prc1Δ::LEU2 hrd1Δ::HIS asi1Δ::loxP*), respectively.

ASI3 deletion was introduced in YWO 636 (*MAT α ura3-1 his3-11,15 leu2-3,112 trp1-1ade2-1ocre can1-100 prc1Δ::LEU2*) and YWO 1343 (*MAT α ura3-1 his3-11,15 leu2-3,112 trp1-1ade2-1ocre can1-100 prc1Δ::LEU2 hrd1Δ::HIS*) to achieve the strains YWO 2151 (*MAT α ura3-1 his3-11,15 leu2-3,112 trp1-1ade2-1ocre can1-100 prc1Δ::LEU2 asi3Δ::URA3*) and YWO 2153 (*MAT α ura3-1 his3-11,15 leu2-3,112 trp1-1ade2-1ocre can1-100 prc1Δ::LEU2 hrd1Δ::HIS asi3Δ::URA3*), respectively. Therefore, the gene disruption cassette *loxP-URA3-loxP* was amplified using the pair of primers Asi3delfor / Asi3delrev as well as pUG72 as template DNA. Removal of the *URA3* auxotrophy marker was achieved by the expression of the Cre recombinase, which was introduced by the plasmid pSH63 and led to the strains YWO 2157 (*MAT α ura3-1 his3-11,15 leu2-3,112 trp1-1ade2-1ocre can1-100 prc1Δ::LEU2 asi3Δ::loxP*) and YWO 2159 (*MAT α ura3-1 his3-11,15 leu2-3,112 trp1-1ade2-1ocre can1-100 prc1Δ::LEU2 hrd1Δ::HIS asi3Δ::loxP*), respectively.

UBC6 and UBC7 deletions were introduced in YWO 636 (*MAT α ura3-1 his3-11,15 leu2-3,112 trp1-1ade2-1ocre can1-100 prc1Δ::LEU2*) and YWO 1526 (*MAT**a** ura3-1 his3-11,15 leu2-3,112 trp1-1ade2-1ocre can1-100 prc1Δ::LEU2 doa10Δ::kanMX*) to achieve the strains YWO 2160 (*MAT α ura3-1 his3-11,15 leu2-3,112 trp1-1ade2-1ocre can1-100 prc1Δ::LEU2 ubc6Δ::His5+*), YWO 2147 (*MAT α ura3-1 his3-11,15 leu2-3,112 trp1-1ade2-1ocre can1-100 prc1Δ::LEU2 ubc7Δ::His5+*) and YWO 2154 (*MAT**a** ura3-1 his3-11,15 leu2-3,112 trp1-1ade2-1ocre can1-100 prc1Δ::LEU2 doa10Δ::kanMX ubc6Δ::His5+*), YWO 2150 (*MAT**a** ura3-1 his3-11,15 leu2-3,112 trp1-1ade2-1ocre can1-100 prc1Δ::LEU2 doa10Δ::kanMX ubc7Δ::His5+*), respectively. Therefore, the gene disruption cassette *loxP-His5+-loxP* was amplified using the pair of primers delUBC6for / delUBC6rev and delUBC7for / delUBC7rev, respectively, as well as pUG27 as templated DNA.

2.4.15 Construction of plasmids

All oligonucleotides and plasmids used for generation of new plasmids in this work are listed in Table 9 and Table 10, respectively.
The gene coding for the *GFP* variant of plasmid pWO621 contains the sequence for an asparagine residue (N_{604}) instead of a lysine residue. The sequence coding for the asparagine residue was substituted for the sequence coding for a lysine residue in a mutagenesis-PCR using the primer MutLys, leading to the plasmid pWO1476.

pWO1456 was created, by amplifying the *TDH3* terminator, using pCT67 as template and the pair of primers TDH3forNheI / TDH3revEcoRI. The 1.549 kb DNA fragment was digested with NheI-HF and EcoRI-HF. GFP_{fast} was amplified using pWX204 as template and the pair of primers GFPfor / eGFPrev. The 753 bp DNA fragment was digested with PacI and NheI-HF. pMA1 was digested with PacI and EcoRI-HF, the remaining 7.345 kb fragment was purified using extraction of DNA fragments out of agarose gels. In ligation reaction all three fragments were ligated.
The GFP_{fast} variant in pWO1456 contains a sequence coding for the HDEL sequence, which is the ER retention signal. This sequence was removed in a mutagenesis-PCR using the primer Mutfast, leading to the plasmid pWO1477.

For *in vivo* ubiquitination assays the sequence coding for His_6-Ub had to be introduced into pRS424. pRS424 contains HindIII restriction sites. One in the multiple cloning site and one in the *TRP1* auxotrophy marker gene. In a mutagenisis-PCR with the primer TRPmutHindIII and pRS424 as template DNA, the HindIII restriction side within *TRP1* was removed. The newly generated plasmid pWO1479 ($pRS424^{-hindII}$) and the His_6-Ub containing plasmid pWO1265 were digested with the restriction enzyme HindIII-HF. The 1296 bp long fragment and the linearized $pRS424^{-hindII}$ were ligated, leading to the plasmid pWO1481.

To generate the plasmid pWO1496, [P_{PRC1} − C^*T_{Pdr5}(CS)] was amplified using the pair of primers CT for / CT rev and pBM8 as template DNA. The 2519 bp long DNA fragment, as well as pRS316, were digested with HindIII-HF. Both were ligated, leading to the plasmid pWO1414. The native *PRC1* terminator was amplified using genomic DNA from *S. cerevisiae* as template and the pair of primers CPYTerfor / CPYTerrev. The 242 bp long DNA fragment, as well as pWO1414, were digested with EcoRI-HF and SpeI-HF. Ligation of both led to pWO1496.

To generate the plasmid pWO1486, mutagenesis-PCR with pWO1414 as template DNA and the primer MutCT3 was performed. The native *PRC1* terminator was amplified using genomic DNA from *S. cerevisiae* as template and the pair of primers CPYTerfor / CPYTerrev. The 242 bp long DNA fragment, as well as pWO1486, were digested with EcoRI-HF and SpeI-HF. Ligation of both led to pWO1499.

To generate the plasmid pWO1497, mutagenesis-PCR with pWO1486 as template DNA and the primer MutCT4 was performed. The native *PRC1* terminator was amplified using genomic DNA from *S. cerevisiae* as template and the pair of primers CPYTerfor / CPYTerrev. The 242 bp long DNA fragment, as well as pWO1497, were digested with EcoRI-HF and SpeI-HF. Ligation of both led to pWO1502.

To generate the plasmid pWO1487, mutagenesis-PCR with pWO1414 as template DNA and the primer MutCT7 was performed. The native *PRC1* terminator was amplified using genomic DNA from *S. cerevisiae* as template and the pair of primers CPYTerfor / CPYTerrev. The 242 bp long DNA fragment, as well as pWO1487, were digested with EcoRI-HF and SpeI-HF. Ligation of both led to pWO1500. Mutagenesis-PCR was performed, using pWO1500 as template DNA and the primer MutCT5 and MutCT6, respectively. Successful mutagenesis led to the plasmids pWO1503 and pWO1504, respectively.

pWO1522 was generated in a three-step mutagenesis-PCR. The first PCR was performed, using pWO1496 as template DNA and the primer MutWSC1. The resulting plasmid pWO1520 was used as template DNA for the second mutagenesis-PCR with the primer MutWSC2. The newly generated plasmid pWO1521 was used as template DNA for the final mutagenesis-PCR using the primer MutWSC3. Successful mutagenesis led to the plasmid pWO1522.

For generation of pWO1529, the plasmids pBM8 and pSK007 were digested with the restriction enzymes AgeI-HF and HindIII-HF. The 7,628 bp long DNA fragment generated in the pBM8 digestion was used as vector. The 2,574 bp long DNA fragment created in the pSK007 digestion was used as insert. Ligation of both led to the plasmid pWO1529.

To generate the plasmids pWO1591 and pWO1593, mutagenesis-PCR's with pWO1507 and pWO1534 as template DNA, respectively, and the primer MutCT41 were performed. pWO1591 and pRS314 were digested with KpnI-HF and NotI-HF. The 2,781 bp long DNA fragment was ligated into the linearized vector pRS314, leading to the plasmid pWO1596. pWO1593 and pRS314 were digested with KpnI-HF and NotI-

HF. The 2,769 bp long DNA fragment was ligated into the linearized vector pRS314, leading to the plasmid pWO1595.

The following plasmids were generated via mutagenesis-PCR using appropriate primers and template DNA. The resulting plasmids, template DNA and primers are listed in Table 11.

Table 11: Newly generated plasmids, created via mutagenesis, used primers and template DNA.

Newly generated plasmid	Used primer	Template DNA
pWO1507	MutCT1	pWO1503
pWO1512	MutCT12	pWO1507
pWO1513	MutCT13	pWO1507
pWO1514	MutCT11	pWO1507
pWO1515	MutCT14	pWO 1507
pWO1516	MutCT19	pWO1507
pWO1517	MutCT18	pWO1507
pWO1518	MutCT17	pWO1507
pWO1519	MutCT16	pWO1507
pWO1523	MutCT33	pWO1503
pWO1524	MutCT29	pWO1507
pWO1526	MutCT30	pWO1507
pWO1528	MutCTLHA	pBM8
pWO1538	MutCT34	pWO1523
pWO1551	MutCT35	pWO1496
pWO1552	MutCT36	pWO1496
pWO1553	MutWSC6	pWO1534
pWO1554	MutWSC7	pWO1534
pWO1555	MutWSC5	pWO1534
pWO1602	MutCT42	pWO1507
pWO1603	MutCT42	pWO1534
pWO1604	MutCPY	pWO1496
pWO1605	MutCPY	pWO1499
pWO1606	MutCPY	pWO1507
pWO1607	MutCPY	pWO1553
pWO1608	MutCPY	pWO1554
pWO1609	MutCPY	pWO1555
pWO1610	MutCPY	pWO1502

2.5 Methods in protein biochemistry

2.5.1 Protein sample precipitation for sodium dodecyl sulfate polyacrylamide gel electrophoresis

Urea loading buffer:

200 mM	Tris/HCl pH 6.8
8 M	Urea
5% (w/v)	SDS
0.1 mM	EDTA pH 8.0
1.5% (v/v)	β-Mercaptoethanol
0.05% (w/v)	Bromophenol blue

To precipitate proteins in a protein-containing solution for subsequent SDS-PAGE, a TCA solution was added to a final concentration of 10% (v/v). After vortexing the mixture was incubated on ice for 10 min. After centrifugation at V_{max} in a table centrifuge for 10 min, the protein pellet was washed once with 1 ml of ice-cold acetone. The acetone was discarded and the pellet was dried at RT. After dissolving the precipitated proteins in urea loading buffer at 75°C for 10 min, the samples were subjected to SDS-PAGE, Western blot and immunodetection using protein-specific antibodies.

2.5.2 Sodium dodecyl sulfate polyacrylamide gel electrophoresis (SDS-PAGE)

1 × SDS running buffer:

25 mM	Tris
192 mM	Glycine
0.1% (w/v)	SDS

Table 12: Composition of 4 ml stacking gel (5%) and 5 ml resolving gel (8% and 10%) used for SDS gels.

	Stacking gel	Resolving gel	
	5%	8%	10%
Component	Volume [ml]		
ddH_2O	2.7	2.3	1.9
30% acrylamide mix	0.67	1.3	1.7
1.0 M Tris pH 6.8	0.5	-	-
1.5 M Tris pH 8.8	-	1.3	1.3
10% (w/v) SDS	0.04	0.05	0.05
10% (w/v) APS	0.04	0.05	0.05
TEMED	0.004	0.003	0.002

To separate proteins by molecular mass SDS-PAGE, a discontinuous electrophoretic system, was performed. SDS-PAGE was performed similar to the protocol published in Laemmli 1970 [243]. The matrix used in SDS-PAGE is a polyacrylamide-based discontinuous gel. The SDS gel is composed of a stacking gel and a resolving gel. To achieve ideal separation of proteins a 5% stacking and an 8% or 10% resolving gel were cast using the Mini-PROTEAN Handcast System (Bio-RAD). As running buffer 1 × SDS running buffer was used. The electrophoresis was performed with constant amperage of 30 mA per gel for 60 – 90 min with a maximum voltage of 150 V using the Mini-PROTEAN Tetra Vertical Electrophoresis Cell System (Bio-RAD). In order to identify the approximate size of the separated proteins a molecular-weight size marker was used (PageRuler™ Plus Prestained Protein Ladder, 10 to 250 kDa; Thermo Fisher Scientific).

2.5.3 Tricine sodium dodecyl sulfate polyacrylamide gel electrophoresis (Tricine-SDS-PAGE)

1 × Anode buffer:	1 × Cathode buffer:	1 × Gel buffer:
100 mM Tris	100 mM Tris	3 mM Tris
22.5 mM HCl	100 mM Tricine	1 M HCl
adjusted to pH 8.9	0.1% (w/v) SDS	0.3%(w/v) SDS
	adjusted to pH 8.24	adjusted to pH 8.45

Table 13: Composition of stacking gel (4%), spacer gel (10%) and resolving gel (16%) used for Tricine-SDS gels.

	Stacking gel	Spacer gel	Resolving gel
	4%	10%	16%
Component	Volume [ml]		
ddH_2O	1.7	1.5	1.6
40% acrylamide mix	0.3	1.25	4
3 × Gel buffer	1	1.7	3.3
86% (v/v) Glycerol	-	0.6	1.1

Tricine-SDS-PAGE varies from the classical Laemmli SDS-PAGE by replacing glycine with tricine. Tricine-SDS polyacrylamide gels are used to separated proteins with molecular masses of 1-100 kDa. Preparation of gels and electrophoresis were performed as described in Schägger 2006 [244]. Briefly, the used discontinuous Tricine-SDS gel consists of a 4% stacking gel and two resolving gels of different acrylamide concentration (10% acrylamide and 16% acrylamide, respectively). The exact composition of the gel is shown in Table 13. For electrophoresis the Mini-PROTEAN Tetra Vertical Electrophoresis Cell (Bio-RAD) system was used. The electrophoresis was run at constant voltage of 130 V at RT for 2 hours using both, an anode and a cathode buffer. As molecular-weight size marker the Spectra™ multicolor low range protein ladder from Thermo Fisher Scientific was used.

2.5.4 Western blot

1 × blotting buffer:

25 mM	Tris
192 mM	Glycine
0.02% (w/v)	SDS
20% (v/v)	Methanol

After SDS-PAGE the separated proteins were transferred and immobilized respectively, on the surface of a nitrocellulose membrane (BioTrace™ NT Nitrocellulose Transfer membrane; Pall corporation; Washington; New York; U.S.), a method called Western blot. In this study the wet tank blotting method was used. For blotting a “sandwich” had to be assembled, consisting of the SDS gel, the nitrocellulose membrane, sheets of filter paper (Sartorius; Göttingen; Germany) and fiber pads according to the instructions recommended in the manual of the manufacturer. The blotting chamber (Mini Trans-Blot Cell chamber; Bio-RAD) was filled with ice-cold 1 × blotting buffer. The blotting was performed with constant amperage of 300 mA for 90 min.

2.5.5 Immunodetection

1 × PBS-T:

150 mM	NaCl
22 mM	Na_2HPO_4
2.6 mM	NaH_2PO_4
0.1% (v/v)	Tween-20
adjusted to pH 7.6	

Blocking solution:

1 ×	PBS-T
5% (w/v)	Milk powder or bovine serum albumin fraction V

Detection of the proteins separated by SDS-PAGE and subsequently transferred on the surface of a nitrocellulose membrane was achieved by the use of protein-specific antibodies. Prior to incubation with antibodies, free protein binding sides on the membrane were saturated via 1 hour incubation of the membrane with blocking solution.

Afterwards, the membrane was incubated at 4°C overnight or at RT for 2 hours with protein-specific primary antibody. After washing the membrane three times in 5 ml of 1 × PBS-T for 5 min, the membrane was incubated at RT for 1 hour with secondary antibody or binding protein, which is specific for the constant part of the protein-specific primary antibody used in this study. Additionally, the secondary antibody is fused to the enzyme horseradish peroxidase (HRP), able to convert a luminol-based substrate under emittance of chemiluminescence. Alternatively, specific binding proteins fused to HRP were used, which bind specifically the constant part of corresponding primary antibodies.

After washing the membrane three times in 5 ml of 1 × PBS-T for 5 min the membrane was incubated with an enhanced chemiluminescent substrate (Pierce® ECL Western Blotting Substrate or Western Lightning® Plus-ECL). The chemiluminescent signals were detected by exposure a high performance chemiluminescence film (Amersham Hyperfilm™ ECL; GE Healthcare; Chicago; Illinois; U.S.) and subsequent development using an automated developing machine (OptiMax X-ray Processor; PROTEC).

2.5.6 Preparation of microsomes

Buffer A:

100 mM	Tris pH 9.4
10 mM	DTT
10 mM	NaN_3

Spheroplasting buffer:

1.5 M	Sorbitol
50 mM	Tris-HCl pH 7.5
2 mM	$MgCl_2$
10 mM	NaN_3

Buffer B:

0.2 M	Sorbitol
0.1 M	NaCl
5 mM	$MgCl_2$
10 mM	HEPES pH 7.5
1 mM	NaN_3
1 mM	PMSF
1 ×	Complete inhibitor cocktail

Buffer C:

0.2 M	Sorbitol
0.1 M	NaCl
5 mM	$MgCl_2$
10 mM	HEPES pH 7.4
1 mM	NaN_3

To determine the orientation (chapter 2.5.8) and membrane insertion (chapter 2.5.7) of membrane proteins, microsomes have to be prepared. Yeast main cultures were prepared as described in chapter 2.3.3. 200 OD_{600} of cells, in logarithmic growth phase, were harvested and incubated in 40 ml of synthetic medium containing 0.2% glucose

at 30°C for 1 hour. After harvesting, the cells were resuspended in 20 mM of ice-cold NaN_3 and incubated on ice for 10 min. After an additional washing step, the cells were resuspended in 10 ml of buffer A and further incubated at RT for 10 min. In order to digest the cell wall 10 U of Zymolyase 20T or 2 U of Zymolyase 100T was added per 1 OD_{600} of cells, mixed and incubated at 30°C for 30 min. Afterwards, the spheroplasts were isolated by centrifugation at 5,000 × g and 4°C for 10 min. The spheroplast-containing pellet was resuspended in 1 ml of buffer B. For subsequent cell lysis 3/4th of the sample volume of glass beads (∅ 0.25 – 0.5 mm) was added. Cells were lysed by three intervals of vortexing and chilling on ice for 15 sec, respectively. The supernatant was transferred to a new tube and the glass beads were washed five times with 500 µl of buffer B. The supernatants were pooled and adjusted to a volume of 5 ml. Cell debris was removed by centrifugation at 660 × g and 4°C for 5 min and the microsomes were separated from supernatant via ultracentrifugation at 100,000 × g and 4°C for 1 hour, using an Optima™ TLX-CE preparative ultracentrifuge and TLA-110 fixed-angle rotor. Proteins were precipitated from 1 ml of the supernatant fraction (protein precipitation see chapter 2.5.1) serving as supernatant 1 (S) control. The remaining supernatant was discarded and after resuspending the microsomes in ice-cold buffer C they were immediately frozen and finally stored at -20°C.

2.5.7 Localization studies

Urea loading buffer:

200 mM	Tris/HCl pH 6.8
8 M	Urea
5% (w/v)	SDS
0.1 mM	EDTA pH 8.0
1.5% (v/v)	β-Mercaptoethanol
0.05% (w/v)	Bromophenol blue

Microsomes were prepared as described in chapter 2.5.6. Microsomes were thawed on ice. Six different reaction mixtures were prepared. 250 µl of microsomes, each were treated (1) only with buffer C, or buffer C containing either (2) 1 M KAc or (3) 0.1 M Na_2CO_3 or (4) 1% (w/v) SDS or (5) 1% (v/v) Triton X-100 or (6) 2.5 M urea, on ice for

1 hour, except the SDS-containing mix, which was incubated at RT for 1 hour. Microsomes were separated by centrifugation 100,000 × g at 4°C for 1 hour using a Optima^{TM} TLX-CE preparative ultracentrifuge and TLA-110 fixed-angle rotor. The supernatants were precipitated, serving as supernatant 2 (SN) control (protein precipitation see chapter 2.5.1). The pellets were washed once with the corresponding buffers (100,000 × g at 4°C for 1 hour). The supernatants were discarded and the pellets were incubated in urea loading buffer at 75°C for 10 min. Proteins were separated, using SDS-PAGE and detected by immunoblotting, using the appropriate protein-specific antibodies.

2.5.8 Proteinase K protection assays

Microsomes were prepared as described in chapter 2.5.6. Microsomes were thawed on ice. Three different reaction mixtures were prepared.

1. 250 µl of microsomes adjusted to 1 ml with buffer C.
2. 250 µl of microsomes and 25 µl of proteinase K adjusted to 1 ml with buffer C.
3. 250 µl of microsomes, 25 µl of proteinase K and 1% (v/v) Triton-X100 adjusted to 1 ml with buffer C.

All reactions were incubated on ice for 1 hour. Proteinase K digestion was stopped by adding 110 µl of PMSF (100 mM), mixing and incubating on ice for 10 min. Finally, proteins were precipitated (protein precipitation see chapter 2.5.1). Proteins were separated, using SDS-PAGE and detected by immunoblotting, using the appropriate protein-specific antibodies.

2.5.9 Carboxypeptidase Y activity assay

Carboxypeptidase Y is an exopeptidase of the vacuole (yeast lysosome). *N*-benzoyl-L-tyrosine *p*-nitroanilide (BTpNA) is a substrate for the carboxypeptidase Y. Cleavage of BTpNA produces a yellow product, its absorbance can be measured.
Carboxypeptidase Y activity assays were performed according to Woolford *et al.* 1986 [245]. Summarizing the notable variations briefly, main cultures were prepared as described in chapter 2.3.3. 5 OD_{600} of cells, in logarithmic growth phase, were harvested (2,000 × g; 3 min), washed once with synthetic medium containing 0.2% glucose and finally incubated in 5 ml of synthetic medium containing 0.2% glucose. Cells were incubated at 30°C for 1 hour. Three aliquots of 1 ml each were harvested at 7,000 × g for 2 min in a table centrifuge. One aliquot was processed as described in chapter 2.5.10. The remaining two aliquots were resuspended each in 200 µl of 0.1 M Tris/HCl pH 7.5 and 2.5 mg/ml BTpNA in a ratio 4:1. Cell suspensions were incubated at 37°C for 12 hours. Afterwards, the cells were removed (7,000 × g for 2 min in a table centrifuge). Of the supernatant fraction absorbance was measured at 410 nm.

2.5.10 Cycloheximide-chase analysis and protein extraction

Extraction buffer:

50 mM	Tris/HCl pH 7.5
0.5 mM	EDTA pH 8.0
1 mM	PMSF
1 ×	Complete inhibitor cocktail

Urea loading buffer:

200 mM	Tris/HCl pH 6.8
8 M	Urea
5% (w/v)	SDS
0.1 mM	EDTA pH 8.0
1.5% (v/v)	β-Mercaptoethanol
0.05% (w/v)	Bromophenol blue

To perform degradation kinetics of distinct proteins first the cellular ribosomal protein synthesis has to be inhibited by the application of cycloheximide (CHX).
Therefore, yeast main cultures were prepared as described in chapter 2.3.3. 10 OD_{600} of cells, in logarithmic growth phase, were harvested (2,000 × g; 3 min), washed once with synthetic medium containing 0.2% glucose. Cells were incubated in 2.6 ml of synthetic medium containing 0.2% glucose at 30°C for 1 hour. After application of CHX at a final concentration of 100 µg/ml, 2 OD_{600} of cells were transferred to ice-cold 20 mM NaN_3 at indicated time points, cells were harvested in a table centrifuge at 7,000 × g for 2 min and finally frozen at -80°C or further processed.

Sample preparation:

Cells were resuspended in 100 µl of extraction buffer and lysed mechanically at 4°C for 15 min using glass beads (∅ 0.25 – 0.5 mm). After cell lysis 1 ml of extraction buffer was added and 950 µl of the supernatant fraction was centrifuged at V_{max} in a table centrifuge at 4°C for 20 min. The pellet was incubated in urea loading buffer at 75°C for 10 min. Proteins were separated, using SDS-PAGE and detected by immunoblotting, using appropriate antibodies.

2.5.11 *In vivo* ubiquitination assay

A2 buffer:

6 M	Guanidine-HCl
100 mM	Na_2HPO_4/NaH_2PO_4 pH 8.0
10 mM	Imidazole
250 mM	NaCl
0.5% (v/v)	NP-40

adjusted to pH 8.0 with NaOH

T2 buffer:

50 mM	Na_2HPO_4/NaH_2PO_4 pH 8.0
250 mM	NaCl
20 mM	Imidazole
0.5% (v/v)	NP-40

Urea loading buffer:

200 mM	Tris/HCl pH 6.8
8 M	Urea
5% (w/v)	SDS
0.1 mM	EDTA pH 8.0
1.5% (v/v)	β-Mercaptoethanol
0.05% (w/v)	Bromophenol blue
200 mM	Imidazol

The ubiquitination status of proteins can be analyzed by performing *in vivo* ubiquitination assays according to Geng and Tansey 2008 [246]. Summarizing the notable variations briefly, cells were grown overnight to logarithmic growth phase OD_{600} of 0.8 - 1.5 in synthetic complete medium, containing 0.1 mM $CuSO_4$. 200 OD_{600} of cells, in logarithmic growth phase, were harvested and incubated in 40 ml of synthetic medium containing 0.2% glucose and 0.1 mM $CuSO_4$ at 30°C for 1 hour. Cells were harvested (2,000 × g; 3 min) and incubated in 20 mM NaN_3 on ice for 10 min. After removal of the NaN_3 (in a table centrifuge at 7,000 × g for 2 min) cell lysis was done, using a cell disruptor. Therefore, 800 µl of A2 buffer and 300 µl of glass beads (∅ 0.25 – 0.5 mm) were added to 100 OD_{600} of cells and vortexed at 4°C for 15 min. Then the lysates were precleared at V_{max} for 10 min in a table centrifuge. 2.5% of supernatant was precipitated with 110% TCA, serving as lysate control (protein precipitation see chapter 2.5.1). The remaining supernatant fraction was incubated at RT for 2 hours with Ni-NTA agarose resin to capture all ubiquitinated proteins. After two washing steps with 1 ml of A2 buffer and subsequent three times washing steps with T2 buffer (50 × g; 1 min), the Ni-NTA beads were incubated in each 200 µl of urea loading buffer at 75°C for 10 min. Proteins were separated, using SDS-PAGE and detected by immunoblotting, using appropriate antibodies.

2.5.12 Co-immunoprecipitation experiments

Extraction buffer:

10% (v/v)	Glycerol
50 mM	Tris HCl pH 7.5
0.5 mM	EDTA pH 8.0
200 mM	NaOAc
50 mM	NaF
1 ×	Complete inhibitor cocktail
1 mM	PMSF
1 ×	Pepstatin A
60 mM	β-Glycerophosphate

IP buffer:

165 mM	NaCl
50 mM	Tris HCl pH 7.5
5,5 mM	EDTA pH 8.0
0.05% (v/v)	NP-40
50 mM	NaF
1 ×	Complete inhibitor cocktail
1 mM	PMSF
1 ×	Pepstatin A
60 mM	β-Glycerophosphate
0.5 or 1%	Digitonin

Urea loading buffer:

200 mM	Tris/HCl pH 6.8
8 M	Urea
5% (w/v)	SDS
0.1 mM	EDTA pH 8.0
1.5% (v/v)	β-Mercaptoethanol
0.05% (w/v)	Bromophenol blue

To precipitate protein complexes using appropriate protein-specific antibodies, co-immunoprecipitation experiments were performed. Yeast main cultures were prepared as described in chapter 2.3.3. 150 OD_{600} of cells, in logarithmic growth phase, were harvested and incubated in 40 ml of synthetic medium containing 0.2% glucose at 30°C for 1 hour. Cells were harvested (2,000 × g; 3 min) and incubated in 20 mM NaN_3 on ice for 10 min. After removal of the NaN_3 (in a table centrifuge at 7,000 × g for 2 min) cell were resuspended in 1 ml of extraction buffer and lysed mechanically at 4°C for 15 min using glass beads (∅ 0.25 – 0.5 mm). Glass beads were washed three times with 1 ml of extraction buffer (300 × g for 3 sec). The lysates were collected and finally the volume was adjusted to 5 ml with extraction buffer. Preclearing of lysate was done by centrifugation at 660 × g and 4°C for 5 min. 4 ml of precleared lysate was separated into membrane and supernatant fraction using an Optima™ TLX-CE preparative ultracentrifuge and TLA-110 fixed-angle rotor at 100,000 × g and 4°C for 1 hour. The supernatants were discarded and pellets were washed (100,000 × g and 4°C for 1 hour) with 2 ml of extraction buffer. The supernatants were removed and pellets were solved in 2 ml of IP buffer (containing 1% (w/v) Digitonin) and incubated on a rocking platform at 4°C for 1 hour. Aggregates were removed by centrifugation (100,000 × g and 4°C for 35 min). 10 µl of the supernatant fraction was used for precipitation according to chapter 2.5.1, serving as 1% input sample. The remaining supernatant was divided into two and each part was incubated on a rocking platform with adapted protein-specific antibody at 4°C for 1 h. 7% protein A sepharose was added and incubated at 4°C overnight. After washing three times (400 × g; 1 min) with IP buffer (containing 0.5% digitonin), the pellets were incubated with each 80 µl of urea loading buffer, each, at 75°C for 5 min. Proteins were separated, using SDS-PAGE and detected by immunoblotting, using appropriate antibodies.

3. RESULTS

Proteins containing lesions are recognized by cellular quality control systems and are finally removed to guarantee well balanced protein homeostasis in the cell.

In the endoplasmic reticulum (ER) misfolded secretory proteins are removed by a multi-component system, the so-called ER-associated degradation (ERAD). Depending on the location of the aberrant domain, ERAD substrates are degraded via different pathways. Secretory proteins containing alterations in the ER lumenal domain, the membrane domain or the cytosolic domain are degraded via the ERAD-L, ERAD-M or ERAD-C pathway, respectively (the degradation pathways are explained in detail in the introduction and a brief overview is given in chapter 1.7).

Some years ago, the pathways were classified and for each of them characteristic components were determined that define the respective pathway. The ER membrane protein Der1 was shown to be specific of the ERAD-L degradation pathway but dispensable for degradation of ER proteins with aberrant membrane domain (ERAD-M pathway) [41,42]. However, there are certain ERAD-L substrates that surprisingly show a Der1 independent degradation, such as CTG* and CT* [196]. Other ERAD-L substrates require Der1 for degradation but only to a certain extent, like the *bona fide* ERAD-L substrates KHN and KWW [41,230] (for more details see chapter 1.7).

In general, it is puzzling that some of the proteins, containing a misfolded ER lumenal domain, are degraded without the help of Der1, a protein identified to be essential for the ERAD-L pathway.

In this work a suitable set of ERAD substrates was generated to elucidate in detail under which circumstances Der1 is required for degradation of ER proteins containing lesions in their ER lumenal domain. The substrates additionally contain differences in the folding status of the membrane domain and the composition of the cytosolic part. Furthermore, it was analyzed which components of the ubiquitin-proteasome system participate in these Der1 dependent and independent degradation pathways, which leads to a more detailed picture about the ERAD-L and ERAD-M degradation mechanisms.

3.1 Establishing a suitable set of substrates to analyze differences in the *canonical* ER-associated degradation pathways

The mechanism how substrates of the ERAD pathways are degraded is generally analyzed using artificially misfolded proteins. These artificial proteins contain certain epitopes for analysis in experiments. Lesions are inserted into distinct domains of the secretory proteins to target them for one specific degradation pathway.

The mutated carboxypeptidase Y (CPY*) is frequently used as an ER lumenal misfolded domain, to analyze the ERAD-L degradtion mechanism. An asterisk marks the misfolded form of CPY, it is indicated as CPY*. Under native conditions the carboxypeptidase yscY (CPY), a serine exopeptidase, passes the secretory pathway to reach its final destination, the vacuole (yeast lysosome). Replacement of glycine at position 255 by arginine leads to unfolding and inactivation of the exopeptidase activity. As soluble misfolded protein, CPY* is retained in the ER lumen and finally removed by the ERAD-L pathway ([223] and Figure 6).

In the *bona fide* ERAD substrates CT*, CTL* and CTG*, CPY* is anchored in the ER membrane by a domain representing the last of the 12 transmembrane helices from the multidrug transporter Pdr5 (T_{Pdr5}). In the ER lumen a peptide of 32 amino acids and in the cytosol a peptide of 12 amino acids, the so-called cytosolic sequence (CS), guarantees proper insertion into the ER membrane. Both peptides derive from the last ER lumenal and the last cytosolic part of Pdr5, which are parts up- and downstream of T_{Pdr5}.

Some modification of the nomenclature should give a more detailed information about the origin of the ER lumenal as well as membrane and cytosolic domains in the CPY* derivatives CT*, CTL* and CTG*. They are denoted as C*T_{Pdr5}(CS), C*T_{Pdr5}(CS)Leu2 and C*T_{Pdr5}(CS)GFP.

Since there exists a huge amount of information about degradation of C*T_{Pdr5}(CS), C*T_{Pdr5}(CS)Leu2 and C*T_{Pdr5}(CS)GFP, these CPY* derivatives were taken as basis to establish a suitable set of substrates to analyze the mechanisms of the *canonical* ERAD pathways in more detail.

3.1.1 Use of *bona fide* ERAD substrates C*T$_{Pdr5}$(CS)Leu2 and C*T$_{Pdr5}$(CS)GFP

As indicated above the *bona fide* ERAD substrates C*T$_{Pdr5}$(CS)Leu2 and C*T$_{Pdr5}$(CS)GFP are well characterized. Both are fusion proteins, originating from C*T$_{Pdr5}$(CS). In C*T$_{Pdr5}$(CS) the ERAD-L substrate CPY* is linked to the ER membrane through the last transmembrane helix of Pdr5.

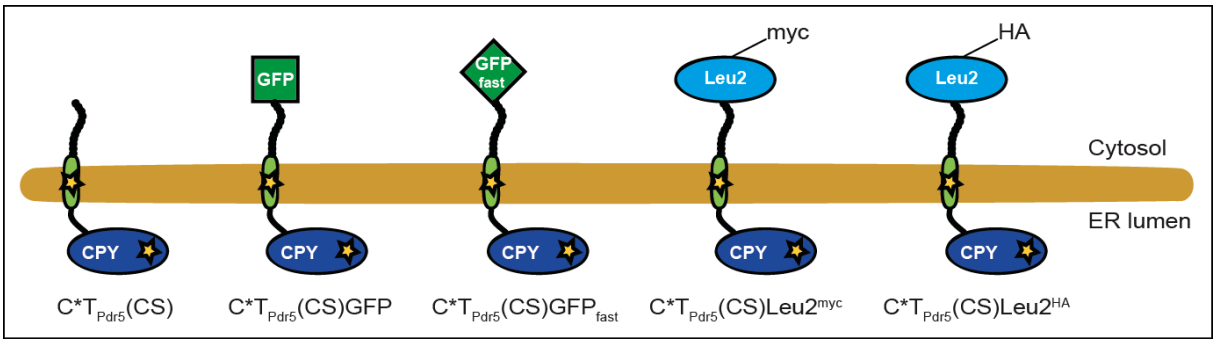

Figure 9: Schematic representation of the ERAD substrates C*T$_{Pdr5}$(CS), C*T$_{Pdr5}$(CS)GFP, C*T$_{Pdr5}$(CS)GFP$_{fast}$, C*T$_{Pdr5}$(CS)Leu2^{myc} and C*T$_{Pdr5}$(CS)Leu2^{HA}.

The oval structure marked with a yellow asterisk, symbolizes the misfolded carboxypeptidase domain (C*), followed by a single-spanning transmembrane helix (T$_{Pdr5}$; green). The membrane domain is labeled with a yellow asterisk, which represents misfolding, because it is the last transmembrane helix from the multidrug transporter Pdr5, which cannot interact with the neighboring transmembrane helices and must therefore considered to be misfolded. The black chain located in the cytosolic part of each C*T$_{Pdr5}$ derivative represents a peptide of 12 amino acids, originating from the C-terminal tail of Pdr5. For C*T$_{Pdr5}$(CS)GFP the green fluorescent protein (GFP) from *Aequorea victoria* is fused to C*T$_{Pdr5}$(CS). C*T$_{Pdr5}$(CS)GFP$_{fast}$ contains a superfast folding GFP variant. In case of C*T$_{Pdr5}$(CS)Leu2^{myc} and C*T$_{Pdr5}$(CS)Leu2^{HA}, C*T$_{Pdr5}$(CS) is fused to the β-iso-propylmalate dehydrogenase (Leu2) and marked either with a myc-Tag or an HA-Tag.

In case of the *bona fide* substrate C*T$_{Pdr5}$(CS)GFP the green fluorescent protein (GFP), referring to the protein isolated from the jellyfish *Aequorea victoria*, is fused to the C-terminus of C*T$_{Pdr5}$(CS). Thus, C*T$_{Pdr5}$(CS)GFP is embedded into the ER membrane containing the misfolded CPY* moiety in the ER lumen and a fluorescent GFP variant as cytosolic domain (Figure 9). Since fluorescence of the GFP moiety in the membrane construct was shown, the cytosolic domain is assumed to be folded [196].

C*T$_{Pdr5}$(CS)Leu2^{myc} was generated for genetic screens [45,194,197,231], the ER lumenal, misfolded CPY* moiety was used to uncover components necessary for ERAD-L substrate degradation. Through the last transmembrane helix of Pdr5, CPY* is recruited to the ER membrane and at the cytosolic part it is linked to the β-iso-propylmalate dehydrogenase (Leu2) (Figure 9) [247]. Functional Leu2 is assumed to be properly folded because if it is present in the cytosol, the cells can complete the leucine

synthesis and are able to grow in medium without leucine. This indicates the Leu2-containing C*T_{Pdr5}(CS)Leu2^{myc} to be a suitable construct for use in genetic screens. For better analysis it was additionally tagged with a myc-Tag (C*T_{Pdr5}(CS)Leu2^{myc}).

Although C*T_{Pdr5}(CS)Leu2^{myc} and C*T_{Pdr5}(CS)GFP differ solely in their properly folded cytosolic domain, degradation of both substrates, Leu2^{myc} and GFP, respectively, was found to be fundamentally different, which is briefly summarized in the following and an overview is given in Table 14.

Table 14: Overview of key components required for degradation of C*T_{Pdr5}(CS)Leu2^{myc} and C*T_{Pdr5}(CS)GFP

A green check mark indicates essential for degradation; a red cross symbol means dispensable for degradation; ~ (tilde) means involved in but not absolutely necessary for degradation. The analyzed ERAD components are Der1, a membrane protein, the ubiquitin ligases Hrd1 and Doa10, the ubiquitin chain elongating ligase Hul5, the ER lumenal and cytosolic Hsp70 chaperones Kar2 and Ssa1, respectively.

	Der1	Hrd1	Doa10	Hul5	Kar2	Ssa1
C*T_{Pdr5}(CS)Leu2^{myc}	✓	✓	✘	✓	✓	✘
C*T_{Pdr5}(CS)GFP	✘	~	✘	✘	✘	✓

C*T_{Pdr5}(CS)Leu2^{myc} is completely stabilized in the absence of Der1 as well as the ubiquitin ligase Hrd1 ([194] and Data published in PhD thesis Stefanie Besser [232]). Furthermore, the ER lumenal Hsp70 chaperone Kar2 is required but the cytosolic Hsp70 chaperone Ssa1 is dispensable for degradation of C*T_{Pdr5}(CS)Leu2^{myc} (Data published in PhD thesis Stefanie Besser [232]). This indicates C*T_{Pdr5}(CS)Leu2^{myc} to be degraded via an ERAD-L degradation mechanism. In addition, the proteasome-associated ubiquitin ligase Hul5 is necessary for the elongation of ubiquitin chains on C*T_{Pdr5}(CS)Leu2^{myc}. In the absence of Hul5, a N-terminal truncated degradation intermediate of C*T_{Pdr5}(CS)Leu2^{myc} accumulates in the ER membrane (truncC*T_{Pdr5}(CS)Leu2^{myc}) [194], which is not further degraded. The myc-Tag is composed of a 13 times repeated sequence of amino acids, on the C-terminus of C*T_{Pdr5}(CS)Leu2^{myc}. Therefore, it may be unstructured and might function as a degron signal and thus, Hul5 might be required for C*T_{Pdr5}(CS)Leu2^{myc} degradation.

On contrary, the cytosolic Hsp70 chaperone Ssa1 is required to degrade the membrane-bound CPY* derivative C*T_{Pdr5}(CS)GFP but the ER lumenal chaperone

Kar2 is dispensable for degradation [196]. C*T$_{Pdr5}$(CS)GFP degradation is unaffected in cells lacking Der1 [196]. This is astonishing, since C*T$_{Pdr5}$(CS)GFP contains the misfolded CPY* moiety in the ER lumen, which was predicted to signal degradation by the ERAD-L pathway. Furthermore, an accumulation of a truncated version of C*T$_{Pdr5}$(CS)GFP is not observed in the absence of Hul5 (Data published in PhD thesis Sonja Kohlmann [248]). In cells lacking Hrd1, degradation of C*T$_{Pdr5}$(CS)GFP is only slightly impaired [196], which suggests the participation of an additional ubiquitin ligase in degradation of C*T$_{Pdr5}$(CS)GFP.

C*T$_{Pdr5}$(CS)GFP does not require Der1 for degradation and in the absence of the ubiquitin ligase Hrd1, C*T$_{Pdr5}$(CS)GFP is only slightly stabilized. Thus, it seems that C*T$_{Pdr5}$(CS)GFP is not degraded via an ERAD-L related mechanism. Since the cytosolic Hsp70 chaperone Ssa1 is required for C*T$_{Pdr5}$(CS)GFP degradation, C*T$_{Pdr5}$(CS)GFP may possibly be degraded in an ERAD-C dependent manner.

However, to analyze the mechanisms of the different ERAD pathways pure ERAD-L, ERAD-M and ERAD-C substrates are required, which are eliminated solely by one of the ERAD branches. These substrates are also called true ERAD substrates. Therefore, it has to be determined, which parts of the *bona fide* ERAD substrates C*T$_{Pdr5}$(CS)Leu2^{myc} and C*T$_{Pdr5}$(CS)GFP have to be changed to generate such true ERAD substrates.

Since the constructs C*T$_{Pdr5}$(CS)Leu2^{myc} and C*T$_{Pdr5}$(CS)GFP are expressed under the control of different promoters, for a genuine comparison all substrates were expressed under the control of the same promoter. First, the *TDH3* promoter (in case of C*T$_{Pdr5}$(CS)GFP [196]) and the *GAL*4 promoter (in case of C*T$_{Pdr5}$(CS)Leu2^{myc} [197]) were replaced by the native *PRC1* promoter. The newly generated constructs C*T$_{Pdr5}$(CS)GFP$_{fast}$ and C*T$_{Pdr5}$(CS)Leu2^{HA} are also expressed under the control of the *PRC1* promoter.

C*T$_{Pdr5}$(CS)GFP contains a GFP variant, which is predicted to fold very slowly and is prone to form dimers [249,250]. Now the question arises, if the slowly folding GFP is recognized as being misfolded, which could explain the participation of the cytosolic Ssa1 chaperone in C*T$_{Pdr5}$(CS)GFP degradation. To investigate this question, the GFP variant in C*T$_{Pdr5}$(CS)GFP was exchanged for a superfast folding variant (GFP$_{fast}$) [250], resulting in C*T$_{Pdr5}$(CS)GFP$_{fast}$.

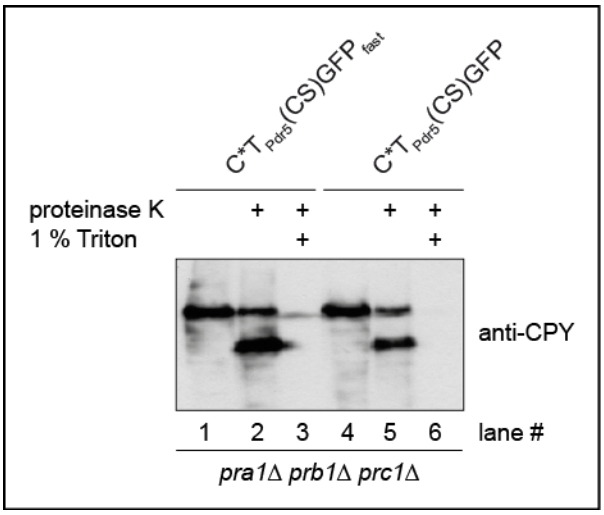

Figure 10: C*T$_{Pdr5}$GFP$_{fast}$ and C*T$_{Pdr5}$GFP are type I membrane proteins with the N-terminal CPY* domain in the ER lumen and a C-terminal GFP in the cytosol.

Microsomes were isolated from lysates of *pra1Δprb1Δprc1Δ* cells, expressing C*T$_{Pdr5}$GFP$_{fast}$ and C*T$_{Pdr5}$GFP. Microsomes were treated for 1 h at 15°C only with buffer or buffer containing either proteinase K (0.5 mg/ml) or proteinase K (0.5 mg/ml) and 1% (v/v) Triton X-100. Digestion was stopped by adding 110 mM PMSF. C*T$_{Pdr5}$GFP$_{fast}$ and C*T$_{Pdr5}$GFP were analyzed by immunoblotting using CPY antibody.

To guarantee that C*T$_{Pdr5}$(CS)GFP$_{fast}$ contains a properly folded cytosolic GFP$_{fast}$ moiety, localization and folding of the construct were determined, the slowly folding GFP- containing variant, C*T$_{Pdr5}$(CS)GFP, served as control. For the localization studies, microsomes were generated and treated with proteinase K, which is a highly active protease with broad cleavage specificity. After proteinase K treatment, all cytosolically exposed proteins and protein domains are digested. The GFP variants are tightly folded, so the digest has to be done at 15°C for 1 hour. In the 2nd and 5th lane of Figure 10 the digested microsomes are shown. There are two bands with different molecular masses, which correspond to the full-length C*T$_{Pdr5}$(CS)GFP$_{fast}$ or C*T$_{Pdr5}$(CS)GFP as well as to the respective truncated versions. Since the truncated versions are detected by immunoblotting using a CPY antibody, it can be presumed that the respective CPY* moieties are protected from proteinase K digestion in the ER lumen and the cytosolically exposed GFP variants are removed. As control full-length C*T$_{Pdr5}$(CS)GFP$_{fast}$ and C*T$_{Pdr5}$(CS)GFP are shown in the fraction containing untreated microsomes (Figure 10; lane 1 and 4). The addition of Triton solubilizes the microsomes and all proteins are exposed for proteinase K digestion (Figure 10; lane 3 and 6).

The ER lumenal CPY* moiety and the cytosolic GFP variant indicates that

C*T$_{Pdr5}$(CS)GFP$_{fast}$ and C*T$_{Pdr5}$(CS)GFP are type I membrane proteins (N$_{out}$; C$_{in}$).

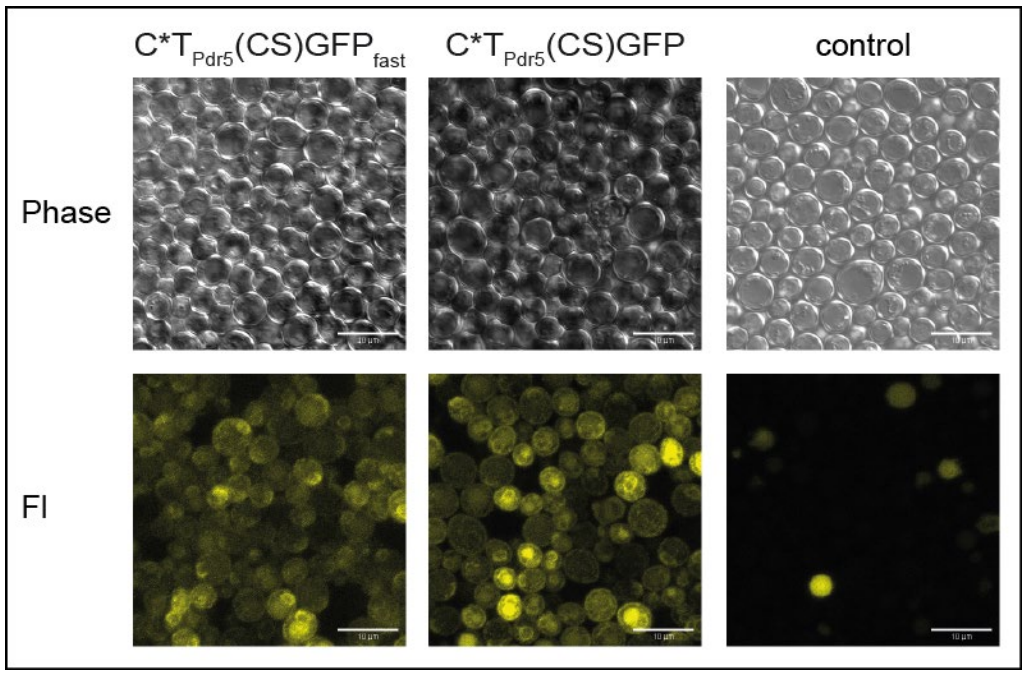

Figure 11: C*T$_{Pdr5}$(CS)GFP$_{fast}$ and C*T$_{Pdr5}$(CS)GFP are ER membrane proteins, containing properly folded GFP variants.

Fluorescence microscopy was used to take images from living cells (*prc1*Δ*hrd1*Δ*doa10*Δ) expressing either C*T$_{Pdr5}$(CS)GFP$_{fast}$, C*T$_{Pdr5}$(CS)GFP or no C*T$_{Pdr5}$(CS)GFP variant. Phase contrast (Phase, upper panel) and fluorescence signals (Fl, lower panel) are shown (scale bar 10 µm).

Folding of the GFP variants was detected by fluorescence microscopy (Figure 11). Cells (*prc1*Δ*hrd1*Δ*doa10*Δ) were taken in which the degradation of C*T$_{Pdr5}$(CS)GFP and C*T$_{Pdr5}$(CS)GFP$_{fast}$ is impaired, to achieve ideal fluorescence signals. The first two pictures of the lower panel in Figure 11 represents fluorescence signals (Fl) of C*T$_{Pdr5}$(CS)GFP$_{fast}$ and C*T$_{Pdr5}$(CS)GFP and indicates that the GFP$_{fast}$ and the GFP moiety of the respective constructs are properly folded. In the negative control, cells expressing no C*T$_{Pdr5}$(CS)GFP variant, solely autofluorescence of the vacuole is detected. Phase contrast images (Phase) of the respective cells are shown in the upper panel of Figure 11.

In conclusion, C*T$_{Pdr5}$(CS)GFP$_{fast}$ as well as C*T$_{Pdr5}$(CS)GFP are type I ER membrane proteins with tightly folded cytoplasmic GFP variant and misfolded ER lumenal CPY* moiety (schematic representation see Figure 9).

Next, it was determined whether the exchange of the slowly folding GFP variant for the superfast folding GFP_{fast} alters the degradation mechanism. The slowly folding GFP variant is recognized by a cytosolic machinery with participation of Ssa1, but is degraded independently of Hul5. The $C^*T_{Pdr5}(CS)$ derivative, which contains a folded Leu2 domain in the cytosol, $C^*T_{Pdr5}(CS)Leu2^{myc}$, requires Hul5 for degradation. Thus, $C^*T_{Pdr5}(CS)GFP_{fast}$ turnover rates were measured in cells lacking Hul5, using cycloheximide-chase analysis. The application of cycloheximide at timepoint 0 min, leads to the inhibition of the ribosomal protein expression. Taking samples at indicated timepoints, degradation kinetics can be measured and analyzed by immunodetection, using appropriate antibodies.

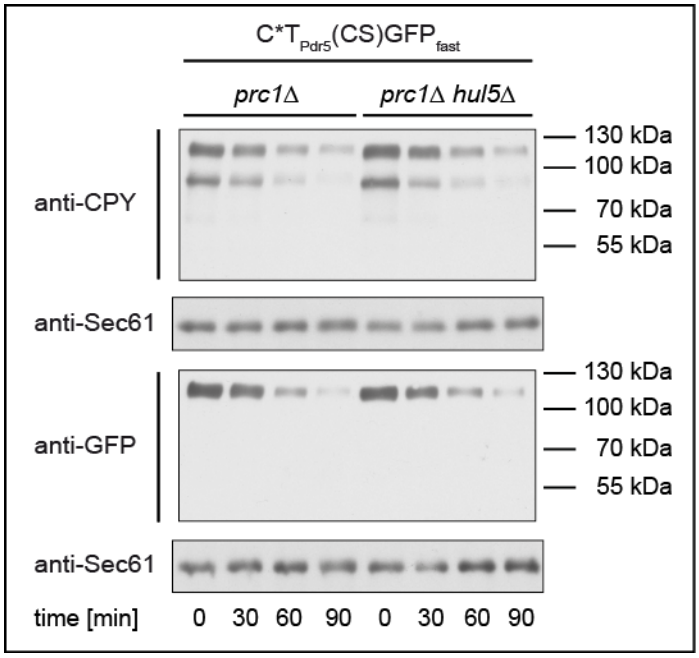

Figure 12: Distinct intermediates occur, Hul5 independent, during the degradation of $C^*T_{Pdr5}(CS)GFP_{fast}$.

Cycloheximide-chase analysis of $C^*T_{Pdr5}(CS)GFP_{fast}$ degradation was performed in *prc1*Δ and *prc1*Δ*hul5*Δ cells. Samples were taken every 30 min after cycloheximide addition. $C^*T_{Pdr5}(CS)GFP_{fast}$ was detected by immunoblotting using CPY antibody and GFP antibody. Sec61 was used as loading control.

The upper part of Figure 12 shows that $C^*T_{Pdr5}(CS)GFP_{fast}$ is degraded via an intermediate. Full-length $C^*T_{Pdr5}(CS)GFP_{fast}$ has a molecular mass of approximately 110 kDa, and the degradation intermediate has a molecular mass of approx. 80 kDa. Both appear after immunoblotting using a CPY antibody. Degradation of $C^*T_{Pdr5}(CS)GFP_{fast}$ is independent of Hul5, since the degradation intermediate appears

also in the presence of Hul5. Full-length C*T$_{Pdr5}$(CS)GFP$_{fast}$ is solely found after immunoblotting using GFP antibody (Figure 12). Solely the membrane fraction is enriched during sample preparation (chapter 2.5.10). Thus, it can be assumed that the degradation intermediate is still membrane-bound. Since it is detected after immunoblotting with CPY antibody and has a molecular mass of approximately 80 kDa, the degradation intermediate seems to be composed of CPY* and the transmembrane domain, resulting in a C*T$_{Pdr5}$(CS) variant. Over time, this intermediate is further degraded. Thus, C*T$_{Pdr5}$(CS) might be an appropriate substrate to analyze the degradation mechanisms of ERAD.

There was also the question, whether the myc-Tag at the cytosolic part of C*T$_{Pdr5}$(CS)Leu2^{myc} affects degradation. Therefore, it was substituted for a single HA-Tag and turnover rates were determined in *prc1*Δ and *prc1*Δ*hul5*Δ cells.

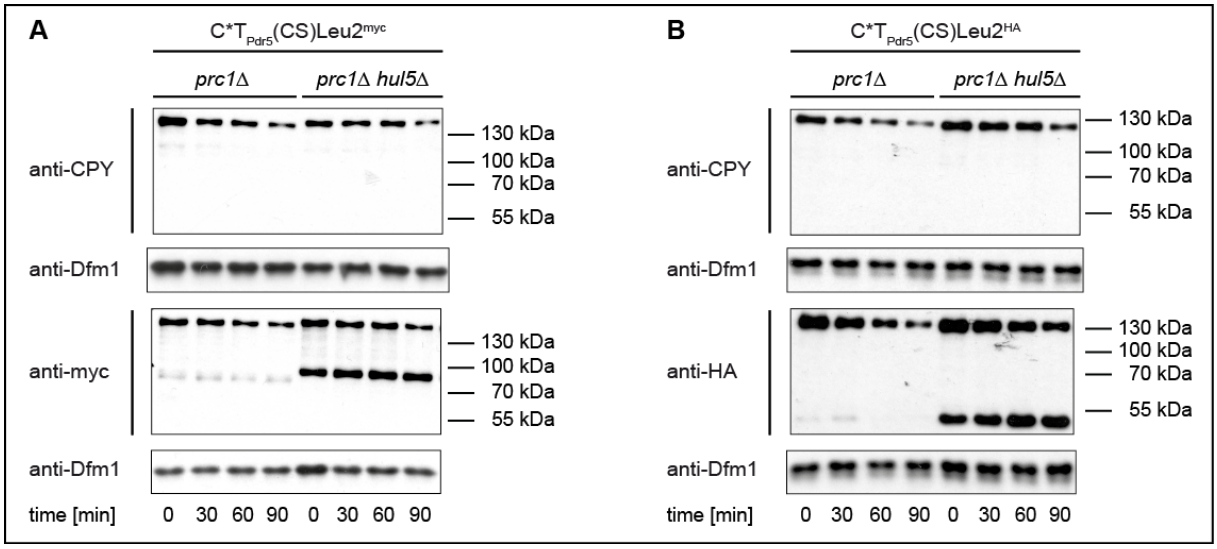

Figure 13: Distinct intermediates occur during the degradation of C*T$_{Pdr5}$(CS)Leu2^{myc} and C*T$_{Pdr5}$(CS)Leu2^{HA}, which are enriched in cells lacking Hul5.

Cycloheximide-chase analysis of C*T$_{Pdr5}$(CS)Leu2^{myc} (**A**) and C*T$_{Pdr5}$(CS)Leu2^{HA} (**B**) degradation were performed in *prc1*Δ and *prc1*Δ*hul5*Δ cells. Samples were taken every 30 min after cycloheximide addition and both, C*T$_{Pdr5}$(CS)Leu2^{myc} and C*T$_{Pdr5}$(CS)Leu2^{HA} were detected by immunoblotting using CPY, myc and HA antibody as indicated. The ER membrane protein Dfm1 was used as loading control.

Figure 13 illustrates that in addition to the respective full-length constructs a truncated version of C*T$_{Pdr5}$(CS)Leu2^{myc} and C*T$_{Pdr5}$(CS)Leu2^{HA} accumulates in the Hul5 deficient cells, but to a smaller extent than in the presence of Hul5. The truncated versions are detected only with myc or HA antibody, respectively, and not after

immunoblotting using CPY antibody. Thus, the truncated versions correspond to T_{Pdr5}(CS)Leu2^{myc} and T_{Pdr5}(CS)Leu2^{HA}.
It can be concluded that the myc-Tag does not serve as a degron signal.

In summary, the "*bona fide* set of substrates", C*T_{Pdr5}(CS)GFP, C*T_{Pdr5}(CS)GFP$_{fast}$, C*T_{Pdr5}(CS)Leu2^{myc} and C*T_{Pdr5}(CS)Leu2^{HA} have the C*T_{Pdr5}(CS) core containing an ER lumenal misfolded CPY* moiety in common, but are degraded differently. This calls for a closer look at the variables for the various degradation pathways.
But first, it should be analyzed whether Hul5 is required to degrade the common core C*T_{Pdr5}(CS). For analyzation, an HA epitope was added to the cytosolic part and thus, C*T_{Pdr5}(CS)^{HA} was generated (Figure 14).

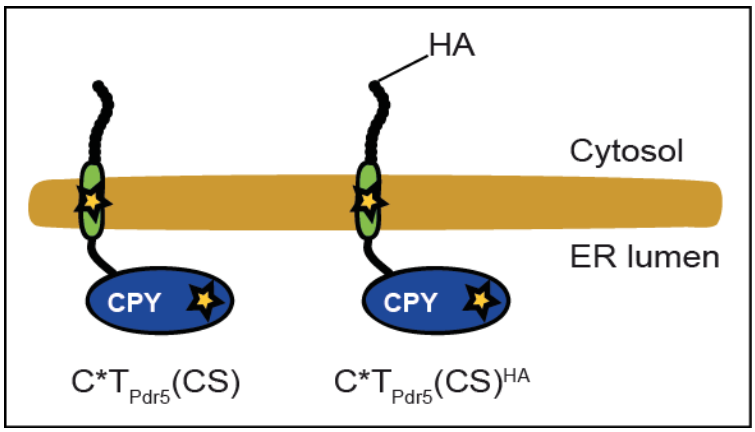

Figure 14: Schematic representation of ERAD substrates C*T_{Pdr5}(CS) and C*T_{Pdr5}(CS)^{HA}.
The oval structure marked with an asterisk symbolizes the misfolded carboxypeptidase domain (C*), followed by a single-spanning transmembrane helix, shown in green. The membrane domain labeled with a yellow asterisk represents the last transmembrane helix from the multidrug transporter Pdr5 (T_{Pdr5}). The black chain located in the cytosolic part of the C*T derivatives represents a peptide of 12 amino acids, originating from the C-terminal tail of Pdr5 (CS). The cytosolic part of C*T_{Pdr5}(CS)^{HA} is tagged with a single HA epitope (YPYDVPDYA).

First, localization studies were performed, to determine whether C*T_{Pdr5}(CS)^{HA} is an integral membrane protein. Microsomes were generated from crude lysate of cells lacking the main vacuolar proteases (*pra1*Δ*prb1*Δ*prc1*Δ). This strain was selected to prevent unspecific protein degradation by the highly active and robust vacuolar proteases. To exclude contamination of the microsomal fraction with cytosolic proteins, the cytosolic phosphoglycerate kinase (PGK) was analyzed. Microsomes were treated with detergent and finally pellet (microsomes) and supernatant 1 (S) were separated by centrifugation. Treatment of the microsomes with 1 M potassium acetate (KAc) or

2.5 M urea removed peripheral proteins. Treatment with 0.1 M sodium carbonate (Na_2CO_3) removed proteins with distinct topologies; such as peripheral proteins on the microsomal surface, as well as all proteins, which were captured in the microsomes and peripheral proteins, located at the inner membrane of the microsomes. Treatment with 1% SDS or 1% Triton solubilized the microsomes, and all proteins were released into the supernatant 2 (SN).

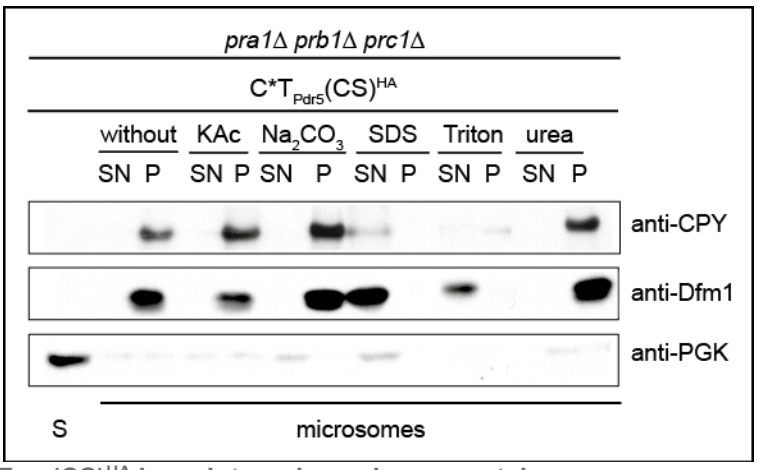

Figure 15: C*T$_{Pdr5}$(CS)^{HA} is an integral membrane protein.

Microsomes and supernatant 1 (S) were separated from lysate of *pra1Δprb1Δprc1Δ* cells expressing C*T$_{Pdr5}$(CS)^{HA}. Microsomes were treated only with buffer (without) or buffer containing either 1 M potassium acetate (KAc) or 0.1 M sodium carbonate (Na_2CO_3) or 1% (w/v) SDS (SDS) or 1% (v/v) Triton X-100 (Triton) or 2.5 M urea (urea), followed by centrifugation. Receiving supernatant 2 (SN) and pellet (P), which were analyzed by immunoblotting. C*T$_{Pdr5}$(CS)^{HA} was detected using CPY antibody. The integral ER membrane protein Dfm1 was visualized using Dfm1 antibody. As control for separating supernatant 1 (S) and microsomes, the soluble cytosolic protein PGK was detected using PGK antibody.

As illustrated in Figure 15 C*T$_{Pdr5}$(CS)^{HA} is still in the membrane fraction although the microsomes were treated with potassium acetate, sodium carbonate or urea. It is only released when the microsomes were completely solubilized with SDS or Triton, respectively. As positive control, the integral ER membrane protein Dfm1 was analyzed. As expected, it was shown that C*T$_{Pdr5}$(CS)^{HA} and Dfm1 are integral ER membrane proteins.

In addition, it was investigated, if the CPY* moiety of C*T$_{Pdr5}$(CS)^{HA} is located in the ER lumen and thus C*T$_{Pdr5}$(CS)^{HA} is a type I membrane protein. Therefore, proteinase protection assays were performed with intact microsomes (Figure 16). Microsomes were treated only with buffer or buffer containing either proteinase K or proteinase K and 1% Triton. Proteinase K is a highly active protease with broad cleavage specificity.

After proteinase K treatment cytosolically exposed protein domains are digested.

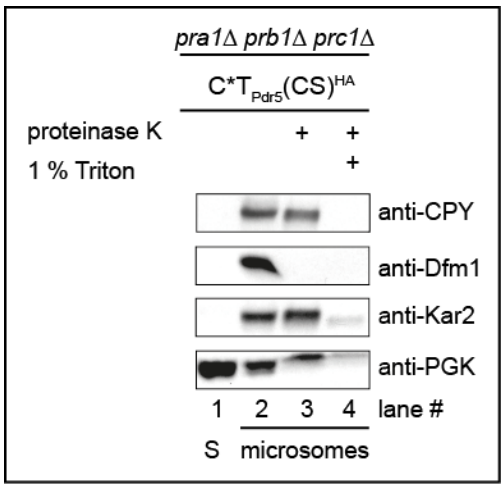

Figure 16: C*T$_{Pdr5}$(CS)^{HA} is a membrane protein with the N-terminal CPY* domain in the ER lumen and a C-terminal tail (CS) containing an HA-Tag in the cytosol.

Microsomes and supernatant (S) were separated from lysate of *pra1Δprb1Δprc1Δ* cells expressing C*T$_{Pdr5}$(CS)^{HA}. Microsomes were treated only with buffer or buffer containing either proteinase K (0.5 mg/ml) or proteinase K (0.5 mg/ml) and 1% (v/v) Triton X-100. Digestion was stopped by adding 110 mM PMSF. C*T$_{Pdr5}$(CS)^{HA} was analyzed by immunoblotting using CPY antibody. The ER membrane protein Dfm1 was visualized using Dfm1 antibody. Kar2, as a control for ER lumenal soluble proteins, was analyzed using Kar2 antibody. As a control for separating supernatant (S) and microsomes, the soluble cytosolic protein PGK was detected using PGK antibody.

Figure 16 reveals that the CPY* moiety of C*T$_{Pdr5}$(CS)^{HA} is protected from proteinase K digestion (Figure 16; lane 3; anti-CPY). As a control, the integral ER membrane protein Dfm1, containing several transmembrane helices [147,251], is shown to be digested (Figure 16; lane 3; anti-Dfm1). As positive control, Kar2 is analyzed. As a soluble ER lumenal protein, it is captured in the microsomes, and not accessible to proteinase K digestion (Figure 16; lane 3; Kar2 detection).
This proves that C*T$_{Pdr5}$(CS)^{HA} is an integral membrane protein with type I orientation (N_{out}; C_{in}), carrying the CPY* moiety in the ER lumen.

Finally, it is analyzed whether Hul5 is involved in degradation of C*T$_{Pdr5}$(CS)^{HA}.

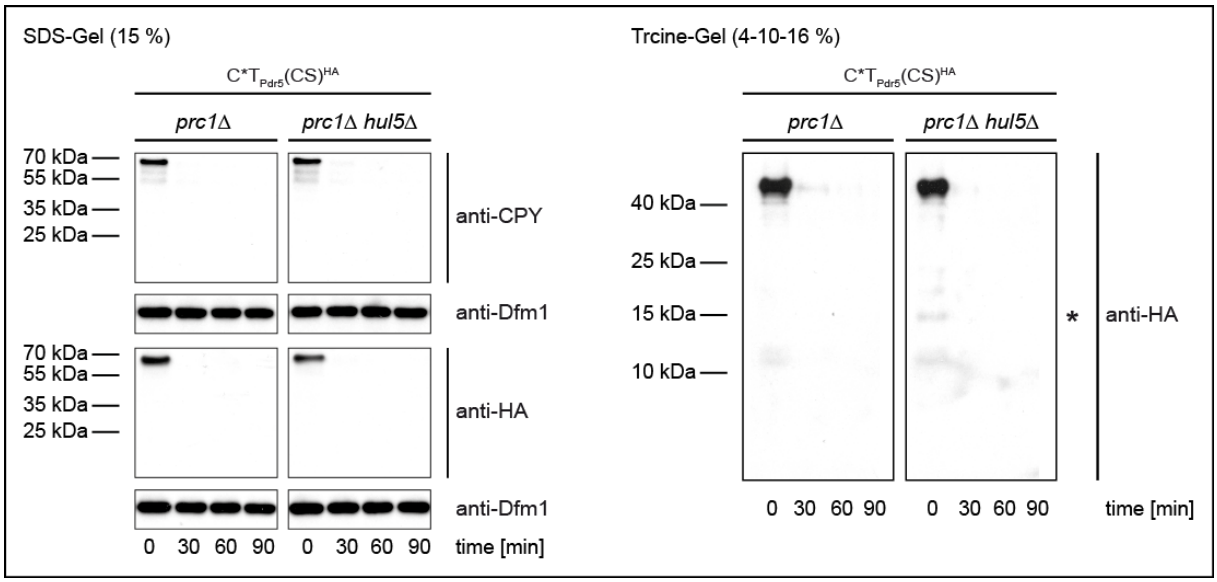

Figure 17: Distinct intermediates occur during the degradation of C*T$_{Pdr5}$(CS)^{HA}.
Cycloheximide-chase analysis of C*T$_{Pdr5}$(CS)^{HA} degradation was performed in *prc1*Δ and *prc1*Δ*hul5*Δ cells.
Samples were taken every 30 min after cycloheximide addition. Proteins were separated in gel electrophoresis using a 15% SDS-gel and a 4-10-16% Tricin-gel. C*T$_{Pdr5}$(CS)^{HA} was detected by immunoblotting using CPY antibody and HA antibody. Dfm1 was used as loading control.

Figure 17 shows turnover rates of C*T$_{Pdr5}$(CS)^{HA} in *prc1*Δ and *prc1*Δ*hul5*Δ cells. The left side illustrates separation on a 15% SDS-gel. Immunoblotting using CPY antibody indicated full-length C*T$_{Pdr5}$(CS)^{HA} as well as degradation intermediates with smaller molecular masses. Immunoblotting with HA antibody indicates only full-length C*T$_{Pdr5}$(CS)^{HA}, using a 15% SDS-gel. On the right side the same samples were separated on a 4-10-16% Tricin-gel. Immunoblotting with HA antibody reveals a degradation intermediate of C*T$_{Pdr5}$(CS)^{HA}, with a molecular mass of approx. 15 kDa, in the absence of Hul5 (Figure 17; right side highlited with an asterisk). Since the signal is very weak, exposure over longer time period is shown in Figure S1. Thus, it can be assumed that C*T$_{Pdr5}$(CS)^{HA} is degraded via a membrane-bound intermediate, which is composed of the cytosolic part containing the HA-Tag and membrane domain of C*T$_{Pdr5}$(CS)^{HA}, since solely the membrane fractions are enriched during sample preparation. In addition, Hul5 facilitates degradation of the intermediate, because an accumulation of the intermediate occurs in the absence of Hul5.

In summary, degradation of the "*bona fide* set of substrates", C*T$_{Pdr5}$(CS)GFP, C*T$_{Pdr5}$(CS)GFP$_{fast}$, C*T$_{Pdr5}$(CS)Leu2^{myc} and C*T$_{Pdr5}$(CS)Leu2^{HA} differs although they are composed of a misfolded ER lumenal domain, an aberrant membrane part and a

properly folded cytosolic domain. On account of this, they are not adequate substrates to search for differences in ERAD-L and ERAD-M pathways. They all contain the membrane-anchored CPY*, known as C*T$_{Pdr5}$(CS), this substrate serves as basis to establish an additional set of ERAD substrates, which is shown in the following chapter.

3.1.2 Transforming old into new, the C*T derivatives

C*T$_{Pdr5}$(CS) is composed of the mutated misfolded carboxypeptidase (CPY*) in the ER lumen. It further contains the last transmembrane helix of Pdr5, which was generated to analyze the degradation of membrane-bound ERAD-L substrates [196]. Interestingly, both substrates, membrane-bound C*T$_{Pdr5}$(CS) and ER lumenal, soluble CPY*, are degraded via different pathways (an overview is given in Table 15).

Table 15: Overview of key components required for degradation of the CPY* and the membrane-bound C*T$_{Pdr5}$(CS)

A green check mark indicates essential for degradation; a red cross symbol means dispensable for degradation; ~ (tilde) means involved in but not absolutely necessary for degradation. The analyzed ERAD components are Der1, a membrane protein, the ubiquitin ligase Hrd1, the ER lumenal Hsp70 chaperones Kar2 and the AAA ATPase Cdc48.

	Der1	Hrd1	Kar2	Cdc48
CPY*	✓	✓	✓	✓
C*T$_{Pdr5}$(CS)	✗	~	✗	✓

CPY* and C*T$_{Pdr5}$(CS) are degraded via the ubiquitin-proteasome system (UPS) [43,44,196]. Prior to degradation both substrates require Cdc48 to be extracted out of the ER [105,190,196]. While CPY* degradation is completely abolished in cells lacking the ER membrane embedded ubiquitin ligase Hrd1, C*T$_{Pdr5}$(CS) is not fully stabilized [53,196]. This indicates that another ubiquitin ligase must be involved in C*T$_{Pdr5}$(CS) degradation. Furthermore, in contrast to CPY* degradation, C*T$_{Pdr5}$(CS) is independently degraded of the ER membrane-embedded Der1 [62,196].This is surprising, since it was shown that Der1 is recruited to the *HRD* ligase complex, built by Hrd1 and the misfolding receptor Hrd3 [41,42,60] and is therefore indispensable for ERAD-L substrate degradation. Additionally, in contrast to soluble ERAD-L substrate degradation, membrane-bound C*T$_{Pdr5}$(CS) degradation is independent of the Hsp70

chaperone Kar2 [49,196]. This is puzzling, since Kar2 scaffolds misfolded ER lumenal proteins. It retains them until they are either modified and folded or eliminated by ERAD [196].

Vashist and Ng as well as Carvalho *et al.* defined Der1 as a central player of the ERAD-L pathway and showed that Der1 is dispensable for the ERAD-M pathway [41,42].

The transmembrane domain of C*T$_{Pdr5}$(CS), originates from Pdr5, a multi-spanning membrane protein. This single helix bears polar residues, which can build up interactions with the other membrane helices of Pdr5 in its native environment. As orphan helix, the polar residues could lead to misfolding and be a determinant for retention and degradation [196]. Thus, the transmembrane domain of C*T$_{Pdr5}$(CS) could possibly be a degron. This could be an explanation for the fundamentally different degradation behavior of CPY* and C*T$_{Pdr5}$(CS). Furthermore, C*T$_{Pdr5}$(CS) might be degraded via an ERAD-M mechanism and not by the ERAD-L pathway.

Before analyzing the C*T$_{Pdr5}$(CS) degradation mechanism in more detail, additional considerations should be made.

C*T$_{Pdr5}$(CS) is expressed under the control of the strong *TDH3* promoter (P$_{TDH3}$). Overexpression of misfolded ER proteins, however, leads to ER stress and ERAD saturation. Under such stress conditions the unfolded protein response (UPR) is activated and proteins are in part degraded in the vacuole [252].

According to this, any influence of C*T$_{Pdr5}$(CS) overexpression by the *TDH3* promoter must be excluded. Therefore, the *TDH3* promoter and the *TDH3* terminator were substituted for the *PRC1* promoter (P$_{PRC1}$) and *PRC1* terminator (T$_{PRC1}$).

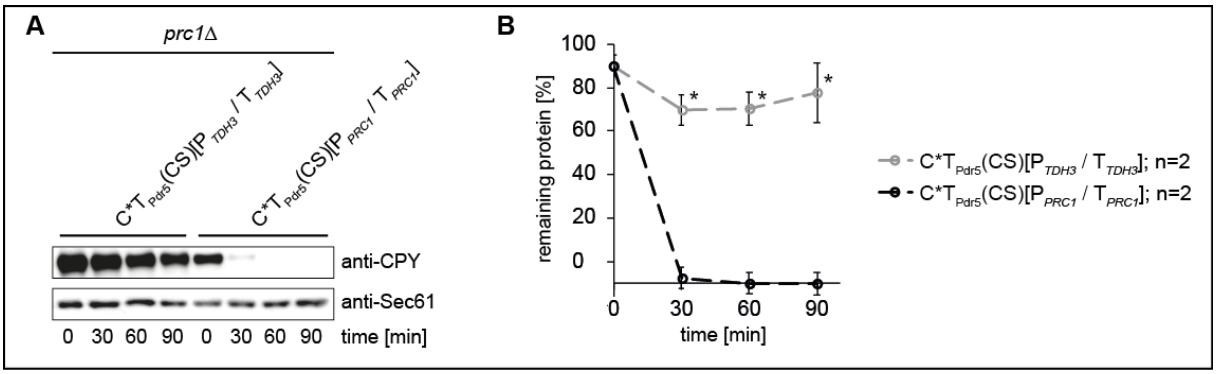

Figure 18: Expression of C*T$_{Pdr5}$(CS) under the control of the *PRC1* promoter and the *PRC1* terminator.

A: Cycloheximide-chase analysis of C*T$_{Pdr5}$(CS) degradation was performed in *prc1*Δ cells. Samples were taken every 30 min after cycloheximide addition and C*T$_{Pdr5}$(CS) was detected by immunoblotting using CPY antibody. Sec61 was used as loading control.
B: The quantification represents the data of two independent experiments. Error bars indicate the respective standard error of the mean (SEM). *P < 0.05, unpaired two-sample *t*-test.

Substitution of the *TDH3* promoter and terminator for the *PRC1* promoter and terminator results in much less C*T$_{Pdr5}$(CS) protein in the cell (Figure 18). These protein amounts are ideal to follow the protein in further experiments.

With the established C*T$_{Pdr5}$(CS) [P$_{PRC1}$; T$_{PRC1}$] construct degradation kinetics of the substrate in cells lacking Der1 had to be repeated, because Vashist and Ng [41] attribute a critical role for Der1 in ERAD-L but not in ERAD-M substrate degradation.

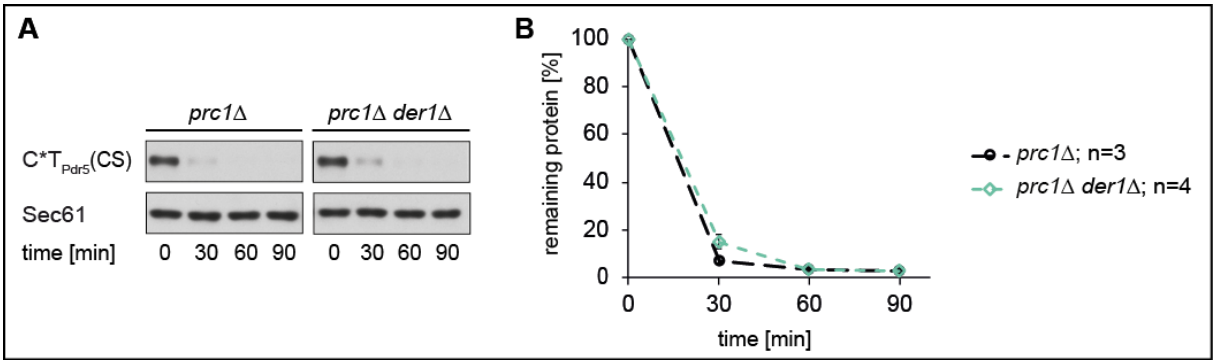

Figure 19: C*T$_{Pdr5}$(CS) is a member of the ERAD-M substrate family due to its Der1 independent degradation.

A: Cycloheximide-chase analysis of C*T$_{Pdr5}$(CS) degradation was performed in *prc1*Δ and *prc1*Δ*der1*Δ cells.
Samples were taken every 30 min after cycloheximide addition (t=0 min) and C*T$_{Pdr5}$(CS) was detected by immunoblotting using CPY antibody. Sec61 was used as loading control.
B: The quantification represents the data of up to four independent experiments. Error bars indicate the respective standard error of the mean (SEM). *P < 0.05, unpaired two-sample *t*-test relative to the control (*prc1*Δ).

Figure 19 shows that Der1 is dispensable for degradation of the C*T$_{Pdr5}$(CS) construct, expressed under control of the native *PRC1* promoter and the *PRC1* terminator. On contrary, degradation of the soluble ERAD-L substrate CPY* is dependent on Der1 [62]. This supports the hypothesis that C*T$_{Pdr5}$(CS) is degraded via the ERAD-M pathway, despite the fact that it contains a fully ERAD-L compatible lumenal protein portion: CPY*.

Recently, it was shown that the Der1 homolog Dfm1 (Der1-like family member) [147] is responsible for the retrotranslocation of the *bona fide* ERAD-M substrate HMG2-GFP [106]. Consequently, it was analyzed whether Dfm1 is involved in degradation of the expected ERAD-M substrate C*T$_{Pdr5}$(CS). Since it was shown that cells can undergo rapid suppression in the absence of Dfm1, in case of ERAD-M substrate overexpression [106], all cells (*prc1*Δ*dfm1*Δ *and prc1*Δ*der1*Δ*dfm1*Δ) were always freshly transformed with plasmid encoding the various C*T derivatives, before use in experiments.
To exclude any possible overlapping function of the homologous pair, Der1 and Dfm1, in the degradation of C*T$_{Pdr5}$(CS), degradation kinetics were also performed in *prc1*Δ*der1*Δ*dfm1*Δ cells (Figure 20).

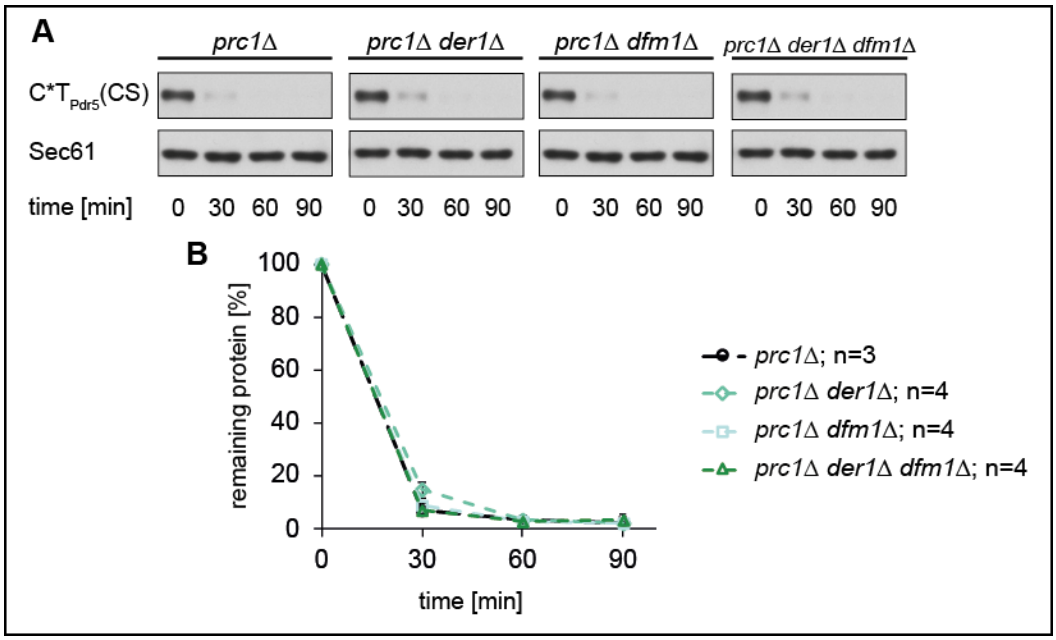

Figure 20: Dfm1 is not required for degradation of C*T$_{Pdr5}$(CS).

A: Cycloheximide-chase analysis of C*T$_{Pdr5}$(CS) degradation was performed in *prc1*Δ; *prc1*Δ*der1*Δ; *prc1*Δ*dfm1*Δ and *prc1*Δ*der1*Δ*dfm1*Δ cells.
Samples were taken every 30 min after cycloheximide addition (t=0 min) and C*T$_{Pdr5}$(CS) was detected by immunoblotting using CPY antibody. Sec61 was used as loading control.
B: The quantification represents the data of up to four independent experiments. Error bars indicate the respective standard error of the mean (SEM). *P < 0.05, unpaired two-sample *t*-test relative to the control (*prc1*Δ).

Figure 20 indicates that Dfm1 does not participate in the degradation of C*T$_{Pdr5}$(CS). An overlapping function of Der1 and Dfm1 is not observed, because there is no additional stabilization of C*T$_{Pdr5}$(CS) in *prc1*Δ*der1*Δ*dfm1*Δ cells.

The next question was, which ubiquitin ligases participate in ubiquitination of C*T$_{Pdr5}$(CS). In the absence of the ubiquitin ligase Hrd1, C*T$_{Pdr5}$(CS) degradation is only slightly impaired ([196] and Figure 21). Thus, another ubiquitin ligase in addition to Hrd1 seems to be involved in ubiquitination of C*T$_{Pdr5}$(CS). It was shown that the Asi complex participates in ubiquitination of ERAD-M substrates [155,156]. The Asi complex, which is located in the inner nuclear membrane (INM), consists of two RING Ubiquitin ligases, Asi1 and Asi3 [67,68]. ER proteins with intracellular domains smaller than 60 kDa are able to move to the INM and thus C*T$_{Pdr5}$(CS) seems to be accessible for the Asi complex. In cycloheximide-chase analysis degradation kinetics of C*T$_{Pdr5}$(CS) were determined in cells lacking components of either the Asi complex or Hrd1 or both ligases (Figure 21).

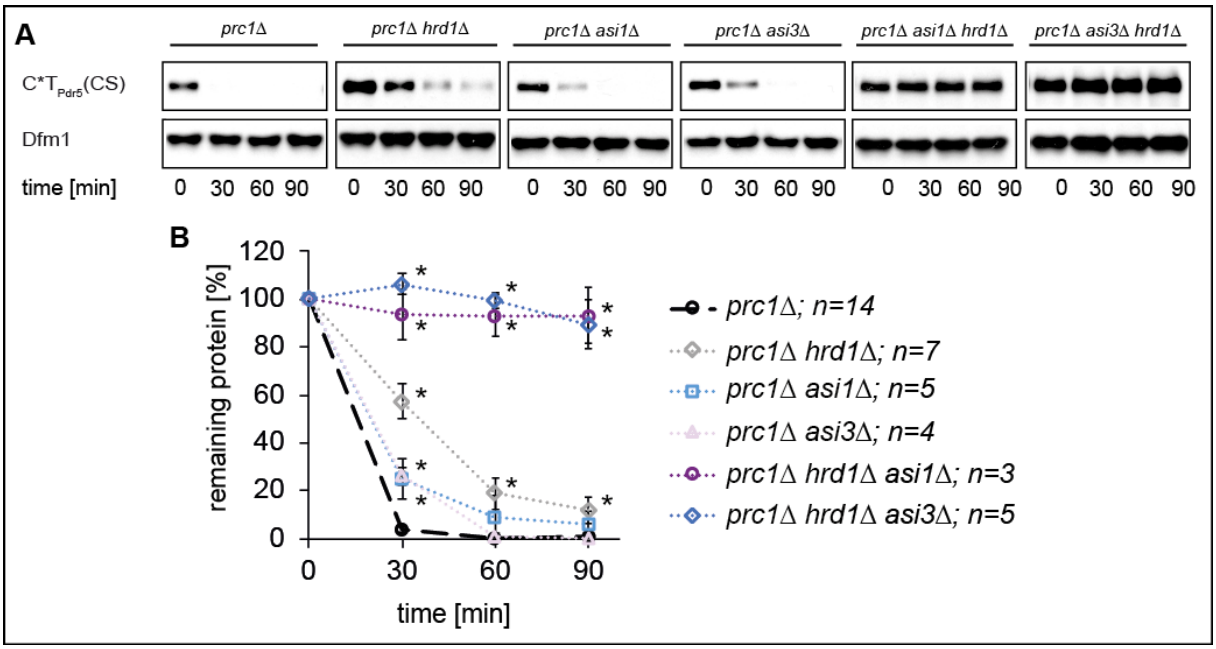

Figure 21: C*T_{Pdr5}(CS) degradation is Hrd1 and Asi complex dependent.

A: Cycloheximide-chase analysis of C*T_{Pdr5}(CS) degradation was performed in *prc1Δ; prc1Δhrd1Δ; prc1Δasi1Δ; prc1Δasi3Δ; prc1Δhrd1Δasi1Δ* and *prc1Δhrd1Δasi3Δ* cells.
Samples were taken every 30 min after cycloheximide addition (t=0 min) and C*T_{Pdr5}(CS) was detected by immunoblotting using CPY antibody. Dfm1 was used as loading control.
B: The quantification represents the data of up to 14 independent experiments. Error bars indicate the respective standard error of the mean (SEM). *P < 0.05, unpaired two-sample *t*-test relative to the control (*prc1Δ*).

Deletion of either Asi1, Asi3 or Hrd1 have only minor effect on degradation of C*T_{Pdr5}(CS). However, C*T_{Pdr5}(CS) is completely stabilized in cells depleted of Hrd1 and components of the Asi complex (Figure 21). This shows that the ubiquitin ligases Hrd1 and the Asi complex are prerequisites for degradation of C*T_{Pdr5}(CS), able to take over the ubiquitination process when one or the other ligase is missing.

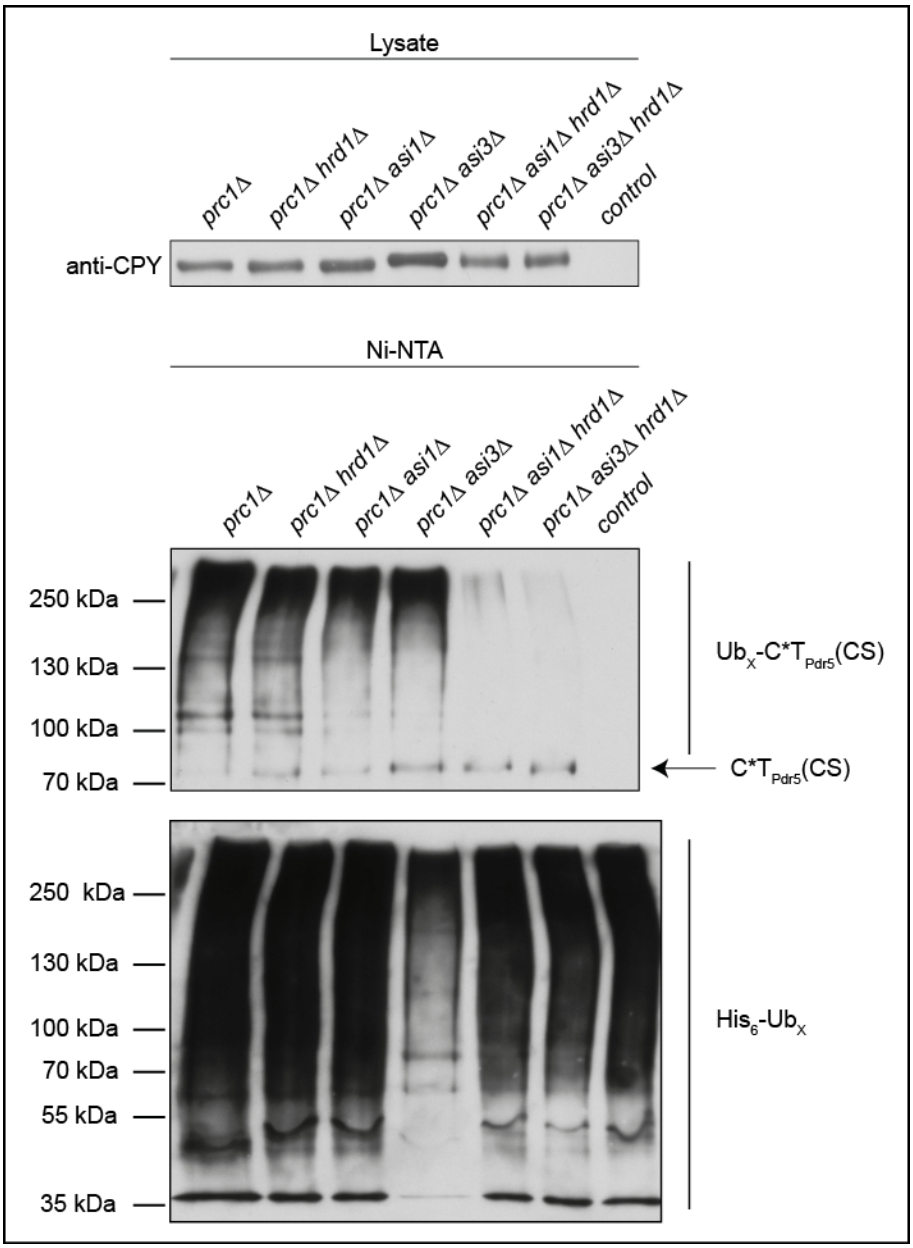

Figure 22: Hrd1 and the Asi complex are responsible for ubiquitination of C*T$_{Pdr5}$(CS).
Ubiquitination was analyzed in cells (genotype as indicated) expressing C*T$_{Pdr5}$(CS) and His$_6$-tagged ubiquitin (Ub). Cell lysates (input) were incubated with Ni-NTA resin under denaturing conditions to pull down all His$_6$-ubiquitinated proteins. C*T$_{Pdr5}$(CS) was detected by immunoblotting with CPY antibody and His antibody was used to visualize all bound Ub$_X$-proteins.

In vivo ubiquitination assays were performed according to the instructions described in chapter 2.5.11 of the material and methods part, to analyze whether Hrd1 and the Asi complex are indeed involved in polyubiquitination of C*T$_{Pdr5}$(CS). Briefly His$_6$-tagged ubiquitin and C*T$_{Pdr5}$(CS) were co-expressed in cells with genotypes as indicated. Cells used for ubiquitination assays were deficient of endogenous CPY. All polyubiquitinated proteins, modified with His$_6$-Tag, were captured by a Ni-NTA resin.

Figure 22 reveals that polyubiquitination of C*T$_{Pdr5}$(CS) is not affected in cells lacking Hrd1. In contrast, polyubiquitination of C*T$_{Pdr5}$(CS) is slightly reduced in cells, which are deficient in components of the Asi complex. Double deletion of the Asi complex and Hrd1 leads to non-ubiquitinated C*T$_{Pdr5}$(CS).

This demonstrates that the ubiquitin ligases Hrd1 and the Asi complex are responsible for ubiquitination and degradation of C*T$_{Pdr5}$(CS). Obviously, the absence of any of the two ligases leaves enough capacity to nearly fully polyubiquitinate the substrate.

In summary, it was shown that the C*T$_{Pdr5}$(CS) construct – under the control of native *PRC1* promoter and *PRC1* terminator – is degraded independently of Der1. For its degradation the ubiquitin ligases Hrd1 and the Asi comlex are required. In contrast, the *bona fide* ERAD-L substrate CPY* is degraded Der1 dependent and polyubiquitination of CPY* is only achieved by the ubiquitin ligase Hrd1 [53,62].

Thus, it can be postulated that the membrane domain of C*T$_{Pdr5}$(CS) signals for an ERAD-M degradation mechanism, although C*T$_{Pdr5}$(CS) contains in addition a misfolded ER lumenal CPY* moiety in the ER lumen.

Next, it was analyzed whether the lesion in the membrane part of C*T$_{Pdr5}$(CS) is sufficient for retention or whether the CPY* moiety is required.

Therefore, carboxypeptidase Y activity assay was performed, according to the instructions described in chapter 2.5.9 of the materials and methods part. In brief, cells expressing the ERAD substrate C*T$_{Pdr5}$(CS) and the respective control substrate CT$_{Pdr5}$(CS) containing the active CPY are incubated for 12 hours with *N*-benzoyl-L-tyrosine *p*-nitroanilide (BTpNA), which is a substrate for the fully active carboxypeptidase Y (CPY) in the vacuole.

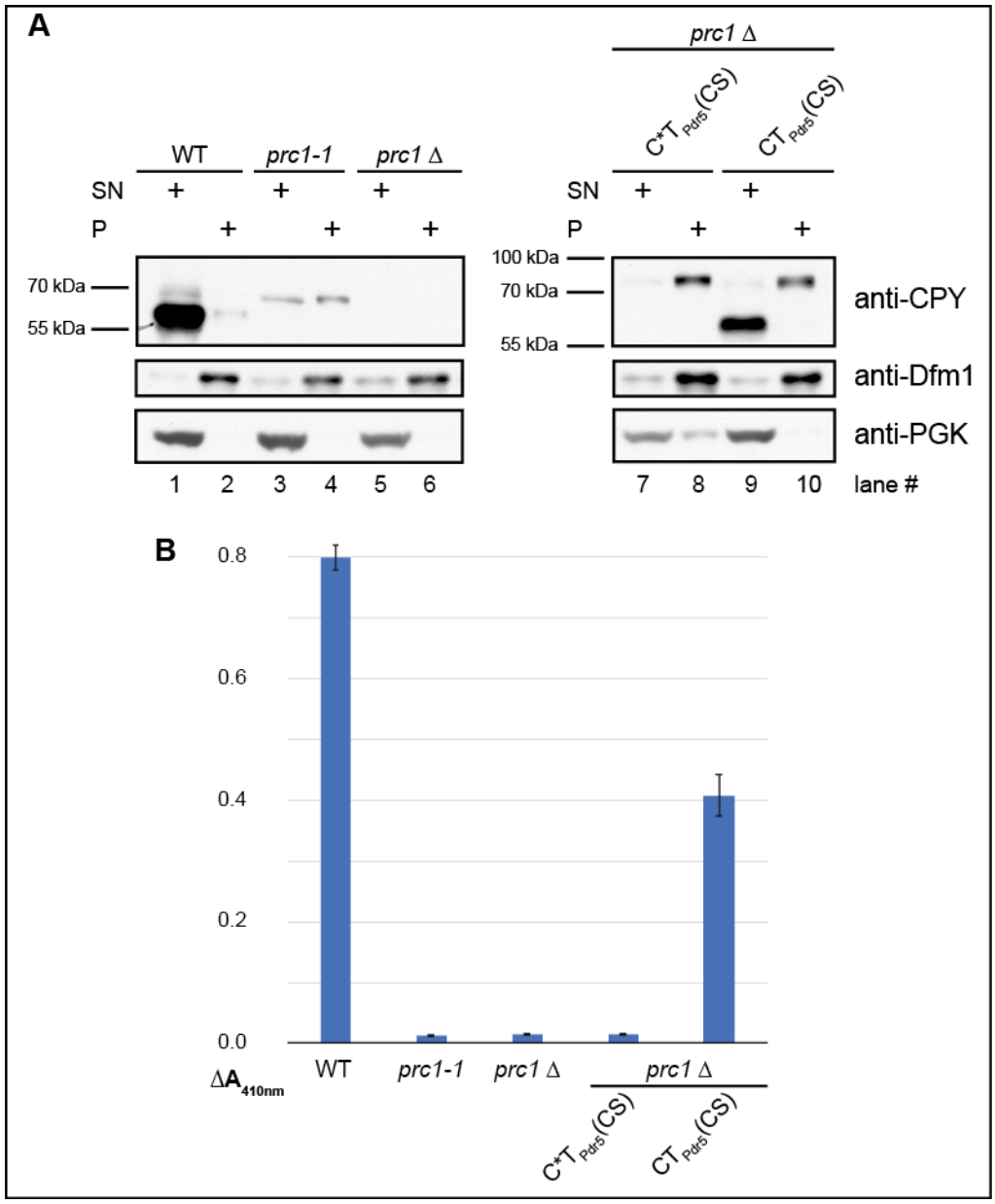

Figure 23: ER lumenal CPY* moiety of C*T$_{Pdr5}$(CS) is required for retention in the ER

A: Localization of the carboxypeptidase Y (CPY) and its derivatives (WT, endogenous CPY; *prc1-1*, endogenous CPY*; *prc1*Δ, lacking endogenous CPY) was determined in cells expressing the indicated variants. Pellet (P) and supernatant (SN) were separated from lysate and analyze by immunoblotting. CPY variants were detected using CPY antibody. The integral ER membrane protein Dfm1 was visualized using Dfm1 antibody. As control for separating pellet and supernatant, the soluble cytosolic protein PGK was detected using PGK antibody.
B: Cells were incubated for 12 h with BTpNA and absorbance was measured at 410 nm (ΔA_{410nm}). The quantification represents the data of five independent experiments. Error bars indicate the respective standard error of the mean (SEM). *P < 0.05, unpaired two-sample *t*-test relative to the control (WT).

Active CPY can be found in the vacuole (Figure 23 A; lane 1), there it is able to cleave BTpNA, generating a yellow product. Its absorbance can be measured at a wavelength of 410 nm (Figure 23 B; WT). Mutated carboxypeptidase (CPY*) is retained in the ER

(Figure 23 A; lane 4) and is not able to cleave BTpNA (Figure 23 B; *prc1-1*). In cells expessing CT_{Pdr5}(CS) turnover of BTpNA can be measured (Figure 23 B) and a CPY moiety in the vacuole (SN) occurs (Figure 23 A; lane 9). In cells expressing C^*T_{Pdr5}(CS), which contains a misfolded carboxypeptidase moiety, BTpNA turnover does not occur (Figure 23 B). In addition, C^*T_{Pdr5}(CS) was found in the membrane fraction (Figure 23 A; lane 8), indicating a retention of C^*T_{Pdr5}(CS) in the ER membrane.
This shows that the ER lumenal misfolded CPY* moiety and not the aberrant membrane part of C^*T_{Pdr5}(CS) leads to ER retention.

Based on the ERAD-M substrate C^*T_{Pdr5}(CS), a substrate with a properly folded membrane domain, should be generated to determine the mechanism of ERAD-L substrate degradation. The newly generated substrate should be expressed under the same expression conditions [P_{PRC1}; T_{PRC1}] than C^*T_{Pdr5}(CS). Therefore, the T_{Pdr5} has to be substituted for a native transmembrane domain, which is single spanning without polar residues. Possible interactions with ER proteins have to be excluded, because they might indirectly influence ERAD targeting. The transmembrane domain of the plasma membrane protein Wsc1 was selected [41,253], resulting in C^*T_{Wsc1}(CS). A schematic representation of C^*T_{Wsc1}(CS) is shown in Figure 24.

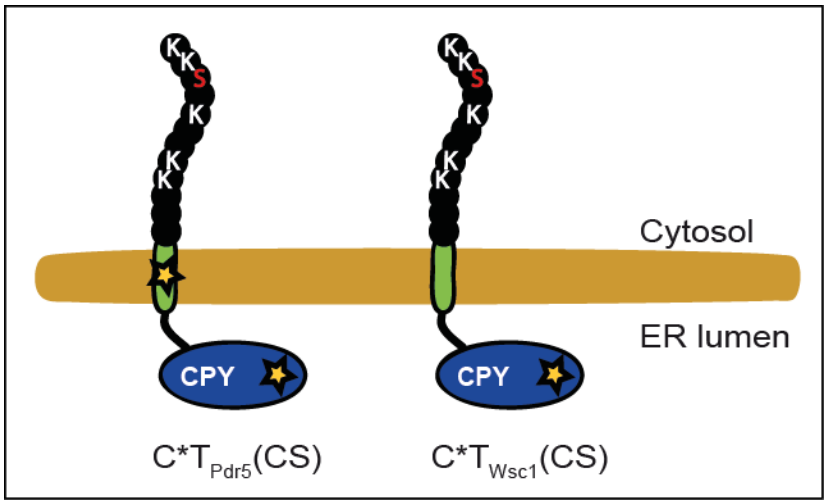

Figure 24: Schematic representation of ERAD substrates C*T$_{Pdr5}$(CS) and C*T$_{Wsc1}$(CS).
The oval structure marked with an asterisk symbolizes the misfolded carboxypeptidase domain (C*), followed by a single-spanning transmembrane helix, shown in green. The membrane domain labeled with a yellow asterisk represents the last transmembrane helix from the multidrug transporter Pdr5 (T$_{Pdr5}$), which signals misfolding. The unlabeled membrane domain represents the proper transmembrane helix from Wsc1 (T$_{Wsc1}$). The black chain located in the cytosolic part of the C*T derivatives represents a peptide of 12 amino acids, originating from the C-terminal tail of Pdr5 (CS). (CS) contains amongst others five lysine (K) and one serine (S) residue, which are highlighted in white and red, respectively.

C*T$_{Wsc1}$(CS) was shown to be an integral membrane protein with type I orientation (N_{out}; C_{in}), by treating microsomes with detergent and digesting microsomes with proteinase K (data shown in the diploma thesis of Dorothea Mandlmeir [239]).

Then, degradation kinetics of the ERAD-M substrate C*T$_{Pdr5}$(CS) and the newly generated substrate, C*T$_{Wsc1}$(CS), were compared, in cells lacking endogenous CPY (*prc1*Δ).

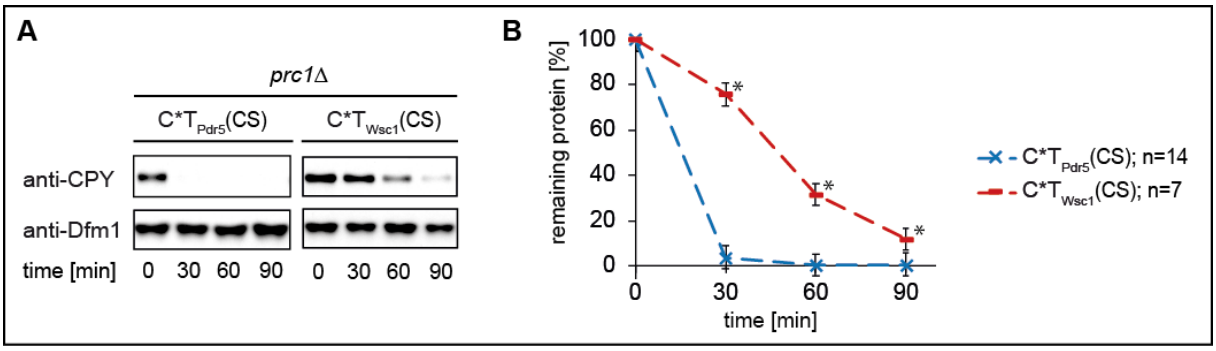

Figure 25: C*T$_{Wsc1}$(CS) is degraded with a different kinetics than the ERAD-M substrate C*T$_{Pdr5}$(CS).

A: Cycloheximide-chase analysis of C*T$_{Pdr5}$(CS) and C*T$_{Wsc1}$(CS) degradation was performed in *prc1*Δ cells.
Samples were taken every 30 min after cycloheximide addition (t=0 min) and C*T derivatives were detected by immunoblotting using CPY antibody. Dfm1 was used as loading control.
B: The quantification represents the data of up to 14 independent experiments. Error bars indicate the respective standard error of the mean (SEM). *P < 0.05, unpaired two-sample *t*-test relative to the control (C*T$_{Pdr5}$(CS)).

As shown in Figure 25, degradation of C*T$_{Wsc1}$(CS) ($t_{\frac{1}{2}}$ ~ 50 min) is much slower than degradation of C*T$_{Pdr5}$(CS) ($t_{\frac{1}{2}}$ ~ 15 min).

This indicates that C*T$_{Wsc1}$(CS) and C*T$_{Pdr5}$(CS) might be degraded via different pathways.

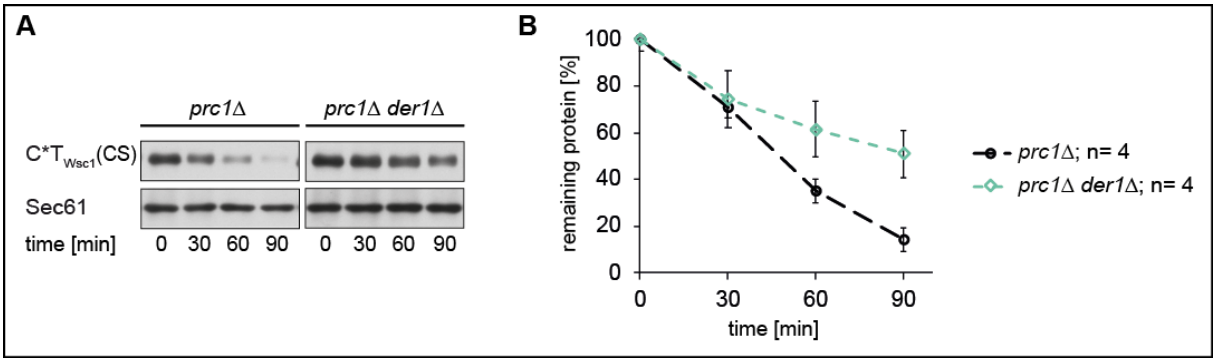

Figure 26: C*T$_{Wsc1}$(CS) degradation is affected by Der1 and therefore it is an ERAD-L substrate.

A: Cycloheximide-chase analysis of C*T$_{Wsc1}$(CS) degradation was performed in *prc1*Δ and *prc1*Δ*der1*Δ cells.
Samples were taken every 30 min after cycloheximide addition (t=0 min) and C*T$_{Wsc1}$(CS) was detected by immunoblotting using CPY antibody. Sec61 was used as loading control.
B: The quantification represents the data of four independent experiments. Error bars indicate the respective standard error of the mean (SEM). *P < 0.05, unpaired two-sample *t*-test relative to the control (*prc1*Δ).

Since in C*T$_{Wsc1}$(CS) the ERAD-L substrate CPY* is anchored in the membrane via a properly folded membrane helix, C*T$_{Wsc1}$(CS) should indeed be degraded by the

ERAD-L pathway. To determine the participation of Der1, a key component of the ERAD-L pathway, in degradation of C*T$_{Wsc1}$(CS) cycloheximide-chase experiments were performed (Figure 26). As can be seen, degradation of C*T$_{Wsc1}$(CS) is significantly retarded in cells lacking Der1. This leads to the assumption that C*T$_{Wsc1}$(CS) is an ERAD-L substrate family member.

The Der1 homolog [147], Dfm1 participates in the retrotranslocation of some distinct ERAD-M substrates [106] and it is also involved in the degradation of ERAD-C substrates [159], which contain a misfolded domain in the cytosol.
Participation of Dfm1 in degradation of the membrane-bound ERAD-L substrate, C*T$_{Wsc1}$(CS), should be excluded, since they contain properly folded membrane domain and intact cytosolic domain.

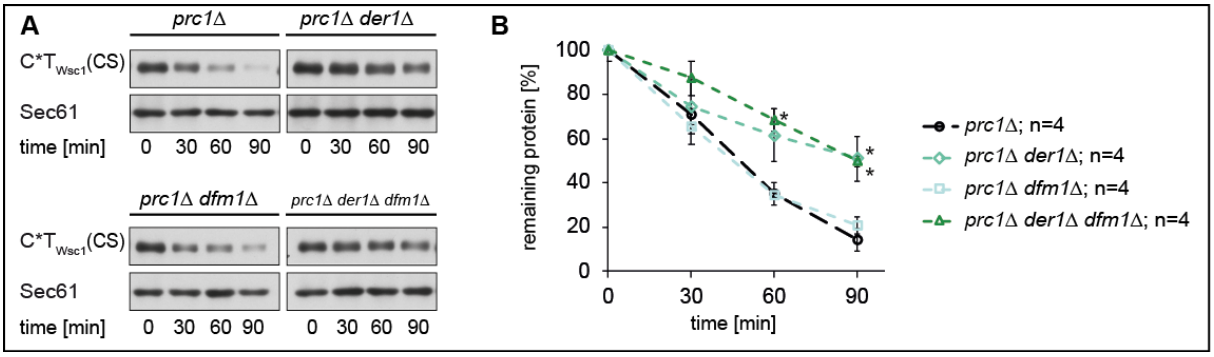

Figure 27: Dfm1 has no function in the degradation of the ERAD-L substrate C*T$_{Wsc1}$(CS).

A: Cycloheximide-chase analysis of C*T$_{Wsc1}$(CS) degradation was performed in *prc1*Δ; *prc1*Δ*der1*Δ*; prc1*Δ*dfm1*Δ *and prc1*Δ*der1*Δ*dfm1*Δ cells.
Samples were taken every 30 min after cycloheximide addition (t=0 min) and C*T$_{Wsc1}$(CS) was detected by immunoblotting using CPY antibody. Sec61 was used as loading control.
B: The quantification represents the data of four independent experiments. Error bars indicate the respective standard error of the mean (SEM). *P < 0.05, unpaired two-sample *t*-test relative to the control (*prc1*Δ).

Turnover rates shown in Figure 27 reveal that degradation of C*T$_{Wsc1}$(CS) is not affected in the absence of Dfm1. Furthermore, an overlapping effect of the homologous pair, Der1 and Dfm1, in degradation of C*T$_{Wsc1}$(CS) is not observed.

Table 16: Overview of the different requirements for C*T$_{Pdr5}$(CS) and C*T$_{Wsc1}$(CS) degradation

A green check mark indicates indispensable for degradation; a red cross symbol means dispensable for degradation; ~ (tilde) means involved in but not absolutely necessary for degradation. The ERAD components including the membrane protein Der1 and the ubiquitin ligases Hrd1 and Asi complex and their participation in degradation of the indicated substrates are shown.

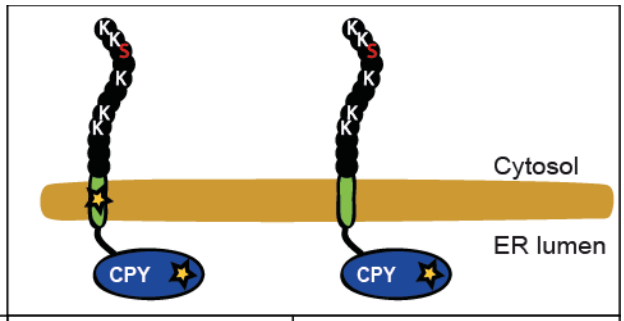

Name	C*T$_{Pdr5}$(CS)	C*T$_{Wsc1}$(CS)
cytosolic domain	CS: peptide of 12 amino acids (RVPKKNGKLSKK)	CS: peptide of 12 amino acids (RVPKKNGKLSKK)
membrane domain	T$_{Pdr5}$: last transmembrane helix of Pdr5	T$_{Wsc1}$: transmembrane helix of Wsc1
ER lumenal domain	CPY*	CPY*
Half-life time	approx. 15 min	approx. 50 min
Der1	✗	~
Hrd1	~	
Asi complex	~	
Hrd1 and Asi complex	✓	

In summary, membrane-anchored substrates carrying one and the same ER lumenal misfolded protein (CPY*) but differently folded transmembrane domains (C*T$_{Pdr5}$(CS) and C*T$_{Wsc1}$(CS)) follow different degradation pathways, concerning the required ubiquitin ligases and the helper proteins of the ER membrane. An overview of the differences in degradation is given in Table 16.

In brief, polyubiquitination of C*T$_{Pdr5}$(CS), containing an aberrant membrane domain, is mediated by the ubiquitin ligase Hrd1 together with the nuclear Asi complex. Since

Der1 is dispensable for this degradation process, C*T_{Pdr5}(CS) belongs to the ERAD-M substrate class. Substitution of the Pdr5 transmembrane domain with the properly folded membrane domain of Wsc1 leads to the construct C*T_{Wsc1}(CS) [P_{PRC1}; T_{PRC1}]. Degradation changes fundamentally, with a half-life of 50 min. In addition, Der1 participates in degradation of the newly generated substrate C*T_{Wsc1}(CS). Therefore, it is postulated to be degraded via an ERAD-L degradation mechanism. Degradation mechanism of proteins containing an ER lumenal misfolded domain and native membrane part, such as C*T_{Wsc1}(CS) is analyzed in the following chapter. Thus, in Table 16 it is not further mentioned.

3.2 More detailed mechanism of ER-associated degradation pathways, using a set of membrane-bound CPY* derivatives

In the first part of this thesis, a set of membrane-bound CPY* derivatives were established to scrutinize mechanistic differences in ERAD.

For easier comparison, they are composed of a related modular structure. In the ER lumen they contain the misfolded carboxypeptidase (CPY*) domain, which is required for ER retention. The CPY* derivatives are anchored in the ER membrane through either an aberrant membrane domain (C*T$_{Pdr5}$(CS)) or a properly folded one (C*T$_{Wsc1}$(CS)) (Figure 24).

Despite the fact that the ER lumenal CPY* moiety of C*T$_{Pdr5}$(CS) is an ERAD-L substrate, the membrane-bound C*T$_{Pdr5}$(CS) was shown to be degraded via an ERAD-M degradation mechanism, since its degradation is independent of Der1 (Figure 19). Obviously, the Pdr5 membrane part converts the degradation mechanism from ERAD-L to ERAD-M. Furthermore, it was shown that prior to degradation, C*T$_{Pdr5}$(CS) is ubiquitinated by the ubiquitin ligase Hrd1, which is embedded in the ER membrane and the Asi complex, located in the inner nuclear membrane (Figure 22). Thus, C*T$_{Pdr5}$(CS) can be used to further analyze ERAD-M degradation mechanism.

Exchange of the aberrant Pdr5 membrane portion against the properly folded Wsc1 domain leads to C*T$_{Wsc1}$(CS). It was shown that C*T$_{Wsc1}$(CS) is degraded via an ERAD-L related degradation mechanism, since Der1 is involved (Figure 26).

Der1 is a key component of the ERAD-L degradation mechanism [41,42], responsible for the recognition of ER lumenal misfolded proteins as well as it participates in the retrotranslocation [57,95]. Therefore, it introduces ERAD-L substrates into the ER membrane ([61,62] and reviewed in [6,40]) and it is in complex with Hrd1 [41,60–62], which is strongly suggested to form the retrotranslocon (chapter 1.3). But there is a discrepancy between degradation of the *bona fide* ERAD-L substrate CPY* and the membrane-anchored C*T$_{Wsc1}$(CS). Degradation of CPY* is completely abolished in the absence of Der1 [62], in contrast, C*T$_{Wsc1}$(CS) degradation is only slightly impaired in cells lacking Der1 (Figure 26), which was also observed for some other ERAD-L substrates, KHN and KWW ([41] and more details in chapter 1.7).

Now, it should be analyzed under which circumstances Der1 is essential for degradation and in which cases it is dispensable for degradation. Therefore, various C*T derivatives were designed. Finally, the analysis of their degradation gives a detailed picture about the ERAD-L and ERAD-M degradation mechanisms.

3.2.1 Proteins with a misfolded ER lumenal domain and a properly folded membrane domain are classified as ERAD-L substrates, as long as they are not containing either lysine or serine residues in their cytosolic part

C*T_{Wsc1}(CS) is composed of the *bona fide* ERAD-L substrate CPY* in the ER lumen required for ER retention (Figure 23) and T_{Wsc1}, the properly folded membrane domain of Wsc1[41]. Degradation of C*T_{Wsc1}(CS) is only slightly impaired in the absence of Der1. This is surprising, because it Der1 is a key component essential for ERAD-L degradation. This disagreement should be solved in the following.

At the cytosolic part C*T_{Wsc1}(CS) contains a peptide of 12 amino acids, the so-called cytosolic sequence (CS) (Figure 24). Amongst others the (CS) contains a serine (S) and five lysine (K) residues. These amino acids can be modified with ubiquitin [116,117]. However, it is possible that these residues contain a critical role in degradation. For instance, they might signal for an additional degradation mechanism independent of Der1, which might be an explanation for the reduced stabilization of C*T_{Wsc1}(CS) in the absence of Der1. To investigate this assumption, constructs were designed, which differ in the composition of the cytosolic part.

Therefore, the cytosolic part was shortened (ΔCS) and either a lysine, a serine or, as control, an alanine residue were added, leading to the substrates C*T_{Wsc1}(ΔCS)A, C*T_{Wsc1}(ΔCS)S and C*T_{Wsc1}(ΔCS)K (Figure 28).

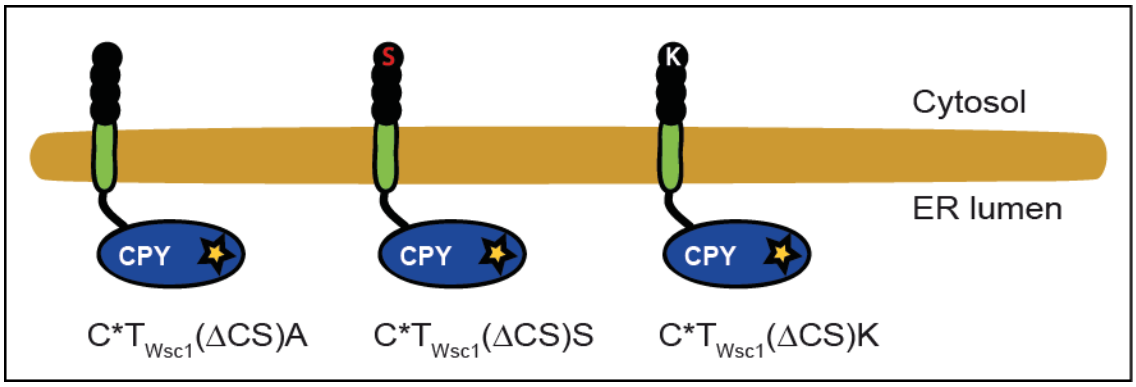

Figure 28: Schematic representation of ERAD substrates C*T$_{Wsc1}$(ΔCS)A, C*T$_{Wsc1}$(ΔCS)S and C*T$_{Wsc1}$(ΔCS)K.

The oval structure marked with an asterisk symbolizes the misfolded carboxypeptidase domain (C*), followed by the transmembrane helix from Wsc1 (T$_{Wsc1}$), shown in green. The black chain located in the cytosolic part of the C*T derivative represents the truncated peptide of three amino acids (arginine-valine-proline), originating from the C-terminal tail of Pdr5 (ΔCS), containing an additional lysine (K), serine (S) or alanine (A) residue. These lysine and serine residues are highlighted in white and red, respectively. The alanine residue, as control, is not highlighted.

First, localization and topology of the substrates C*T$_{Wsc1}$(ΔCS)A, C*T$_{Wsc1}$(ΔCS)S and C*T$_{Wsc1}$(ΔCS)K were determined as described in material and methods. The C*T$_{Wsc1}$(ΔCS) derivatives were shown to be integral membrane proteins with type I orientation (N$_{out}$; C$_{in}$) (Figure S2 and Figure S3). Furthermore, the ER lumenal CPY* moiety is required for ER retention, because the control constructs, containing the native CPY moiety, are found proteolytically active in the vacuole (Figure S4).

Then, participation of Der1 in degradation of the C*T$_{Wsc1}$ derivatives was determined. For ERAD-L substrate degradation Der1 is in complex with the ubiquitin ligase Hrd1. Thereby, Der1 delivers the proteins to the ligase [6,61,62]. Then, the ubiquitin ligase Hrd1 attaches polyubiquitin chains to ERAD-L substrates prior to their degradation by the 26S proteasome [43,150]. Therefore, degradation kinetics in cells lacking Der1 and Hrd1 were measured, using cycloheximide-chase experiments.

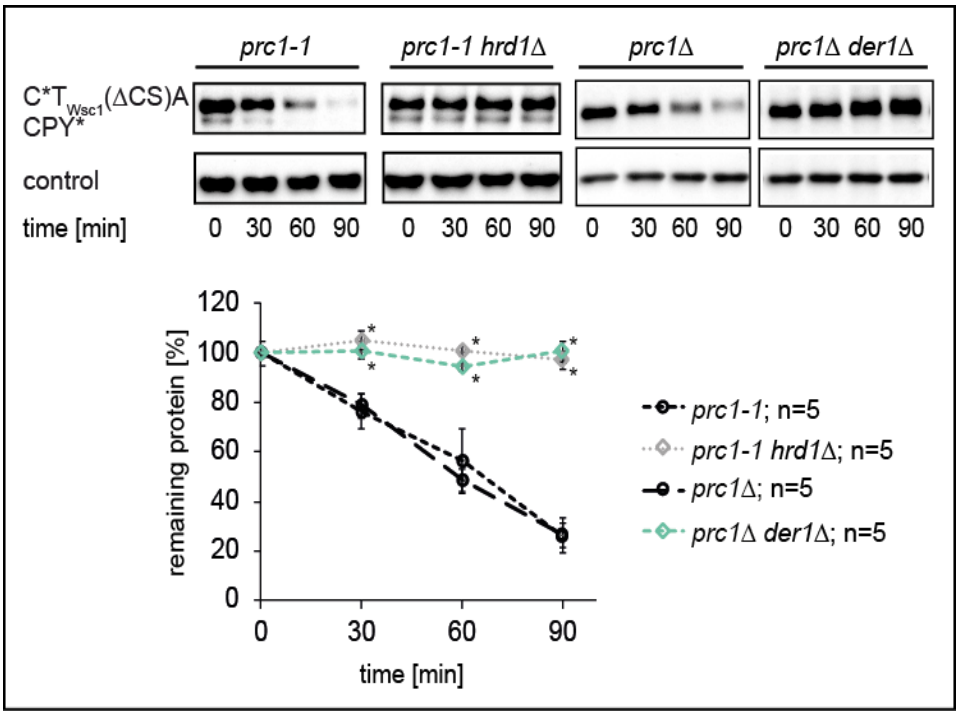

Figure 29: C*T$_{Wsc1}$(ΔCS)A degradation is Der1 and Hrd1 dependent.

A: Cycloheximide-chase analysis of C*T$_{Wsc1}$(ΔCS)A degradation was performed in *prc1Δ*; *prc1Δder1Δ* cells and *prc1-1*; *prc1-1 hrd1Δ* cells.
Samples were taken every 30 min after cycloheximide addition (t=0 min) and C*T$_{Wsc1}$(ΔCS)A was detected by immunoblotting using CPY antibody. Dfm1 was used as loading control for the *prc1-1*; *prc1-1 hrd1Δ* pair and Sec61 for the *prc1Δ*; *prc1Δ der1Δ* pair respectively.
B: The quantification represents the data of five independent experiments. Error bars indicate the respective standard error of the mean (SEM). *P < 0.05, unpaired two-sample *t*-test relative to the control (*prc1Δ* and *prc1-1*).

Figure 29 uncovers that the ubiquitin ligase Hrd1 and its complex partner Der1 are indispensable for the degradation of C*T$_{Wsc1}$(ΔCS)A.

Since Der1 transfers ERAD-L substrates to the ubiquitin ligase Hrd1 for ubiquitination [6,61,62], polyubiquitination of C*T$_{Wsc1}$(ΔCS)A was analyzed in cells lacking either Der1 or Hrd1.

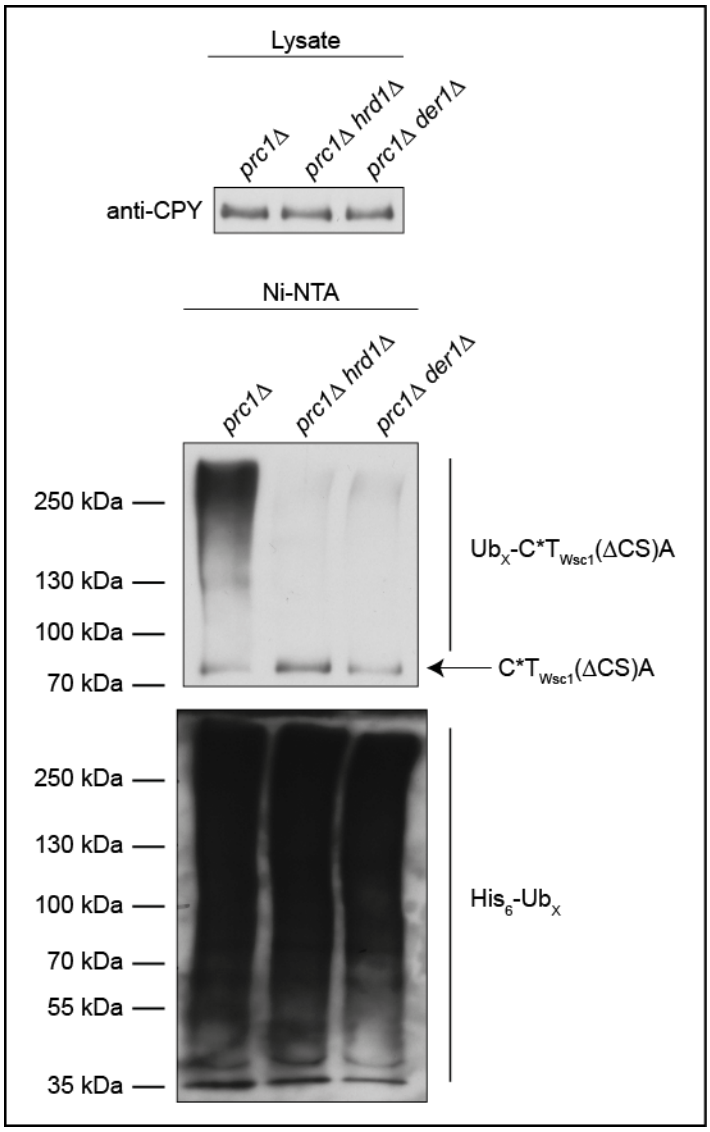

Figure 30: Ubiquitination of C*T$_{Wsc1}$(ΔCS)A is mediated by the ubiquitin ligase Hrd1 and its complex partner Der1.

Ubiquitination was analyzed in cells (genotype as indicated) expressing C*T$_{Wsc1}$(ΔCS)A and His$_6$-tagged ubiquitin (Ub). Cell lysates (input) were incubated with Ni-NTA resin under denaturing conditions to pull down all His$_6$-ubiquitinated proteins. C*T$_{Wsc1}$(ΔCS)A was detected by immunoblotting with CPY antibody and the amount of bound polyubiquitinated proteins (His$_6$-Ub$_X$) was visualized with His antibody.

Figure 30 shows that Hrd1 is the only ligase responsible for the polyubiquitination of C*T$_{Wsc1}$(ΔCS)A (Figure 30). Additionally, in the absence of Der1, C*T$_{Wsc1}$(ΔCS)A is also not polyubiquitinated (Figure 30).

In comparison, C*T$_{Wsc1}$(CS), which contains serine and lysine residues in its cytosolic part, is only slightly stabilized in cells lacking Der1. This supports the assumption that an amino acid, which can be ubiquitinated in the cytosolic part of ER lumenal misfolded, membrane-bound proteins, signals for an additional Der1 independent

degradation mechanism. In addition, this substantiates C*T$_{Wsc1}$(ΔCS)A to be an *bona fide* ERAD-L substrate, whereby recognition for degradation is supposed to occur via the ER lumenal part of the substrate.

Next, it should be determined whether the presence of a serine or lysine residue, or both instead of alanine in the cytosolic part of ERAD-L substrates, changes their degradation dependency on Der1. The alteration in degradation would probably propose that these residues can be identified by a Der1 independent degradation mechanism, in addition to the ERAD-L degradation process.
In order to answer this, degradation kinetics of C*T$_{Wsc1}$(ΔCS)S were performed in cells lacking either Hrd1 or Der1 (Figure 31).

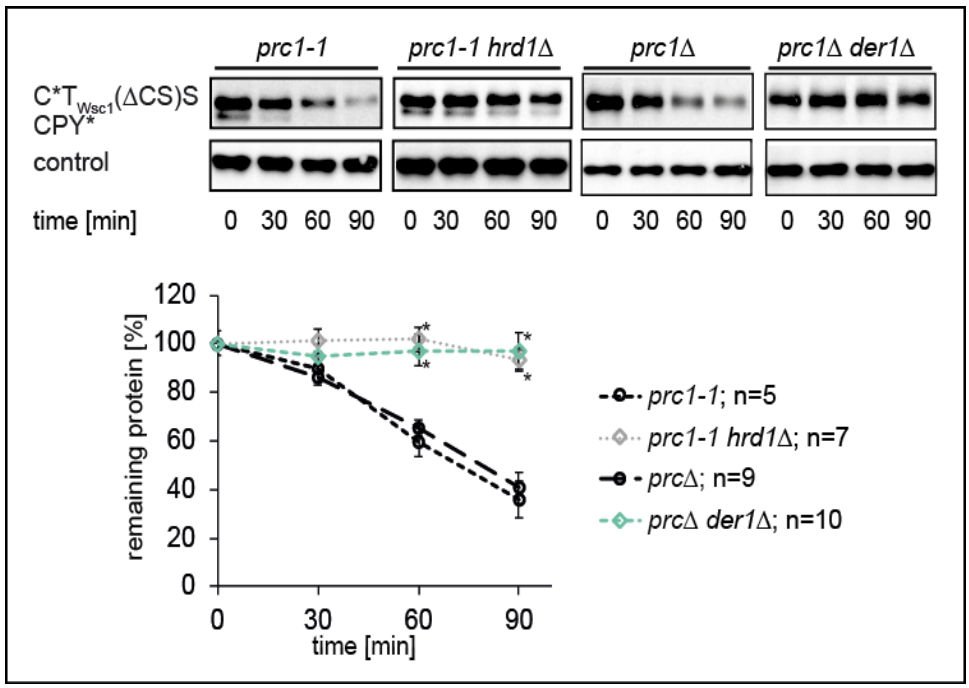

Figure 31: C*T$_{Wsc1}$(ΔCS)S degradation is Der1 and Hrd1 dependent.

A: Cycloheximide-chase analysis of C*T$_{Wsc1}$(ΔCS)S degradation was performed in *prc1*Δ; *prc1*Δ*der1*Δ cells and *prc1-1*; *prc1-1 hrd1*Δ cells.
Samples were taken every 30 min after cycloheximide addition (t=0 min) and C*T$_{Wsc1}$(ΔCS)S was detected by immunoblotting using CPY antibody. Dfm1 was used as loading control for the *prc1-1*; *prc1-1 hrd1*Δ pair and Sec61 for the *prc1*Δ; *prc1*Δ *der1*Δ pair respectively.
B: The quantification represents the data of up to 10 independent experiments. Error bars indicate the respective standard error of the mean (SEM). *P < 0.05, unpaired two-sample *t*-test relative to the control (*prc1*Δ and *prc1-1*).

Figure 31 reveals that C*T$_{Wsc1}$(ΔCS)S is still degraded in a Der1 and Hrd1 dependent manner.

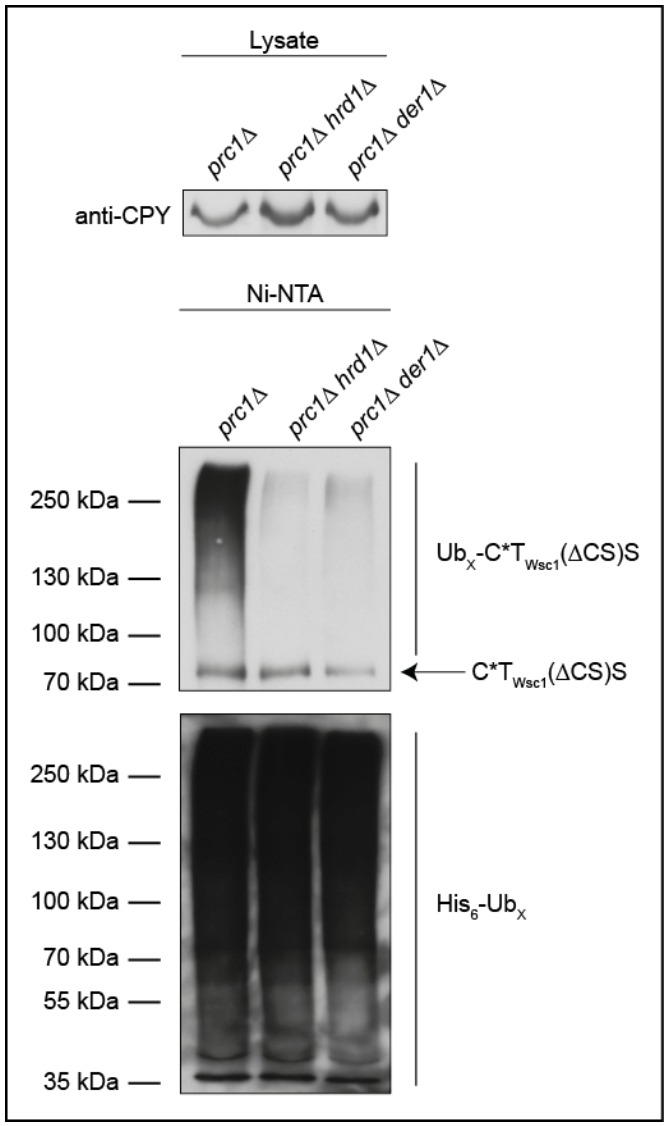

Figure 32: Ubiquitination of C*T$_{Wsc1}$(ΔCS)S is mediated by the ubiquitin ligase Hrd1. Without Der1 C*T$_{Wsc1}$(ΔCS)S cannot be delivered to the ligase.

Ubiquitination was analyzed in cells (genotype as indicated) expressing C*T$_{Wsc1}$(ΔCS)S and His$_6$-tagged ubiquitin (Ub). Cell lysates (input) were incubated with Ni-NTA resin under denaturing conditions to pull down all His$_6$-ubiquitinated proteins. C*T$_{Wsc1}$(ΔCS)S was detected by immunoblotting with CPY antibody and the amount of bound polyubiquitinated proteins (His$_6$-Ub$_X$) was visualized with His antibody.

Consistent with the lack of polyubiquitinated C*T$_{Wsc1}$(ΔCS)S in cells singly depleted of Hrd1 and Der1, there is a perfect correlation between the degradation rates and the ubiquitination of C*T$_{Wsc1}$(ΔCS)S (Figure 32).

Der1 and Hrd1 are key components of the ERAD-L degradation pathway. Here, it was shown that they are essentially required for degradation of C*T$_{Wsc1}$(ΔCS)A and C*T$_{Wsc1}$(ΔCS)S. This shows that serine residues in the cytosolic domain of ERAD-L substrates do not alter the degradation.

Next, it was analyzed whether lysine residues in the cytosolic domain influence the ERAD-L degradation mechanism.

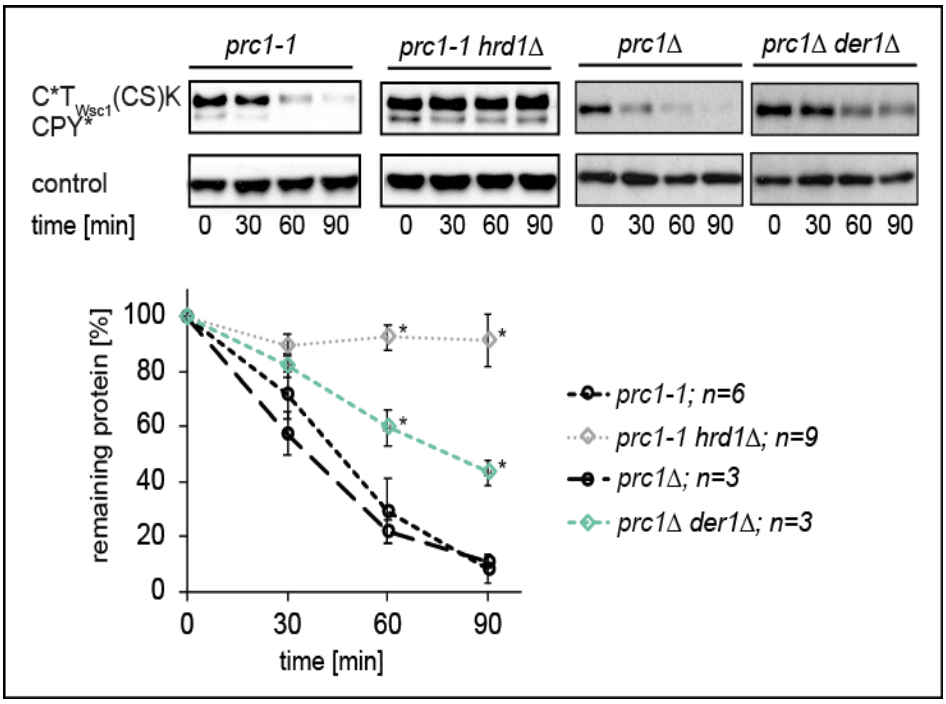

Figure 33: C*T$_{Wsc1}$(ΔCS)K degradation is Hrd1 dependent and only partly affected by Der1 deficiency.

A: Cycloheximide-chase analysis of C*T$_{Wsc1}$(ΔCS)K degradation was performed in *prc1Δ*; *prc1Δder1Δ* cells and in *prc1-1*; *prc1-1 hrd1Δ* cells.
Samples were taken every 30 min after cycloheximide addition (t=0 min). C*T$_{Wsc1}$(ΔCS)K was detected by immunoblotting using CPY antibody. Dfm1 was used as loading control for the *prc1-1*; *prc1-1 hrd1Δ* pair and Sec61 for the *prc1Δ*; *prc1Δ der1Δ* pair respectively.
B: The quantification represents the data of up to 9 independent experiments. Error bars indicate the respective standard error of the mean (SEM). *P < 0.05, unpaired two-sample *t*-test relative to the control (*prc1Δ* and *prc1-1*).

Figure 33 illustrates that the ubiquitin ligase Hrd1 is indispensable for C*T$_{Wsc1}$(ΔCS)K degradation. Surprisingly, degradation of C*T$_{Wsc1}$(ΔCS)K is only slightly impaired, but not abrogated in the absence of Der1. This suggests that a lysine residue, in the cytosolic part of ER lumenal misfolded proteins with properly folded membrane domain, can be identified by a mechanism, which leads to Der1 independent degradation. Simultaneously the ERAD-L degradation pathway, which leads to degradation in a Der1 dependent manner, is operating.

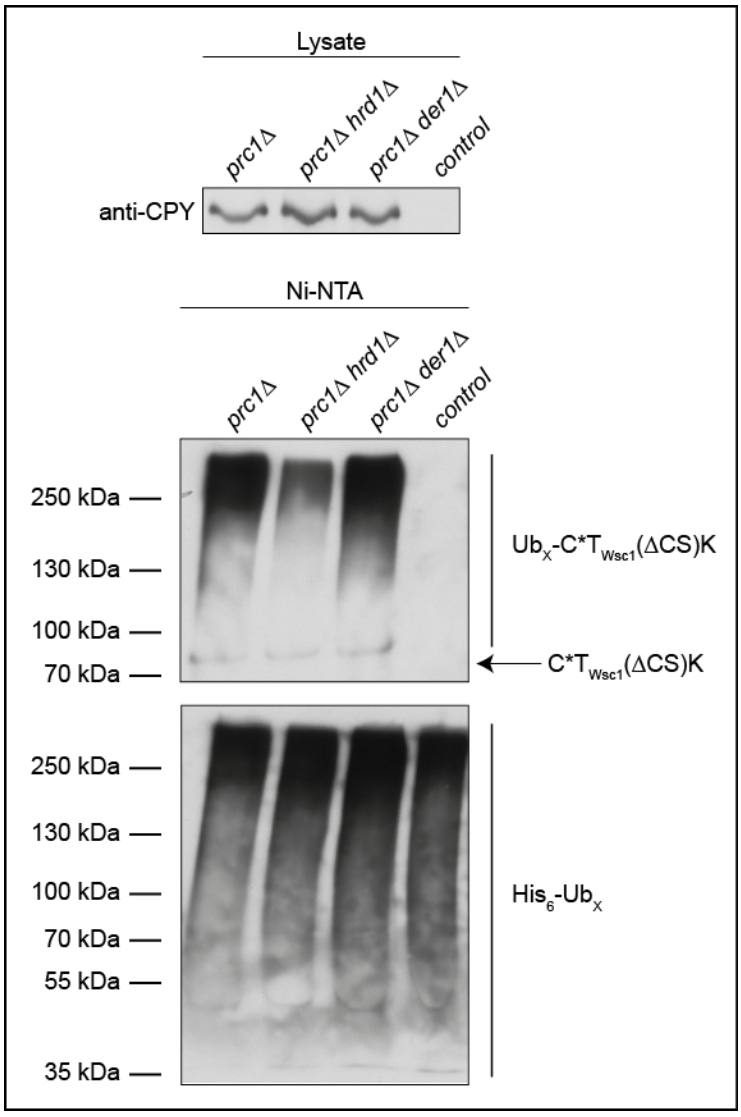

Figure 34: Ubiquitination of C*T$_{Wsc1}$(ΔCS)K is not only mediated by the ubiquitin ligase Hrd1.
Ubiquitination was analyzed in cells (genotype as indicated) expressing C*T$_{Wsc1}$(ΔCS)K and His$_6$-tagged ubiquitin (Ub). Cell lysates (input) were incubated with Ni-NTA resin under denaturing conditions to pull down all His$_6$-ubiquitinated proteins. C*T$_{Wsc1}$(ΔCS)K was detected by immunoblotting with CPY antibody and the amount of bound polyubiquitinated proteins (His$_6$-Ub$_X$) was visualized with His antibody.

Polyubiquitination analysis of C*T$_{Wsc1}$(ΔCS)K in *hrd1*Δ and in *der1*Δ cells, respectively was performed (Figure 34). C*T$_{Wsc1}$(ΔCS)K is still ubiquitinated (Ub$_X$-C*T$_{Wsc1}$(ΔCS)K) in cells lacking Der1, which is in agreement with the measured degradation rates (Figure 33).

Unexpectedly, polyubiquitinated C*T$_{Wsc1}$(ΔCS)K is found in the absence of Hrd1. This contradicts with the complete stabilization of C*T$_{Wsc1}$(ΔCS)K in *hrd1*Δ cells (Figure 33) and suggests that another ubiquitin ligase might be involved in the ubiquitination of C*T$_{Wsc1}$(ΔCS)K. Yet, this ubiquitination mark is not sufficient to signal the final

elimination.

There are two possible candidates for the residual ubiquitination of C*T_{Wsc1}(ΔCS)K. One is the ER membrane embedded RING ubiquitin ligase Doa10, which is a key component of ERAD-C substrate ubiquitination [69,139,158] and responsible for ubiquitination of some ERAD-M substrates [66]. The other candidate is the Asi complex, which is located in the inner nuclear membrane and is formed by the RING ubiquitin ligases Asi1 and Asi3. It is involved in ERAD-M substrate ubiquitination [67,68,157].

To distinguish, which ubiquitin ligase is additionally required for the ubiquitination of C*T_{Wsc1}(ΔCS)K, *in vivo* ubiquitination assays were performed in different yeast strains, all depleted of the mentioned ligases (genotypes as indicated in Figure 35).

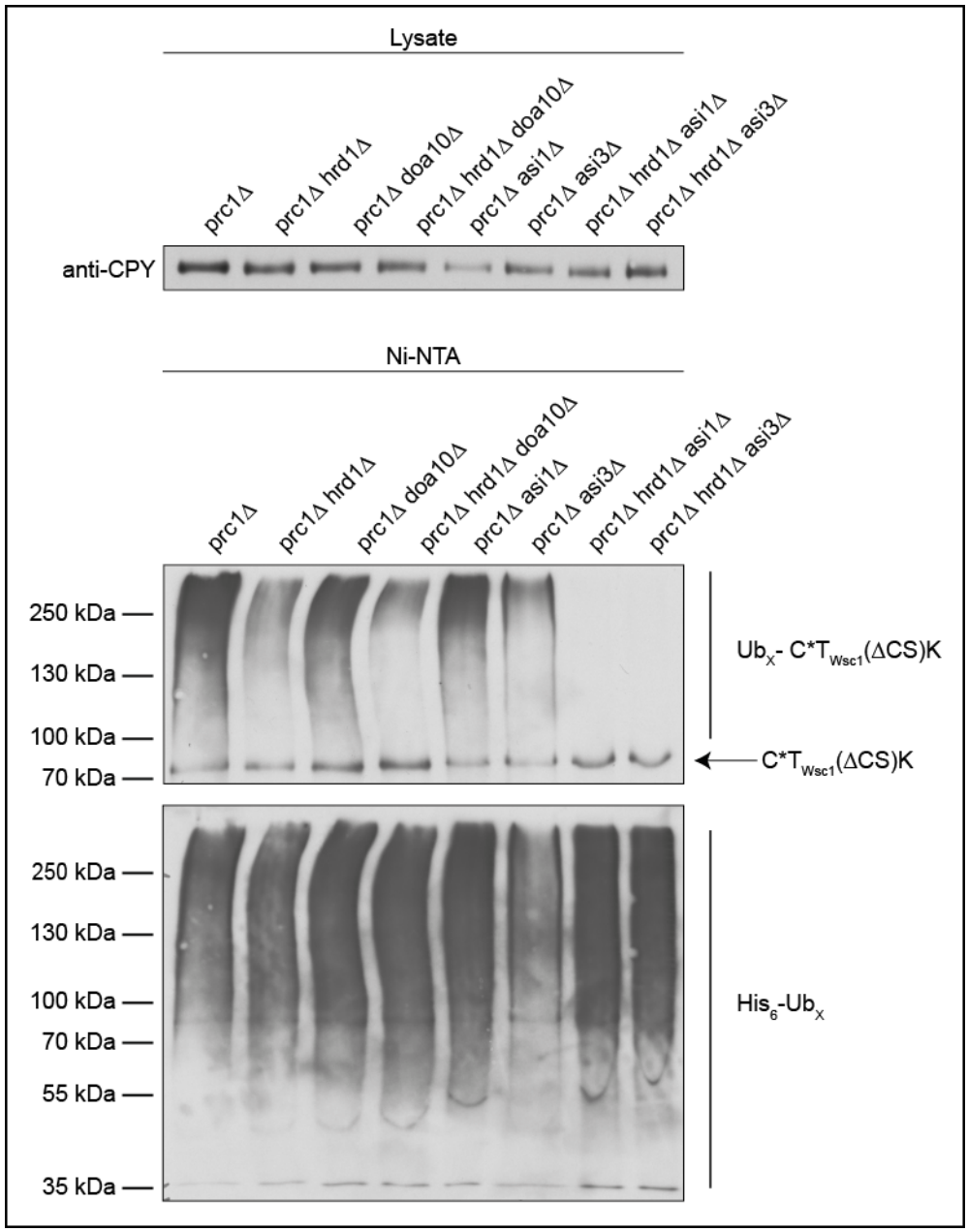

Figure 35: Ubiquitination of C*T$_{Wsc1}$(ΔCS)K is mediated by the ubiquitin ligase Hrd1 and the Asi complex.

Ubiquitination was analyzed in cells (genotype as indicated) expressing C*T$_{Wsc1}$(ΔCS)K and His$_6$-tagged ubiquitin (Ub). Cell lysates (input) were incubated with Ni-NTA resin under denaturing conditions to pull down all His$_6$-ubiquitinated proteins. C*T$_{Wsc1}$(ΔCS)K was detected by immunoblotting with CPY antibody and the amount of bound polyubiquitinated proteins (His$_6$-Ub$_X$) was visualized with His antibody.

Ubiquitination of C*T$_{Wsc1}$(ΔCS)K still occurs when only Hrd1, Asi, Asi3 or Doa10 are depleted. Since ubiquitinated C*T$_{Wsc1}$(ΔCS)K is found in *prc1*Δ*doa10*Δ as well as in *prc1*Δ*hrd1*Δ*doa10*Δ it can be assumed that the ligase Doa10 does not participate in the degradation of C*T$_{Wsc1}$(ΔCS)K. However, ubiquitination of C*T$_{Wsc1}$(ΔCS)K is

completely abolished in cells depleted of Hrd1 together with components of the Asi complex (Figure 35). This indicates that both ligases, the Asi complex and Hrd1 are required to ubiquitinate C*T$_{Wsc1}$(ΔCS)K. Interestingly, only the ubiquitination mark mediated by Hrd1 leads to degradation of C*T$_{Wsc1}$(ΔCS)K.

Table 17: Overview of the different requirements for C*T$_{Wsc1}$(ΔCS)A, C*T$_{Wsc1}$(ΔCS)S and C*T$_{Wsc1}$(ΔCS)K degradation

A green check mark indicates indispensable for degradation; a red cross symbol means dispensable for degradation; ~ (tilde) means involved in but not absolutely necessary for degradation; a green check mark with parenthesis indicates indispensable for degradation but for ubiquitination it is required but not indispensable; a red cross symbol with parenthesis indicates dispensable for degradation but participate in ubiquitination; n.a. corresponds to not necessary to analyze. The ERAD components including the membrane protein Der1 and the ubiquitin ligases Hrd1 and Asi complex and their participation in degradation of the indicated substrates are shown.

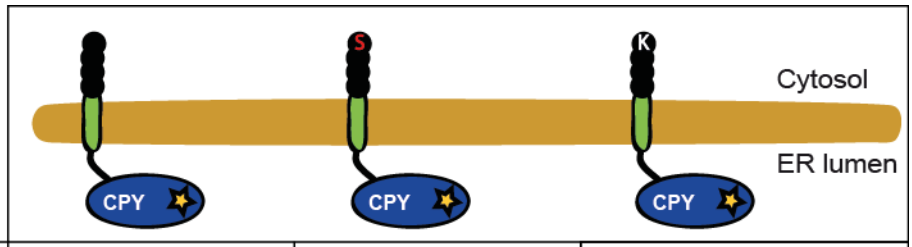

Name	C*T$_{Wsc1}$(ΔCS)A	C*T$_{Wsc1}$(ΔCS)S	C*T$_{Wsc1}$(ΔCS)K
cytosolic domain	ΔCS: truncated peptide (RVPA)	ΔCS: truncated peptide (RVPS)	ΔCS: truncated peptide (RVPK)
membrane domain	T$_{Wsc1}$: transmembrane helix of Wsc1	T$_{Wsc1}$: transmembrane helix of Wsc1	T$_{Wsc1}$: transmembrane helix of Wsc1
ER lumenal domain	CPY*	CPY*	CPY*
Der1	✓	✓	~
Hrd1	✓	✓	(✓)
Asi complex	✗	✗	(✗)
Hrd1 and Asi complex	n. a.	n. a.	✓

In summary, ER lumenal misfolded proteins, with a properly folded membrane domain, lacking lysine residues in the cytosolic part are degraded by the ERAD-L pathway. This is due to the fact that solely Hrd1 is required for ubiquitination and Der1 is

indispensable in the degradation mechanism. This implies that proteins with a misfolded ER lumenal domain and a properly folded membrane domain, lacking any lysine residues in the cytosolic part (Table 17) are true ERAD-L substrates.
In comparison, degradation of proteins with a misfolded ER lumenal domain, a properly folded membrane domain containing lysine residues in the cytosolic part of the protein, is slightly retarded in the absence of Der1. These proteins are ubiquitinated by Hrd1 and the nuclear Asi complex. While the Hrd1 catalyzed ubiquitin chains are indispensable for degradation, the Asi complex mediated ubiquitination signal does astonishingly not lead to elimination of the protein. Its function has to be established.
These substrates are recognized in part by the ERAD-L pathway and in addition by a Der1 independent recognition process (Table 17).
The nuclear Asi complex participates in ubiquitination of C*T_{Wsc1}(ΔCS)K (Figure 35) and it is involved in degradation of the *bona fide* ERAD-M substrate C*T_{Pdr5}(CS), which is also independent of Der1 (Figure 22 and Figure 19). Thus, one might assume that the ERAD-M degradation pathway operates in degradation of C*T_{Wsc1}(ΔCS)K, described as Der1 independent degradation mechanism. Therefore, C*T_{Wsc1}(ΔCS)K is called an ERAD-L/M substrate.

3.2.1.1 Serine and lysine residues in the cytosolic part of membrane proteins, with a misfolded ER lumenal domain and a properly folded membrane domain, dictate the need of ubiquitin-conjugating enzyme

As shown above, ubiquitination of the ERAD-L substrates C*T_{Wsc1}(ΔCS)A and C*T_{Wsc1}(ΔCS)S is mediated only by Hrd1, whereas Hrd1 as well as the Asi complex participate in ubiquitination of C*T_{Wsc1}(ΔCS)K. Since ubiquitination is mediated by an enzymatic cascade, which is composed of a ubiquitin-activating enzyme, a ubiquitin-conjugating enzyme and a ubiquitin ligase, the question was open, whether serine and lysine residues in the cytosolic part of proteins with misfolded ER lumenal domain and properly folded membrane domain, dictate the requirement of different ubiquitin-conjugating enzymes.

In the ERAD-L pathway, collaboration between the ubiquitin ligase Hrd1 and the ubiquitin-conjugating enzymes (Ubc's) Ubc1, Ubc6 and Ubc7 was established [43,149,154].

For degradation of ERAD-M substrates Hrd1 was found to collaborate with Ubc1 and Ubc7 [65,196]. Additionally, the Asi complex, together with Ubc6 and Ubc7, was discovered to be involved in degradation of ERAD-M substrates [68].

Consequently, degradation of the *bona fide* ERAD-L substrates C*T$_{Wsc1}$(ΔCS)A, C*T$_{Wsc1}$(ΔCS)S and the ERAD-L/M substrate C*T$_{Wsc1}$(ΔCS)K was determined in cells lacking either Ubc1, Ubc6 or Ubc7.

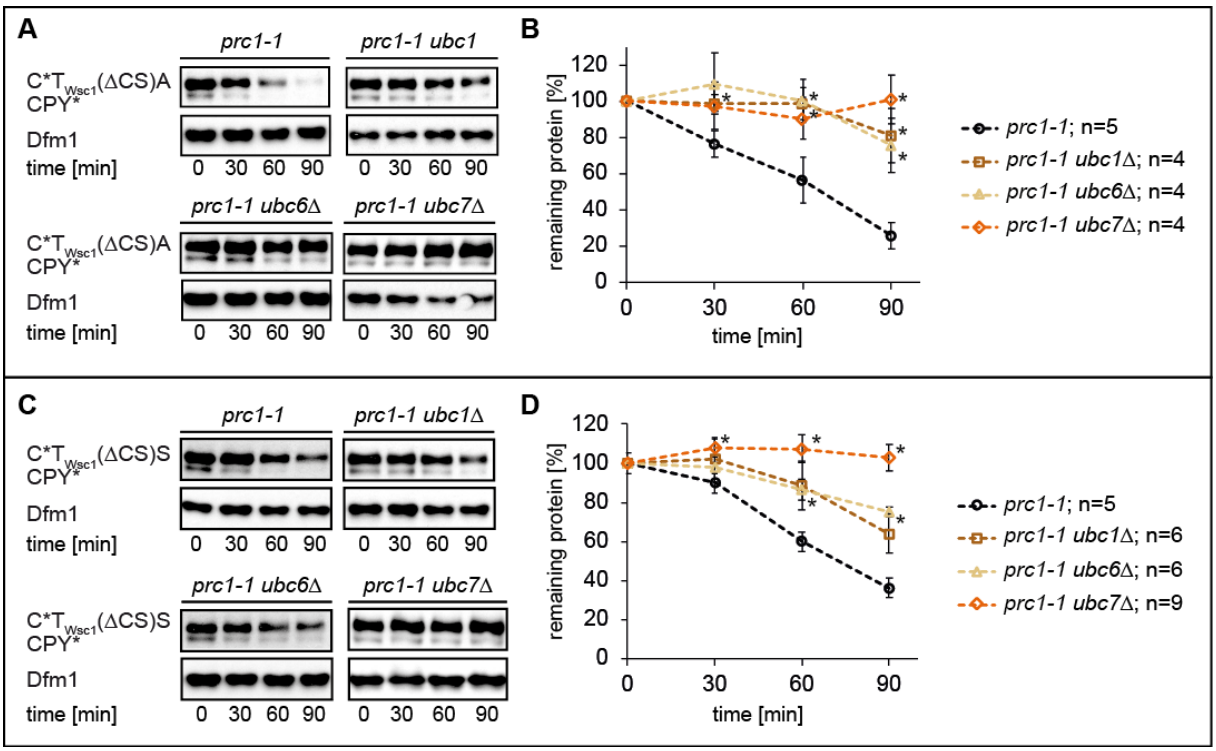

Figure 36: Degradation of C*T$_{Wsc1}$(ΔCS)A and C*T$_{Wsc1}$(ΔCS)S is dependent on the ubiquitin-conjugating enzymes Ubc1, Ubc6 and Ubc7.

A+C: Cycloheximide-chase analysis of C*T$_{Wsc1}$(ΔCS)A and C*T$_{Wsc1}$(ΔCS)S degradation were performed in *prc1-1; prc1-1 ubc1Δ; prc1-1 ubc6Δ and prc1-1 ubc7Δ* cells.
Samples were taken every 30 min after cycloheximide addition (t=0 min) and C*T$_{Wsc1}$(ΔCS)A and C*T$_{Wsc1}$(ΔCS)S were detected by immunoblotting using CPY antibody. Dfm1 was used as loading control.
B+D: The quantifications represent the data of up to 9 independent experiments. Error bars indicate the respective standard error of the mean (SEM). *P < 0.05, unpaired two-sample *t*-test relative to the control (*prc1-1*).

Ubc7 as well as Ubc1 and Ubc6 are indispensable for degradation of C*T$_{Wsc1}$(ΔCS)A (Figure 36; **A+B**). In contrast, only Ubc7 is absolutely required for degradation of C*T$_{Wsc1}$(ΔCS)S, while the absence of Ubc1 and Ubc6 does only partly diminish its degradation (Figure 36; **C+D**).

Although C*T$_{Wsc1}$(ΔCS)A and C*T$_{Wsc1}$(ΔCS)S had been classified as ERAD-L

substrates, and as such achieve ubiquitination by the Hrd1 ligase, the need for ubiquitin-conjugating enzymes obviously varies.

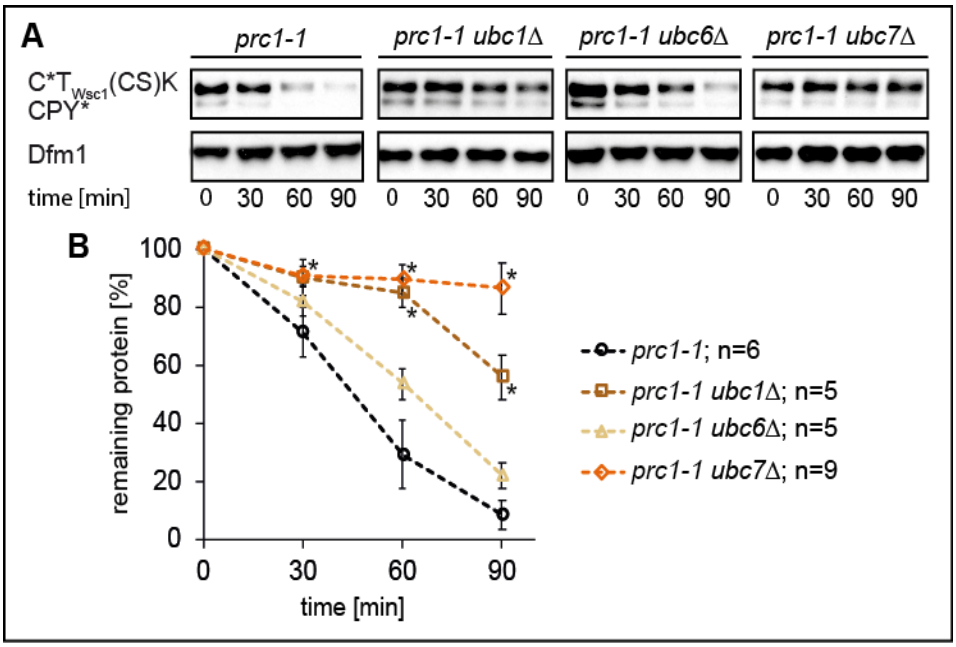

Figure 37: The degradation of C*T$_{Wsc1}$(ΔCS)K requires Ubc7 and is dependent on Ubc1.
A: Cycloheximide-chase analysis of C*T$_{Wsc1}$(ΔCS)K degradation was performed in *prc1-1; prc1-1 ubc1Δ; prc1-1 ubc6Δ and prc1-1 ubc7Δ* cells.
Samples were taken every 30 min after cycloheximide addition (t=0 min) and C*T$_{Wsc1}$(ΔCS)K was detected by immunoblotting using CPY antibody. Dfm1 was used as loading control.
B: The quantification represents the data of up to 9 independent experiments. Error bars indicate the respective standard error of the mean (SEM). *P < 0.05, unpaired two-sample *t*-test relative to the control (*prc1-1*).

In contrast to C*T$_{Wsc1}$(ΔCS)A and C*T$_{Wsc1}$(ΔCS)S, Ubc6 is not at all required for degradation of C*T$_{Wsc1}$(ΔCS)K (Figure 37). However, C*T$_{Wsc1}$(ΔCS)K degradation depends on the ubiquitin-conjugating enzyme Ubc7 and its degradation is slightly impaired in cells lacking Ubc1 (Figure 37).

It is still not clear, how the retention signal, which is the misfolded CPY* moiety in the ER lumen, communicates with the cytosolic recognition process of the polytopic membrane substrate.

3.2.1.2 *Involvement of the AAA ATPase Cdc48 in the extraction of proteins, with misfolded ER lumenal domain and proper membrane domain, out of the ER membrane, independent of the composition of their cytosolic part*

The AAA ATPase Cdc48 is required to extract all yet known ERAD-substrates out of the ER membrane [103,105,158,164,189–194]. Thus, it is expected that Cdc48 is required for degradation of ER lumenal misfolded proteins with properly folded membrane domain, containing lysine residues in the cytosolic part of the protein. As a representative of the so-called ERAD-L/M substrates C*T$_{Wsc1}$(CS) was used (Figure 24). As control turnover rates of the membrane-bound ERAD-L substrate C*T$_{Wsc1}$(ΔCS) were measured.

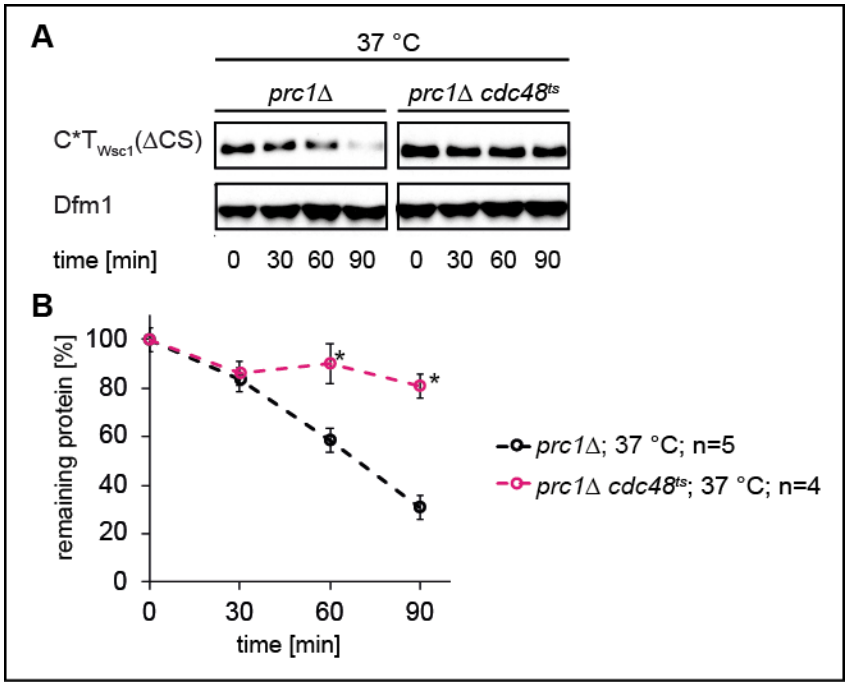

Figure 38: Cdc48 is necessary for degradation of C*T$_{Wsc1}$(ΔCS).

A: Cycloheximide-chase analysis of C*T$_{Wsc1}$(ΔCS) degradation was performed in *prc1*Δ; and *prc1*Δ *cdc48^{ts}* cells.
Main cultures were grown at 25°C. Then they were shifted to 37°C for 60 min prior to taking samples every 30 min after cycloheximide addition (t=0 min). C*T$_{Wsc1}$(ΔCS) was detected by immunoblotting using CPY antibody. Dfm1 was used as loading control.
B: The quantification represents the data of up to five independent experiments. Error bars indicate the respective standard error of the mean (SEM). *P < 0.05, unpaired two-sample *t*-test relative to the control (*prc1*Δ cells at 37°C).

For degradation studies, a strain was used, which carries a temperature-sensitive allele of Cdc48 (*cdc48-T413R*, called *cdc48^{ts}*). There are no considerable metabolic changes in the *cdc48^{ts}* mutant under these permissive conditions (25°C) and cells

behave like wildtype. After shift for one hour to the restrictive temperature 37°C, Cdc48 is inactivated, which leads to abolished degradation of all Cdc48 client proteins.

Figure 38 illustrates that the true ERAD-L substrate C*T$_{Wsc1}$(ΔCS) is completely stabilized the *cdc48^{ts}* mutant under restrictive temperature (37°C).

This supports the fact that Cdc48 is required for degradation of membrane localized ERAD-L substrates. To test whether Cdc48 is also required to extract ERAD-L/M proteins out of the ER membrane, degradation kinetics were measured in the *cdc48^{ts}* mutant strain, expressing C*T$_{Wsc1}$(CS).

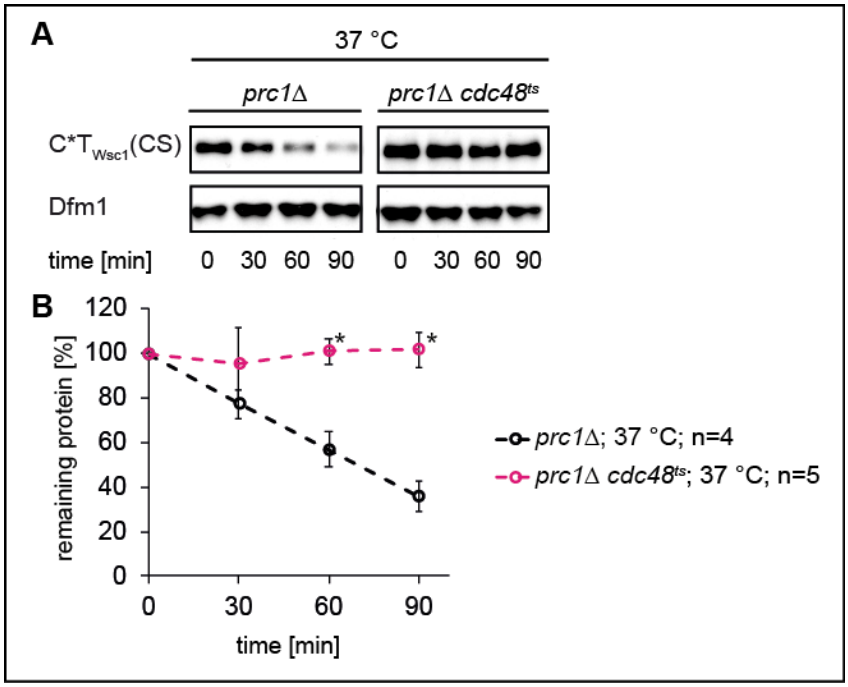

Figure 39: Cdc48 is necessary for degradation of C*T$_{Wsc1}$(CS).

A: Cycloheximide-chase analysis of C*T$_{Wsc1}$(CS) degradation was performed in *prc1*Δ; and *prc1*Δ *cdc48^{ts}* cells.
Main cultures were grown at 25°C. Then they were shifted to 37°C for 60 min prior to taking samples every 30 min after cycloheximide addition (t=0 min). C*T$_{Wsc1}$(CS) was detected by immunoblotting using CPY antibody. Dfm1 was used as loading control.
B: The quantification represents the data of up to five independent experiments. Error bars indicate the respective standard error of the mean (SEM). *P < 0.05, unpaired two-sample *t*-test relative to the control (*prc1*Δ cells at 37°C).

C*T$_{Wsc1}$(CS) is completely stabilized in the *cdc48^{ts}* mutant under restrictive conditions (Figure 39). This shows that Cdc48 is required for extraction of membrane-bound ERAD-L substrates, as well as membrane proteins degraded by the ERAD-L pathway and in addition by the Der1 independent ERAD-M degradation pathway, which is called the ERAD-L/M pathway.

Table 18: Overview of the different requirements for C*T_{Wsc1}(ΔCS)A, C*T_{Wsc1}(ΔCS)S and C*T_{Wsc1}(ΔCS)K degradation

A green check mark indicates indispensable for degradation; a red cross symbol means dispensable for degradation; ~ (tilde) means involved in but not absolutely necessary for degradation; a green check mark with parenthesis indicates indispensable for degradation but for ubiquitination it is required but not indispensable; a red cross symbol with parenthesis indicates dispensable for degradation but participate in ubiquitination; n.a. corresponds to not necessary to analyze. The ERAD components including the homologous pair of membrane proteins, Der1 and Dfm1, the ubiquitin ligases Hrd1 and Asi complex, the ubiquitin-conjugating enzymes Ubc1, Ubc6 and Ubc7 and the AAA ATPase Cdc48 and their participation in degradation of the indicated substrates are shown.

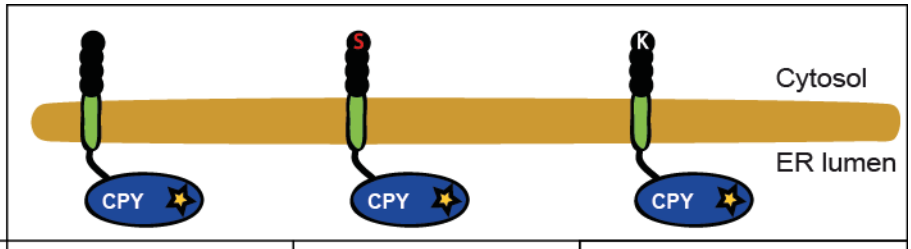

Name	C*T_{Wsc1}(ΔCS)A	C*T_{Wsc1}(ΔCS)S	C*T_{Wsc1}(ΔCS)K
cytosolic domain	ΔCS: truncated peptide (RVPA)	ΔCS: truncated peptide (RVPS)	ΔCS: truncated peptide (RVPK)
membrane domain	T_{Wsc1} : transmembrane helix of Wsc1	T_{Wsc1} : transmembrane helix of Wsc1	T_{Wsc1} : transmembrane helix of Wsc1
ER lumenal domain	CPY*	CPY*	CPY*
Der1	✓	✓	~
Hrd1	✓	✓	(✓)
Asi complex	✗	✗	(✗)
Hrd1 and Asi complex	n. a.	n. a.	✓
Ubc1	✓	~	~
Ubc6	✓	~	✗
Ubc7	✓	✓	✓
Cdc48	✓		

In summary the composition of the cytosolic part of ER membrane-bound substrates with an ER lumenal misfolded domain and an intact membrane part, directs their degradation pathway (an overview is given in Table 18 and briefly summarized in the following). Degradation of such membrane substrates lacking lysine residues in the cytosolic part (C*T$_{Wsc1}$(ΔCS)A and C*T$_{Wsc1}$(ΔCS)S) is abrogated when Der1 is absent. These substrates are treated like true ERAD-L substrates. For the ubiquitination and final degradation of these substrates, the ubiquitin ligase Hrd1, in collaboration with the ubiquitin-conjugating enzymes Ubc1, Ubc6 and Ubc7 is required. As for all known ERAD substrates the AAA ATPase Cdc48 is responsible for membrane extraction, prior to terminal degradation in the cytosol.

On contrary, a Der1 independent cytosolic recognition process seems to identify the cytosolic lysine residue and thus participate in the degradation of C*T$_{Wsc1}$(ΔCS)K. This Der1 independent degradation process was suggested to be the canonical ERAD-M pathway, because for ubiquitination of C*T$_{Wsc1}$(ΔCS)K, the Hrd1 ligase as well as the Asi complex, in collaboration with the ubiquitin-conjugating enzymes Ubc1 and Ubc7, are required. However, solely Hrd1 mediated ubiquitination induces final elimination.

Therefore, the already established ERAD-L and ERAD-M degradation mechanisms, suggested by Vashist and Ng 2004 [41] are extended in the following way. ER lumenal, soluble, misfolded proteins, such as CPY*, KHN and PrA*, as well as membrane-bound proteins with an intact membrane domain, a misfolded ER lumenal domain and lacking any lysine residues in the cytosolic part of the protein, as present in the newly designed substrates C*T$_{Wsc1}$(ΔCS) and C*T$_{Wsc1}$(ΔCS)A can be classified as *bona fide* ERAD-L substrates. The availability of a single lysine residue in the cytosolic part of these proteins is sufficient to be identified by a Der1 independent process additionally to the ERAD-L degradation mechanism. Thus, they are expected to be degraded by the ERAD-L/M pathway to highlight the Der1 dependent and the Der1 independent mechanism, which both are required to degrade these class of substrates.

3.2.2 Nondegradable ER membrane-bound ERAD substrates

As shown in the previous chapter (chapter 3.2.1), membrane-bound proteins with an ER lumenal misfolded domain, a properly folded membrane domain, lacking lysine residues in the cytosolic part are degraded via the established ERAD-L pathway, requiring the membrane protein Der1 and the ubiquitin ligase Hrd1. In contrast to these ERAD-L substrates, proteins with a misfolded ER lumenal domain, a properly folded membrane domain, containing a lysine residue in the cytosolic part are not true ERAD-L substrates: a Der1 independent degradation process recognizes the lysine residue and leads to a Der1 independent degradation pathway in addition to the ERAD-L degradation pathway. These substrates are not only ubiquitinated by the Hrd1 ligase, but also by the Asi complex. However, only Hrd1 mediated ubiquitination leads to degradation of these substrates. This degradation mechanism is described as the ERAD-L/M pathway.

In summary, the cytosolic part of membrane proteins containing a properly folded membrane domain and a misfolded ER lumenal domain directs their degradation pathway considerably.

Replacement of the intact transmembrane helix (T_{Wsc1}) by a misfolded one, as exemplified by C*T_{Pdr5}(CS) leads to degradation completely independent of Der1 (Figure 19). C*T_{Pdr5}(CS) is ubiquitinated by the ligases Hrd1 as well as the Asi complex (Figure 22). Based on its Der1 independent degradation C*T_{Pdr5}(CS) is classified by Vashist and Ng [41] as ERAD-M substrate.

The question arises, whether the cytosolic part of ERAD-M substrates affects their degradation, as it is the case for membrane proteins with misfolded ER lumenal domain but intact membrane domain.

To explore this question, the substrate C*T_{Pdr5}(ΔCS) was generated, which is a truncated version of the ERAD-M substrate C*T_{Pdr5}(CS) – with only the three amino acids (arginine, valine, proline) in the cytosolic part – (Figure 40).

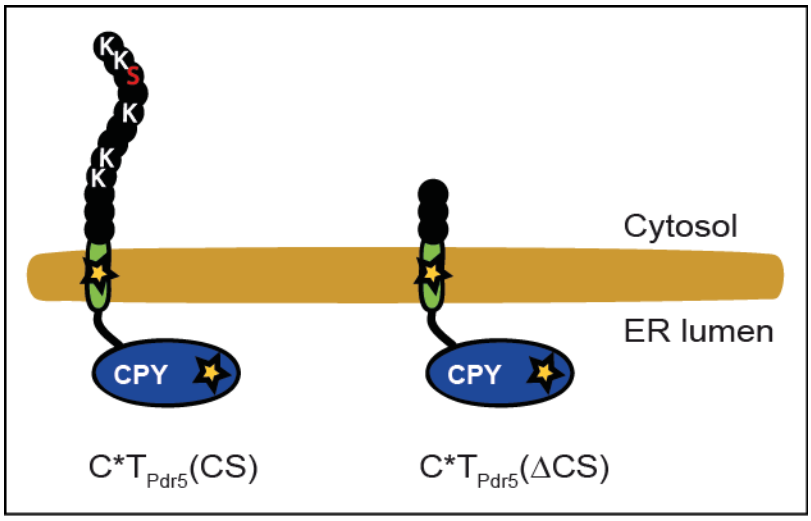

Figure 40: Schematic representation of ERAD substrates C*T$_{Pdr5}$(CS) and C*T$_{Pdr5}$(ΔCS).

The oval structure marked with an asterisk symbolizes the misfolded carboxypeptidase domain (C*), followed by the last transmembrane helix from Pdr5 (T$_{Pdr5}$), which signals misfolding, shown in green with yellow asterisk. The black chain located in the cytosolic part of the C*T$_{Pdr5}$(CS) represents a peptide of 12 amino acids, originating from the C-terminal tail of Pdr5 (CS). In C*T$_{Pdr5}$(ΔCS) the cytosolic peptide is truncated down to three amino acids (arginine-valine-proline). The lysine (K) and serine (S) residues of the (CS) are highlighted in white and red, respectively.

First, localization and topology of C*T$_{Pdr5}$(ΔCS) were determined as described in material and methods. C*T$_{Pdr5}$(ΔCS) was shown to be an integral membrane protein with type I orientation (N_{out}; C_{in}) (Figure S5 and Figure S6). Furthermore, the ER lumenal CPY* moiety is required for ER retention, because the control construct, CT$_{Pdr5}$(ΔCS), containing the native CPY moiety, is proteolytically active in the vacuole (Figure S7).

Then, degradation of C*T$_{Pdr5}$(ΔCS) in comparison to the full-length C*T$_{Pdr5}$(CS) was examined, using cycloheximide-chase analysis.

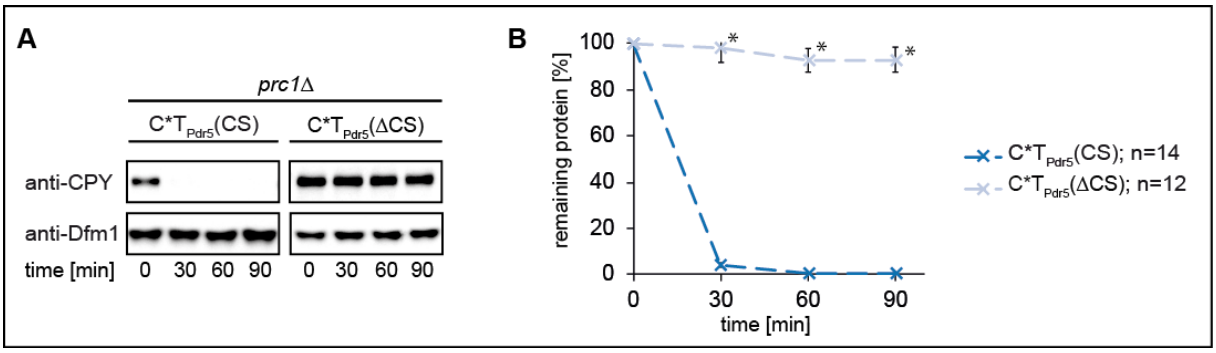

Figure 41: C*T$_{Pdr5}$(ΔCS) is a not degraded at all.

A: Cycloheximide-chase analysis of C*T$_{Pdr5}$(CS) and C*T$_{Pdr5}$(ΔCS) degradation was performed in *prc1*Δ cells.
Samples were taken every 30 min after cycloheximide addition (t=0 min) and C*T$_{Pdr5}$ derivatives were detected by immunoblotting using CPY antibody. Dfm1 was used as loading control.
B: The quantification represents the data of up to 14 independent experiments. Error bars indicate the respective standard error of the mean (SEM). *P < 0.05, unpaired two-sample *t*-test relative to the control (C*T$_{Pdr5}$(CS)).

Surprisingly, in contrast to the full-length protein, C*T$_{Pdr5}$(ΔCS) is not degraded at all, although it carries a misfolded ER lumenal domain as well as a misfolded transmembrane domain like the full-length substrate C*T$_{Pdr5}$(CS) (Figure 41). Contrary to C*T$_{Pdr5}$(ΔCS), the rapidly turned over C*T$_{Pdr5}$(CS) protein contains a cytosolic part with serine as well as lysine residues (Figure 40; an overview is given in Table 19). The fact that C*T$_{Pdr5}$(ΔCS) is not degraded at all, may have various reasons: ubiquitination, retrotranslocation or extraction out of the ER membrane may be impaired.

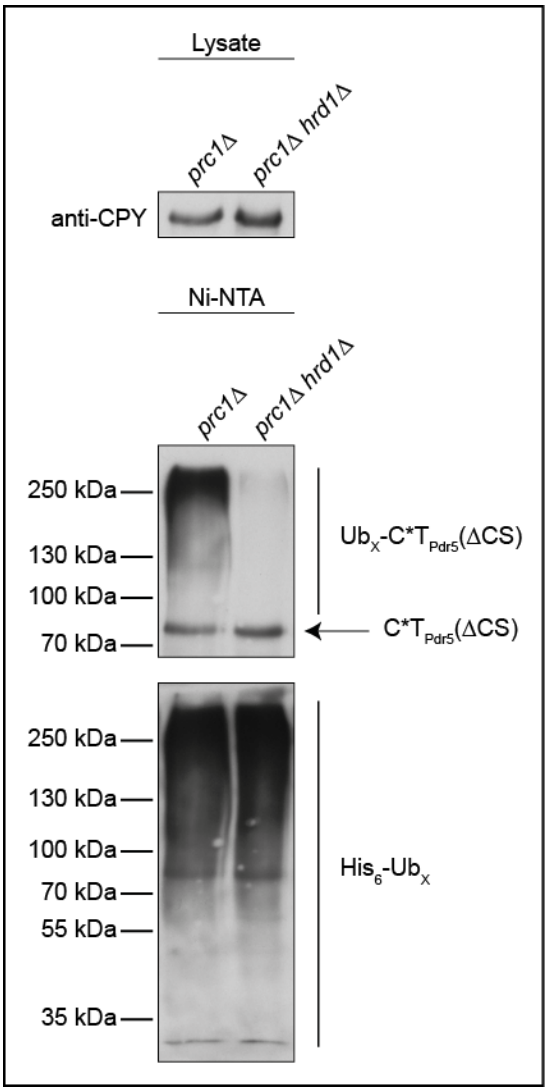

Figure 42: Ubiquitination of C*T$_{Pdr5}$(ΔCS) is mediated by the ubiquitin ligase Hrd1.

Ubiquitination was analyzed in *prc1*Δ and *prc1*Δ*hrd1*Δ cells, expressing C*T$_{Pdr5}$ (ΔCS) and His$_6$-tagged ubiquitin (Ub). Cell lysates (input) were incubated with Ni-NTA resin under denaturing conditions to pull down all His$_6$-ubiquitinated proteins. C*T$_{Pdr5}$(ΔCS) was detected by immunoblotting with CPY antibody and the amount of bound polyubiquitinated proteins (His$_6$-Ub$_X$) was visualized with His antibody.

To check if C*T$_{Pdr5}$(ΔCS) degradation failed because of impaired ubiquitination, *in vivo* ubiquitination assays were performed as described before. Astonishingly, C*T$_{Pdr5}$(ΔCS) is polyubiquitinated (Figure 42), although it is not degraded (Figure 41).

Since ubiquitination occurs but degradation is abolished the question was, which ubiquitin ligase mediates ubiquitination of the protein. Both, the ubiquitin ligases Hrd1 and the Asi complex are involved in C*T$_{Pdr5}$(CS) ubiquitination (Figure 22). Accordingly, they are potential candidates to ubiquitinate the truncated C*T$_{Pdr5}$(ΔCS). Figure 42

reveals that C*T$_{Pdr5}$(ΔCS) is not ubiquitinated at all in cells depleted of Hrd1.

This leads to the conclusion that Hrd1 is the only ligase required for the ubiquitination of C*T$_{Pdr5}$(ΔCS).

Table 19: Overview of the different requirements for C*T$_{Pdr5}$(CS) and C*T$_{Pdr5}$(ΔCS) degradation

A green check mark indicates indispensable for degradation; a red cross symbol means dispensable for degradation; ~ (tilde) means involved in but not absolutely necessary for degradation; a red cross symbol with parenthesis indicates dispensable for degradation but participate in ubiquitination. The ERAD components including the membrane protein Der1 and the ubiquitin ligases Hrd1 and Asi complex, and their participation in degradation of the indicated substrates are shown.

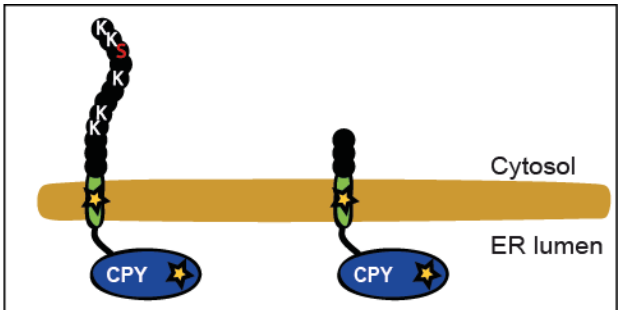

Name	C*T$_{Pdr5}$(CS)	C*T$_{Pdr5}$(ΔCS)
cytosolic domain	CS: peptide of 12 amino acids (RVPKKNGKLSKK)	ΔCS: truncated peptide (RVP)
membrane domain	T$_{Pdr5}$: last transmembrane helix of Pdr5	T$_{Pdr5}$: last transmembrane helix of Pdr5
ER lumenal domain	CPY*	CPY*
Der1	✗	
Hrd1	~	(✗)
Asi complex	✗	→ not degraded at all
Hrd1 and Asi complex	✓	

Since C*T_{Pdr5}(ΔCS) is ubiquitinated via Hrd1 but still remains in the ER membrane (Figure 42 and Figure 41), it can be assumed that its retrotranslocation or membrane extraction is impaired. These considerations are supported by data recently published. The ligase Hrd1 associates via its transmembrane helices with ERAD-L, as well as with ERAD-M substrates [65,95,96]. Furthermore, Hrd1 is under debate to form a channel to allow retrotranslocation of ERAD substrates [59,91,97] (for more details see chapter 1.3, and reviewed in [6]).

The cytosolic or the membrane part of C*T_{Pdr5}(ΔCS) do not provide any amino acid, which can be ubiquitinated. Hence, it is possible that the ER lumenal CPY* moiety of C*T_{Pdr5}(ΔCS) undergoes initial retrotranslocation through the retrotranslocon, formed by Hrd1 amongst others [59], until it is accessible to be ubiquitinated. However, for some reason final retrotranslocation is abolished and C*T_{Pdr5}(ΔCS) accumulates in the ER membrane instead of terminal elimination (Figure 41).

Accumulation of C*T_{Pdr5}(ΔCS) in the ER membrane can have various reasons. Possibly the release of the nondegradable substrate from the retrotranslocon is impaired or the membrane domain of C*T_{Pdr5}(ΔCS), is prevented to enter into the retrotranslocon.

The aberrant membrane domain (T_{Pdr5}) of C*T_{Pdr5}(ΔCS) is the last transmembrane helix of Pdr5, a multi-spanning membrane protein. In its native environment it interacts with partner helices via polar residues. However, as an orphan helix these polar residues are exposed and may lead to an oligomerization of several C*T_{Pdr5}(ΔCS) in the ER membrane, which possibly prevents their degradation.

To explore, whether C*T_{Pdr5}(ΔCS) oligomerizes, either an HA or a V5 epitope were introduced into C*T_{Pdr5}(ΔCS), leading to the substrates C*$^{HA}T_{Pdr5}$(ΔCS) and C*$^{V5}T_{Pdr5}$(ΔCS), respectively. Any influence of either the HA or the V5 epitope had to be excluded. Therefore, both were inserted between the ER lumenal CPY* moiety and the membrane domain (T_{Pdr5}) of C*T_{Pdr5}(ΔCS) (Figure 43).

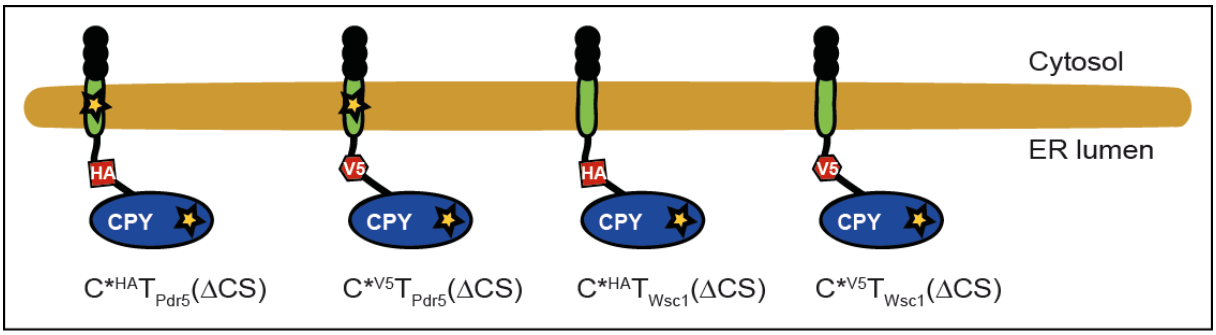

Figure 43: Schematic representation of ERAD substrates $C^{*HA}T_{Pdr5}(\Delta CS)$, $C^{*V5}T_{Pdr5}(\Delta CS)$, $C^{*HA}T_{Wsc1}(\Delta CS)$ and $C^{*V5}T_{Wsc1}(\Delta CS)$.

The oval structure marked with an asterisk symbolizes the misfolded carboxypeptidase domain (C*), followed by the last transmembrane helix from Pdr5, which signals misfolding, shown in green with yellow asterisk, or the proper transmembrane helix from Wsc1, shown in green, respectively. C* is linked to T_{Pdr5} and T_{Wsc1} via a linker. This linker is based on 32 amino acids upstream of the last transmembrane helix of Pdr5 (T_{Pdr5}). An HA-Tag or V5-Tag is integrated in this linker. The black chain located in the cytosolic part represents the truncated peptide of three amino acids (arginine-valine-proline), originating from the C-terminal tail of Pdr5 (ΔCS).

As control, HA-tagged, as well as V5-tagged versions of $C^*T_{Wsc1}(\Delta CS)$ were generated (Figure 43). $C^{*HA}T_{Wsc1}(\Delta CS)$ and $C^{*V5}T_{Wsc1}(\Delta CS)$ contain the intact membrane domain (T_{Wsc1}). This native membrane helix contains only hydrophobic residues and thus should not lead to oligomerization.

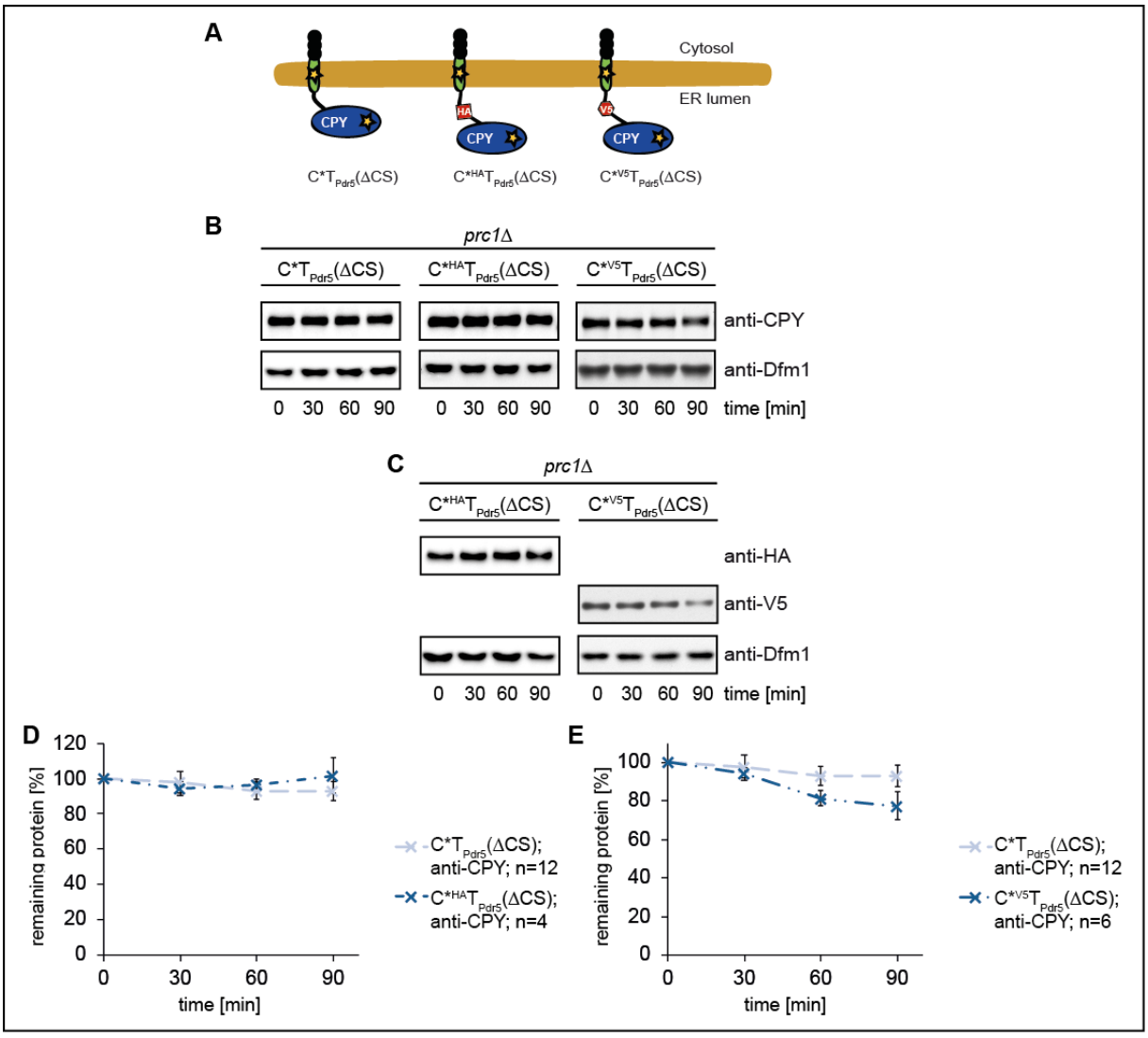

Figure 44: The ERAD substrates C*T$_{Pdr5}$(ΔCS), C*^{HA}T$_{Pdr5}$(ΔCS) and C*^{V5}T$_{Pdr5}$(ΔCS) follow the same degradation kinetics.

A: Schematic representation of the ERAD substrates C*T$_{Pdr5}$(ΔCS), C*^{HA}T$_{Pdr5}$(ΔCS) and C^{V5}*T$_{Pdr5}$(ΔCS); for more detail see Figure 40 and Figure 43.
B+C: Cycloheximide-chase analysis of C*T$_{Pdr5}$(ΔCS), C*^{HA}T$_{Pdr5}$(ΔCS) and C^{V5}*T$_{Pdr5}$(ΔCS) degradation was performed in *prc1*Δ cells.
Samples were taken every 30 min after cycloheximide addition (t=0 min) and C*T$_{Pdr5}$(ΔCS) derivatives were detected by immunoblotting using CPY antibody as well as HA and V5 antibodies. Dfm1 was used as loading control.
D+E: The quantifications represent the data of up to 12 independent experiments. Error bars indicate the respective standard error of the mean (SEM). *P < 0.05, unpaired two-sample *t*-test relative to the control (C*T$_{Pdr5}$(ΔCS)).

Degradation kinetics of C*^{HA}T$_{Pdr5}$(ΔCS) and C*^{V5}T$_{Pdr5}$(ΔCS) were measured, to exclude any alterations, triggered by the insertion of the HA or V5 epitope, respectively. For that, not only the CPY* moiety was detected, but also the HA and V5 epitopes (Figure 44; **B+C**). Both constructs show the same turnover rates as the untagged C*T$_{Pdr5}$(ΔCS) (Figure 44; **D+E**), indicating that neither the HA nor the V5 epitope have an influence

on degradation.

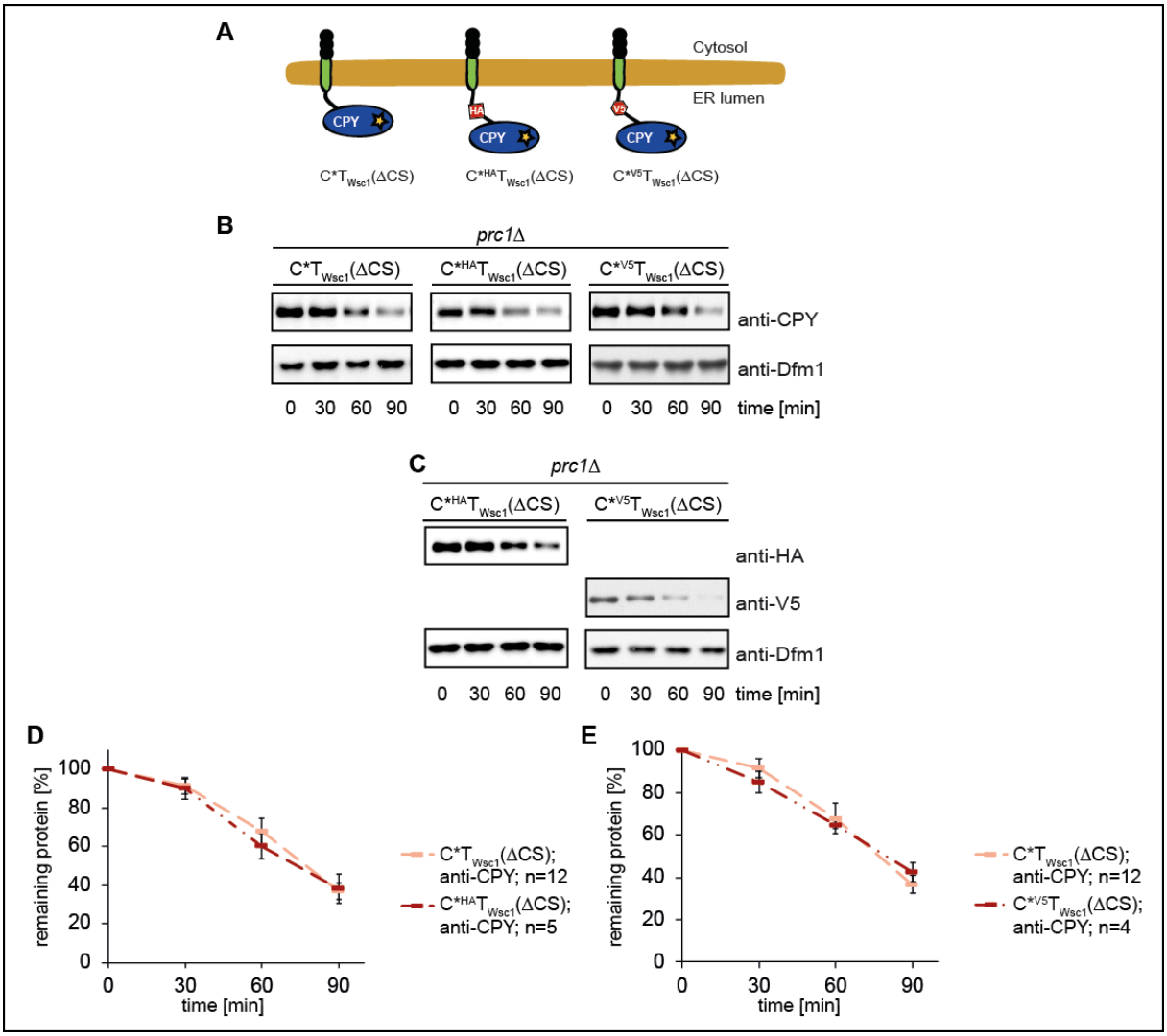

Figure 45: The ERAD substrates C*T$_{Wsc1}$(ΔCS), C*^{HA}T$_{Wsc1}$(ΔCS) and C*^{V5}T$_{Wsc1}$(ΔCS) exhibit the same degradation kinetics.

A: Schematic representation of the ERAD substrates C*T$_{Wsc1}$(ΔCS), C*^{HA}T$_{Wsc1}$(ΔCS) and C^{V5}*T$_{Wsc1}$(ΔCS); for more detail see Figure 40 and Figure 43.
B+C: Cycloheximide-chase analysis of C*T$_{Wsc1}$(ΔCS), C*^{HA}T$_{Wsc1}$(ΔCS) and C^{V5}*T$_{Wsc1}$(ΔCS) degradation was performed in *prc1*Δ cells.
Samples were taken every 30 min after cycloheximide addition (t=0 min) and C*T$_{Wsc1}$(ΔCS) derivatives were detected by immunoblotting using CPY antibody, as well as HA and V5 antibodies. Dfm1 was used as loading control.
D+E: The quantifications represent the data of up to 12 independent experiments. Error bars indicate the respective standard error of the mean (SEM). *P < 0.05, unpaired two-sample *t*-test relative to the control (C*T$_{Wsc1}$(ΔCS)).

For the control substrates C*^{HA}T$_{Wsc1}$(ΔCS) and C*^{V5}T$_{Wsc1}$(ΔCS) degradation was analyzed in cycloheximide-chase analysis, using CPY, HA and V5 antibodies (Figure 45; **B+C**). Tagged as well as untagged control substrates are degraded with the same kinetics (Figure 45; **D+E**).

Thus, it can be assumed that the HA as well as the V5 epitopes do not influence the degradation of C*T_{Pdr5}(ΔCS) and the "control" substrate C*T_{Wsc1}(ΔCS).

Possible oligomerization of C*T_{Pdr5}(ΔCS) can be determined, by performing co-immunoprecipitation experiments. Therefore, crude lysate from cells co-expressing C*$^{HA}T_{Pdr5}$(ΔCS) and C*$^{V5}T_{Pdr5}$(ΔCS) was precleared, membranes were isolated and washed. After membrane solubilization by digitonin treatment, C*$^{HA}T_{Pdr5}$(ΔCS) and C*$^{V5}T_{Pdr5}$(ΔCS) were precipitated using either HA or V5 antibody, respectively.

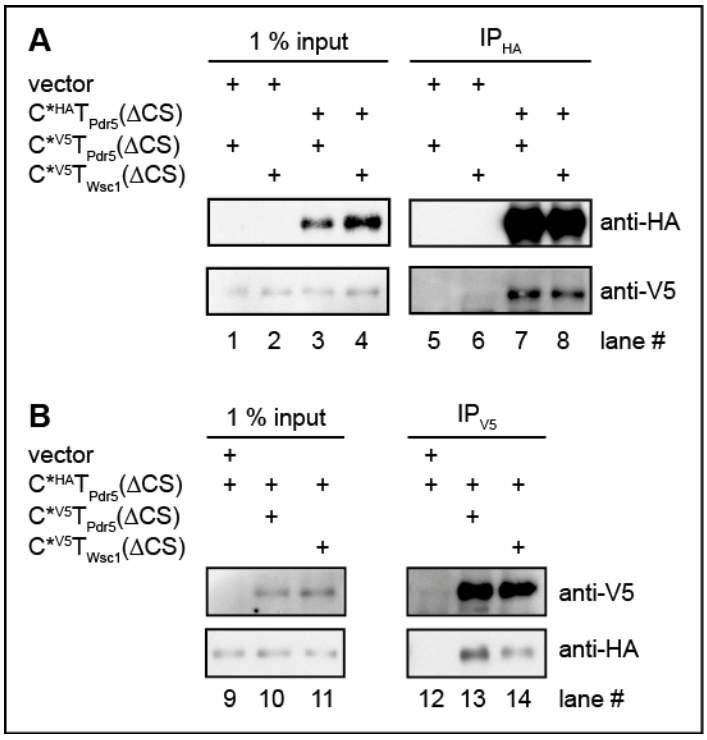

Figure 46: C*T_{Pdr5}(ΔCS) might oligomerize possibly independently of the membrane domain (T_{Pdr5}).

Isolated membranes from cells (*prc1*Δ) expressing C*T(ΔCS) derivatives as indicated (vector correspond to plasmid, containing no C*T(ΔCS) derivative), were solubilized with digitonin and subjected to immunoprecipitation with antibodies against either the HA epitope (upper part) or V5 epitope (lower part). The precipitates (IP) as well as the input control (1% input) were analyzed by SDS-PAGE and immunoblotting using HA and V5 antibodies.

Co-precipitation of C*$^{V5}T_{Pdr5}$(ΔCS) and C*$^{HA}T_{Pdr5}$(ΔCS) was shown, using a HA antibody, (Figure 46A; lane 7). Surprisingly, the control substrate C*$^{V5}T_{Wsc1}$(ΔCS) also co-precipitates with C*$^{HA}T_{Pdr5}$(ΔCS) in a precipitation using HA antibody (Figure 46A; lane 8). No unspecific binding of C*$^{V5}T_{Pdr5}$(ΔCS) or C*$^{V5}T_{Wsc1}$(ΔCS) is detected using the HA antibody in this experimental setup (Figure 46A; lane 5 and 6).

Vice versa, C*$^{HA}T_{Pdr5}$(ΔCS) is co-precipitated, in a precipitation either with

C*^{V5}T$_{Pdr5}$(ΔCS) (Figure 46B; lane 13), or the “control” substrate C*^{V5}T$_{Wsc1}$(ΔCS) (Figure 46B; lane 14) using a V5 antibody.

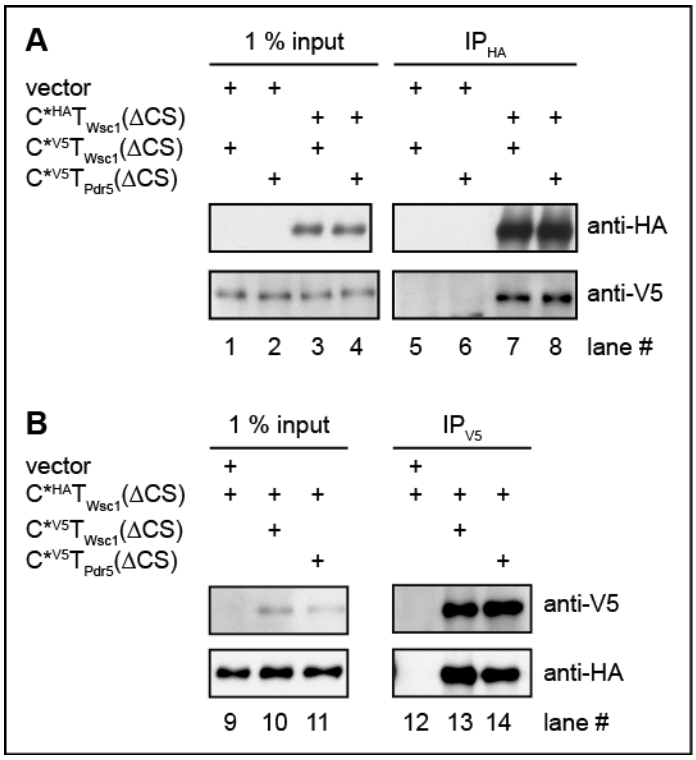

Figure 47: C*T$_{Wsc1}$(ΔCS) oligomerizes.

Isolated membranes from cells (*prc1*Δ) expressing C*T(ΔCS) derivatives as indicated (vector correspond to plasmid, containing no C*T(ΔCS) derivative), were solubilized with digitonin and subjected to immunoprecipitation with antibodies against either the HA epitope (upper part) or V5 epitope (lower part). The precipitates (IP) as well as the input control (1% input) were analyzed by SDS-PAGE and immunoblotting using HA and V5 antibodies.

Additionally, co-precipitation of C*^{HA}T$_{Wsc1}$(ΔCS) and C*^{V5}T$_{Wsc1}$(ΔCS) is detected, using either HA (Figure 47A; lane 7) or V5 antibody (Figure 47B; lane 13). As well as co-precipitation of C*^{V5}T$_{Pdr5}$(ΔCS) and C*^{HA}T$_{Wsc1}$(ΔCS) is detected, using either HA (Figure 47A; lane 8) or V5 antibody (Figure 47B; lane 14)

These data support an oligomerization of membrane-bound CPY* derivatives, lacking a cytosolic part.

However, a homogeneous oligomerization of C*T$_{Pdr5}$(ΔCS) moieties as well as a heterogeneous oligomerization of C*T$_{Pdr5}$(ΔCS) and C*T$_{Wsc1}$(ΔCS) moieties were shown. This indicates that C*T$_{Pdr5}$(ΔCS) degradation is not prevented by oligomerization.

3.2.3 Proteins with misfolded ER lumenal and aberrant membrane domains require a cytosolic lysine residue for degradation

For membrane proteins with a misfolded ER lumenal domain and a properly folded membrane domain (C*T_{Wsc1}(ΔCS) derivatives) it had been shown that the cytosolic part affects the degradation (chapter 3.2.1). Briefly, C*T_{Wsc1} derivatives lacking lysine residues in the cytosolic part are degraded by the established ERAD-L pathway, in a Der1 and Hrd1 dependent manner. Interestingly, C*T_{Wsc1} derivatives containing lysine residues in the cytosolic part are degraded in addition to the ERAD-L degradation mechanism, in a Der1 independent manner. In this so-called ERAD-L/M degradation process, substrate ubiquitination is mediated by the ubiquitin ligases Hrd1 and the Asi complex. But only ubiquitination mediated by Hrd1 is mandatory for degradation.
ER lumenal misfolded proteins with aberrant membrane parts are not degraded at all, in case they are lacking a cytosolic part (Figure 41). Thus, it seems that the cytosolic part of these proteins also affects degradation. Similar to the substrates containing a properly folded membrane part, C*T_{Pdr5}(ΔCS) derivatives were designed, varying only in the cytosolic part. C*T_{Pdr5}(ΔCS) derivatives were generated possessing either a lysine, a serine or an alanine residue as control at the cytosolic C-terminus (Figure 48), resulting in C*T_{Pdr5}(ΔCS)A, C*T_{Pdr5}(ΔCS)S and C*T_{Pdr5}(ΔCS)K.

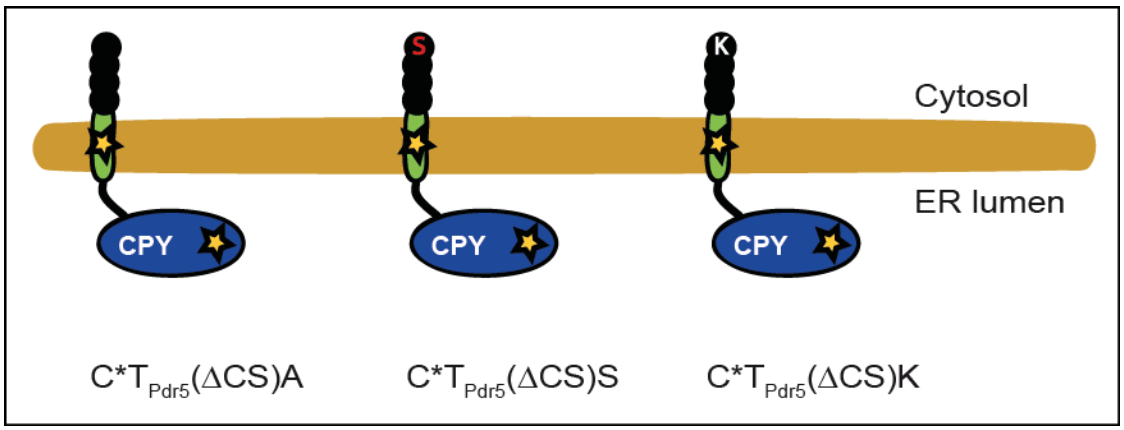

Figure 48: Schematic representation of ERAD substrates C*T_{Pdr5}(ΔCS)A, C*T_{Pdr5}(ΔCS)S and C*T_{Pdr5}(ΔCS)K.

The oval structure marked with an asterisk symbolizes the misfolded carboxypeptidase domain (C*), followed by the last transmembrane helix from Pdr5 (T_{Pdr5}), which signals misfolding, shown in green with a yellow asterisk. The black chain located in the cytosolic part of the C*T derivative represents the truncated peptide of three amino acids (arginine-valine-proline), originating from the C-terminal tail of Pdr5 (ΔCS) containing an additional lysine (K), serine (S) or alanine (A) residue. These lysine and serine residues are highlighted in white and red, respectively. The alanine, as control, is not highlighted.

First, localization and topology of the C*T$_{Pdr5}$(ΔCS) derivatives were determined as described in material and methods. C*T$_{Pdr5}$(ΔCS)A, C*T$_{Pdr5}$(ΔCS)S and C*T$_{Pdr5}$(ΔCS)K were shown to be integral membrane proteins with type I orientation (N$_{out}$; C$_{in}$) (Figure S8 and Figure S9).

Subsequently, degradation of the characterized C*T$_{Pdr5}$(ΔCS)A, or C*T$_{Pdr5}$(ΔCS)S, or C*T$_{Pdr5}$(ΔCS)K was analyzed using cycloheximide-chase assays.

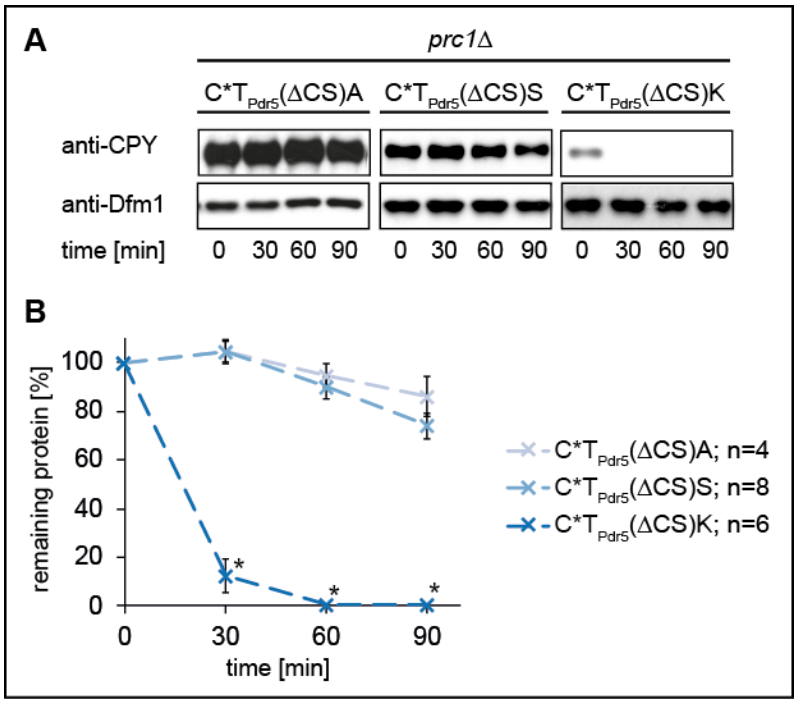

Figure 49: C*T$_{Pdr5}$(ΔCS)K is degraded, whereas the substrates C*T$_{Pdr5}$(ΔCS)S and C*T$_{Pdr5}$(ΔCS)A are not.

A: Cycloheximide-chase analysis of C*T$_{Pdr5}$(ΔCS)K, C*T$_{Pdr5}$(ΔCS)S and C*T$_{Pdr5}$(ΔCS)A degradation was performed in *prc1*Δ cells.
Samples were taken every 30 min after cycloheximide addition (t=0 min) and C*T$_{Pdr5}$(ΔCS) derivatives were detected by immunoblotting using CPY antibody. Dfm1 was used as loading control.
B: The quantification represents the data of up to 8 independent experiments. Error bars indicate the respective standard error of the mean (SEM). *P < 0.05, unpaired two-sample *t*-test relative to the control (C*T$_{Pdr5}$(ΔCS)K).

The control substrate C*T$_{Pdr5}$(ΔCS)A is rather stabilized within 90 minutes of chase (Figure 49). Also C*T$_{Pdr5}$(ΔCS)S degradation is very slow and could hardly be measured within 90 minutes of chase. The unpaired two-sample t-test showed no significant discrepancy of the measured C*T$_{Pdr5}$(ΔCS)A and C*T$_{Pdr5}$(ΔCS)S degradation kinetics.

In contrast, a single lysine residue in the cytosolic part of the C*T$_{Pdr5}$(ΔCS) derivative,

C*T_{Pdr5}(ΔCS)K, leads to fast degradation of the misfolded protein (Figure 49). In comparison, the degradation kinetics of C*T_{Pdr5}(ΔCS)K and the full-length C*T_{Pdr5}(CS), containing several lysine residues, they seem to be equal (Figure 19 and Figure 49).
These results lead to the assumption that the cytosolic part of proteins with misfolded ER lumenal domain and misfolded membrane domain affects their degradation, as it is the case for ER lumenal misfolded proteins with intact membrane domain.
Since C*T_{Pdr5}(ΔCS) is ubiquitinated but not degraded (Figure 42 and Figure 41), ubiquitination of the cytosolic variants is further analyzed.

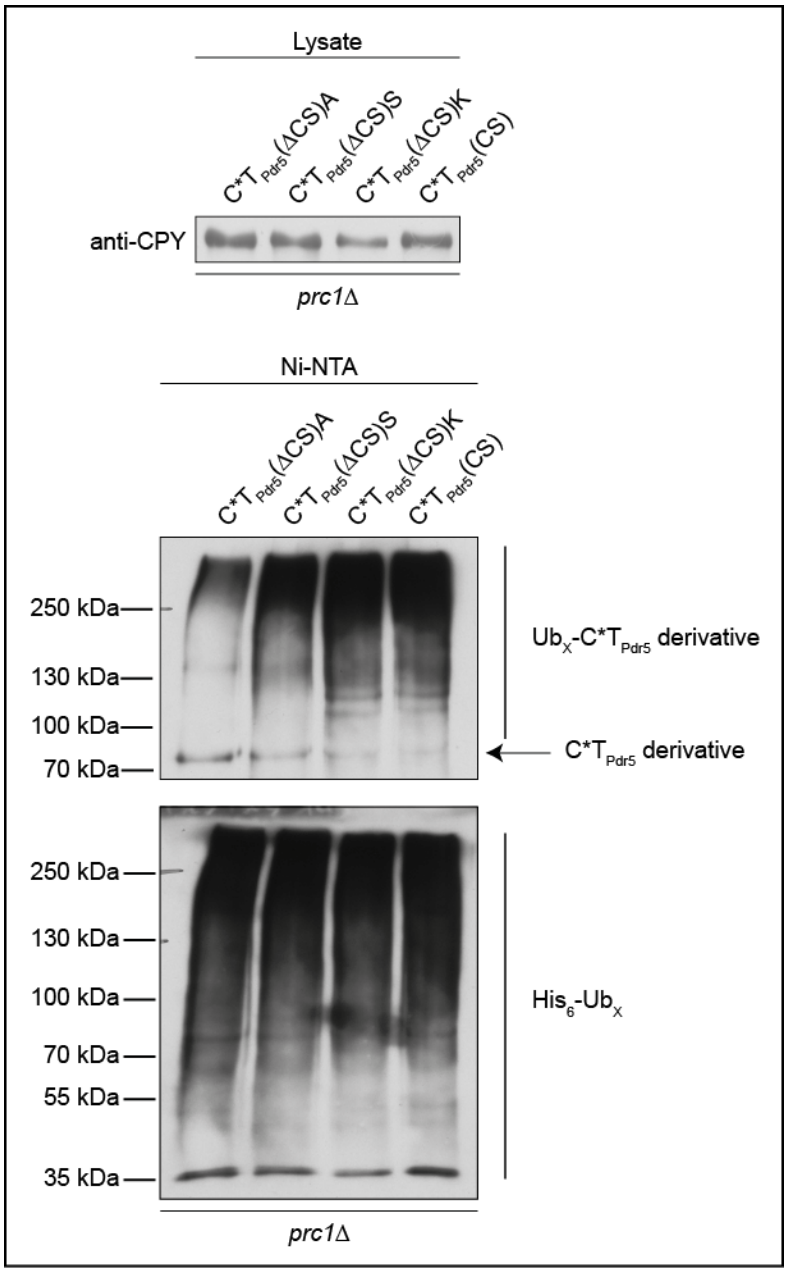

Figure 50: C*T$_{Pdr5}$(ΔCS)A and C*T$_{Pdr5}$(ΔCS)S are still ubiquitinated although not degraded.
Ubiquitination was analyzed in *prc1*Δ cells expressing His$_6$-tagged ubiquitin (Ub) and either C*T$_{Pdr5}$(ΔCS)A or C*T$_{Pdr5}$(ΔCS)S or C*T$_{Pdr5}$(ΔCS)K or C*T$_{Pdr5}$(CS). Cell lysates (input) were incubated with Ni-NTA resin under denaturing conditions to pull down all His$_6$-ubiquitinated proteins. C*T$_{Pdr5}$ derivatives were detected by immunoblotting with CPY antibody and the amount of bound polyubiquitinated proteins (His$_6$-Ub$_X$) was visualized with His antibody.

Indeed, C*T$_{Pdr5}$(ΔCS)A and C*T$_{Pdr5}$(ΔCS)S are polyubiquitinated (Figure 50), although not degraded (Figure 49). The introduction of a single serine residue to the cytosolic part of C*T$_{Pdr5}$(ΔCS) does not change the ubiquitination pattern although serine is an amino acid, which is known to be able to be ubiquitinated [116,117]. Since ubiquitination is mediated in the cytosol, it can be assumed that C*T$_{Pdr5}$(ΔCS)S is ubiquitinated at its

N-terminal CPY* moiety. Therefore, the CPY* moiety of C*T$_{Pdr5}$(ΔCS)S has probably to be initially retrotranslocated. Hrd1 is obviously the ubiquitin ligase involved in retrotranslocation as it is shown for the nondegradable substrate, C*T$_{Pdr5}$(ΔCS) (Figure 42).

The degradable substrate C*T$_{Pdr5}$(ΔCS)K is ubiquitinated and when compared to C*T$_{Pdr5}$(CS), the ubiquitination patterns seem to be equal (Figure 50).
This might be a hint that C*T$_{Pdr5}$(ΔCS)K and C*T$_{Pdr5}$(CS) are both finally retrotranslocated, ubiquitinated and degraded by the ERAD-M pathway, as it was shown for C*T$_{Pdr5}$(CS) (chapter 3.1.2).

Table 20: Overview of the different requirements for C*T$_{Pdr5}$(CS), C*T$_{Pdr5}$(ΔCS), C*T$_{Pdr5}$(ΔCS)A, C*T$_{Pdr5}$(ΔCS)S and C*T$_{Pdr5}$(ΔCS)K degradation

A green check mark indicates indispensable for degradation; a red cross symbol means dispensable for degradation; ~ (tilde) means involved in but not absolutely necessary for degradation; a red cross symbol with parenthesis indicates dispensable for degradation but participate in ubiquitination. The ERAD components including the membrane protein Der1 and the ubiquitin ligases Hrd1 and Asi complex, and their participation in degradation of the indicated substrates are shown.

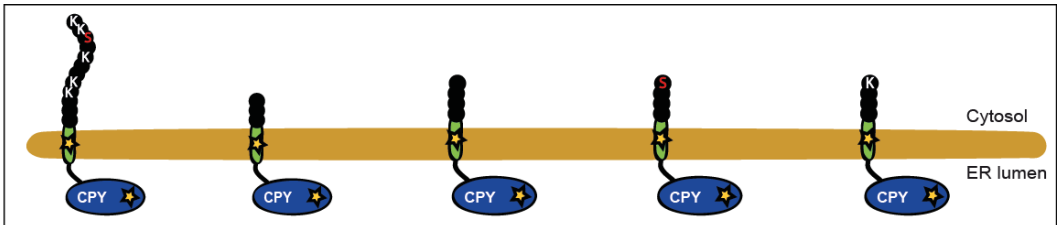

Name	C*T$_{Pdr5}$(CS)	C*T$_{Pdr5}$(ΔCS)	C*T$_{Pdr5}$(ΔCS)A	C*T$_{Pdr5}$(ΔCS)S	C*T$_{Pdr5}$(ΔCS)K
cytosolic domain	CS: peptide of 12 amino acids (RVPKKNGKLSKK)	ΔCS: truncated peptide (RVP)	ΔCS: truncated peptide (RVPA)	ΔCS: truncated peptide (RVPS)	ΔCS: truncated peptide (RVPK)
membrane domain	T$_{Pdr5}$: last transmembrane helix of Pdr5	T$_{Pdr5}$: last transmembrane helix of Pdr5	T$_{Pdr5}$: last transmembrane helix of Pdr5	T$_{Pdr5}$: last transmembrane helix of Pdr5	T$_{Pdr5}$: last transmembrane helix of Pdr5
ER lumenal domain	CPY*	CPY*	CPY*	CPY*	CPY*
Der1	✗				✗
Hrd1	~	(✗)	→ not degraded at all	→ not degraded at all	~
Asi complex	~	→ not degraded at all			~
Hrd1 and Asi complex	✓				✓

Brief summary of the current results shows that CPY* derivatives with an aberrant membrane part are solely degraded, if these proteins carry a lysine residue in their cytosolic part. Ubiquitination, which leads to rapid degradation, is mediated by Hrd1 and the Asi complex. Both ubiquitination marks signal for their final elimination by the ERAD-M degradation mechanism In case of the cytosolic lysine residue is lacking, these substrates are not degraded at all. However, Hrd1 mediates initial retrotranslocation, but final membrane extraction is impaired. (an overview is given in Table 20).

These results emphasize an extraordinary role for lysine residues in the cytosolic part of CPY* derivatives with either misfolded or intact membrane domains. These lysine residues fundamentally influence the degradation process.

3.2.4 A lysine residue in the aberrant membrane domain of proteins, with misfolded ER lumenal domain, is required for their degradation

Lysine residues in the cytosolic part of membrane-bound ERAD substrates with an ER lumenal misfolded domain have an extraordinary role to direct degradation. Thus, it seemed possible that lysine residues, located in the aberrant membrane domain, also have an extraordinary influence on degradation. New substrates were created in which tyrosine residues in the membrane domain of the nondegradable substrate C*T_{Pdr5}(ΔCS), were replaced by lysine residues.

The membrane domain of C*T_{Pdr5}(ΔCS) is the last transmembrane helix out of 12 of the multidrug transporter Pdr5. In its native environment, it associates with other membrane helices of Pdr5 via its polar residues, such as tyrosine, cysteine and asparagine. Tyrosine residues appear at position +2, +8, +13 and +20 within this membrane domain, substitution with lysine leads to the substrates $C^{*}T_{Pdr5}^{Y1\rightarrow K}$(ΔCS); $C^{*}T_{Pdr5}^{Y2\rightarrow K}$(ΔCS); $C^{*}T_{Pdr5}^{Y3\rightarrow K}$(ΔCS) and $C^{*}T_{Pdr5}^{Y4\rightarrow K}$(ΔCS) (Figure 51).

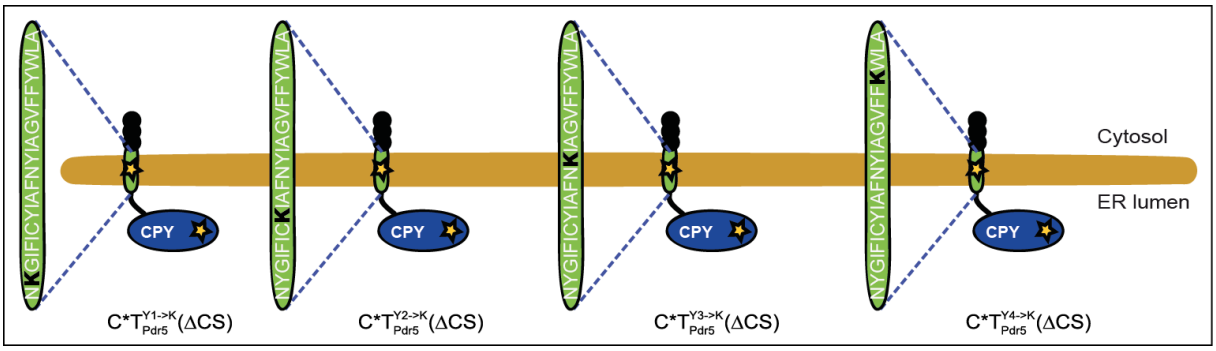

Figure 51: Schematic representation of ERAD substrates $C^{*}T_{Pdr5}^{Y1\rightarrow K}$(ΔCS); $C^{*}T_{Pdr5}^{Y2\rightarrow K}$(ΔCS); $C^{*}T_{Pdr5}^{Y3\rightarrow K}$(ΔCS) and $C^{*}T_{Pdr5}^{Y4\rightarrow K}$(ΔCS).

The oval structure marked with an asterisk symbolizes the misfolded carboxypeptidase domain (C*), followed by the last transmembrane helix from Pdr5 (T_{Pdr5}), which signals misfolding, shown in green with a yellow asterisk. T_{Pdr5} contains four tyrosine residues (Y1-4). These residues are replaced by lysine as indicated in dark black (**K**). The black chain located in the cytosolic part represents a truncated peptide of three amino acids, originating from the C-terminal tail of Pdr5 (ΔCS).

First, it was shown that $C^{*}T_{Pdr5}^{Y1\rightarrow K}$(ΔCS); $C^{*}T_{Pdr5}^{Y2\rightarrow K}$(ΔCS); $C^{*}T_{Pdr5}^{Y3\rightarrow K}$(ΔCS) and $C^{*}T_{Pdr5}^{Y4\rightarrow K}$(ΔCS) are integral membrane proteins with type I orientation (N_{out}; C_{in}) (Figure S10 and Figure S11).

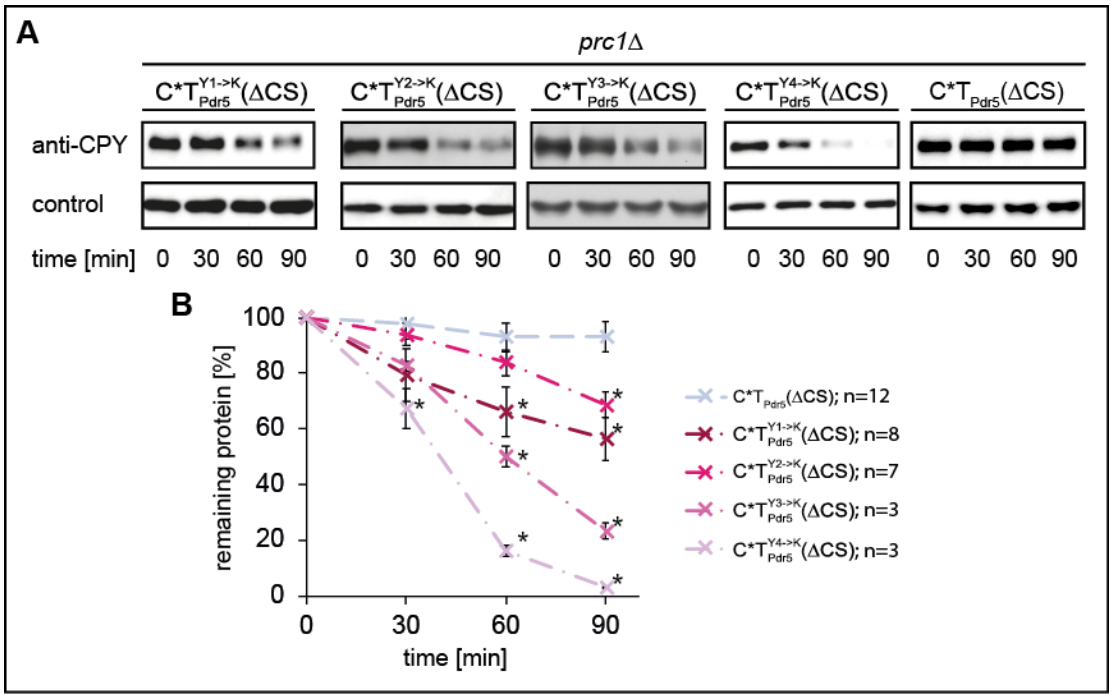

Figure 52: Lysine within the membrane domain leads to degradation.

A: Cycloheximide-chase analysis of C*T$_{Pdr5}$(ΔCS); C*T$^{Y1\rightarrow K}_{Pdr5}$(ΔCS); C*T$^{Y2\rightarrow K}_{Pdr5}$(ΔCS); C*T$^{Y3\rightarrow K}_{Pdr5}$(ΔCS) and C*T$^{Y4\rightarrow K}_{Pdr5}$(ΔCS) degradation was performed in *prc1*Δ cells.
Samples were taken every 30 min after cycloheximide addition (t=0 min) and C*T$_{Pdr5}$(ΔCS) derivatives were detected by immunoblotting using CPY antibody. Dfm1 was used as loading control.
B: The quantification represents the data of up to 12 independent experiments. Error bars indicate the respective standard error of the mean (SEM). *P < 0.05, unpaired two-sample *t*-test relative to the control (C*T$_{Pdr5}$(ΔCS)).

Figure 52 indicates that the introduction of a single lysine residue in the membrane domain of the former nondegradable substrate C*T$_{Pdr5}$(ΔCS) leads to degradation. Additionally, there is a correlation between turnover rate and the position of the lysine residue within the membrane domain in distance to the ER lumen. The closer the lysine residue is located to the cytosolic face of the membrane domain, the faster the protein is degraded (Figure 52). C*T$^{Y4\rightarrow K}_{Pdr5}$(ΔCS) is almost completely degraded, the lysine residue at position +20 is in close proximity to the cytosol). Merely 30% of C*T$^{Y1\rightarrow K}_{Pdr5}$(ΔCS) are degraded within 90 minutes of chase. In case of the lysine residue is positioned at position +2, close to the ER lumen.

In summary, not only lysine residues in the cytosolic part, but also lysine residues within the membrane helix, lead to degradation of the former nondegradable substrate C*T$_{Pdr5}$(ΔCS).

Next, it was explored, which ubiquitin ligase is required for ubiquitination of the four tyrosine-lysine exchanged substrates.

$C^{*}T_{Pdr5}^{Y3\rightarrow K}$(ΔCS) was chosen as representative for all tyrosine-lysine exchanged substrates. It contains a lysine residue within the membrane domain at position +14. Since it was shown that proteins with a misfolded ER lumenal domain, a misfolded membrane domain and lysine residues in the cytosolic part are ubiquitinated and finally degraded by the ubiquitin ligases Hrd1 and the Asi complex, they are good candidates for ubiquitination and degradation of $C^{*}T_{Pdr5}^{Y3\rightarrow K}$(ΔCS). First, turnover rates of $C^{*}T_{Pdr5}^{Y3\rightarrow K}$(ΔCS) in cells lacking the ubiquitin ligase Hrd1 were measured, using cycloheximide-chase analysis.

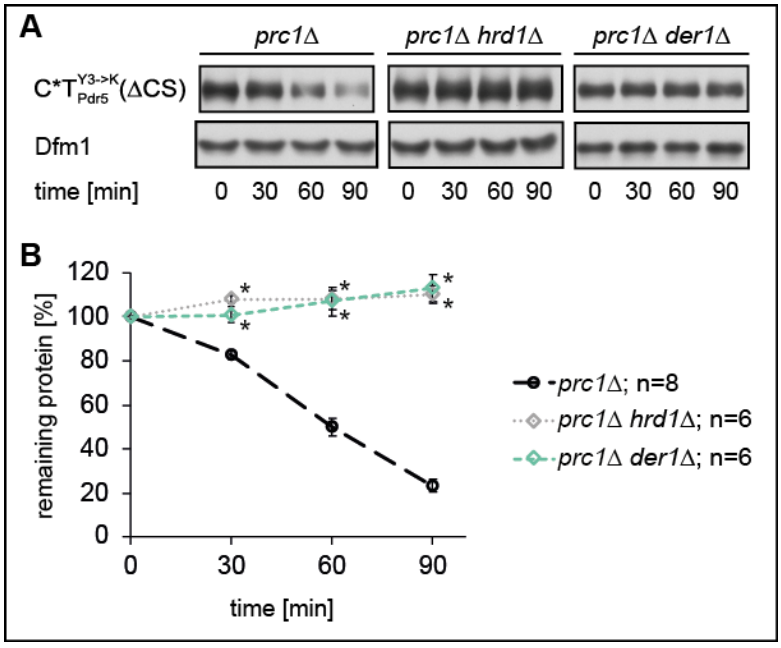

Figure 53: In contrast to ERAD-M substrates, $C^{*}T_{Pdr5}^{Y3\rightarrow K}$(ΔCS) is Hrd1 and Der1 dependent degraded.

A: Cycloheximide-chase analysis of $C^{*}T_{Pdr5}^{Y3\rightarrow K}$(ΔCS) degradation was performed in *prc1*Δ; *prc1*Δ*hrd1*Δ and *prc1*Δ*der1*Δ cells.

Samples were taken every 30 min after cycloheximide addition (t=0 min) and $C^{*}T_{Pdr5}^{Y3\rightarrow K}$(ΔCS) was detected by immunoblotting using CPY antibody. Dfm1 was used as loading control.
B: The quantification represents the data of up to 8 independent experiments. Error bars indicate the respective standard error of the mean (SEM). *P < 0.05, unpaired two-sample *t*-test relative to the control (*prc1*Δ).

Surprisingly, $C^{*}T_{Pdr5}^{Y3\rightarrow K}$(ΔCS) degradation is abrogated in *hrd1*Δ cells (Figure 53). Thus, it is obvious that Hrd1 is the only ligase involved in degradation of $C^{*}T_{Pdr5}^{Y3\rightarrow K}$(ΔCS). This makes it unnecessary to determine degradation kinetics in cells lacking components of the Asi complex.

Although the membrane domain of $C^{*}T^{Y3\rightarrow K}_{Pdr5}$(ΔCS) is misfolded and possesses a lysine residue in the membrane domain, it is completely stabilized in cells lacking Hrd1, which is contrary to the Hrd1 and Asi complex dependent ERAD-M substrate degradation (Figure 21). Thus, it should be analyzed whether the *HRD* ligase complex partner Der1 is involved in degradation of $C^{*}T^{Y3\rightarrow K}_{Pdr5}$(ΔCS). Figure 53 reveals that $C^{*}T^{Y3\rightarrow K}_{Pdr5}$(ΔCS) is completely stabilized in cells lacking Der1. This indicates that $C^{*}T^{Y3\rightarrow K}_{Pdr5}$(ΔCS) is not degraded via the ERAD-M degradation mechanism although it contains an aberrant membrane part.

Additionally, ubiquitination assays were performed to investigate, whether Hrd1 is indeed responsible for ubiquitination of $C^{*}T^{Y3\rightarrow K}_{Pdr5}$(ΔCS).

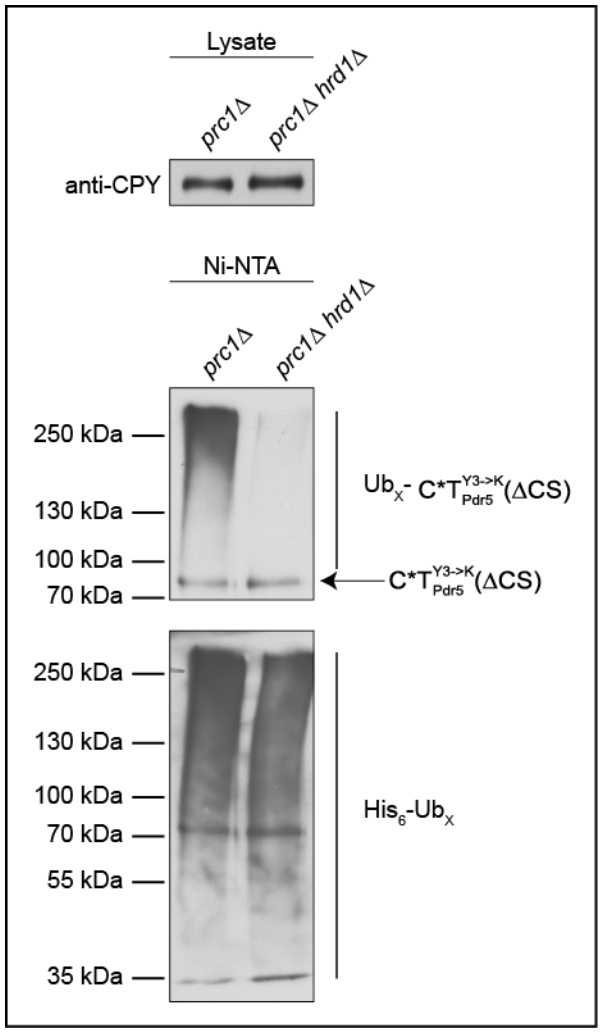

Figure 54: Ubiquitination of $C^{*}T^{Y3\rightarrow K}_{Pdr5}$ (ΔCS) is mediated by the ubiquitin ligase Hrd1.

Ubiquitination was analyzed in *prc1*Δ and *prc1*Δ*hrd1*Δ cells expressing $C^{*}T^{Y3\rightarrow K}_{Pdr5}$ (ΔCS) and His_6-tagged ubiquitin (Ub). Cell lysates (input) were incubated with Ni-NTA resin under denaturing conditions, to pull down all His_6-ubiquitinated proteins. $C^{*}T^{Y3\rightarrow K}_{Pdr5}$ (ΔCS) was detected by immunoblotting with CPY antibody and the amount of bound polyubiquitinated proteins (His_6-Ub_X) was visualized with His antibody.

Ubiquitination was analyzed in cells expressing both, $C^{*}T^{Y3\rightarrow K}_{Pdr5}$ (ΔCS) and His_6-tagged ubiquitin. In *hrd1*Δ cells, $C^{*}T^{Y3\rightarrow K}_{Pdr5}$ (ΔCS) is not ubiquitinated anymore (Figure 54). This demonstrates that Hrd1 is the only ligase involved in ubiquitination of $C^{*}T^{Y3\rightarrow K}_{Pdr5}$ (ΔCS).

Finally, it could be shown that proteins with a misfolded ER lumenal domain and an aberrant membrane part, lacking a cytosolic domain are nondegradable. They become degradable, only when lysine residues are located in the cytosolic domain or in the

aberrant membrane part. If a lysine residue is located in the cytosolic part, the proteins are ubiquitinated by the ubiquitin ligase Hrd1 together with the Asi complex. Their final elimination is independent of Der1 (an overview is given in Table 21). This stands in contrast to proteins possessing lysine residues in the membrane domain. These proteins are ubiquitinated only by the Hrd1 ligase and their terminal degradation is Der1 dependent.

Table 21: Overview of the different requirements in C^*T_{Pdr5}(CS), C^*T_{Pdr5}(ΔCS) and $C^*T^{Y3\rightarrow K}_{Pdr5}$ (ΔCS) degradation

A green check mark indicates indispensable for degradation; a red cross symbol means dispensable for degradation; ~ (tilde) means involved in but not absolutely necessary for degradation; a red cross symbol with parenthesis indicates dispensable for degradation but participate in ubiquitination. The ERAD components including the membrane protein Der1 and the ubiquitin ligases Hrd1 and Asi complex, and their participation in degradation of the indicated substrates are shown.

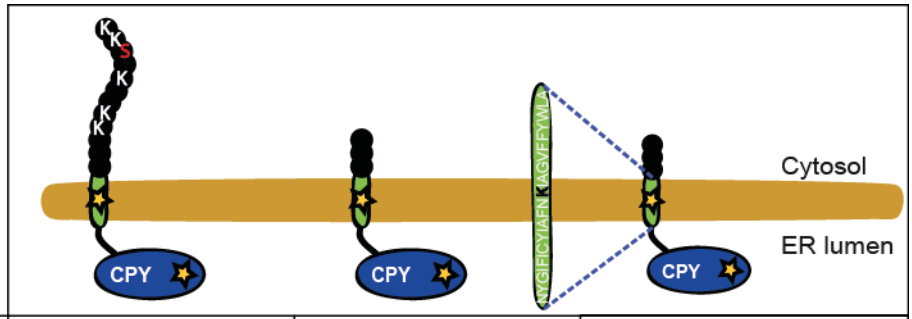

Name	C^*T_{Pdr5}(CS)	C^*T_{Pdr5}(ΔCS)	$C^*T^{Y3->K}_{Pdr5}$(ΔCS)
cytosolic domain	CS: peptide of 12 amino acids (RVPKKNGKLSKK)	ΔCS: truncated peptide (RVP)	ΔCS: truncated peptide (RVP)
membrane domain	T_{Pdr5} : last transmembrane helix of Pdr5	T_{Pdr5} : last transmembrane helix of Pdr5	T_{Pdr5} : last transmembrane helix of Pdr5 **containing lysine**
ER lumenal domain	CPY*	CPY*	CPY*
Der1	✗		✓
Hrd1	~	(✗)	✓
Asi complex	~	→ not degraded at all	
Hrd1 and Asi complex	✓		

3.2.5 Lysine residues in the misfolded ER lumenal domain of proteins with an aberrant membrane part do not influence the degradation mechanism

To analyze if the extraordinary role of lysine residues to influence degradation is restricted to their location in the cytosolic domain and in the membrane part, further C*T_{Pdr5}(ΔCS) derivatives were designed. Two serine residues (S548 and S562), which are located in the amino acid stretch between membrane domain and ER lumenal CPY* were substituted for lysine residues (Figure 55).

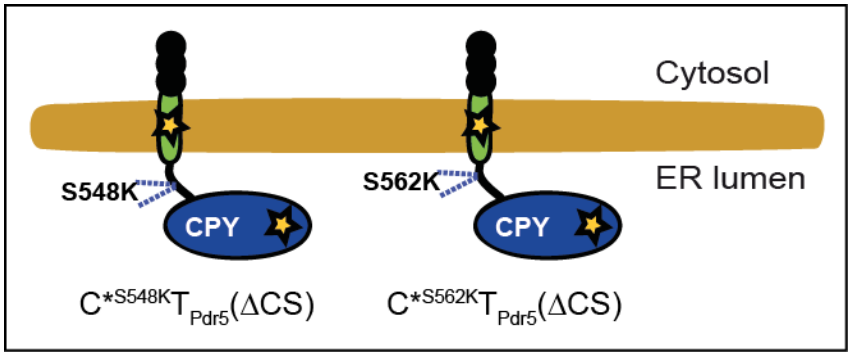

Figure 55: Schematic representation of ERAD substrates C*^{S548K}T_{Pdr5}(ΔCS) and C*^{S562K}T_{Pdr5}(ΔCS).

The oval structure marked with an asterisk symbolizes the misfolded carboxypeptidase domain (C*), followed by the last transmembrane helix from Pdr5, which signals misfolding, shown in green with a yellow asterisk. C* is linked to T_{Pdr5} via a linker. This linker is based on 32 amino acids upstream of the last transmembrane helix of Pdr5 (T_{Pdr5}). In this linker the two serine residues, mutated to lysine, are illustrated. The black chain located in the cytosolic part represents the truncated peptide of three amino acids (arginine-valine-proline), originating from the C-terminal tail of Pdr5 (ΔCS).

First, C*^{S548K}T_{Pdr5}(ΔCS) and C*^{S562K}T_{Pdr5}(ΔCS) localization and topology were determined, indicating that they are integral membrane proteins with type I orientation (N_{out}; C_{in}) (Figure S12 and Figure S13).

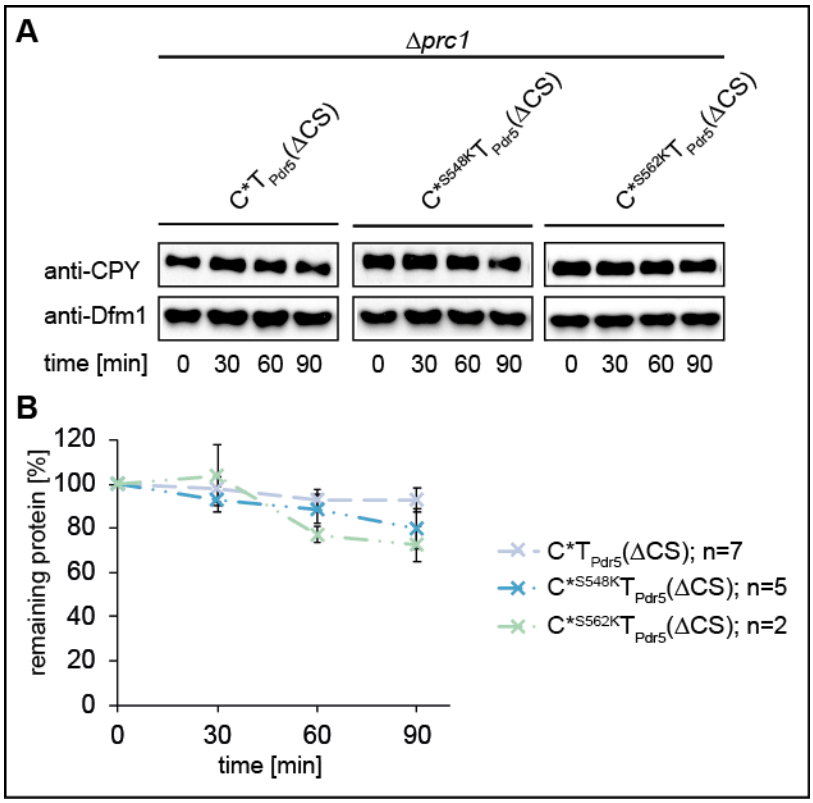

Figure 56: Lysines in the ER lumenal part of C*T$_{Pdr5}$(ΔCS) derivatives did not affect the capability for degradation.

A: Cycloheximide-chase analysis of C*^{S548K}T$_{Pdr5}$(ΔCS) and C*^{S562K}T$_{Pdr5}$(ΔCS) degradation was performed in *prc1*Δ cells.
Samples were taken every 30 min after cycloheximide addition (t=0 min) and C*T$_{Pdr5}$(ΔCS) derivatives were detected by immunoblotting using CPY antibody. Dfm1 was used as loading control.
B: The quantification represents the data of up to 7 independent experiments. Error bars indicate the respective standard error of the mean (SEM). *P < 0.05, unpaired two-sample *t*-test relative to the control (C*T$_{Pdr5}$(ΔCS)).

Then, degradation kinetics of the newly generated C*^{S548K}T$_{Pdr5}$(ΔCS) and C*^{S562K}T$_{Pdr5}$(ΔCS) as well as the established nondegradable substrate C*T$_{Pdr5}$(ΔCS) were measured. Figure 56 shows complete stabilization within 90 min of chase for all of the tested C*T$_{Pdr5}$(ΔCS) variants.

In summary, the extraordinary role of lysine residues to influence degradation of proteins, which possess an ER lumenal misfolded domain and an aberrant membrane part, is restricted to their location in the cytosolic part and in the membrane domain because lysine residues located in the ER lumenal domain do not lead to degradation of proteins with a misfolded ER lumenal domain and an aberrant membrane part.

3.2.6 Function of serine residues in the cytosolic part of ER lumenal misfolded proteins with aberrant membrane domain

ERAD substrates with a misfolded ER lumenal domain and an aberrant membrane part, lacking a cytosolic part are not degraded at all. Such ERAD substrates are C*T_{Pdr5}(ΔCS) and C*T_{Pdr5}(ΔCS)A (schematic representation Figure 40 and Figure 48; degradation kinetics Figure 41 and Figure 49). Surprisingly, these nondegradable substrates are still polyubiquitinated by the ubiquitin ligase Hrd1 (Figure 42). Besides its function as a ubiquitin ligase, several ERAD studies provide evidence for the participation of Hrd1 in retrotranslocation [59,97]. Based on this, nondegradable C*T_{Pdr5}(ΔCS) variants might undergo initial retrotranslocation through Hrd1 until they are ubiquitinated. It seems that the N-terminal CPY* moiety is ubiquitinated since these nondegradable substrates do not possess an amino acid, which can be ubiquitinated in their membrane or cytosolic parts. However, final retrotranslocation and thus degradation is impaired in some way.

Interestingly, presence of a single lysine residue in the cytosolic part results in rapid degradation which is shown for the lysine-containing substrates, C*T_{Pdr5}(ΔCS)K and C*T_{Pdr5}(CS) (schematic representation Figure 24 and Figure 48; degradation Figure 19 and Figure 49). Prior to final elimination, the lysine-containing substrates have to be terminally retrotranslocated.

In general, the composition of the cytosolic part determines the degradation fate of proteins containing a misfolded ER lumenal domain as well as an aberrant membrane part.

The question arises, whether a ubiquitination mark in the cytosolic part has to be recognized, or whether the lysine residue itself has to be identified, to trigger complete retrotranslocation and final degradation.

Lysine is the *canonical* amino acid for ubiquitination [116,254]. Ubiquitin can also be attached to hydroxylated amino acids, such as serine and threonine [116,255], forming an oxy-ester bond. A construct was designed, containing only a serine residue instead of lysine (Figure 48 and Figure 57). This construct, C*T_{Pdr5}(ΔCS)S, is ubiquitinated but not degraded at all (Figure 49 and Figure 50). This leads to the assumption that only lysine is able to direct complete retrotranslocation. To analyze this, a steric interference of serine with the C-terminus of the substrate should be excluded. Therefore,

C*T_{Pdr5}(ΔCS)S was extended by an alanine, resulting in the substrate C*T_{Pdr5}(ΔCS)SA (Figure 57).

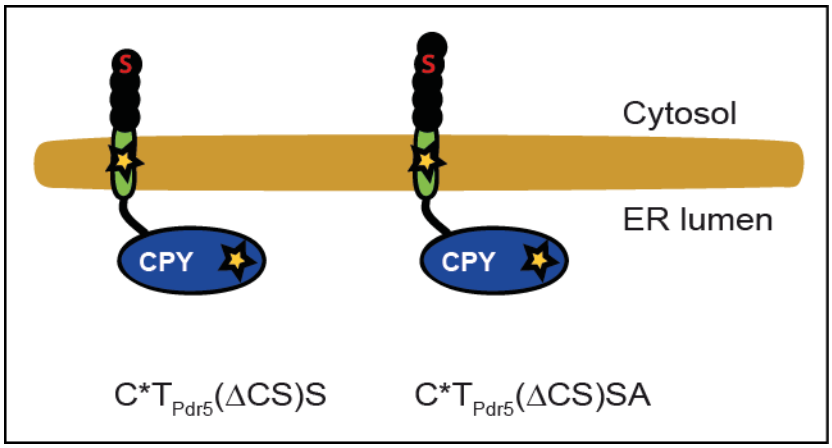

Figure 57: Schematic representation of ERAD substrates C*T_{Pdr5}(ΔCS)S and C*T_{Pdr5}(ΔCS)SA.
The oval structure marked with an asterisk symbolizes the misfolded carboxypeptidase domain (C*), followed by the last transmembrane helix from Pdr5 (T_{Pdr5}), which signals misfolding, shown in green with a yellow asterisk. The black chain located in the cytosolic part of the C*T derivative represents the truncated peptide of three amino acids (arginine-valine-proline), originating from the C-terminal tail of Pdr5 (ΔCS) containing an additional serine (S) residue or serine and alanine residue (SA). This serine residue is highlighted in red and the alanine residue as control is not highlighted.

C*T_{Pdr5}(ΔCS)SA was shown to be an integral membrane protein with type I orientation (N_{out}; C_{in}), by treating microsomes with detergent and digesting microsomes with proteinase K (Figure S14 and Figure S15).

Then, turnover rates were measured, performing cycloheximide-chase analysis.

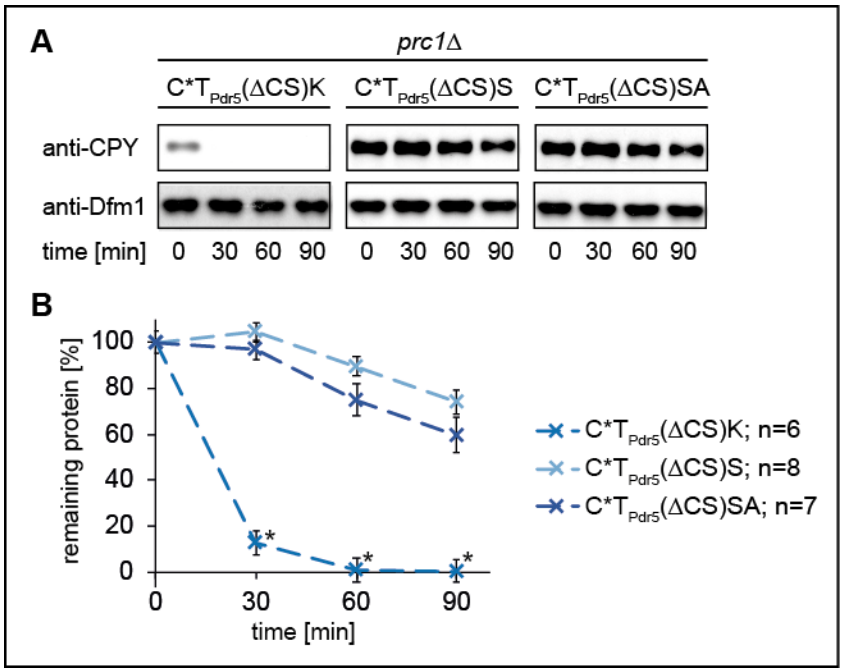

Figure 58: C*T$_{Pdr5}$(ΔCS)K is degraded, whereas the substrates C*T$_{Pdr5}$(ΔCS)S and C*T$_{Pdr5}$(ΔCS)SA are not.

A: Cycloheximide-chase analysis of C*T$_{Pdr5}$(ΔCS)K, C*T$_{Pdr5}$(ΔCS)S and C*T$_{Pdr5}$(ΔCS)SA degradation was performed in *prc1*Δ cells.
Samples were taken every 30 min after cycloheximide addition (t=0 min) and C*T$_{Pdr5}$(ΔCS) derivatives were detected by immunoblotting using CPY antibody. Dfm1 was used as loading control.
B: The quantification represents the data of up to 8 independent experiments. Error bars indicate the respective standard error of the mean (SEM). *P < 0.05, unpaired two-sample *t*-test relative to the control (C*T$_{Pdr5}$(ΔCS)K).

Figure 58 demonstrates that C*T$_{Pdr5}$(ΔCS)SA is stabilized to the same extent as C*T$_{Pdr5}$(ΔCS)S. In comparison, a lysine residue in the cytosolic part leads to degradation with a half-life of 15 minutes. This might indicate that there is no steric interference of the serine residue at the C-terminus.

Since C*T$_{Pdr5}$(ΔCS)S is still ubiquitinated although not degraded (Figure 49 and Figure 50) it was analyzed, whether C*T$_{Pdr5}$(ΔCS)SA is also ubiquitinated.

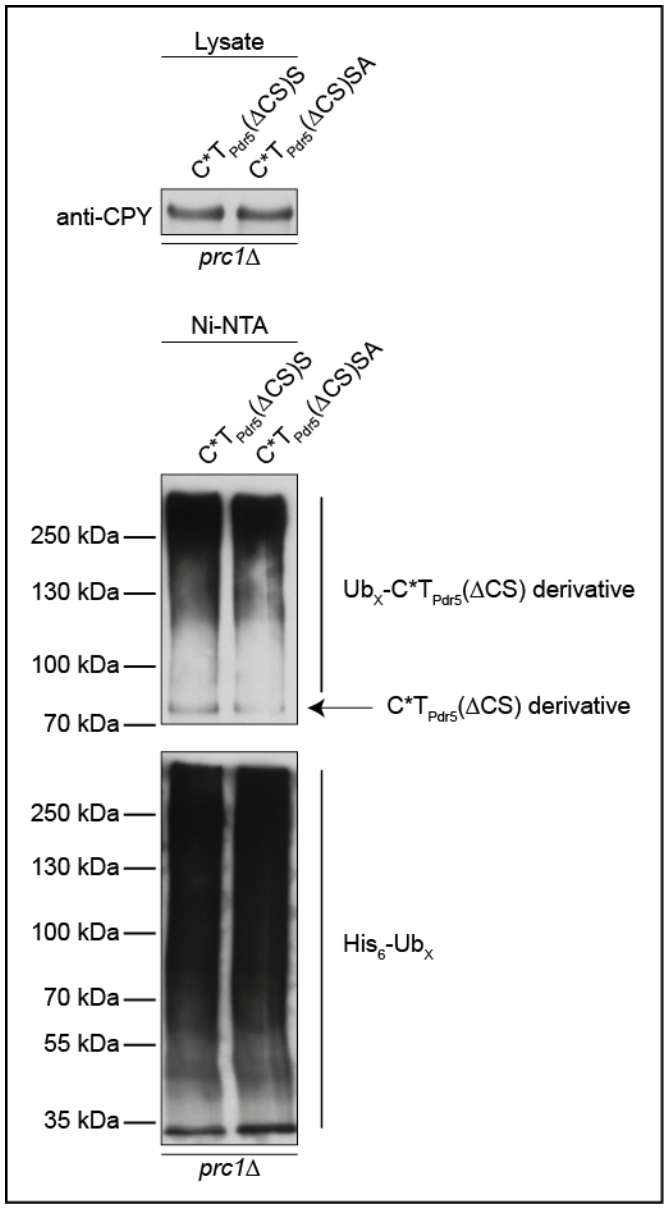

Figure 59: There is no difference in the ubiquitination pattern of C*T$_{Pdr5}$(ΔCS)S and C*T$_{Pdr5}$(ΔCS)SA.

Ubiquitination was analyzed in *prc1*Δ cells expressing C*T$_{Pdr5}$(ΔCS) derivative (as indicated) and His$_6$-tagged ubiquitin (Ub). Cell lysates (input) were incubated with Ni-NTA resin under denaturing conditions, to pull down all His$_6$-ubiquitinated proteins. C*T$_{Pdr5}$(ΔCS) derivatives were detected by immunoblotting with CPY antibody and the amount of bound polyubiquitinated proteins (His$_6$-Ub$_X$) was visualized with His antibody.

In vivo ubiquitination assays reveal that Ub$_X$-C*T$_{Pdr5}$(ΔCS)SA and Ub$_X$-C*T$_{Pdr5}$(ΔCS)S comprise the same ubiquitination patterns (Figure 59). Since ubiquitination of ER proteins is conducted in the cytosol, the ER proteins have to retrograde pass the ER membrane. But it was shown that polyubiquitinated C*T$_{Pdr5}$(ΔCS)SA is not degraded in a time period of 90 minutes of chase and thus accumulates in the ER membrane. It is assumed that C*T$_{Pdr5}$(ΔCS)SA is initially retrotranslocated and ubiquitinated,

however, final retrotranslocation is impaired.

Table 22: Overview of the different requirements for C*T$_{Pdr5}$(CS), C*T$_{Pdr5}$(ΔCS), C*T$_{Pdr5}$(ΔCS)A, C*T$_{Pdr5}$(ΔCS)S, C*T$_{Pdr5}$(ΔCS)SA and C*T$_{Pdr5}$(ΔCS)K degradation

A green check mark indicates indispensable for degradation; a red cross symbol means dispensable for degradation; ~ (tilde) means involved in but not absolutely necessary for degradation; a red cross symbol with parenthesis indicates dispensable for degradation but participate in ubiquitination. The ERAD components including the membrane protein Der1 and the ubiquitin ligases Hrd1 and Asi complex, and their participation in degradation of the indicated substrates are shown.

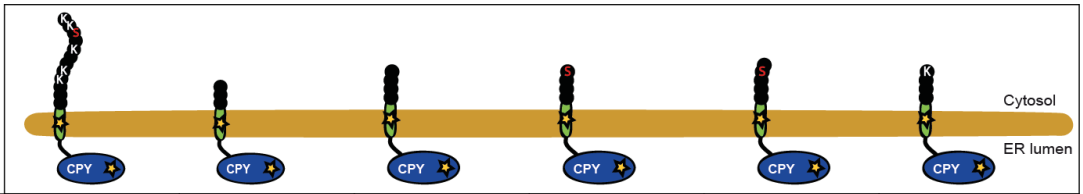

Name	C*T$_{Pdr5}$(CS)	C*T$_{Pdr5}$(ΔCS)	C*T$_{Pdr5}$(ΔCS)A	C*T$_{Pdr5}$(ΔCS)S	C*T$_{Pdr5}$(ΔCS)SA	C*T$_{Pdr5}$(ΔCS)K
cytosolic domain	CS: peptide of 12 amino acids (RVPKKNGKLSKK)	ΔCS: truncated peptide (RVP)	ΔCS: truncated peptide (RVPA)	ΔCS: truncated peptide (RVPS)	ΔCS: truncated peptide (RVPSA)	ΔCS: truncated peptide (RVPK)
membrane domain	T$_{Pdr5}$: last transmembrane helix of Pdr5	T$_{Pdr5}$: last transmembrane helix of Pdr5	T$_{Pdr5}$: last transmembrane helix of Pdr5	T$_{Pdr5}$: last transmembrane helix of Pdr5	T$_{Pdr5}$: last transmembrane helix of Pdr5	T$_{Pdr5}$: last transmembrane helix of Pdr5
ER lumenal domain	CPY*	CPY*	CPY*	CPY*	CPY*	CPY*
Der1	✗					✗
Hrd1	~	(✗)	→ not degraded at all	→ not degraded at all	→ not degraded at all	~
Asi complex	~	→ not degraded at all				~
Hrd1 and Asi complex	✓					✓

In summary CPY* derivatives with a misfolded membrane domain, containing serine residues in close proximity to the membrane are ubiquitinated but not degraded in a time period of 90 minutes of chase. This suggests that initial retrotranslocation occurs, but final retrotranslocation is impaired (an overview is given in Table 22).

Next, it is examined, whether a serine residue at different positions in the cytosolic part is recognized. Therefore, a C*T$_{Pdr5}$(CS) derivative was created, containing a serine residue in the cytosolic part in some distance to the ER membrane.

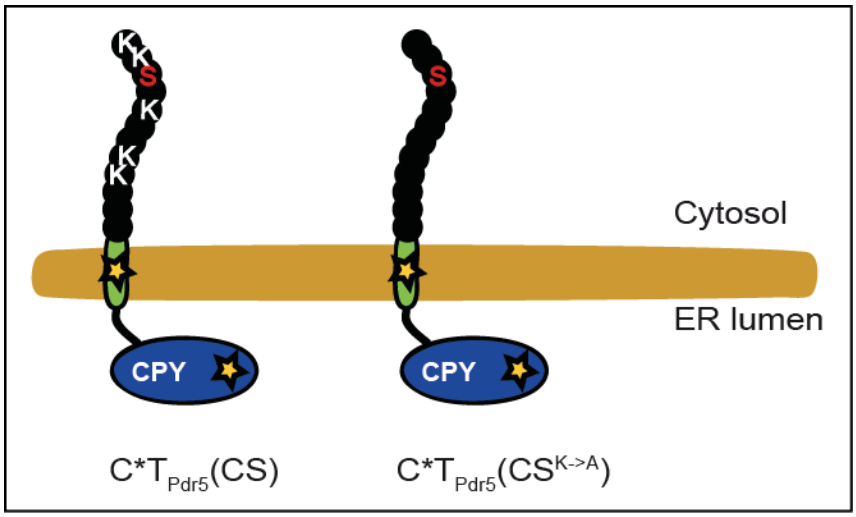

Figure 60: Schematic representation of ERAD substrates C*T$_{Pdr5}$(CS) and C*T$_{Pdr5}$(CS$^{K->A}$).
The oval structure marked with an asterisk symbolizes the misfolded carboxypeptidase domain (C*), followed by the last transmembrane helix from Pdr5 (T$_{Pdr5}$), which signals misfolding, shown in green with a yellow asterisk. The black chain located in the cytosolic part of the C*T derivative represents a peptide of 12 amino acids, originating from the C-terminal tail of Pdr5 (CS). The peptide contains five lysine residues (K) and a single serine residue (S). These lysine and serine residues are highlighted in white and red, respectively. In C*T$_{Pdr5}$(CS$^{K->A}$) all lysine residues of the (CS) were replaced by alanine.

The cytosolic part of C*T$_{Pdr5}$(CS) includes five lysine residues and a single serine residue, which is located at position +10 in distance to the ER membrane.

All lysine residues in the cytosolic part of C*T$_{Pdr5}$(CS) were substituted for alanine, resulting in the serine-only substrate C*T$_{Pdr5}$(CS$^{K->A}$) (Figure 60).

C*T$_{Pdr5}$(CS$^{K->A}$) is an integral membrane protein with type I orientation (N_{out}; C_{in}). This was shown in proteinase K protection assays (Figure S16). Furthermore, the ER lumenal CPY* moiety is required for ER retention, because the control construct, CT$_{Pdr5}$(CS$^{K->A}$), containing the native CPY moiety, is proteolytically active in the vacuole (Figure S17).

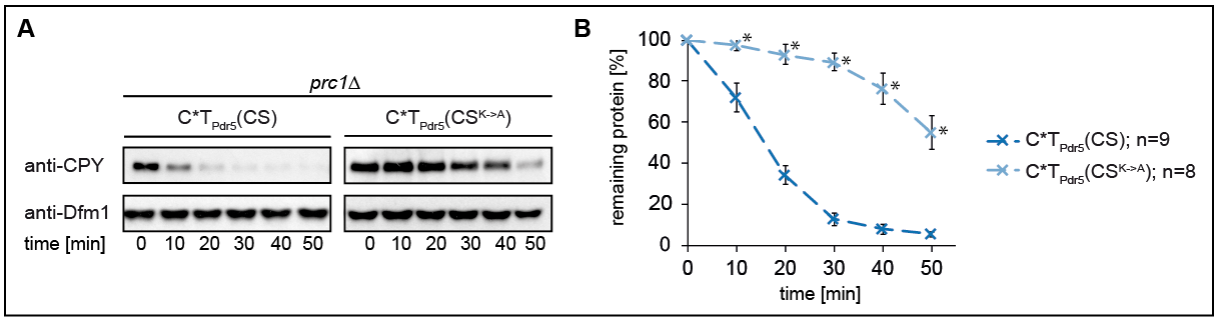

Figure 61: C*T$_{Pdr5}$(CS) and C*T$_{Pdr5}$(CS$^{K->A}$) are degraded with different kinetics within 50 min of chase.

A: Cycloheximide-chase analysis of C*T$_{Pdr5}$(CS) and C*T$_{Pdr5}$(CS$^{K->A}$) degradation was performed in *prc1*Δ cells.
Samples were taken every 10 min after cycloheximide addition (t=0 min) and C*T$_{Pdr5}$(CS) derivatives were detected by immunoblotting using CPY antibody. Dfm1 was used as loading control.
B: The quantification represents the data of up to 9 independent experiments. Error bars indicate the respective standard error of the mean (SEM). *P < 0.05, unpaired two-sample *t*-test relative to the control (C*T$_{Pdr5}$(CS)).

In Figure 61 turnover rates of C*T$_{Pdr5}$(CS) and C*T$_{Pdr5}$(CS$^{K->A}$) are compared. The lysine-rich and serine-containing construct, C*T$_{Pdr5}$(CS), is degraded with a half-life of 15 minutes, whereas the half-life of the serine-only construct, C*T$_{Pdr5}$(CS$^{K->A}$), is ~50 minutes. This shows that a serine residue located in some distance to the membrane induces slow degradation of the construct. Thus, C*T$_{Pdr5}$(CS$^{K->A}$) is completely retrotranslocated prior to degradation. On contrary, degradation is hardly detectable within 90 minutes of chase if the serine residue is located in close proximity to the ER membrane, as it was shown for the construct, C*T$_{Pdr5}$(ΔCS)S (Figure 58). Retrotranslocation of C*T$_{Pdr5}$(ΔCS)S failed, because it remains in the membrane.

In chapter 3.1.2, it was shown that the lysine-rich and serine-containing construct, C*T$_{Pdr5}$(CS), is degraded via the ERAD-M pathway, in a Der1 independent manner, and ubiquitinated by the ubiquitin ligase Hrd1 together with the Asi complex.
C*T$_{Pdr5}$(CS) and C*T$_{Pdr5}$(CS$^{K->A}$) differ only in the presence of lysine residues in the cytosolic part but are degraded with different turnover rates (schematic representation Figure 60; degradation Figure 61). Degradation mechanism of C*T$_{Pdr5}$(CS$^{K->A}$) was further analyzed.

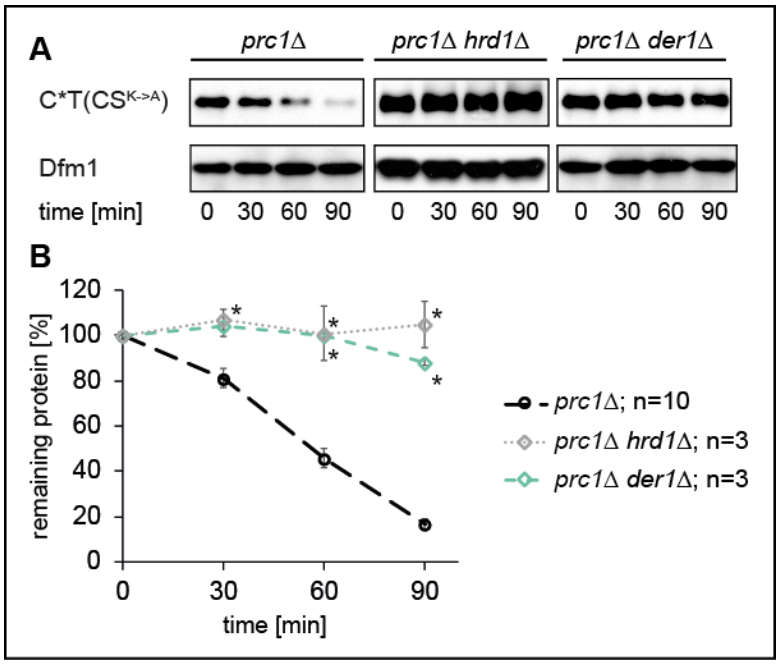

Figure 62: C*T_{Pdr5}($CS^{K->A}$) degradation is Hrd1 and Der1 dependent.

A: Cycloheximide-chase analysis of C*T_{Pdr5}($CS^{K->A}$) degradation was performed in *prc1Δ; prc1Δhrd1Δ* and *prc1Δder1Δ* cells.
Samples were taken every 30 min after cycloheximide addition (t=0 min) and C*T_{Pdr5}($CS^{K->A}$) was detected by immunoblotting using CPY antibody. Dfm1 was used as loading control.
B: The quantification represents the data of up to 10 independent experiments. Error bars indicate the respective standard error of the mean (SEM). *P < 0.05, unpaired two-sample *t*-test relative to the control (*prc1Δ*).

First, degradation kinetics in cells lacking the ubiquitin ligase Hrd1, were measured. Complete stabilization of C*T_{Pdr5}($CS^{K->A}$) was observed (Figure 62). This indicates that Hrd1 is the only ligase involved in degradation of the serine-only construct. The Asi complex does not seem to play any role. This is surprising, because C*T_{Pdr5}($CS^{K->A}$) and the ERAD-M substrate C*T_{Pdr5}(CS) differ only in the presence of lysine residues in the cytosolic part and both contain an ER lumenal misfolded domain (CPY*) as well as an aberrant membrane part (T_{Pdr5}).

According to the classification of ERAD substrates by Vashist and Ng 2004 [41] as well as Carvalho et al. 2006 [42] containing an aberrant membrane might be degraded via the ERAD-M pathway. Astonishingly, degradation of C*T_{Pdr5}($CS^{K->A}$) is abolished in cells lacking Der1 (Figure 62). This shows that a serine residue in the cytosolic part of ER lumenal misfolded proteins, with misfolded membrane domain directs the protein to another degradation pathway, as a lysine residue positioned in the same domain.

Previous publications uncovered a participation of Dfm1 in ERAD-C as well as ERAD-M substrate degradation [86,106]. C*T$_{Pdr5}$(CS$^{K->A}$) contains a misfolded membrane domain and a cytosolic serine residue. Thus, Dfm1 is a candidate that might possibly participate in degradation of C*T$_{Pdr5}$(CS$^{K->A}$).

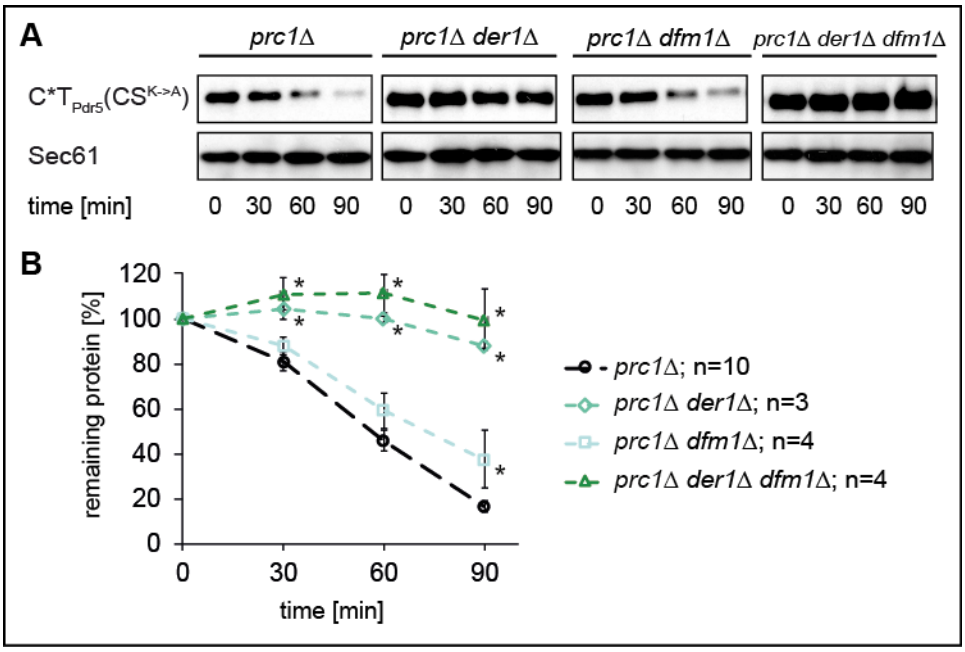

Figure 63: Dfm1 is slightly involved in C*T$_{Pdr5}$(CS$^{K->A}$) degradation.

A: Cycloheximide-chase analysis of C*T$_{Pdr5}$(CS$^{K->A}$) degradation was performed in *prc1*Δ; *prc1*Δ*der1*Δ*; prc1*Δ*dfm1*Δ *and prc1*Δ*der1*Δ*dfm1*Δ cells.
Samples were taken every 30 min after cycloheximide addition (t=0 min) and C*T$_{Pdr5}$(CS$^{K->A}$) was detected by immunoblotting using CPY antibody. Sec61 was used as loading control.
B: The quantification represents the data of up to 10 independent experiments. Error bars indicate the respective standard error of the mean (SEM). *P < 0.05, unpaired two-sample *t*-test relative to the control (*prc1*Δ).

Figure 63 demonstrates that C*T$_{Pdr5}$(CS$^{K->A}$) degradation is only slightly impaired in cells lacking Dfm1, but completely stabilized when Der1 is missing.
Thus, C*T$_{Pdr5}$(CS$^{K->A}$) degradation is dependent on both, Der1 and Dfm1, but to very different extent.
Since Der1 as well as Dfm1 are in complex with the ubiquitin ligase Hrd1 [86], *in vivo* ubiquitination assays might give further information whether they are required for C*T$_{Pdr5}$(CS$^{K->A}$) ubiquitination.

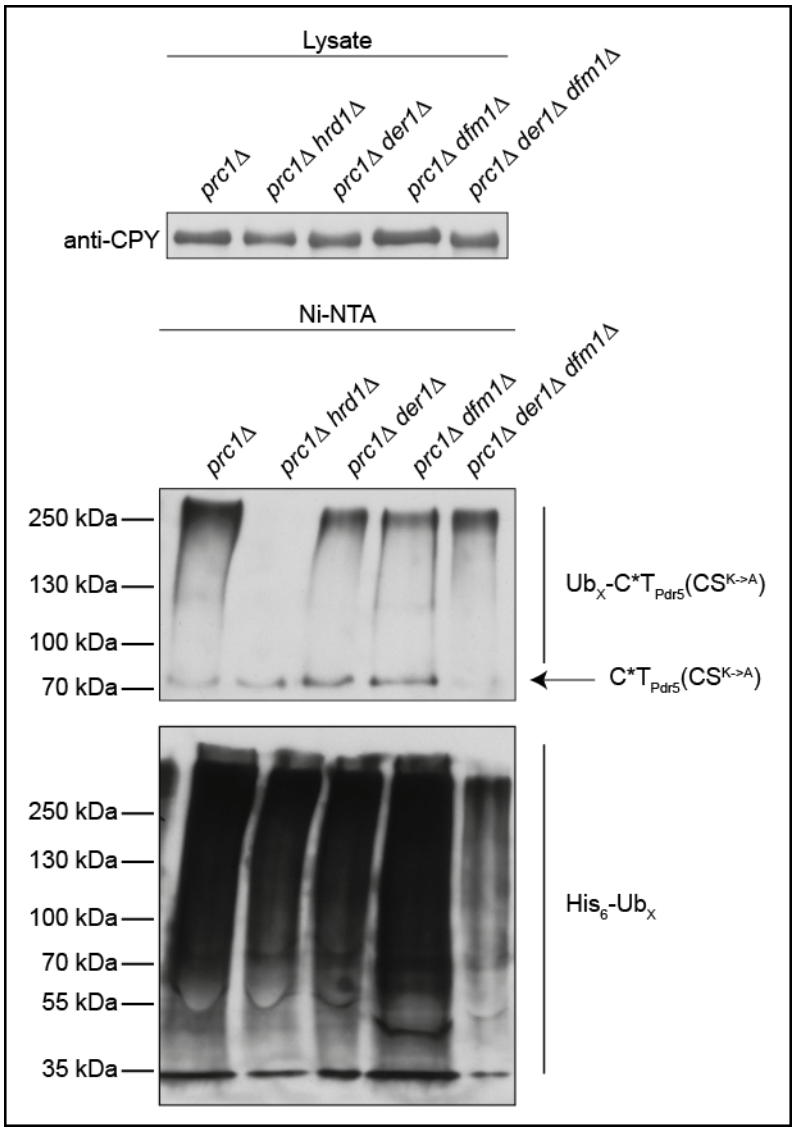

Figure 64: Ubiquitination of C*T$_{Pdr5}$(CS$^{K->A}$) is mediated by the ubiquitin ligase Hrd1. In cells lacking Der1 or Dfm1, C*T$_{Pdr5}$(CS$^{K->A}$) is still ubiquitinated.

Ubiquitination was analyzed in cells (genotype as indicated) expressing C*T$_{Pdr5}$(CS$^{K->A}$) and His$_6$-tagged ubiquitin (Ub). Cell lysates (input) were incubated with Ni-NTA resin under denaturing conditions to pull down all His$_6$-ubiquitinated proteins. C*T$_{Pdr5}$(CS$^{K->A}$) was detected by immunoblotting with CPY antibody and the amount of bound polyubiquitinated proteins (His$_6$-Ub$_X$) was visualized with His antibody.

C*T$_{Pdr5}$(CS$^{K->A}$) ubiquitination is only conducted by the ubiquitin ligase Hrd1. In cells lacking either Der1 or Dfm1, C*T$_{Pdr5}$(CS$^{K->A}$) is still ubiquitinated (Figure 64).

Since Der1 and Dfm1 are a homologous pair of membrane proteins and both are required for C*T$_{Pdr5}$(CS$^{K->A}$) degradation. They might have an overlapping function in degradation of C*T$_{Pdr5}$(CS$^{K->A}$). Therefore, ubiquitination was additionally analyzed in cells depleted for both, Der1 and Dfm1. Astonishingly, C*T$_{Pdr5}$(CS$^{K->A}$) is found to be ubiquitinated in cells double depleted of Der1 and Dfm1 (Figure 64).This indicates that

a Der1 and Dfm1 have no overlapping function and a Der1 and Dfm1 independent process participates in the recruitment of $C^*T_{Pdr5}(CS^{K->A})$ to the ubiquitin ligase Hrd1.

In brief summary, a serine residue in the cytosolic part of CPY* derivatives with a misfolded membrane domain induces only degradation, if the serine residue is located in some distance to the ER membrane. Der1, Dfm1 and a Der1 and Dfm1 independent process seems to be involved upstream of $C^*T_{Pdr5}(CS^{K->A})$ ubiquitination. Hrd1 seems to be the only ligase required for ubiquitination of the serine-only substrate.
In comparison, a lysine residue in the cytosolic part of CPY* derivatives with misfolded membrane domain, leads to degradation in a Der1 independent manner and ubiquitination of these substrates is mediated by the ubiquitin ligases Hrd1 and the Asi complex (Figure 19, Figure 21 and Figure 22).

A lysine residue located within the aberrant membrane domain of an ER lumenal misfolded protein, lacking a cytosolic part, triggers degradation dependent on Der1 and Hrd1 (Figure 53). To investigate whether serine residues located within the membrane domain also induce degradation, new substrates were generated.

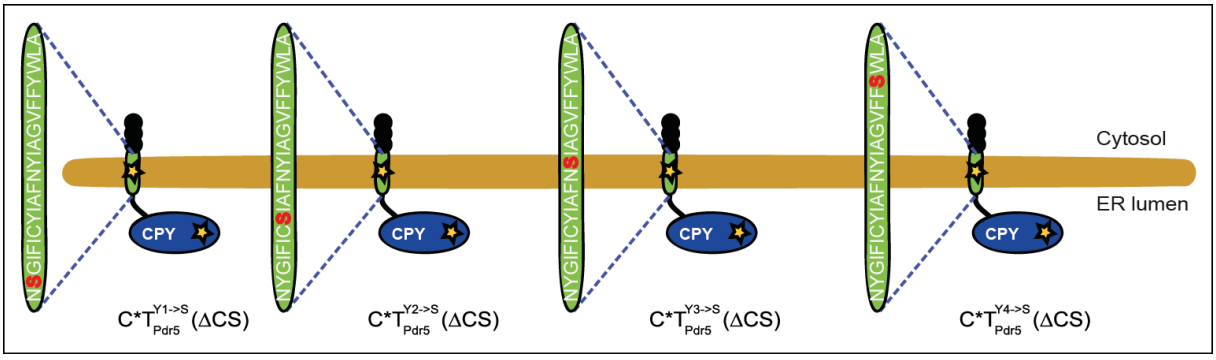

Figure 65: Schematic representation of ERAD substrates $C^*T^{Y1\rightarrow S}_{Pdr5}$ (ΔCS); $C^*T^{Y2\rightarrow S}_{Pdr5}$ (ΔCS); $C^*T^{Y3\rightarrow S}_{Pdr5}$ (ΔCS) and $C^*T^{Y4\rightarrow S}_{Pdr5}$ (ΔCS).

The oval structure marked with an asterisk symbolizes the misfolded carboxypeptidase domain (C*), followed by the last transmembrane helix from Pdr5 (T_{Pdr5}), which signals misfolding, shown in green with a yellow asterisk. T_{Pdr5} contains four tyrosine residues (Y1-4). These residues are replaced by serine as indicated in dark red (S). The black chain located in the cytosolic part represents a truncated peptide of three amino acids (arginine-valine-proline), originating from the C-terminal tail of Pdr5 (ΔCS).

Therefore, serine residues were introduced at the same positions within the aberrant membrane domain as lysine in the former constructs (Figure 51 and Figure 65). $C^{*}T_{Pdr5}^{Y1\rightarrow S}$(ΔCS); $C^{*}T_{Pdr5}^{Y2\rightarrow S}$(ΔCS); $C^{*}T_{Pdr5}^{Y3\rightarrow S}$(ΔCS) and $C^{*}T_{Pdr5}^{Y4\rightarrow S}$(ΔCS) were shown to be integral membrane proteins with type I orientation (N_{out}; C_{in}), by treating microsomes with detergent and digesting microsomes with proteinase K (Figure S18 and Figure S19).

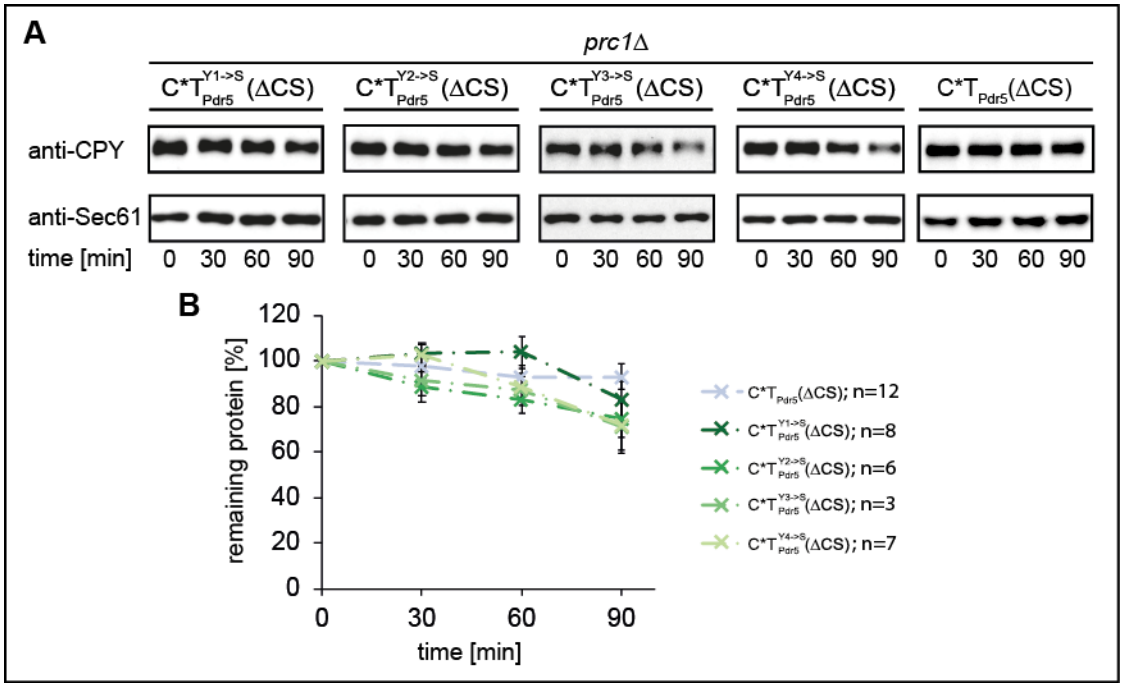

Figure 66: Serine residues in the membrane domain do not induce degradation.

A: Cycloheximide-chase analysis of $C^{*}T_{Pdr5}$(ΔCS); $C^{*}T_{Pdr5}^{Y1\rightarrow S}$(ΔCS); $C^{*}T_{Pdr5}^{Y2\rightarrow S}$(ΔCS); $C^{*}T_{Pdr5}^{Y3\rightarrow S}$(ΔCS) and $C^{*}T_{Pdr5}^{Y4\rightarrow S}$(ΔCS) degradation was performed in *prc1*Δ cells. Samples were taken every 30 min after cycloheximide addition (t=0 min) and $C^{*}T_{Pdr5}$(ΔCS) derivatives were detected by immunoblotting using CPY antibody. Sec61 was used as loading control.
B: The quantification represents the data of up to 12 independent experiments. Error bars indicate the respective standard error of the mean (SEM). *P < 0.05, unpaired two-sample *t*-test relative to the control ($C^{*}T_{Pdr5}$(ΔCS)).

Degradation kinetics of the membrane mutants, containing serine residues, reveal that they are not degraded at all (Figure 66). This indicates that introduction of a serine residue, into the aberrant membrane domain of ER lumenal misfolded proteins lacking cytosolic parts, does not induce degradation.

Only cytosolically located serine residues induce degradation if they are located in some distance to the ER membrane. Thus, it should be distinguished whether the ubiquitination mark at the serine or whether the prolonged cytosolic part causes successful retrotranslocation and final degradation of CPY* derivatives with a misfolded membrane domain.

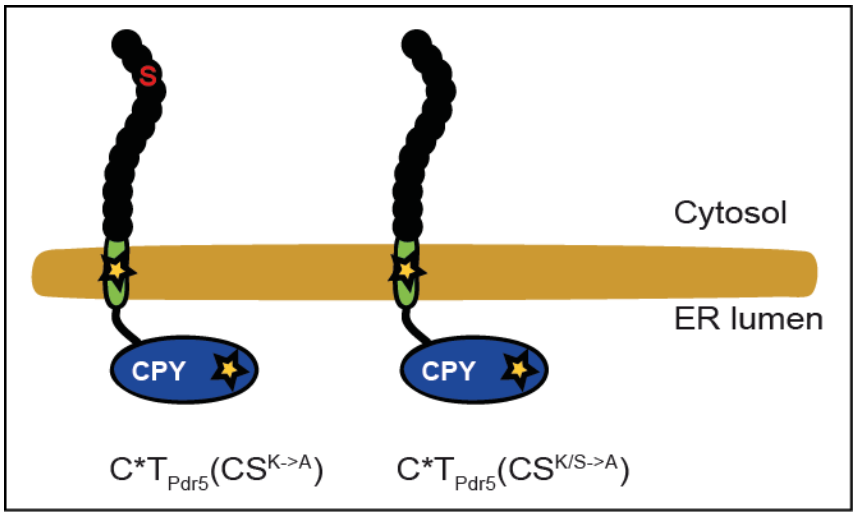

Figure 67: Schematic representation of ERAD substrates C*T$_{Pdr5}$(CS$^{K->A}$) and C*T$_{Pdr5}$(CS$^{K/S->A}$).

The oval structure marked with an asterisk symbolizes the misfolded carboxypeptidase domain (C*), followed by the last transmembrane helix from Pdr5 (T$_{Pdr5}$), which signals misfolding, shown in green with a yellow asterisk. The black chain located in the cytosolic part of the C*T$_{Pdr5}$ derivative represents a peptide of 12 amino acids, originating from the C-terminal tail of Pdr5 (CS). The peptide contains five lysine residues (K) and a single serine residue (S). In C*T$_{Pdr5}$(CS$^{K->A}$) all lysine residues of the (CS) are replaced by alanine, in C*T$_{Pdr5}$(CS$^{K/S->A}$) the serine residue of the (CS) is replaced by alanine, additionally, and is highlighted in red.

Therefore, a new substrate was created, which contains a prolonged cytosolic part without any amino acid that can be ubiquitinated. In order to receive such a substrate the cytosolic serine residue of C*T$_{Pdr5}$(CS$^{K->A}$) was substituted for an alanine residue, resulting in C*T$_{Pdr5}$(CS$^{K/S->A}$) (Figure 67).

Analysis of topology and localization showed that C*T$_{Pdr5}$(CS$^{K/S->A}$) is an integral membrane protein with type I orientation (N$_{out}$; C$_{in}$) (Figure S20). Furthermore, the ER lumenal CPY* moiety is required for ER retention, because the control construct, CT$_{Pdr5}$(CS$^{K/S->A}$), containing the native CPY moiety, is proteolytically active in the vacuole (Figure S21).

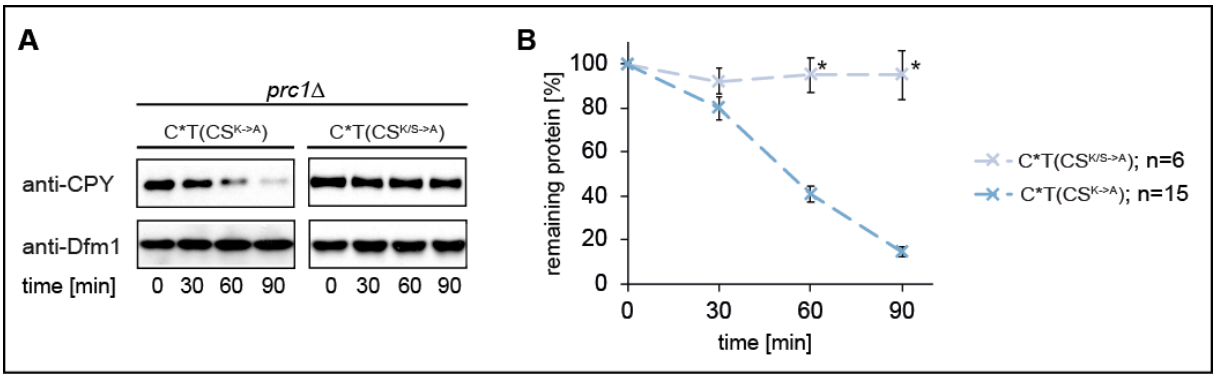

Figure 68: C*T$_{Pdr5}$(CS$^{K/S->A}$) is not degraded at all.

A: Cycloheximide-chase analysis of C*T$_{Pdr5}$(CS$^{K->A}$) and C*T$_{Pdr5}$(CS$^{K/S->A}$) degradation was performed in *prc1*Δ cells.
Samples were taken every 30 min after cycloheximide addition (t=0 min) and C*T$_{Pdr5}$(CS) derivatives were detected by immunoblotting using CPY antibody. Dfm1 was used as loading control.
B: The quantification represents the data of up to 15 independent experiments. Error bars indicate the respective standard error of the mean (SEM). *P < 0.05, unpaired two-sample *t*-test relative to the control (C*T$_{Pdr5}$(CS$^{K->A}$)).

C*T$_{Pdr5}$(CS$^{K/S->A}$) is not degraded at all (Figure 68), leading to the assumption that not the presence of a cytosolic part but a ubiquitination mark triggers final degradation.
In chapter 3.2.2 it was shown that a cytosolically truncated version - C*T$_{Pdr5}$(ΔCS) - lacking any residue, which can be ubiquitinated, is also not degraded, but ubiquitinated by the ubiquitin ligase Hrd1. Thus, it is possible that C*T$_{Pdr5}$(CS$^{K/S->A}$) is also ubiquitinated by Hrd1 but not degraded. This should be further investigated.

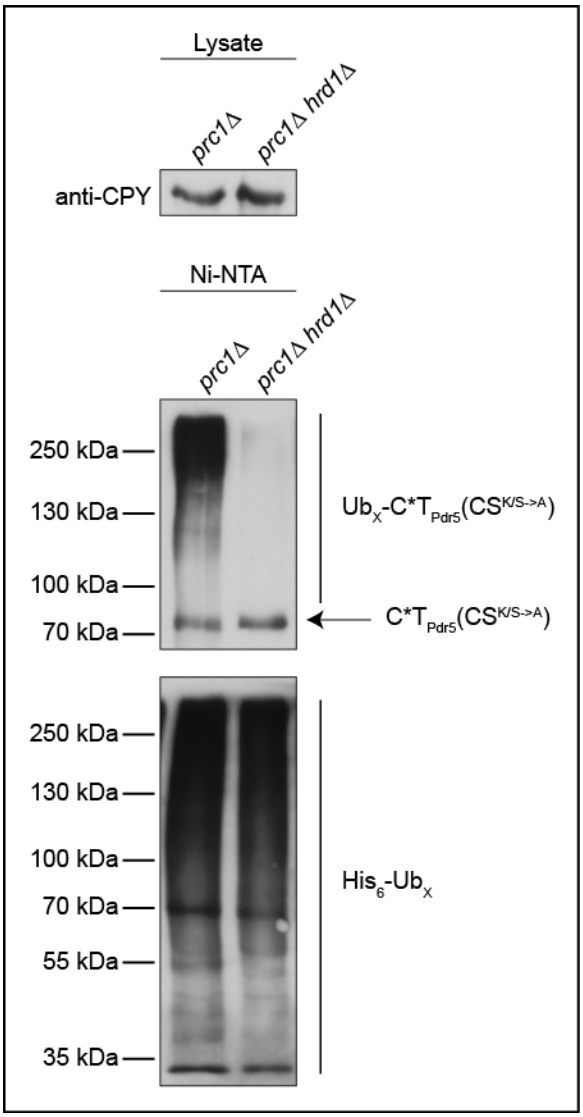

Figure 69: Ubiquitination of C*T$_{Pdr5}$(CS$^{K/S->A}$) is mediated by the Hrd1 ubiquitin ligase.
Ubiquitination was analyzed in *prc1*Δ cells expressing C*T$_{Pdr5}$ derivative and His$_6$-tagged ubiquitin (Ub). Cell lysates (input) were incubated with Ni-NTA resin under denaturing conditions to pull down all His$_6$-ubiquitinated proteins. C*T$_{Pdr5}$ derivatives were detected by immunoblotting with CPY antibody and the amount of bound polyubiquitinated proteins (His$_6$-Ub$_X$) was visualized with His antibody.

Figure 69 illustrates, that C*T$_{Pdr5}$(CS$^{K/S->A}$) is still ubiquitinated. However, degradation kinetics does not show any turnover (Figure 68). The substrate must be ubiquitinated at the CPY* moiety, because membrane domain (T$_{Pdr5}$) and cytosolic part (CS$^{K/S->A}$) lacking any amino acid that can be ubiquitinated. Since C*T$_{Pdr5}$(CS$^{K/S->A}$) is not degraded, the CPY* moiety must undergo initial retrotranslocation for ubiquitination to occur. However, final retrotranslocation is abolished in some way.

In summary, this proves that a ubiquitination mark for proteasomal degradation at the cytosolic serine residue has to be present to trigger complete retrotranslocation.

However, the attachment of ubiquitin chains to either lysine or serine residues leads to different degradation pathways.

The cytosolic part of C*T$_{Pdr5}$(CS) contains five lysine residues, as well as a single serine residue. To analyze, whether there is a hierarchy of directing pathways by the lysine or serine residues, new substrates were generated, which contain only lysine residues in their cytosolic part.

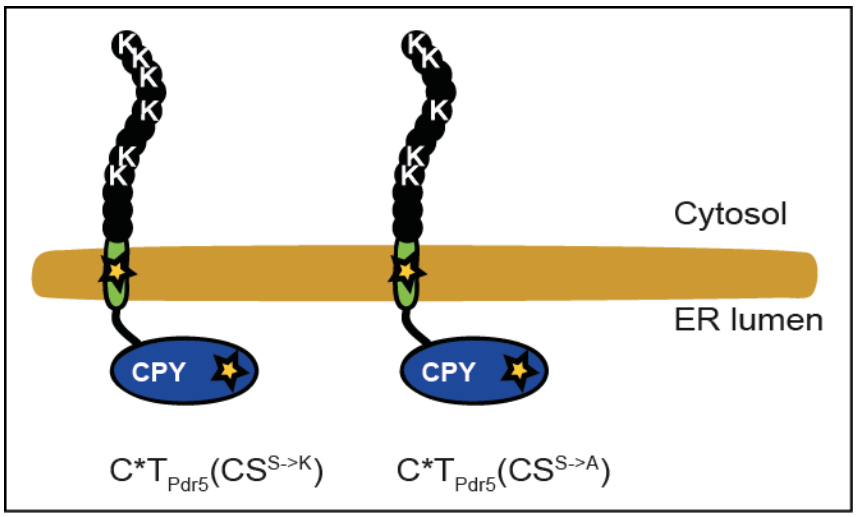

Figure 70: Schematic representation of ERAD substrates C*T$_{Pdr5}$(CS$^{S->K}$) and C*T$_{Pdr5}$(CS$^{S->A}$). The oval structure marked with an asterisk symbolizes the misfolded carboxypeptidase domain (C*), followed by the last transmembrane helix from Pdr5 (T$_{Pdr5}$), which signals misfolding, shown in green with a yellow asterisk. The black chain located in the cytosolic part of the C*T derivative represents a peptide of 12 amino acids, originating from the C-terminal tail of Pdr5 (CS). The peptide contains five lysine residues (K) and a single serine residue (S). The serine residue is replaced by lysine or alanine, respectively. Lysine residues of the (CS) are highlighted in white.

Therefore, the serine residue in the cytosolic part of C*T$_{Pdr5}$(CS) was substituted for a lysine or an alanine residue, respectively (Figure 70).

Analysis of topology and localization showed that C*T$_{Pdr5}$(CS$^{S->K}$) and C*T$_{Pdr5}$(CS$^{S->A}$) are integral membrane proteins with type I orientation (N_{out}; C_{in}) (Figure S22 and Figure S23).

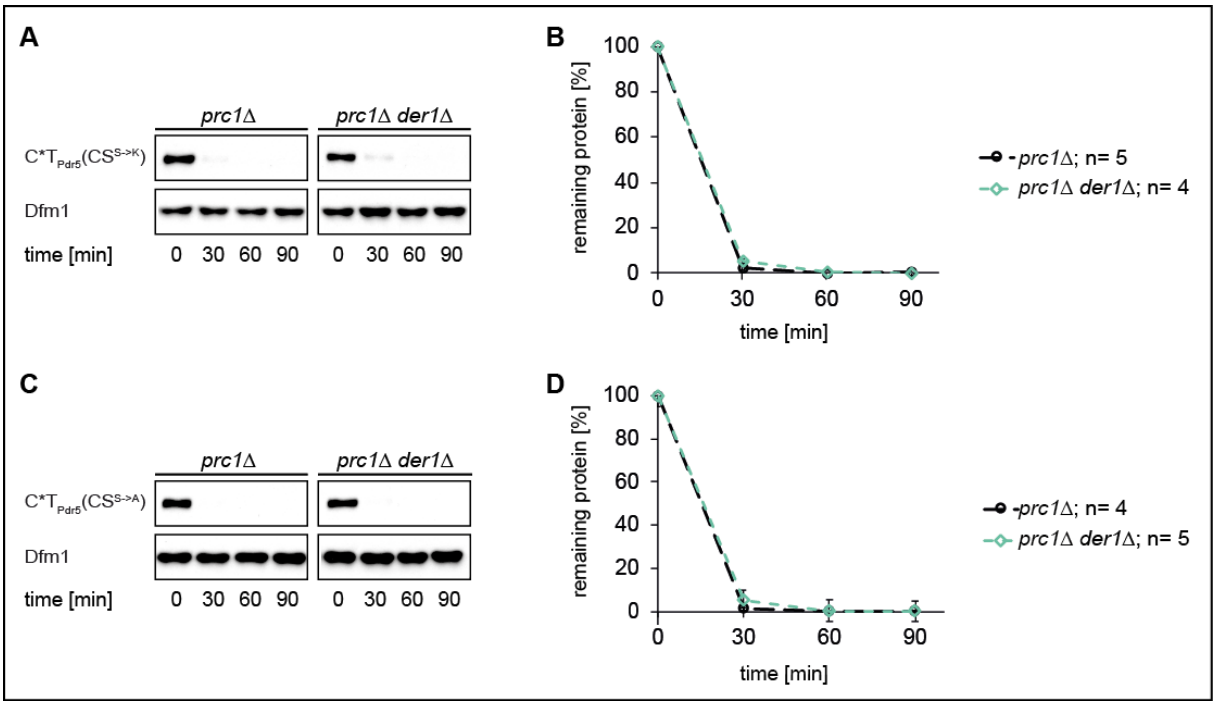

Figure 71: The degradation of C*T$_{Pdr5}$(CS$^{S->K}$) and C*T$_{Pdr5}$(CS$^{S->A}$) is not dependent on Der1.
A+C: Cycloheximide-chase analysis of C*T$_{Pdr5}$(CS$^{S->K}$) and C*T$_{Pdr5}$(CS$^{S->A}$) degradation was performed in *prc1*Δ and *prc1*Δ*der1*Δ cells.
Samples were taken every 30 min after cycloheximide addition (t=0 min) and C*T$_{Pdr5}$(CS) derivatives were detected by immunoblotting using CPY antibody. Dfm1 was used as loading control.
B+D: The quantifications represent the data of up to five independent experiments. Error bars indicate the respective standard error of the mean (SEM). *P < 0.05, unpaired two-sample t-test relative to the control (*prc1*Δ).

Figure 71 illustrates that both lysine-only substrates have a half-life of 15 minutes, which is comparable to the turnover rates of C*T$_{Pdr5}$(CS) and C*T$_{Pdr5}$(ΔCS)K (Figure 19 and Figure 49). Furthermore, all substrates, with an ER lumenal misfolded domain and an aberrant membrane part, containing lysine in the cytosolic part are degraded independently of Der1 (Figure 71 and Figure 19). This shows that the serine residue has no influence on degradation of the lysine-rich and serine-containing construct C*T$_{Pdr5}$(CS).

In vivo ubiquitination assays were performed, to compare the ubiquitination patterns of the lysine-only substrates with C*T$_{Pdr5}$(CS), which is the lysine-rich and serine-containing construct.

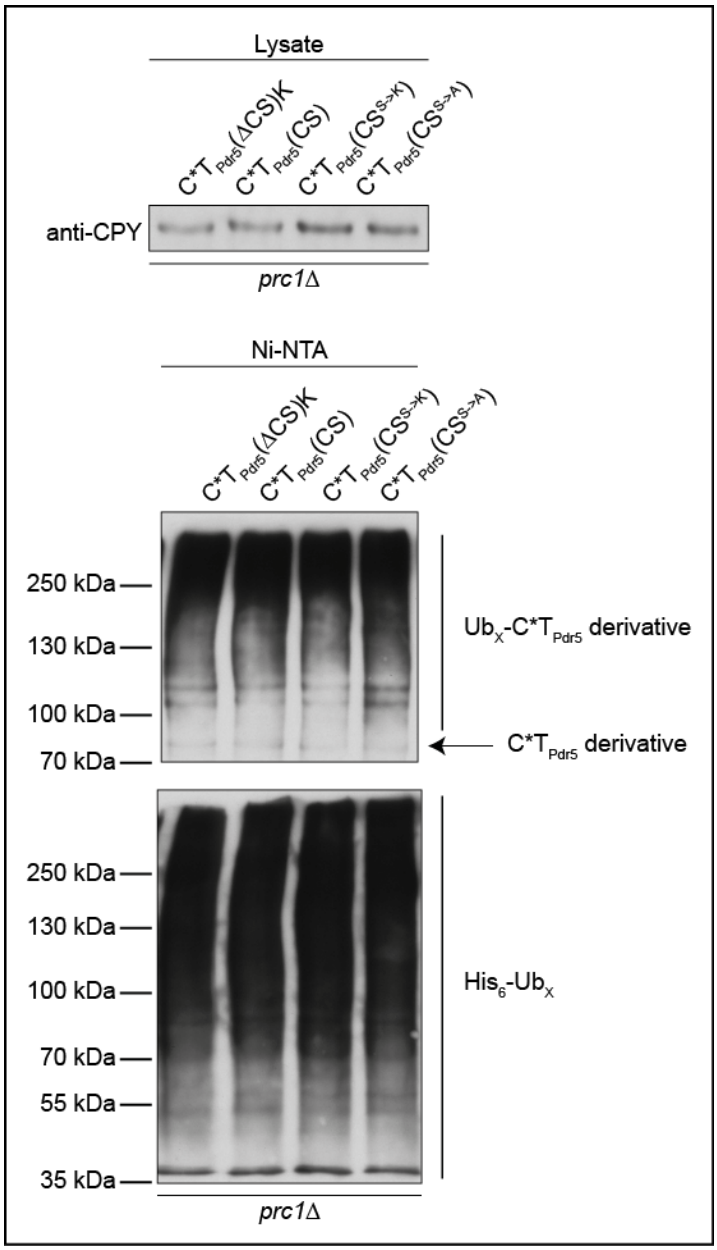

Figure 72: C*T$_{Pdr5}$(ΔCS), C*T$_{Pdr5}$(CS), C*T$_{Pdr5}$(CS$^{S->K}$) and C*T$_{Pdr5}$(CS$^{S->A}$) possess equal ubiquitination patterns

Ubiquitination was analyzed in *prc1*Δ cells expressing C*T$_{Pdr5}$ derivative and His$_6$-tagged ubiquitin (Ub). Cell lysates (input) were incubated with Ni-NTA resin under denaturing conditions to pull down all His$_6$-ubiquitinated proteins. C*T$_{Pdr5}$ derivatives were detected by immunoblotting with CPY antibody and the amount of bound polyubiquitinated proteins (His$_6$-Ub$_X$) was visualized with His antibody.

Figure 72 shows same ubiquitination patterns for the lysine-containing constructs C*T$_{Pdr5}$(ΔCS)K, C*T$_{Pdr5}$(CS$^{S->K}$) and C*T$_{Pdr5}$(CS$^{S->A}$). Additionally, C*T$_{Pdr5}$(CS) shows the same ubiquitination pattern. This demonstrates that serine residues have no influence on ubiquitination if they colocalize with lysine residues. Together with the data of the degradation kinetics this indicates that in case of both, lysine and serine

residues, in the cytosolic part, lysine is sufficient to trigger ubiquitination and induce fast degradation.

Table 23: Overview of the different requirements for C*T$_{Pdr5}$(CS), C*T$_{Pdr5}$(ΔCS)S, C*T$_{Pdr5}$(CS$^{K->A}$), C*T$_{Pdr5}$(CS$^{K/S->A}$), C*T$_{Pdr5}$(CS$^{S->A}$) and C*T$_{Pdr5}$(CS$^{S->K}$) degradation

A green check mark indicates indispensable for degradation; a red cross symbol means dispensable for degradation; ~ (tilde) means involved in but not absolutely necessary for degradation; a red cross symbol with parenthesis indicates dispensable for degradation but participate in ubiquitination; n.a. corresponds to not necessary to analyze. The ERAD components including the membrane protein Der1 and the ubiquitin ligases Hrd1 and Asi complex, and their participation in degradation of the indicated substrates are shown.

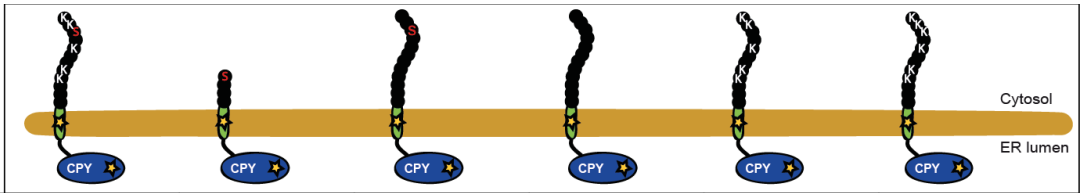

Name	C*T$_{Pdr5}$(CS)	C*T$_{Pdr5}$(ΔCS)S	C*T$_{Pdr5}$(CS$^{K->A}$)	C*T$_{Pdr5}$(CS$^{K/S->A}$)	C*T$_{Pdr5}$(CS$^{S->A}$)	C*T$_{Pdr5}$(CS$^{S->K}$)
cytosolic domain	CS: peptide of 12 amino acids (RVPKKNGKLSKK)	ΔCS: truncated peptide (RVPS)	CS: peptide of 12 amino acids (RVPAANGALSAA)	CS: peptide of 12 amino acids (RVPAANGALAAA)	CS: peptide of 12 amino acids (RVPKKNGKLAKK)	CS: peptide of 12 amino acids (RVPKKNGKLKKK)
membrane domain	T$_{Pdr5}$: last transmembrane helix of Pdr5	T$_{Pdr5}$: last transmembrane helix of Pdr5	T$_{Pdr5}$: last transmembrane helix of Pdr5	T$_{Pdr5}$: last transmembrane helix of Pdr5	T$_{Pdr5}$: last transmembrane helix of Pdr5	T$_{Pdr5}$: last transmembrane helix of Pdr5
ER lumenal domain	CPY*	CPY*	CPY*	CPY*	CPY*	CPY*
Der1	✗	→ not degraded at all	✓	→ not degraded at all	✗	✗
Hrd1	~		✓			
Asi complex	~		✗			
Hrd1 and Asi complex	✓		n. a.			

In summary, the classification of substrates with a misfolded membrane domain into a separate class of ERAD-M substrates should be considered (an overview is given in Table 23 and briefly summarized in the following).

Proteins with a misfolded ER lumenal domain and an aberrant membrane domain are degraded via different mechanisms, depending on the incidence of lysine and serine residues at different positions.

Proteins possessing lysine residues within the aberrant membrane part, as well as proteins possessing cytosolic serine residues in distance to the ER membrane, belong to a Der1 dependent degradation pathway with Hrd1 as the only ubiquitin ligase involved in ubiquitination of these substrates.

In comparison, proteins possessing lysine residues in their cytosolic part are members of a Der1 independent degradation pathway. In this pathway, ubiquitination is

conducted by the ubiquitin ligases Hrd1 together with the Asi complex. These group of substrates show characteristics of the ERAD-M degradation pathway (Figure 19, Figure 21 and Figure 22).

A further group of nondegradable substrates (C*T_{Pdr5}(ΔCS) and C*T_{Pdr5}(ΔCS)A but also C*T_{Pdr5}($CS^{K/S->A}$)), is composed of an ER lumenal misfolded domain, an aberrant membrane part, and containing neither lysine nor serine residues in their cytosolic part nor in their membrane domain, respectively. Within this group substrate ubiquitination is mediated by Hrd1, but final retrotranslocation and thus degradation of these substrates is abolished.

3.2.7 Participation of ubiquitin-conjugating enzymes and Cdc48 in degradation pathways

Degradation mechanisms of C*T$_{Pdr5}$(CS) and C*T$_{Pdr5}$(CS$^{K->A}$) are further analyzed. Participation of ubiquitin-conjugating enzymes in the elimination of either the serine and lysine rich substrate C*T$_{Pdr5}$(CS), or the serine-only substrate C*T$_{Pdr5}$(CS$^{K->A}$), is determined in the following. The canonical ERAD ubiquitin-conjugating enzymes are analyzed, these are Ubc1, Ubc6 and Ubc7 [43,65,68,149,154,196].

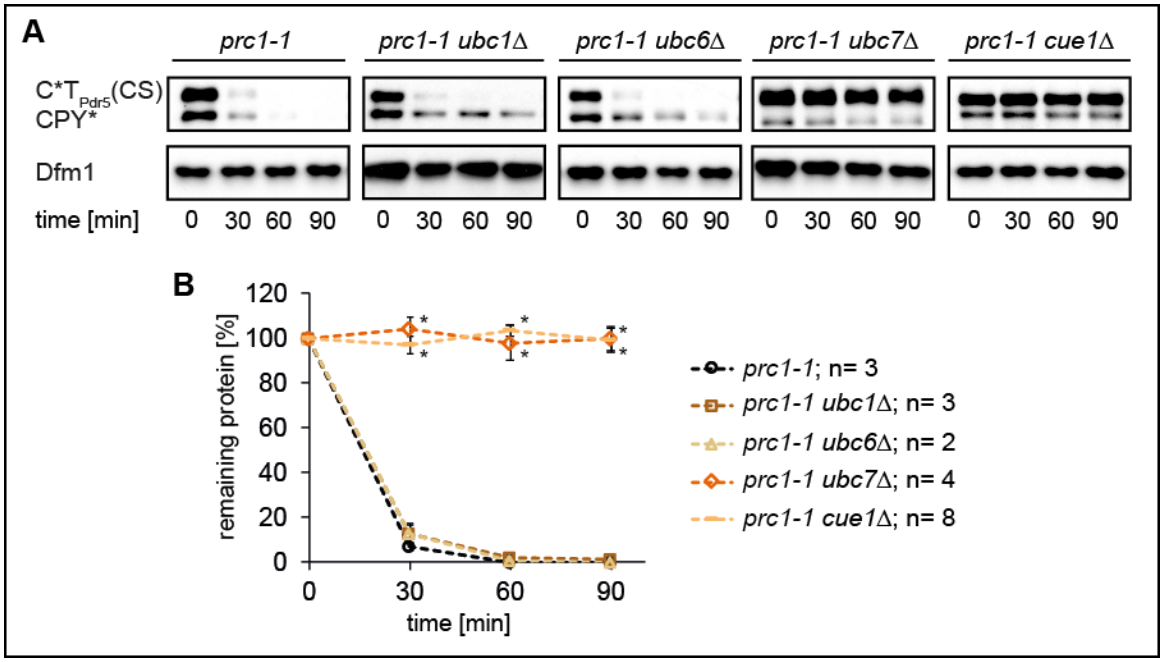

Figure 73: The degradation of C*T$_{Pdr5}$(CS) requires Ubc7 together with its membrane anchor protein Cue1.

A: Cycloheximide-chase analysis of C*T$_{Pdr5}$(CS) degradation was performed in *prc1-1; prc1-1 ubc1Δ; prc1-1 ubc6Δ; prc1-1 ubc7Δ* and *prc1-1 cue1Δ* cells.
Samples were taken every 30 min after cycloheximide addition (t=0 min) and C*T$_{Pdr5}$(CS) was detected by immunoblotting using CPY antibody. Dfm1 was used as loading control.
B: The quantification represents the data of up to 8 independent experiments. Error bars indicate the respective standard error of the mean (SEM). *P < 0.05, unpaired two-sample *t*-test relative to the control (*prc1-1*).

Turnover rates of C*T$_{Pdr5}$(CS) were measured in cells, each singly depleted of Ubc1, Ubc6 or Ubc7, respectively. As illustrated in Figure 73, solely Ubc7 is indispensable for degradation of C*T$_{Pdr5}$(CS). Previous publications showed that Ubc7 is activated by its membrane anchor protein Cue1. Cue1 facilitates and stabilizes the growing polyLys48chain [151–153].

Turnover rates were measured in cells lacking the Ubc7 membrane anchor protein Cue1 to exclude any indirect effects of Ubc7 depletion. This shows a complete stabilization of C*T_{Pdr5}(CS) in cells depleted of Cue1 (Figure 73).

C*T_{Pdr5}(CS), degradation is dependent on the ligases Hrd1 and the Asi complex. A participation of the ubiquitin-conjugating enzyme Ubc7, together with its membrane anchor protein Cue1 was demonstrated.

Ubiquitin chain elongation mediated by the Ubc7/Cue1 pair is more efficient, when an initial ubiquitination is present on the client proteins [152]. For ERAD-C substrates it was recently shown that Ubc6 is responsible for priming the substrate for further ubiquitination [139]. Chain formation and elongation in this case is then mediated by Ubc7 in collaboration with Cue1 [139].

In vivo ubiquitination assays were performed, to investigate whether there are alterations in the ubiquitination pattern of C*T_{Pdr5}(CS). Therefore, cells were used, which are depleted for the mentioned ubiquitin-conjugating enzymes (Figure 74).

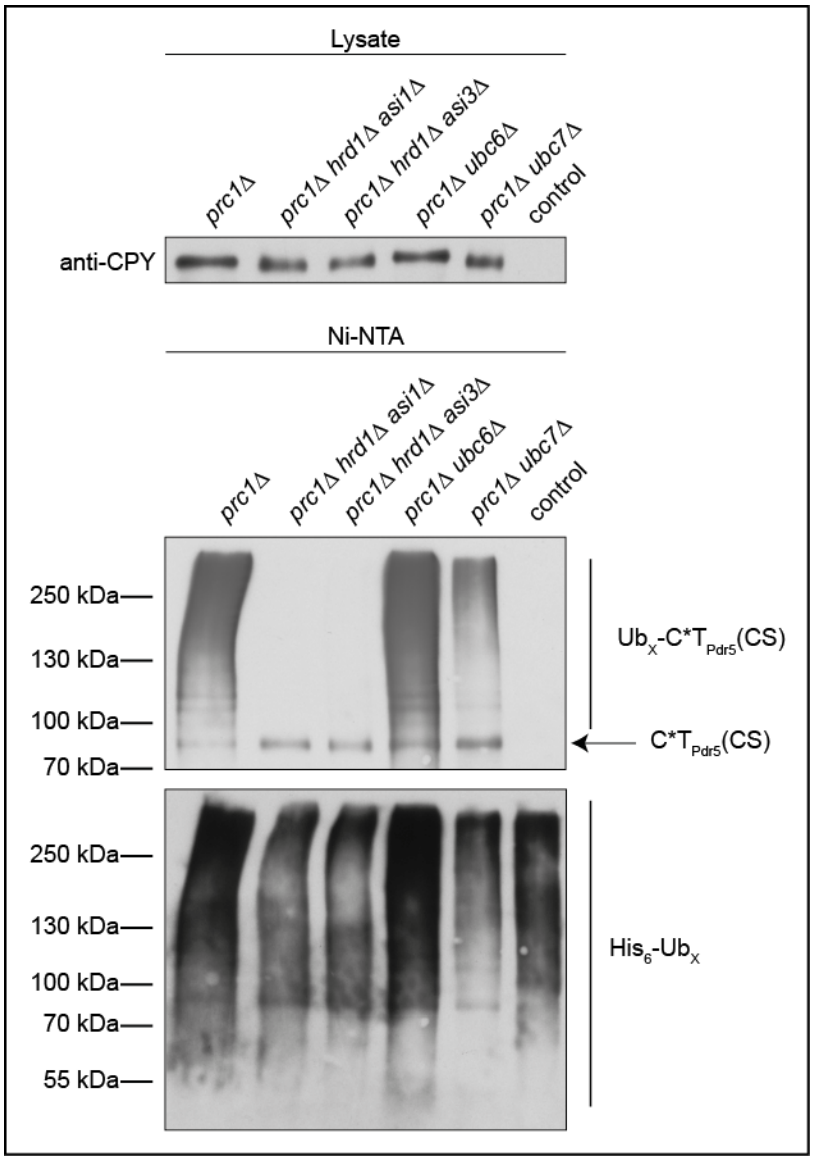

Figure 74: Responsible for ubiquitination of C*T$_{Pdr5}$(CS) are Hrd1 and the Asi complex, together with the ubiquitin-conjugating enzyme Ubc7.

Ubiquitination was analyzed in cells (genotype as indicated) expressing C*T$_{Pdr5}$(CS) and His$_6$-tagged ubiquitin (Ub). Cell lysates (input) were incubated with Ni-NTA resin under denaturing conditions to pull down all His$_6$-ubiquitinated proteins. C*T$_{Pdr5}$(CS) was detected by immunoblotting with CPY antibody and the amount of bound polyubiquitinated proteins (His$_6$-Ub$_X$) was visualized with His antibody.

Figure 74 reveals that ubiquitination of C*T$_{Pdr5}$(CS) is unaffected in cells depleted of Ubc6, proving that Ubc6 is not involved in C*T$_{Pdr5}$(CS) priming and ubiquitination at all. Additionally, residual ubiquitination of C*T$_{Pdr5}$(CS) is observed in cells lacking Ubc7. This indicates that another ubiquitin-conjugating enzyme participates in ubiquitination of C*T$_{Pdr5}$(CS).

Ubiquitination of C*T$_{Pdr5}$(CS) is abolished in cells depleted for Hrd1 as well as the Asi complex, which serves as negative control, because these ligases are indispensable for C*T$_{Pdr5}$(CS) ubiquitination (Figure 74).

The following analysis shows, which ubiquitin-conjugating enzymes participate in degradation and ubiquitination of the serine-only construct, C*T$_{Pdr5}$(CS$^{K->A}$).

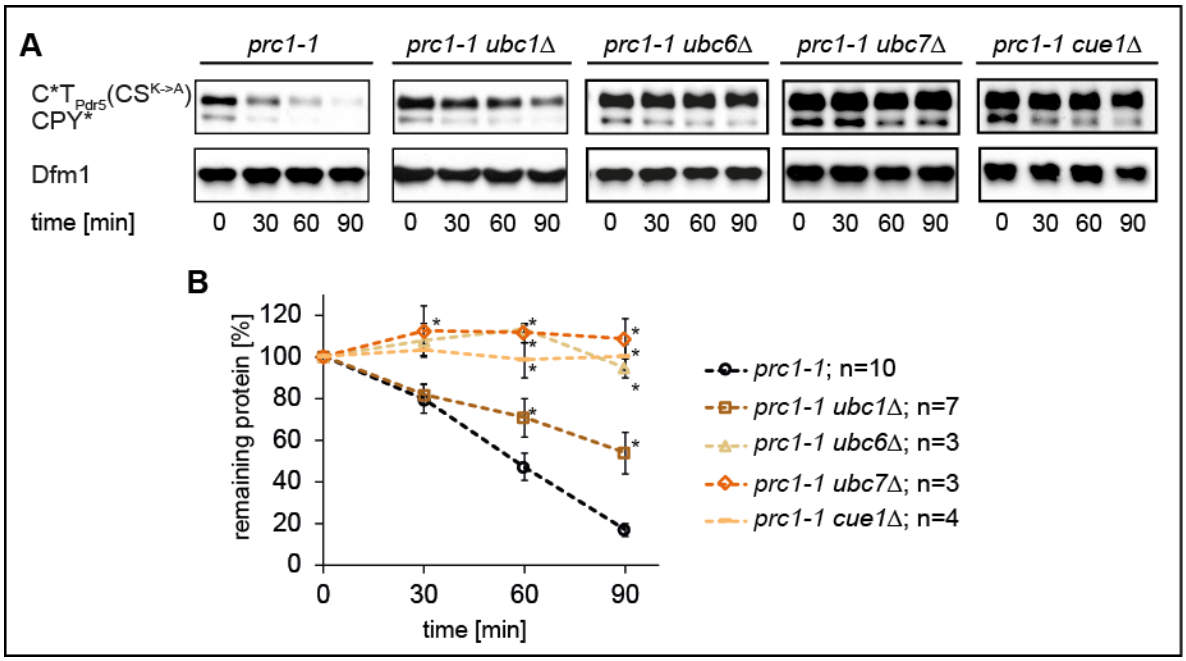

Figure 75: The degradation of C*T$_{Pdr5}$(CS$^{K->A}$) requires Ubc6 and Ubc7 together with its membrane anchor protein Cue1 and is affected by Ubc1.

A: Cycloheximide-chase analysis of C*T$_{Pdr5}$(CS$^{K->A}$) degradation was performed in *prc1-1; prc1-1 ubc1Δ; prc1-1 ubc6Δ; prc1-1 ubc7Δ* and *prc1-1 cue1Δ* cells.
Samples were taken every 30 min after cycloheximide addition (t=0 min) and C*T$_{Pdr5}$(CS$^{K->A}$) was detected by immunoblotting using CPY antibody. Dfm1 was used as loading control.
B: The quantification represents the data of up to 10 independent experiments. Error bars indicate the respective standard error of the mean (SEM). *P < 0.05, unpaired two-sample *t*-test relative to the control (*prc1-1*).

Figure 75 illustrates that C*T$_{Pdr5}$(CS$^{K->A}$) degradation is abolished in cells lacking Ubc6, Ubc7 and Cue1. In cells depleted of Ubc1, degradation is only slightly affected. This indicates that Ubc6, Ubc7 and Cue1 are indispensable for C*T$_{Pdr5}$(CS$^{K->A}$) degradation, but Ubc1 is not mandatory for degradation.

Generally, it is shown that degradation of C*T$_{Pdr5}$(CS$^{K->A}$) fundamentally differs from C*T$_{Pdr5}$(CS) degradation.

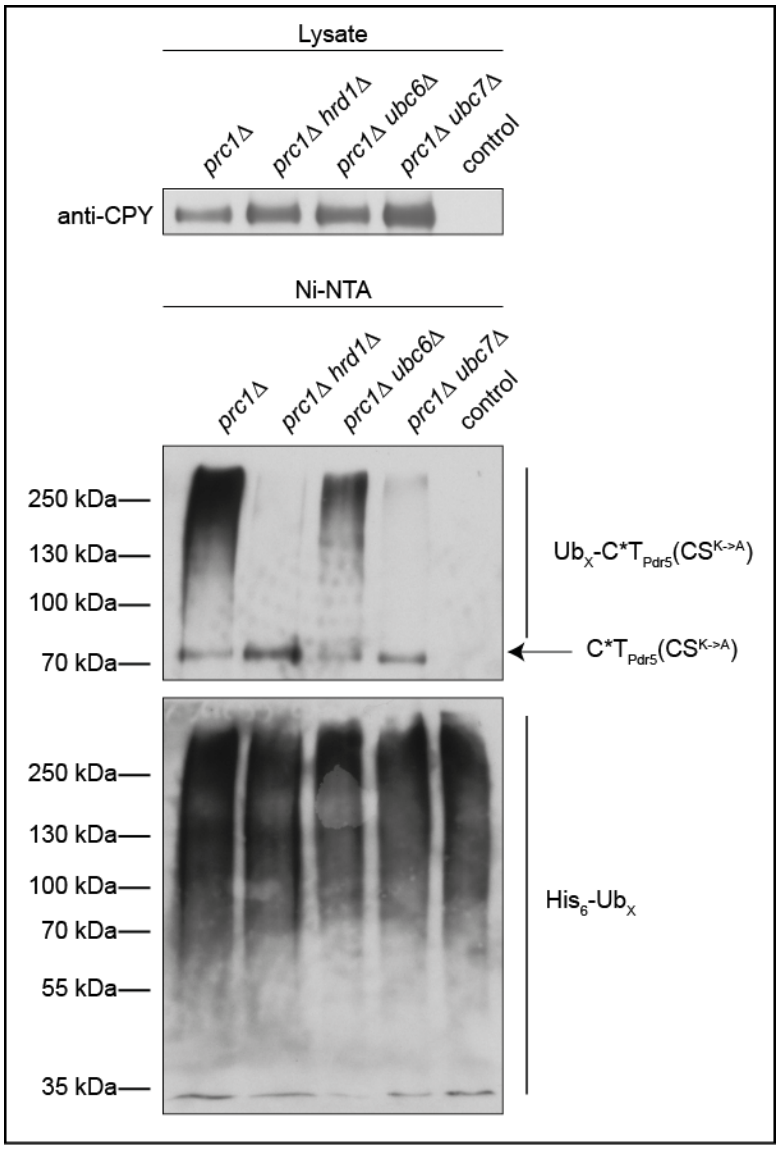

Figure 76: Ubiquitination of C*T$_{Pdr5}$(CS$^{K->A}$) is mediated by the ubiquitin ligase Hrd1 together with the ubiquitin-conjugating enzymes Ubc6 and Ubc7.

Ubiquitination was analyzed in cells (genotype as indicated) expressing C*T$_{Pdr5}$(CS$^{K->A}$) and His$_6$-tagged ubiquitin (Ub). Cell lysates (input) were incubated with Ni-NTA resin under denaturing conditions to pull down all His$_6$-ubiquitinated proteins. C*T$_{Pdr5}$(CS$^{K->A}$) was detected by immunoblotting with CPY antibody and the amount of bound polyubiquitinated proteins (His$_6$-Ub$_X$) was visualized with His antibody.

C*T$_{Pdr5}$(CS$^{K->A}$), containing a single serine residue in the cytosolic domain, is not ubiquitinated in *ubc7*Δ cells. This matches with the turnover rates, which show no degradation of C*T$_{Pdr5}$(CS$^{K->A}$) in these cells. Interestingly, there is significant ubiquitination in cells depleted of Ubc6, although it is not degraded in the absence of Ubc6 (Figure 76 and for comparison Figure 75). Degradation in *ubc1*Δ cells is only slightly impaired. Thus, it is possible that Ubc1 together with Ubc7 are responsible for ubiquitination of C*T$_{Pdr5}$(CS$^{K->A}$) in *ubc6*Δ cells.

Ubc6 was shown to cooperate with the ubiquitin ligases Doa10 and the Asi complex [67,68]. For ubiquitination of the ERAD-M substrate, C*T$_{Pdr5}$(CS), Hrd1 was found to collaborate with Ubc7. But ubiquitination of C*T$_{Pdr5}$(CS$^{K->A}$) is achieved by Hrd1 together with the ubiquitin-conjugating enzymes Ubc1, Ubc6 and Ubc7. Ubiquitination of C*T$_{Pdr5}$(CS$^{K->A}$) is triggered only by Hrd1 and neither by the Asi complex nor Doa10 (Figure S24). Any indirect effects of Doa10 should be excluded. Degradation kinetics and ubiquitination assays were performed in the absence of Doa10. As control substrate C*T$_{Pdr5}$(CS) was used, because it is degraded independently of Ubc6 and Doa10.

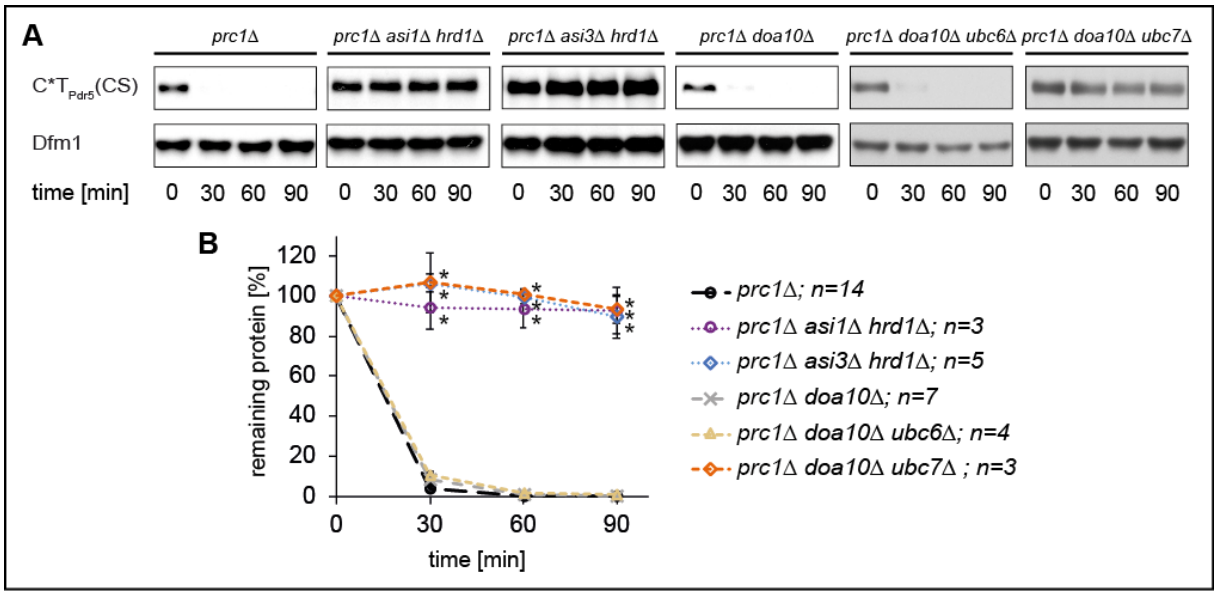

Figure 77: The degradation of C*T$_{Pdr5}$(CS) requires Ubc7 together with its membrane anchor protein Cue1.

A: Cycloheximide-chase analysis of C*T$_{Pdr5}$(CS) degradation was performed in *prc1Δ; prc1Δasi1Δhrd1Δ; prc1Δasi3Δhrd1Δ; prc1Δdoa10Δ; prc1Δdoa10Δubc6Δ* and *prc1Δdoa10Δubc7Δ* cells.
Samples were taken every 30 min after cycloheximide addition (t=0 min) and C*T$_{Pdr5}$(CS) was detected by immunoblotting using CPY antibody. Dfm1 was used as loading control.
B: The quantification represents the data of up to 14 independent experiments. Error bars indicate the respective standard error of the mean (SEM). *P < 0.05, unpaired two-sample *t*-test relative to the control (*prc1Δ*).

The ERAD-M substrate C*T$_{Pdr5}$(CS), which is completely stabilized in the absence of both, Hrd1 as well as the Asi complex, shows the same turnover rates in the absence as in the presence of Doa10 (Figure 77).
This indicates that deletion of Doa10 does not affect degradation of C*T$_{Pdr5}$(CS). It is still dependent on Hrd1, the Asi complex and Ubc7.

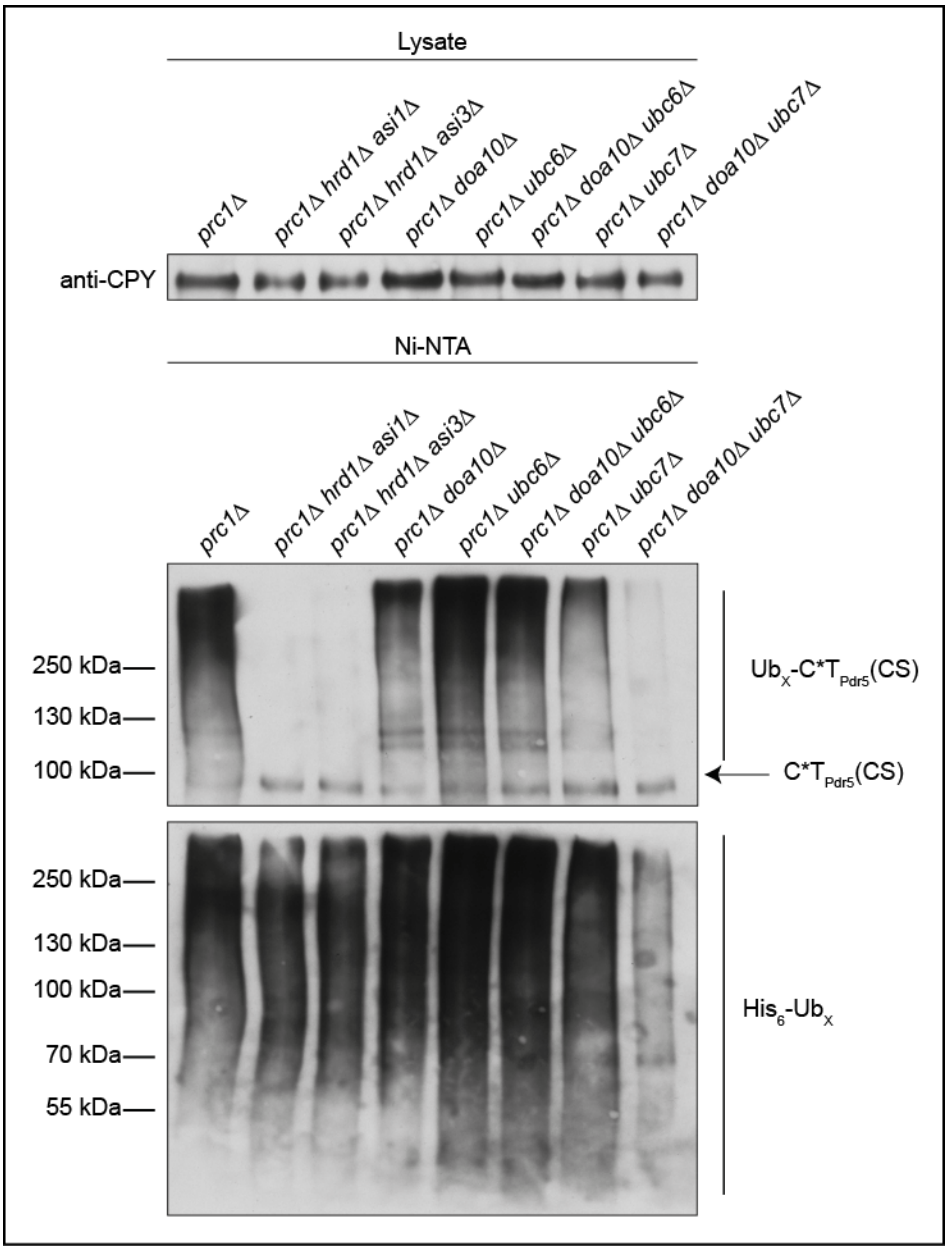

Figure 78: Ubiquitination of C*T$_{Pdr5}$(CS) is mediated by the ubiquitin ligase Hrd1 together with the ubiquitin-conjugating enzymes Ubc6 and Ubc7.

Ubiquitination was analyzed in cells (genotype as indicated) expressing C*T$_{Pdr5}$(CS) and His$_6$-tagged ubiquitin (Ub). Cell lysates (input) were incubated with Ni-NTA resin under denaturing conditions to pull down all His$_6$-ubiquitinated proteins. C*T$_{Pdr5}$(CS) was detected by immunoblotting with CPY antibody and the amount of bound polyubiquitinated proteins (His$_6$-Ub$_X$) was visualized with His antibody.

In vivo ubiquitination assays were also performed in the absence of Doa10.

In the absence of Doa10 and Ubc6 ubiquitination of C*T$_{Pdr5}$(CS) is unaffected, whereas ubiquitination of C*T$_{Pdr5}$(CS) is abolished in cells depleted of Doa10 and Ubc7. This indicates that Ubc6 is dispensable for ubiquitination of C*T$_{Pdr5}$(CS), which is consistent with the measured turnover rates (Figure 77). Interestingly, ubiquitination is found in

cells singly depleted of Ubc7 but C*T$_{Pdr5}$(CS) ubiquitination is abolished in cells lacking both, Ubc7 and Doa10 (Figure 78). However, the amount of bound polyubiquitinated proteins containing His$_6$-tagged ubiquitin, which was analyzed using His antibody, is also reduced (Figure 78).

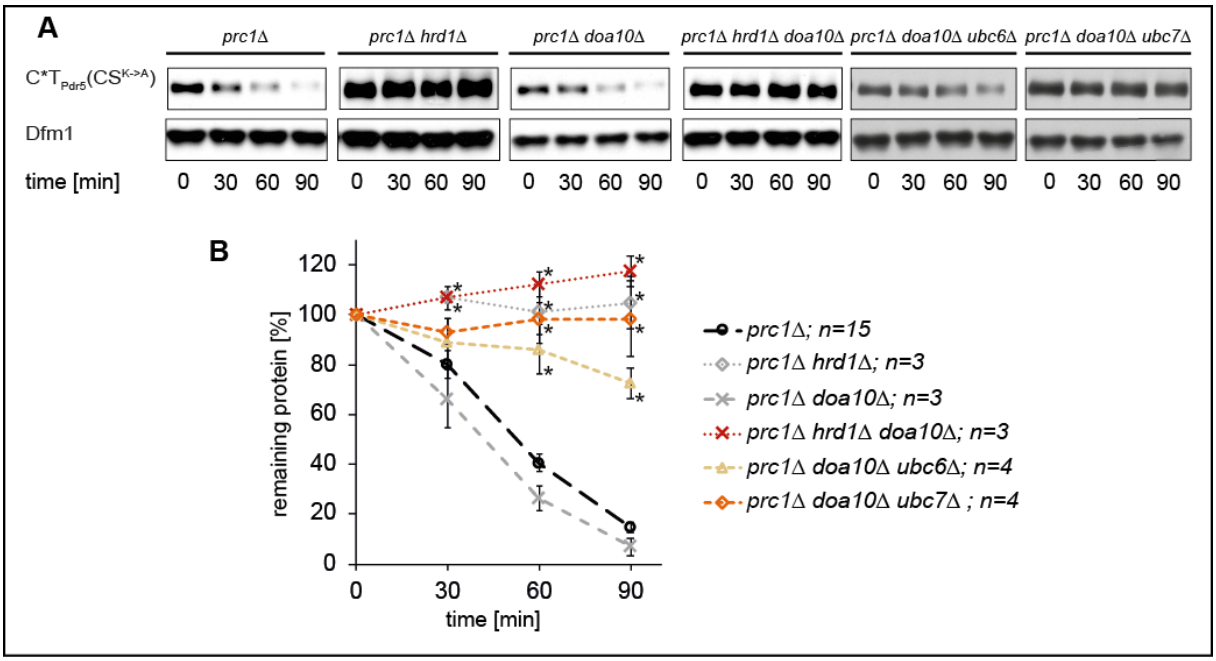

Figure 79: The degradation of C*T$_{Pdr5}$(CS$^{K->A}$) requires Ubc6 and Ubc7 and is independent of the ubiquitin ligase Dao10 .

A: Cycloheximide-chase analysis of C*T$_{Pdr5}$(CS$^{K->A}$) degradation was performed in *prc1Δ; prc1Δhrd1Δ; prc1Δdoa10Δ; prc1Δhrd1Δdoa10Δ; prc1Δdoa10Δubc6Δ* and *prc1Δdoa10Δubc7Δ* cells. Samples were taken every 30 min after cycloheximide addition (t=0 min) and C*T$_{Pdr5}$(CS$^{K->A}$) was detected by immunoblotting using CPY antibody. Dfm1 was used as loading control.
B: The quantification represents the data of up to 15 independent experiments. Error bars indicate the respective standard error of the mean (SEM). *P < 0.05, unpaired two-sample *t*-test relative to the control (*prc1Δ*).

Next, turnover rates of C*T$_{Pdr5}$(CS$^{K->A}$), containing only a single serine in the cytosolic part, in the absence of Doa10 were measured. As shown above, degradation of C*T$_{Pdr5}$(CS$^{K->A}$) is abolished in cells lacking either Hrd1 or Ubc6 or Ubc7. It is unaffected in cells depleted of Doa10 (Figure 79) indicating that degradation of C*T$_{Pdr5}$(CS$^{K->A}$) is independent of Doa10.

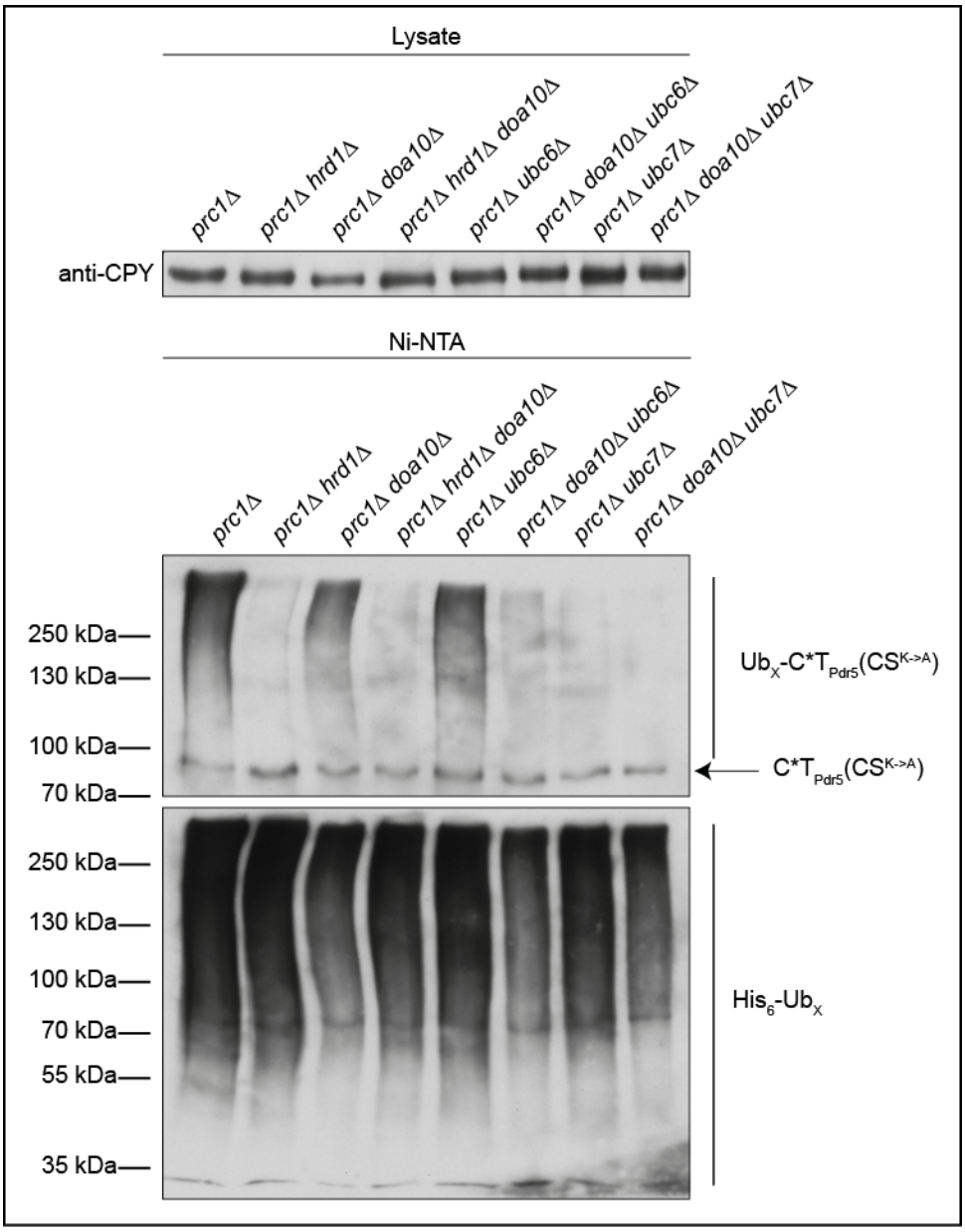

Figure 80: Ubiquitination of C*T$_{Pdr5}$(CS$^{K->A}$) is mediated by the Ubiquitin ligase Hrd1 together with the Ubiquitin-conjugating enzymes Ubc6 and Ubc7.

Ubiquitination was analyzed in cells (genotype as indicated) expressing C*T$_{Pdr5}$(CS$^{K->A}$) and His$_6$-tagged ubiquitin (Ub). Cell lysates (input) were incubated with Ni-NTA resin under denaturing conditions to pull down all His$_6$-ubiquitinated proteins. C*T$_{Pdr5}$(CS$^{K->A}$) was detected by immunoblotting with CPY antibody and the amount of bound polyubiquitinated proteins (His$_6$-Ub$_X$) was visualized with His antibody.

In vivo ubiquitination assays confirm that Hrd1 is the only ligase responsible for ubiquitination of C*T$_{Pdr5}$(CS$^{K->A}$). Deletion of Doa10 has no influence on C*T$_{Pdr5}$(CS$^{K->A}$) ubiquitination (Figure 80). Ubc7 participates in the ubiquitination of C*T$_{Pdr5}$(CS$^{K->A}$) because ubiquitination signals cannot be observed in its absence.

Astonishingly, significant ubiquitination is observed in cells lacking Ubc6, but ubiquitination is abolished in cells doubly depleted of Ubc6 and Doa10 (Figure 80).

In summary, C*T_{Pdr5}(CS) is ubiquitinated by the ubiquitin ligases Hrd1 and the Asi complex in cooperation with the ubiquitin-conjugating enzyme Ubc7 and its membrane anchor protein Cue1. Residual ubiquitination of C*T_{Pdr5}(CS) in cells deleted for Ubc7 suggests that another ubiquitin-conjugating enzyme participates in C*T_{Pdr5}(CS) ubiquitination.
On contrary, final transfer of ubiquitin to C*T_{Pdr5}($CS^{K->A}$) is only mediated by the ligase Hrd1. In addition, the ubiquitin-conjugating enzymes Ubc1, Ubc6 and Ubc7 participate, but the extent differs. Ubc6 and Ubc7 are indispensable, whereas ubiquitination is only slightly impaired in cells lacking Ubc1.

Ultimately, the ubiquitinated ERAD substrates must be pulled out of the ER membrane. For all yet known ERAD substrates this is mediated by the AAA ATPase Cdc48 [103,105,158,164,189–194]. Since it was shown that degradation of C*T_{Pdr5}(CS) and C*T_{Pdr5}($CS^{K->A}$) differ fundamentally, participation of Cdc48, in both degradation pathways, is determined.

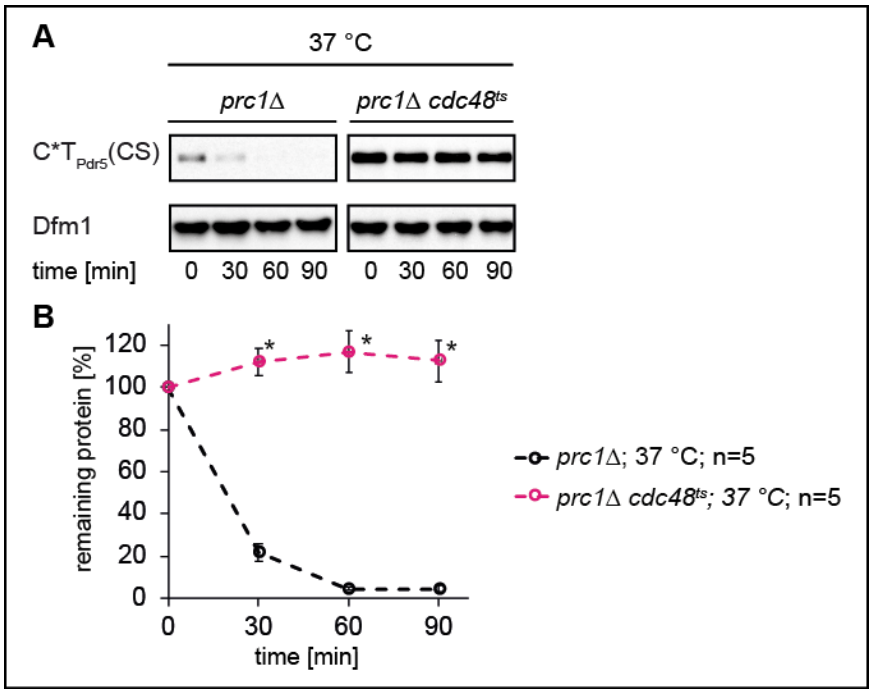

Figure 81: Cdc48 is necessary for the degradation of C*T$_{Pdr5}$(CS).

A: Cycloheximide-chase analysis of C*T$_{Pdr5}$(CS) degradation was performed in *prc1*Δ; and *prc1*Δ *cdc48^{ts}* cells.
Main cultures were grown at 25°C. Then they were shifted to 37°C for 60 minutes prior to taking samples every 30 min after cycloheximide addition (t=0 min). C*T$_{Pdr5}$(CS) was detected by immunoblotting using CPY antibody. Dfm1 was used as loading control.
B: The quantification represents the data of five independent experiments. Error bars indicate the respective standard error of the mean (SEM). *P < 0.05, unpaired two-sample *t*-test relative to the control (*prc1*Δ cells at 37°C).

Therefore, turnover rates of the two substrates were measured in cells carrying either active Cdc48 or the temperature sensitive *cdc48^{ts}* mutant. At the restrictive temperature (37°C) the *cdc48^{ts}* mutant is inactive. Degradation of C*T$_{Pdr5}$(CS) is impaired under restrictive conditions in the *cdc48^{ts}* mutant (Figure 81). This indicates that Cdc48 participates in its degradation.

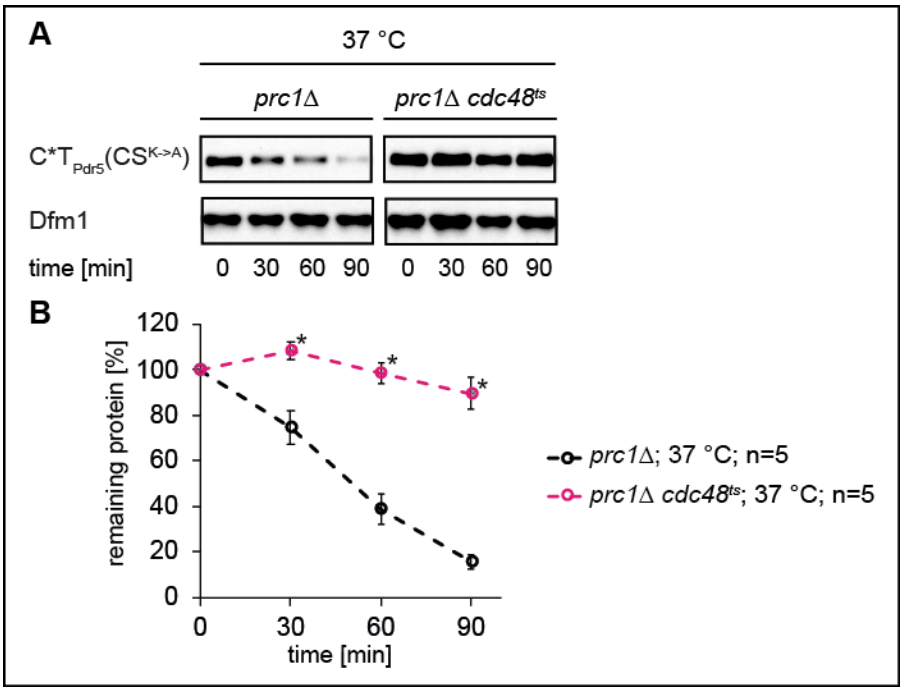

Figure 82: Cdc48 is necessary for the degradation of C*T$_{Pdr5}$(CS$^{K->A}$).

A: Cycloheximide-chase analysis of C*T$_{Pdr5}$(CS$^{K->A}$) degradation was performed in *prc1*Δ; and *prc1*Δ *cdc48^{ts}* cells.
Main cultures were grown at 25°C. Then they were shifted to 37°C for 60 minutes prior to taking samples every 30 min after cycloheximide addition (t=0 min). C*T$_{Pdr5}$(CS$^{K->A}$) was detected by immunoblotting using CPY antibody. Dfm1 was used as loading control.
B: The quantification represents the data of five independent experiments. Error bars indicate the respective standard error of the mean (SEM). *P < 0.05, unpaired two-sample *t*-test relative to the control (*prc1*Δ cells at 37°C).

Figure 82 shows that degradation of C*T$_{Pdr5}$(CS$^{K->A}$) is also impaired in the *cdc48^{ts}* mutant at restrictive conditions. Thus, Cdc48 is indispensable for C*T$_{Pdr5}$(CS$^{K->A}$) degradation.

Thus, after they are ubiquitinated, both, the lysine-containing as well as the serine-containing substrates are pulled out of the ER by the AAA ATPase Cdc48.

Table 24: Overview of the different requirements in C*T$_{Pdr5}$(CS) and in C*T$_{Pdr5}$(CS$^{K->A}$) degradation

A green check mark indicates indispensable for degradation; a red cross symbol means dispensable for degradation; ~ (tilde) means involved in but not absolutely necessary for degradation; a red cross symbol with parenthesis indicates dispensable for degradation but participate in ubiquitination; n.a. corresponds to not necessary to analyze. The ERAD components including the homologous pair of membrane proteins, Der1 and Dfm1, the ubiquitin ligases Hrd1 and Asi complex, the ubiquitin-conjugating enzymes Ubc1, Ubc6 and Ubc7 as well as the membrane anchor protein Cue1 and the AAA ATPase Cdc48 and their participation in degradation of the indicated substrates are shown.

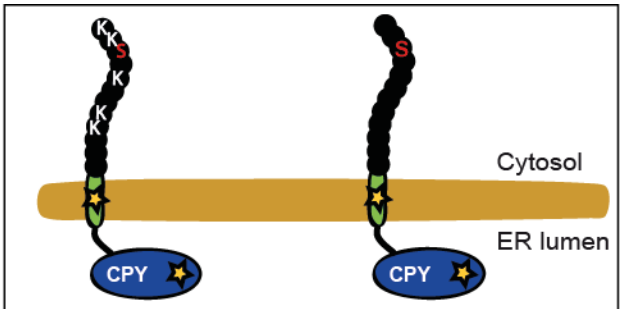

Name	C*T$_{Pdr5}$(CS)	C*T$_{Pdr5}$(CS$^{K->A}$)
cytosolic domain	CS: peptide of 12 amino acids (RVPKKNGKLSKK)	CS: peptide of 12 amino acids (RVPAANGALSAA)
membrane domain	T$_{Pdr5}$: last transmembrane helix of Pdr5	T$_{Pdr5}$: last transmembrane helix of Pdr5
ER lumenal domain	CPY*	CPY*
Der1	✗	✓
Dfm1	✗	~
Hrd1	~	✓
Asi complex	~	✗
Hrd1 and Asi complex	✓	n. a.
Ubc1	✗	~
Ubc6	✗	✓
Ubc7	✓	✓
Cue1	✓	✓
Cdc48	✓	✓

4. DISCUSSION

A quality control system in the ER monitors the secretory proteins to guarantee that only properly folded and correctly modified proteins are further transported. Aberrant proteins are directed to degradation. However, the ER lacks a proteolytic system. Thus, the proteins have to be retrograde transported across the ER membrane to the cytosol. There the major protease, the 26S proteasome, is responsible for their final breakdown ([43] republished in [44]). All components required for elimination of aberrant ER proteins are summarized as the ER-associated degradation (ERAD).

Depending on the location of the proteins' lesion – in the ER lumen, the membrane domain or the cytosolic domain – , the secretory proteins are removed by the ERAD-L, ERAD-M or ERAD-C degradation mechanism, respectively. An overview of the different ERAD pathways is given in chapter 1.7 of this work.

In each of the ERAD branches special proteins exist, which are essentially required for degradation, the so-called central players. During the last decades, the degradation mechanisms of the different ERAD branches were identified by the use of specifically designed, artificially misfolded proteins, called ERAD substrates. An overview of the central players of the different ERAD branches and the respective ERAD substrates is given in Table 1 in the introduction part of this work.

The ER membrane protein Der1 was shown to be a central player in the ERAD-L degradation mechanism [41,60–62]. Der1 is required for the introduction of proteins, containing a lesion in the ER lumenal domain, into the ER membrane ([61,62] and reviewed in [6,40]). Furthermore, it is in complex with the *HRD* ligase complex, which is composed of the ubiquitin ligase Hrd1 and Hrd3 [42,53,54,57,59,60], which is a receptor for misfolded proteins. According to the current classification, established by Vashist and Ng [41] as well as Carvalho *et al.* [42], al proteins containing a lesion in the ER lumen and require Der1 for degradation are ERAD-L substrates. On contrary, they proclaimed that ER proteins with aberrant membrane parts are degraded without the need of Der1, the so-called ERAD-M substrates.

However, in cells lacking Der1, it was shown that degradation of some ERAD-L substrates is only slightly impaired ([41] and Figure 33). This posed the question on the current classification.

In this work a new set of ERAD substrates was generated, which contain related

modular structures, composed of misfolded carboxypeptidase Y (CPY*) in the ER lumen and either the native, properly folded Wsc1 transmembrane helix or the last transmembrane helix of Pdr5, which is an orphan transmembrane helix and thus signals misfolding (representatives are shown in Figure 24). Using these substrates, it was shown that the composition of the cytosolic part directs the proteins degradation fate. These different degradation mechanisms are summarized and discussed in the following chapters, with a focus on Der1.

4.1 Hul5 seems to be involved in the degradation mechanism of ERAD substrates with an aberrant membrane part

Degradation of the *bona fide* substrates C*T_{Pdr5}(CS)Leu2^{myc} and C*T_{Pdr5}(CS)GFP is well characterized (an overview is given in Table 14). Although both are composed of an obviously related modular structure – CPY* as ER lumenal misfolded domain, an aberrant membrane part (T_{Pdr5}) and a properly folded cytosolic domain, GFP or Leu2, respectively – they are degraded via different mechanisms. C*T_{Pdr5}(CS)Leu2^{myc} is eliminated via the ERAD-L degradation mechanism [194]. In addition, a degradation intermediate consisting of T_{Pdr5}(CS)Leu2^{myc} appears and accumulates in the absence of the proteasome-associated ubiquitin ligase Hul5 ([194] and Figure 13). On contrary, C*T_{Pdr5}(CS)GFP is degraded by components of the ERAD-C pathway [196], without the participation of Hul5 (Data published in PhD thesis Stefanie Besser [232]). To test whether the slowly folding GFP variant, folding takes about 2-4 hours [256], in the cytosolic domain serves as a degron, it was substituted for a superfast folding variant (GFP_{fast}) (Figure 9). Previously, GFP_{fast} was shown to fold 7-fold faster than the other GFP variant [250]. Surprisingly, C*T_{Pdr5}(CS)GFP_{fast} is removed by a different degradation intermediate containing the membrane-anchored CPY*, which is a C*T_{Pdr5} derivative and is further degraded (Figure 12). This observation stands in contrast to C*T_{Pdr5}(CS)Leu2^{myc} degradation, where a membrane-bound N-terminally truncated version accumulates in the absence of Hul5, composed of the membrane part and the cytosolic domain, T_{Pdr5}(CS)Leu2^{myc} ([194] and Figure 13).

An explanation for the different degradation intermediates might be that the GFP_{fast} moiety is recognized by some cytosolic recognition process, which may lead to the removal of the cytosolic part only, because the membrane-bound CPY* is still

observed. The cytosolic Hsp70 chaperone family participate in recognition of the slowly folding GFP in the former substrate C*T_{Pdr5}(CS)GFP [196]. Thus, it is possible that the cytosolic Hsp70 chaperone Ssa1 recognizes the C*T_{Pdr5}(CS)GFP_{fast}, which possibly leads to removal of the GFP_{fast} moiety. This should be further analyzed.

Furthermore, it was excluded that the myc-Tag, which is composed of 13 times the myc epitope, in C*T_{Pdr5}(CS)$Leu2^{myc}$ might serve as a degradation signal, since a single HA-Tag-containing variant, C*T_{Pdr5}(CS)$Leu2^{HA}$, is also degraded by an N-terminally truncated membrane-bound intermediate, dependent on Hul5 (Figure 13).

All GFP- and Leu2-containing constructs are composed of the membrane-bound CPY* and thus share a common core structure, the so-called C*T_{Pdr5}(CS). Surprisingly, the cytosolically HA-tagged version of this common core, C*$T_{Pdr5}$$(CS)^{HA}$, is degraded via a membrane-bound intermediate in cells lacking Hul5 (Figure 17). The size of the intermediate indicates that it is composed of the membrane-bound cytosolic part of C*$T_{Pdr5}$$(CS)^{HA}$ - a peptide of 12 amino acids and the HA-Tag as well as T_{Pdr5}. This shows that first the CPY* moiety is degraded, possibly it loops out through the retrotranslocon and thus is exposed for digestion by the proteasome. This was shown for the CPY* moiety of the C*T_{Pdr5}(CS)$Leu2^{myc}$ construct [194]. The remaining $T_{Pdr5}$$(CS)^{HA}$ part is composed of the aberrant T_{Pdr5} membrane domain, the cytosolic sequence and the HA epitope. It is possible that ubiquitin chain elongation mediated by Hul5 is required for the extraction of aberrant membrane parts out of the ER membrane, because the aberrant membrane parts of the constructs C*T_{Pdr5}(CS)$Leu2^{myc}$, C*T_{Pdr5}(CS)$Leu2^{HA}$, and C*$T_{Pdr5}$$(CS)^{HA}$ accumulate in absence of the ubiquitin ligase Hul5 (Figure 13 and Figure 17). This hypothesis is maintained by the observation, that the Leu2myc-containing ERAD-M substrate Sec61-2L is also degraded via a membrane-bound degradation intermediate, dependent on Hul5 [194].

To test whether Hul5 is involved in degradation of proteins containing lesions in the membrane domain, a new substrate has to be generated with a properly folded membrane domain and a misfolded ER lumenal domain as well as a properly folded cytosolic domain. In addition, it should contain a cytosolic and an ER lumenal epitope for analysis in immunoblotting, for instance a cytosolically HA tagged version of the C*T_{Wsc1}(CS) substrate.

4.2 ERAD-M degradation mechanism

In this work direct evidence was provided that C*T_{Pdr5}(CS) is eliminated by an ERAD-M degradation mechanism. Originally, C*T_{Pdr5}(CS), which consists of the ER membrane-anchored, misfolded *bona fide* ERAD-L substrate CPY* [196], was generated to analyze the degradation mechanism of membrane-bound ERAD-L substrates. Unfortunately, the sequence of the transmembrane domain codes for an orphan helix of Pdr5 and thus it can serve as a degron [41]. This might change the construct into an ERAD-M substrate. In this work it was finally shown because the ER membrane protein Der1, a key component of the ERAD-L pathway [196], is not involved in degradation of C*T_{Pdr5}(CS) (Figure 19).

Furthermore, in this work it was uncovered that the inner nuclear membrane-bound ubiquitin ligase Asi complex together with the ER membrane-bound ubiquitin ligase Hrd1 are prerequisites for ubiquitination and final elimination of C*T_{Pdr5}(CS) (Figure 21 and Figure 22). Previously, it was shown that the Asi complex is involved in the removal of distinct ERAD-M substrates, which are incorrectly located in the INM [67,68]. This is consistent with the conclusion that C*T_{Pdr5}(CS) is degraded by the ERAD-M pathway.

The cooperation of a ubiquitin ligase and one or several ubiquitin-conjugating enzymes results in the formation of polyubiquitin chains. The ubiquitin-conjugating enzymes Ubc6 and Ubc7 are known to be involved in the ERAD-M degradation mechanism [65–68,149,155,157]. Here, it was shown that Ubc7 is necessary for C*T_{Pdr5}(CS) degradation (Figure 73). Furthermore, ablation of Cue1, the membrane anchor protein and activator of Ubc7, has the same effect (Figure 73). Previously, it was shown that C*T_{Pdr5}(CS) degradation is impaired in cells lacking both, Ubc1 and Ubc7 [196]. But degradation was not shown in cells singularly depleted of Ubc1 or Ubc7. Thus, it is possible that the stabilization of C*T_{Pdr5}(CS) in the double mutant is only caused by the absence of Ubc7. Furthermore, Ubc7 participates in various cellular functions. In this work, it was additionally shown that without recruitment of Ubc7 to the ER membrane by Cue1, C*T_{Pdr5}(CS) is not degraded at all (Figure 73). Cooperation of Hrd1 only with Ubc7 is capable to polyubiquitinate substrate proteins [149,257]. This seems to be facilitated by the partial unfolding of the substrate by the ligase [258]. But this ubiquitination mark is insufficient for degradation, since C*T_{Pdr5}(CS) is not degraded in cells lacking Ubc7 (Figure 73). Surprisingly, *in vivo* ubiquitination assays reveal residual ubiquitination of

C*T_{Pdr5}(CS) in these cells (Figure 74). This observation strongly suggests that an additional ubiquitin-conjugating enzyme is involved in ubiquitination of C*T_{Pdr5}(CS). A collaboration of Ubc7 and an additional ubiquitin-conjugating enzyme is also assumed because earlier it was found that Ubc7 is extremely proficient in forming Lys48 ubiquitin chains but less efficient in decorating lysine residues of substrate proteins with ubiquitin [152,153]. In addition, it was shown that Ubc7 works in tandem with Ubc6 in ubiquitination of a certain Doa10 substrate [139]. Ubc6 primes the substrate protein, by attaching a single ubiquitin moiety to either lysine, serine or threonine residues and then Ubc7, together with its membrane anchor and activator protein Cue1, elongates the ubiquitin chain, by forming Lys48 linkages [139]. However, here it was shown that Ubc6 is not required for C*T_{Pdr5}(CS) ubiquitination and degradation (Figure 73 and Figure 74). Thus, it is suggested to look for another ubiquitin-conjugating enzyme. In yeast, there are 13 known ubiquitin-conjugating enzymes. Two of them are involved in transferring the yeast SUMO and yeast Nedd8 homologs [133,134]. It was shown that Ubc6 is not involved in C*T_{Pdr5}(CS) ubiquitination (Figure 74). Since C*T_{Pdr5}(CS) degradation is not affected in cells lacking Ubc1 (Figure 73), it may nevertheless be involved in priming C*T_{Pdr5}(CS), which seems to be a prerequisite for completely efficient ubiquitination by Ubc7. Ubc2 is required for ubiquitination of some ERAD-C substrates [159]. Ubc4 and Ubc5 have redundant functions to mediate monoubiquitination in RING E3-catalyzed pathways [259]. Ubc10 is involved in monoubiquitination of some peroxisomal proteins [260,261]. Thus, Ubc1, Ubc2, Ubc4, Ubc5 and Ubc10 are candidates to work in tandem with Ubc7 in ubiquitination of the ERAD-M substrate C*T_{Pdr5}(CS). Since degradation is completely abrogated in cells depleted for Ubc7, but residual ubiquitination can be detected in *in vivo* ubiquitination assays, it is recommended to analyze ubiquitination in cells double depleted of Ubc7 and either Ubc1, Ubc2, Ubc4, Ubc5 or Ubc10 in further experiments.

In brief summary, it was shown that in the ERAD-M degradation mechanism the ubiquitin ligases Hrd1 as well as the nuclear Asi complex, together with the ubiquitin-conjugating enzyme Ubc7, which is recruited to the ER membrane by Cue1, participate in ubiquitination. Prior to final breakdown the ERAD-M substrates have to be pulled out of the nuclear and ER membrane. This is facilitated by the AAA ATPase Cdc48 (Figure 81). Besides membrane extraction mediated by Cdc48, the ubiquitin ligase Hrd1 is also discussed to form a retrotranslocon for ERAD-M substrates (chapter 1.3). However,

Hrd1 is restricted to the ER and the nuclear Asi complex participates in degradation of ERAD-M substrates. Thus, it may be possible that the Asi complex also forms a retrotranslocon in the INM. However, this has to be further analyzed.

Recently, it was proclaimed that Dfm1, a Der1 homolog [147], is required for retrotranslocation of some ERAD-M substrates [106]. In this work it was shown that Dfm1 does not participate in C*T_{Pdr5}(CS) degradation (Figure 20). Furthermore, it was also revealed that under strong ERAD-M substrate expression, cells lacking Dfm1 undergo adaptive evolution within nine passages of liquid culture, which leads to suppression of the *dfm1*Δ phenotype [106]. This is the reason, why the experiments of this work are always conducted with freshly transformed cells – two passages of liquid culture – and all substrates are expressed under the control of the native *PRC1* promoter. The simplest explanation, why C*T_{Pdr5}(CS) is degraded independently of Dfm1 but the known ERAD-M substrates Sec61-2, Pdr5* and Hmg2-GFP require Dfm1 for degradation, is that Sec61-2, Pdr5* and Hmg2-GFP contain several transmembrane helices and C*T_{Pdr5}(CS) only a single one. The mutations in the transmembrane helices of the multi-spanning membrane-bound substrates may possibly alter the folding of the cytosolic loops between them. Indeed, it is well-known that Dfm1 is involved in degradation of ER membrane-bound proteins containing lesions in their cytosolic parts [86]. Thus, Dfm1 may possibly not facilitate ERAD-M substrate degradation but participate in degradation of membrane-bound substrates with lesions in the cytosolic part. However, the most important question, how Dfm1 facilitates the retrotranslocation of these distinct ERAD substrates, is still open. But it is well-established, that Dfm1 recruits the AAA ATPase Cdc48 to the ER membrane [106–108]. Indeed, Cdc48 is also involved in C*T_{Pdr5}(CS) degradation (Figure 81 and [196]).

In brief summary, it is still an open question whether a retrotranslocon is required in the ERAD-M degradation mechanism, which cannot be answered within the experimental setup of this work. However, recently developped optical sensor systems to follow retrotranslocation of ERAD-C substrates [262] and retrotranslocation studies used for ERAD-L [96,97] as well as ERAD-M substrates [263] might shed more light into the dynamic field of retrotranslocation.

According to the established classification that proteins containing lesions in the membrane part are degraded via the ERAD-M degradation mechanism, composed of

the ubiquitin ligases Hrd1 and Asi complex, the ubiquitin-conjugating enzyme Ubc7, the AAA ATPase Cdc48 and the proteasome. In this work direct evidence was provided that this picture of ERAD-M substrates has to be rearranged, as it is explained in the following.

First, C*T_{Pdr5}(CS) contains lesions in the ER lumenal as well as the membrane part. But using carboxypeptidase activity assays it was demonstrated that the aberrant membrane part is not sufficient for ER retention, because native carboxypeptidase fused to the aberrant membrane part, CT_{Pdr5}(CS), is transported to vacuole where it is proteolytically active (Figure 23). Numerous studies in yeast and mammals show that polar residues within the membrane part, as well as mismatched hydrophobic length of the transmembrane domains, are recognized [264–266], which leads to retention in the ER and finally elimination by ERAD [65,66,267–272]. However, it seems that a portion of these aberrant membrane proteins fails to be recognized and is further transported to the Golgi [273–278]. There, the retrieval receptor Rer1 binds proteins with aberrant membrane parts and shuttles them back to the ER, where they are finally removed by ERAD [273,275,279,280]. Although the quality control systems of the ER and the Golgi are competent to remove aberrant membrane parts, indeed membrane-bound CPY is still able to reach its native environment, the vacuole (Figure 23). The best explanation comes from studies with the Golgi-membrane-localized ubiquitin ligase Tul1. It ubiquitinates membrane proteins, containing polar residues in their membrane parts, and targets them for vacuolar degradation [281]. In addition, Tul1 is also able to sort vacuolar proteins such as the carboxypeptidase S into multivesicular bodies, which deliver the proteins to their final destination, the vacuole [281–283]. In respect of these data, it is possible that the aberrant membrane part containing polar residues linked to the native vacuolar carboxypeptidase Y, CT_{Pdr5}(CS) construct, escapes ER retention and then in the Golgi, it is recognized as a target for the vacuole. In case of C*T_{Pdr5}(CS), which contains the misfolded carboxypeptidase Y, the CPY* moiety serves as a retention signal, and prevents BTpNA substrate turnover in the vacuole (Figure 23).
This shows that aberrant membrane parts of secretory proteins are able to escape the ER quality control mechanism.

Next, in this work it was shown that solely proteins containing an aberrant membrane part are degraded by the ERAD-M mechanism, composing Asi complex and Hrd1, in

case they contain a lysine residue in their cytosolic domain. In absence of cytosolic lysine residues degradation follows another mechanism as discussed in the following chapters.

4.3 Serine residues in the cytosolic part play a special role in degradation of proteins with an aberrant membrane domain and a misfolded ER lumenal domain

Analysis of several designed ERAD-M constructs, C*T_{Pdr5} derivatives, revealed that the amino acid composition of the cytosolic part has a huge influence on degradation. These ERAD-M constructs contain lysine as well as serine residues in their cytosolic part. A special group of these proteins contain only a serine residue in their cytosolic parts (Figure 60). Astonishingly, the serine-only construct is degraded by a different degradation pathway than the variants containing lysine residues in their cytosolic part. A first hint for different degradation pathways was given, by measuring the turnover rates. The lysine-containing ERAD-M substrate C*T_{Pdr5}(CS) is degraded with a half-life of 15 min, in comparison the so-called serine-only construct, C*T_{Pdr5}($CS^{K->A}$), shows slower turnover rates – half-life time ~50 min (Figure 61).

Further analysis of degradation demonstrates that the serine-only substrate requires only Hrd1 for ubiquitination (Figure 64). However, the lysine-containing ERAD-M substrate C*T_{Pdr5}(CS) additionally requires the Asi complex (Figure 21), which is located in the inner nuclear membrane [155]. Membrane-bound proteins with cytosolic domains smaller than 60 kDa are able to reach the INM by lateral diffusion [155,156]. It seems to be possible that both, C*T_{Pdr5}(CS) and C*T_{Pdr5}($CS^{K->A}$), are distributed in the ER membrane as well as in the INM. This might also explain the slower degradation of the serine-containing substrate, because it needs solely the ER localized Hrd1 ligase for degradation.

The need of different ubiquitin-conjugating enzymes for degradation of the constructs, C*T_{Pdr5}(CS) and C*T_{Pdr5}($CS^{K->A}$), might explain why the serine-only construct requires only the ubiquitin ligase Hrd1 but the lysine-containing construct requires both ubiquitin ligases, Hrd1 and Asi complex.

For ubiquitination of C*T_{Pdr5}($CS^{K->A}$) the ubiquitin-conjugating enzymes Ubc1, Ubc6 and Ubc7 are required. It was shown that in cells lacking Ubc7, C*T_{Pdr5}($CS^{K->A}$) is not

ubiquitinated at all (Figure 76). But in the absence of Ubc6, C*T_{Pdr5}($CS^{K->A}$) is still ubiquitinated (Figure 76). Ubc7 is proficient to mediate transfer of lysine48 polyubiquitin chains on previously monoubiquitinated substrates [152,153]. Furthermore, in a distinct case Ubc6 monoubiquitinates at either lysine, serine or threonine residues and then polyubiquitination is achieved by Ubc7, therefore, they cooperate with the ubiquitin ligase Doa10, which is a central player in the ERAD-C degradation mechanism [139]. Astonishingly, in cells lacking both, the ubiquitin-conjugating enzyme Ubc6 as well as the ubiquitin ligase Doa10, C*T_{Pdr5}($CS^{K->A}$) is not ubiquitinated at all (Figure 80). Although, turnover as well as ubiquitination is not affected in cells lacking only Doa10 (Figure 80 and Figure S24). Furthermore, it is recommended to analyze, how Ubc1 is involved in ubiquitination of C*T_{Pdr5}($CS^{K->A}$), by performing further *in vivo* ubiquitination assays in the absence of Ubc1. However, presence of serine residues in the cytosolic part of proteins with an ER lumenal misfolded domain and an aberrant part, alter the requirement of ubiquitin-conjugating enzymes in comparison to proteins containing lysine residues in the cytosolic part. For ubiquitination of the lysine-containing substrates the ubiquitin-conjugating enzyme Ubc7 is required. Ubc6 as well as Ubc1 are dispensable for degradation of the lysine-containing substrates (Figure 73). It was further shown that RING ligase equally bind substrate and E2~Ub conjugate and facilitates their orientation. Thus, the ubiquitin-conjugating enzyme determines the formation of the growing ubiquitin chain. Although it was shown that both, the Hrd1 ubiquitin ligase as well as the nuclear Asi complex cooperate with the ubiquitin-conjugating enzymes Ubc6 and Ubc7, the Asi complex might possibly not be able to mediate ubiquitination on serine residues. To analyze this hypothesis, further *in vitro* ubiquitination experiments have to be performed.

Most surprising was that Der1, a key component of the ERAD-L pathway, is indispensable for C*T_{Pdr5}($CS^{K->A}$) degradation (Figure 62), but it is dispensable for degradation of the lysine-containing ERAD-M substrate C*T_{Pdr5}(CS). Both substrates contain the same ER lumenal misfolded domain and the same aberrant membrane part.

How exactly Der1 contributes to the removal of aberrant proteins is highly investigated but not finally defined. On the one hand, the absence of Der1 initiates ER stress and thus activates the unfolded protein response (UPR) [62]. On the other hand, Der1 is one

of the most upregulated genes during UPR [284]. The UPR is conserved from yeast to man and it is a response to ER stress to restore normal ER function. Therefore, signaling pathways are activated, which increases the expression of molecular chaperones required for protein folding and of proteins required for protein degradation [285]. In ERAD Der1 is involved in degradation of ER lumenal soluble proteins, such as CPY* [61,62], PrA* [62] and KHN [230] but also necessary for membrane-bound ERAD substrates, like KWW [41] and C*T$_{Pdr5}$(CS)Leu2 (Data published in PhD thesis Stefanie Besser [232]) and some C*T$_{Pdr5}$(CS) derivatives (Figure 29, Figure 31, Figure 33, Figure 53, Figure 62 and [97]). It was shown to be dispensable for degradation of ERAD-M substrates, such as the lysine-containing CPY* derivatives C*T$_{Pdr5}$(CS), C*T$_{Pdr5}$(CS$^{S->K}$) and C*T$_{Pdr5}$(CS$^{S->A}$) (Figure 19 and Figure 71), as well as the *bona fide* ERAD-M substrates Sec61-2, Hmg2, Pdr5* and C*T$_{Pdr5}$(CS)GFP, as well as ERAD-C substrates, like Ste6* and KSS [41,42,196].

Since Der1 is substantial for degradation of C*T$_{Pdr5}$(CS$^{K->A}$) and C*T$_{Pdr5}$(CS)Leu2, but dispensable for C*T$_{Pdr5}$(CS) and C*T$_{Pdr5}$(CS)GFP, it may be possible that lysine residues are recognized by the same process as the GFP moiety. It was shown that the GFP moiety is recognized by the cytosolic Hsp70 chaperones [196] and it is assumed that the GFP moiety is removed prior to the membrane-embedded remnant (chapter 3.1.1). For degradation of the remaining C*T$_{Pdr5}$ core structure, the CPY* moiety seems to loop out through the translocon and for elimination of the aberrant membrane part the proteasome-associated ubiquitin ligase Hul5 might be required (chapter 4.1). To test whether the lysine residues in the cytosolic part of the ERAD-M substrate C*T$_{Pdr5}$(CS) are identified by the cytosolic Hsp70 chaperones, its turnover rates have to be measured in a Ssa1 mutant yeast strain in comparison to the serine-only construct, C*T$_{Pdr5}$(CS$^{K->A}$). Since the ER lumenal Hsp70 chaperone Kar2 participates in degradation of C*T$_{Pdr5}$(CS)Leu2 but is dispensable for C*T$_{Pdr5}$(CS) degradation [196,232], it should be further analyzed whether Kar2 is involved in degradation of C*T$_{Pdr5}$(CS) and C*T$_{Pdr5}$(CS$^{K->A}$). Since the CPY* moiety is required for ER retention of C*T$_{Pdr5}$(CS) and C*T$_{Pdr5}$(CS$^{K->A}$) it is still ambiguous how the signal is transferred across the ER membrane. It is possible that the cytosolic part and the ER lumenal part are independently recognized. Therefore, the signal has not to be transferred across the ER membrane. Taken together, these considerations lead to the following model. Lesions as well as exposed lysine residues in the cytosolic part of proteins with an ER

lumenal misfolded domain and an aberrant membrane part might be recognized by the cytosolic Hsp70 chaperones and the cytosolic domain might be finally removed by the cytosolic degradation machinery, including Ssa1. For elimination of the remaining transmembrane part chain elongation mediated by the proteasome-associated ubiquitin ligase Hul5 might be required. The CPY* moiety possibly loops out, which leads to elimination, because in the absence of Hul5 the aberrant membrane part remains in the ER membrane.

It is not finally solved yet whether Der1 contains four [62] or six [251] transmembrane helices. However, its N- and C-terminal parts are exposed to the cytosol [62,147]. Peptide-chain extension at the C-terminus and N-terminal modifications lead to inactivation of Der1 [62,147]. At its N-terminus Der1 is acetylated by the *N*-acetyltransferase NatB. In case of impaired acetylation, Der1 is rapidly degraded by Hrd1 [286]. But overexpression of Der1 is able to rescue the *natB*Δ phenotype [286]. The C-terminus is also important, because it is required for the integration of Der1 into the *HRD* ligase complex. Der1 has an intrinsic propensity to form oligomers [41,60–62] and is recruited by Usa1 [60] to the *HRD* ligase complex, formed by Hrd3 and Hrd1 [42,53,54,57,59,60]. Thereby, the C-terminal part of Usa1 interacts with the C-terminus of Der1. The N-terminus of Usa1 binds Hrd1 via its ubiquitin-like (UBL) domain [60]. Without Usa1, Der1 is not found to associate with the *HRD* ligase complex anymore [42,60]. Alterations in the first ER lumenal loop of Der1 [147] and the first and second transmembrane helices [61] inhibit retrotranslocation of distinct ERAD substrates [61]. In addition, Der1 receives ERAD-L substrates from the Hsp70 chaperone Kar2, the lectin Yos9 as well as the misfolding receptor Hrd3, introduces them into the membrane and shuttles them to the retrotranslocon [6,61,62].

Consistent with the role of Der1 in the ERAD-L degradation mechanism, $C^*T_{Pdr5}(CS^{K->A})$ might be degraded as explained in the following. The cytosolic part of $C^*T_{Pdr5}(CS^{K->A})$ seems not to be recognized as aberrant. As an ERAD-L substrate its CPY* domain might be recognized by Kar2. This has to be determined in further experiments. Then the CPY* moiety is introduced in the ER membrane by Der1 and transferred to the retrotranslocon for elimination, which is built amongst others by the ubiquitin ligase Hrd1 [59,60,95,97]. The aberrant membrane part has to be removed. Therefore, the ubiquitin chain elongation mediated by the proteasome-associated ubiquitin-ligase

Hul5 might be required (Figure 17).

Recently, a C*T_{Pdr5}(CS) derivative, containing only a serine residue in the cytosolic part was declared to be an ERAD-L substrate [97]. The cytosolic lysine residues in the (CS) were substituted for arginine and it was found that this substrate requires Der1 for degradation [97]. This arginine and serine-containing substrate composes of an aberrant membrane part (T_{Pdr5}). To monitor whether the arginine and serine-containing substrate with the aberrant membrane part is an ERAD-L substrate, in this work the lysine residues of C*T_{Pdr5}(CS) were replaced by arginine. Equal turnover rates were found for the C*T_{Pdr5}($CS^{K->R}$) construct compared with C*T_{Pdr5}($CS^{K->A}$). Furthermore, it was shown that both proteins require Der1 for degradation (Figure 63 and Figure S25). But there might possibly be a difference in degradation of C*T_{Pdr5}($CS^{K->A}$) and C*T_{Pdr5}($CS^{K->R}$). The Der1 homolog Dfm1 seems to be slightly involved in degradation of C*T_{Pdr5}($CS^{K->A}$) but not in degradation of C*T_{Pdr5}($CS^{K->R}$) (Figure 63 and Figure S25). However, participation of Dfm1 in degradation of C*T_{Pdr5}($CS^{K->A}$) was hardly detectable (Figure 63). In cycloheximide-analysis, using up to 6 independent experiments, a slight stabilization of C*T_{Pdr5}($CS^{K->R}$) might have been failed to detect in cells lacking Dfm1 (Figure S25). *In vivo* ubiquitination experiments might possibly give an answer, whether Dfm1 participates in C*T_{Pdr5}($CS^{K->R}$) degradation or not. Indeed, Dfm1 is involved in C*T_{Pdr5}($CS^{K->A}$) degradation, which was shown by analyzing polyubiquitination of the substrate in cells lacking Dfm1 (Figure 64). In addition, polyubiquitinated C*T_{Pdr5}($CS^{K->A}$) was found in cells lacking Der1 as well as Dfm1 (Figure 64). This leads to the assumption, that Hrd1 can additionally receive the substrate C*T_{Pdr5}($CS^{K->A}$) independently of Der1 but also independently of Dfm1. Hrd1 is also the only ligase required for C*T_{Pdr5}($CS^{K->A}$) ubiquitination (Figure S24 and Figure 64) and it was shown that Hrd1 is able to bind aberrant membrane parts [41,65]. The simplest explanation is that the ubiquitin ligase Hrd1, itself, binds the substrate. However, here it is assumed that participation of Der1 and Dfm1 increase the efficiency of substrate recruitment.

In any case, the AAA ATPase Cdc48 is required for degradation of the serine-containing substrate (Figure 82), as it is for all ERAD substrates [103,105,158,164,189–194].

4.4 Lysine is dominant in directing the degradation

The ERAD-M substrate C*T_{Pdr5}(CS) contains five lysine residues and a single serine residue in its cytosolic part. Substitution of the lysine residues for alanine, leads to the serine-only substrate C*T_{Pdr5}($CS^{K->A}$). Degradation of C*T_{Pdr5}(CS) and C*T_{Pdr5}($CS^{K->A}$) differs fundamentally, as explained above. Briefly, the lysine-rich and serine-containing substrate C*T_{Pdr5}(CS) was shown to be degraded by the Der1-independent ERAD-M pathway in which the ubiquitin ligases Hrd1 and the Asi complex are key components. The serine-only construct C*T_{Pdr5}($CS^{K->A}$) is degraded dependent on Der1, and the ubiquitin ligase Hrd1. Since both constructs contain the same ER lumenal misfolded and the same aberrant membrane part, the kind of amino acid, which can be ubiquitinated, directs their degradation. C*T_{Pdr5}(CS) contains not only lysine residues but also a single serine residue. Both lysine-only containing constructs show the same turnover rates and the same polyubiquitination pattern as C*T_{Pdr5}(CS) (Figure 19, Figure 71 and Figure 72). In addition, it was shown that they are degraded independently of Der1 (Figure 71).

With the lysine-only constructs C*T_{Pdr5}($CS^{S->A}$) and C*T_{Pdr5}($CS^{S->K}$) it was shown, that in case of a lysine residue is present in the cytosolic part of the protein, the substrate is degraded via an ERAD-M degradation mechanism. The additional serine residue is not mandatory for degradation.

4.5 ERAD-L degradation mechanism

According to the current classification, proteins containing lesions in the ER lumen are degraded by an ERAD-L degradation process [41,42]. They can either be ER lumenal, soluble proteins or ER membrane-bound proteins. It is well-established that the ER membrane protein Der1 is a key component of the ERAD-L degradation mechanism [41,42,60–62]. But there is an inconsistency in its role in the ERAD-L substrate degradation, because there are distinct substrates containing lesions in the ER lumenal domain, although their degradation is slightly impaired in cells lacking Der1 [41,97]. However, they are postulated to be ERAD-L substrates [41,97].

This inconsistency was solved during this work. Therefore, a membrane-bound substrate was generated, by replacing the membrane part of the ERAD-M substrate C*T_{Pdr5}(CS) with a properly folded one (Figure 24). The single spanning transmembrane helix of Wsc1 was chosen, because as a plasma membrane protein Wsc1 does not contain any intrinsic signals for ER retention, that might possibly influence ERAD [41,253]. The new construct, C*T_{Wsc1}(CS) shows slower turnover than the ERAD-M substrate C*T_{Pdr5}(CS) (Figure 25), which indicates that both constructs are differently degraded. This assumption was supported by the fact that the exchange of an aberrant membrane part by a properly folded one, leads to a substrate, which requires to some extent Der1 for degradation (Figure 26). This is consistent with data previously published [41] and indicates that C*T_{Wsc1}(CS) is partly degraded via the ERAD-L degradation mechanism. An overlapping function of the homologous pair Der1 and Dfm1 was also excluded (Figure 27). Der1 is essential for degradation of ERAD-L substrates but C*T_{Wsc1}(CS) is still degraded in the absence of Der1. Consequently, C*T_{Wsc1}(CS) cannot be a true ERAD-L substrate.

Thus, the cytosolic part of C*T_{Wsc1}(CS) was analyzed. It is composed of 12 amino acids, including a serine and several lysine residues (Figure 24). C*T_{Wsc1} derivatives were generated, which contain only either a serine, a lysine or an alanine residue (Figure 28) in their cytosolic part. It was shown, that degradation of the two constructs, containing serine- or alanine, is completely abrogated in the absence of Der1 (Figure 29 and Figure 31). In comparison, degradation of the lysine-containing construct is only slightly impaired in cells lacking Der1 (Figure 33) and it is still ubiquitinated (Figure 34). This provides direct evidence that proteins with ER lumenal misfolded domains

and properly folded membrane parts are only completely stabilized in the absence of Der1, if they are lacking any lysine residues in their cytosolic part. These proteins are true ERAD-L substrates. Additionally, it provides direct evidence that constructs containing lysine residues in the cytosolic part are degraded by the ERAD-L pathway in tandem with a Der1 independent degradation mechanism.

Amongst others, Der1 is in complex with the ubiquitin ligase Hrd1, which is highly discussed to form also the channel of the retrotranslocon (more details are given in chapter 1.3). Der1 facilitates membrane insertion of the hydrophilic, ER lumenal domains [6,61,62]. This role was supported since the alanine- as well as the serine-containing constructs are not ubiquitinated in the absence of Der1 (Figure 30 and Figure 32). All C*T_{Wsc1} derivatives require the ubiquitin ligase Hrd1 for degradation (Figure 29, Figure 31 and Figure 33). Astonishingly, using *in vivo* ubiquitination assays, it was found that C*T_{Wsc1}(ΔCS)K is still ubiquitinated in cells lacking Hrd1 (Figure 34), whereas the ERAD-L substrates, C*T_{Wsc1}(ΔCS)A and C*T_{Wsc1}(ΔCS)S, are not ubiquitinated at all (Figure 30 and Figure 32). This shows that Hrd1 is the only ligase required for ubiquitination and final elimination of ERAD-L substrates. Secondly, it supports the assumption that an additional ubiquitin ligase is involved in the Der1 independent degradation mechanism. This ubiquitin ligase was found to be the Asi complex (Figure 35). However, the ubiquitination mark mediated by the Asi complex is not sufficient to signal degradation, because C*T_{Wsc1}(ΔCS)K is not degraded in the absence of Hrd1 (Figure 33).

Considering the participation of the Asi complex and the Der1-independency, these data strongly suggested that the ERAD-M pathway operates in tandem with the ERAD-L pathway to degrade proteins with ER lumenal misfolded domains and properly folded membrane parts, containing lysine residues in their cytosolic parts. Thus, the mechanism to degrade this group of ERAD substrates was called the ERAD-L/M pathway.

It is currently unclear how and why the lysine residue is recognized. It is recommended to perform co-immunoprecipitation experiments and to determine the binding partners of either the lysine-containing substrate or the alanine-containing one, as a control.

However, it was additionally shown that Ubc1, Ubc6 and Ubc7 participate in degradation of the ERAD-L substrates C*T_{Wsc1}(ΔCS)A and C*T_{Wsc1}(ΔCS)S (Figure 36) but only Ubc1 and Ubc7 are required for degradation of the ERAD-L/M substrate

C*T_{Wsc1}(ΔCS)K (Figure 37). Participation of these ubiquitin-conjugating enzymes was shown by measuring the turnover rates of the indicated constructs.
Ubc7 was shown to work more efficiently, if there is a monoubiquitylated substrate [139,152,153]. Ubc1 and Ubc6 were shown to monoubiquitinate substrates [139,287]. This imply that together with the ubiquitin ligase Hrd1, Ubc1 and Ubc6 possibly monoubiquitinate ERAD-L substrates and thus prime the substrate for polyubiquitination conducted by Ubc7. Further ubiquitination studies have to be performed to improve this model. However, this experimental setup could not explain whether only these ubiquitin-conjugating enzymes are required for ubiquitination or whether some others are additionally involved. Furthermore, the question how these enzymes exactly work in tandem is still open. Thus, further *in vivo* ubiquitination assays have to be performed.
Finally, Cdc48 is required for degradation of ERAD-L/M substrates (Figure 39). As a control, the participation of Cdc48 in degradation of membrane-bound ERAD-L substrates was shown (Figure 38). This is not further surprising since Cdc48 is indispensable for degradation of all yet known ERAD substrates [103,105,158,164,189–194].

In summary in this thesis it was shown that membrane-bound proteins containing a misfolded ER lumenal domain are degraded by an ERAD-L mechanism, essentially require the ER membrane protein Der1 and the ubiquitin ligase Hrd1, in case they do not contain lysine residues in their cytosolic part. In comparison to these true ERAD-L substrates, lysine residues in the cytosolic part change their degradation mechanism to an ERAD-L/M mechanism. For degradation of these substrates a Der1 independent process participates additionally to the ERAD-L mechanism.

4.6 Nondegradable ERAD substrates

The strongest evidence that the cytoplasmic part has an extraordinary role in degradation of membrane-bound ERAD substrates, provides a special group of nondegradable ERAD substrates. These proteins are composed of an ER lumenal misfolded domain (CPY*) as well as an aberrant membrane part (T_{Pdr5}) and a cytosolic part without amino acid, which can be ubiquitinated. This was shown with the substrates C*T_{Pdr5}(ΔCS), C*T_{Pdr5}(ΔCS)A and C*T_{Pdr5}($CS^{K/S->A}$). Preliminary data were shown in the diploma thesis of Frederik Eisele [288]. In this work, it was shown that the length of the cytoplasmic part is not important for degradation. The construct C*T_{Pdr5}(ΔCS), containing a truncated version of the CS as well as the construct C*T_{Pdr5}($CS^{K/S->A}$) containing a longer CS are not degraded at all (Figure 41 and Figure 68). Astonishingly, their ER lumenal domain (CPY*) contains numerous amino acids, which can be ubiquitinated, and also the aberrant membrane part contains a cysteine residue, however, they are not degraded at all. Introduction of a lysine residue in the cytoplasmic part leads to fast degradation by the ERAD-M pathway (chapter 3.1.2). On contrary, a serine residue leads also to degradation, but only in case the serine residue is located in some distance to the ER membrane. This was shown, using the substrates C*T_{Pdr5}(ΔCS)S, serine in distance +4, and C*T_{Pdr5}($CS^{K->A}$), serine in distance +10 to the ER membrane (Figure 49 and Figure 61). Interference of the serine residue with the carboxy-terminus was excluded, because the substrate containing the serine at position +4 and additionally an alanine at the carboxy-terminus is also not degraded within 90 minutes of chase (Figure 58). There might be a trend for degradation of the constructs containing cytosolic serine residues close to the ER membrane, but with the experimental setup of this work this could not be analyzed. It is recommended to measure turnover rates of the constructs containing a cytosolic serine residue in close proximity to the ER membrane over a longer chase period. Thereby it should be considered that translation is irreversibly inhibited by the application of cycloheximide and the cells start to die after a certain time. This may lead to removal of the accumulated serine substrates in the ER membrane by ER-phagy and not by ERAD. How either the serine residue in distance to the ER membrane or the lysine residue affect degradation is discussed in chapters 4.2; 4.3 and 4.4.

Performing oligomerization experiments it was excluded that oligomerization of the nondegradable substrates prevents their degradation. Therefore, either an HA or a V5 epitope was introduced between the ER lumenal misfolded CPY* moiety and the aberrant membrane part. At the cytosolic part these variants contain only three amino acids (arginine-valine-proline), which remain to guarantee proper membrane integration. For control HA- as well as V5-tagged variants of C*T_{Wsc1}(ΔCS) were used. C*T_{Wsc1}(ΔCS) is a CPY* derivative, which contains a properly folded membrane domain (T_{Wsc1}). As a true ERAD-L substrate it is degraded in a Der1 and Hrd1 dependent process (chapter 3.2.1 and Diploma thesis Dorothea Mandlmeir [239]). Neither the HA nor the V5 epitope affect degradation of the membrane-bound CPY* derivatives, when introduced in the ER lumenal part (Figure 44 and Figure 45). In co-immunoprecipitation experiments it was shown that not only the HA- and V5-tagged C*T_{Pdr5}(ΔCS) can be co-precipitated (Figure 46) but also the HA- and V5-tagged C*T_{Wsc1}(ΔCS) control variants (Figure 47). In addition, heterogeneous C*T_{Pdr5}(ΔCS) and C*T_{Wsc1}(ΔCS) forms were found (Figure 46 and Figure 47). During the experimental setup the cellular membrane fraction was enriched and finally the membrane lipids were solubilized by digitonin treatment to obtain the native structure of the membrane-bound proteins [289–291]. In this experimental setup it may be possible that the hydrophobic parts of the substrates' CPY* moiety interact in the environment of the hydrophilic IP buffer, which leads to co-precipitation independently of the real membrane environment. In this experimental setup a possible oligomerization of the ERAD substrates may have been failed to detect.

Astonishingly, the nondegradable substrates are still ubiquitinated (Figure 42, Figure 50 and Figure 69). This indicates that they are accessible to a ubiquitin ligase. Furthermore, it was shown that solely the ER membrane-embedded ubiquitin ligase Hrd1 mediates ubiquitination of the nondegradable substrates (Figure 42 and Figure 69). The cytosolic part of the nondegradable substrates does not contain any amino acid, which can be ubiquitinated. But the ER lumenal misfolded CPY* moiety contains numerous amino acids for ubiquitination. Although the order of events is currently unclear, it is shown that the CPY* moiety is ubiquitinated. Since the CPY* moiety is located in the ER lumen, but ubiquitination mediated by Hrd1 is conducted in the cytosol, the CPY* moiety has to be transferred to the cytosol. Der1 facilitates the membrane insertion of ER lumenal misfolded proteins and mediates the transfer to the

Hrd1 ligase. Recently, it was shown that Hrd1 seems to be part of the retrotranslocon [59]. Unfortunately, ubiquitination of the nondegradable substrates in the absence of Der1 was not analyzed. Further experiments may shed light onto the question, whether Der1 shuttles the nondegradable substrates to Hrd1 or whether Hrd1 itself binds the nondegradable substrates and initiates the transfer of the CPY* moiety into the cytosol, where it is finally ubiquitinated. However, for final retrotranslocation and thus elimination an amino acid for ubiquitination has to present in the cytosolic part of these proteins. This conclusion is consistent with recently published data in the mammalian system. It was found that certain ERAD substrates containing aberrant membrane parts are not degraded at all as long as they do not contain any lysine residues in their cytosolic parts [292]. However, a role for cytosolic serine residues as well as ubiquitination mediated by Hrd1 was not shown for the mammalian ERAD substrates. Furthermore, in this work it was shown that introduction of a lysine residue in the aberrant membrane part of nondegradable substrates leads to degradation of these substrates (Figure 52). In comparison, serine residues within the aberrant membrane parts do not lead to degradation (Figure 66). The aberrant membrane part of these constructs is the last of 12 transmembrane helices of the multi drug transporter Pdr5. It contains four tyrosine residues. In its native environment these residues mediate interaction of the membrane helices. The tyrosine residues are arranged at position +2, +8, +13 and +20. Surprisingly, turnover rates increase the closer the lysine residues are located to the cytosol. In detail, the construct $C^{*}\_T_{Pdr5}^{Y4\rightarrow K}$ (ΔCS) is faster degraded than the construct $C^{*}\_T_{Pdr5}^{Y1\rightarrow K}$ (ΔCS), which contains the tyrosine residue close to the ER lumen at position +2 (Figure 52). These membrane mutants are degraded by an ERAD-L degradation process, because the membrane protein Der1 and the Hrd1 ligase are involved (Figure 53 and Figure 54), which are central players of the ERAD-L pathway. Surprisingly, lysine residues in the cytosolic part lead to an ERAD-M degradation process, which is independent of Der1. The ubiquitin ligases Hrd1 as well as the nuclear Asi complex are involved (chapter 3.1.2). The cryo-EM structure of a Hrd1-Hrd3 hetero tetramer revealed a funnel, which reaches from the cytosol to the ER lumen [59]. It is proposed that this funnel might allow transport in opposite directions [98,99]. These observations lead to the assumption that the lysine-containing membrane variants, which require Hrd1 for ubiquitination and final elimination, are able to slide back and forth. Thus, they are accessible for the RING domain of the ligase and once

they are ubiquitinated they can be finally removed.

For several ERAD substrates it was demonstrated that charged and polar residues in the transmembrane part lead to ER retention [268,293–298]. In at least some cases ER retention is due to complete translocation of the transmembrane domain into the ER lumen [297,299,300]. To support this possibility, membrane integration and topology of the substrates used in this work was determined (Figure S10, Figure S11, Figure S18 and Figure S19).

Another possibility why these substrates are ubiquitinated although not degraded might be because of the ubiquitin chain formation. The formation of ubiquitin chains is a highly flexible and dynamic process (more details in 1.4 and reviewed in [120–122]). All possible linkages within ubiquitin chains are observed [124,125]. Common chains are polyLys48-linked chains which are the *canonical* signal for final degradation by the 26S proteasome [120]. Lys6-linked, Lys11-linked chains and Lys63-linked ubiquitin chains are involved in autophagy [126,127] in the regulation of mitosis [128], hypoxia response [129] and mitophagy [126] or they prevent proteins from proteasomal destruction [70]. Thus, it might be that the nondegradable substrates contain ubiquitin chains, which are not clients for the ubiquitin-proteasome system.

Prior to elimination by the 26S proteasome the proteins have to be pulled out of the ER membrane. The AAA ATPase Cdc48 provides the power for membrane extraction of all yet known ERAD substrates [103,105,158,164,189–194]. It is in complex with several cofactors (chapter 1.5), which mediate substrate recruitment [105]. Cdc48 clients are ubiquitinated proteins. Recently, it was shown that the ubiquitin chains are rearranged by Cdc48 and its cofactors [184–186]. Thus, it might be that the nondegradable substrates are not client proteins of the Cdc48 complex anymore. Consequently, it should be analyzed whether the nondegradable substrates are associated with the Cdc48.

In summary, various membrane-bound ERAD substrates with a related modular structure were generated during this work. For ER retention, all of these substrates possess the misfolded carboxypeptidase Y (CPY*) in the ER lumen (Figure 23, Figure S4, Figure S7, Figure S17 and Figure S21). One part of these substrates consists of an aberrant transmembrane domain, the last transmembrane helices of Pdr5. As an orphan helix it exposes polar residues, which cannot interact with partner domains and thus signals misfolding. The cytosolic part of these substrates influences the degradation mechanism (chapters 3.2.2; 3.2.3 and 3.2.6). This is amazing since they contain two misfolded domains, the ER lumenal and the membrane domain.

If the cytosolic part lacks any amino acid, which can be ubiquitinated, the substrates are not degraded at all, as shown for C*T$_{Pdr5}$(ΔCS), C*T$_{Pdr5}$(ΔCS)A and C*T$_{Pdr5}$(CS$^{K/S->A}$) (Figure 41, Figure 49 and Figure 68). Amino acids to be ubiquitinated are only present in the ER lumenal located CPY* moiety of the substrate. However, they are nevertheless ubiquitinated by Hrd1 (Figure 42 and Figure 69). Since ubiquitination occurs at the cytosolic RING domain of Hrd1 partial retrotransloctaion of the lumenal part has to occur. However, final retrotranslocation is prevented in some way.

Lysine residues in the cytosolic part of these substrates trigger fast degradation in a Der1 independent manner (Figure 19). Therefore, these substrates must at least in part be retrotranslocated. The ubiquitin ligase Hrd1 is proclaimed to be part of the retrotranslocon [6,59,63,78,97]. But ubiquitination of the cytosolic lysine-containing substrates is mediated by the ubiquitin ligase Hrd1 and by the Asi complex (Figure 21 and Figure 22). Hrd1 is restricted to the ER membrane, whereas the Asi complex is solely located in the inner nuclear membrane (INM) [155]. Thus, it can by hypothesized that the Asi complex possibly participates in a retrotranslocation step in the INM.

These cytosolic lysine-containing substrates are degraded by the established ERAD-M pathway. Additional serine residues in the lysine-containing cytosolic part do not further affect the degradation pathway of these substrates. This was shown using the substrates C*T$_{Pdr5}$(CS), C*T$_{Pdr5}$(CS$^{S->A}$) and C*T$_{Pdr5}$(CS$^{S->K}$) (chapter 3.2.3 and 3.2.6). On contrary, substrates lacking lysine residues in the cytosolic part but containing serine residues in some distance to the ER membrane in the cytosolic part are degraded in a Der1 dependent manner (Figure 62). This is astonishing because they have a misfolded membrane domain and according to the established classification by Vashist and Ng [41] as well as Carvalho *et al.* 2006 [42], proteins with misfolded membrane

domains are degraded by the ERAD-M pathway, which is independent of Der1 (Figure 19 and [41,42]). Only Hrd1 and not the Asi complex conduct ubiquitination of the serine-only substrate. This was shown, using the substrate $C^*T_{Pdr5}(CS^{K->A})$ (chapter 3.2.6; an overview is given in Table 24).

In addition, several CPY* derivatives were generated, composed of the ER lumenal misfolded CPY* and the single spanning properly folded Wsc1 transmembrane helix (T_{Wsc1}) (chapter 3.2.1). Analysis of the cytosolic part of these proteins showed that cytosolic lysine residues lead to a Der1 independent degradation mechanism additionally to the ERAD-L degradation. This Der1 independent process might be the ERAD-M degradation pathway, because it was shown that the nuclear Asi complex conducts ubiquitin chain formation at these lysine-containing substrates. However, this ubiquitination signal does not lead to proteasomal degradation. True ERAD-L substrates lacking cytosolic lysine residues and essentially require Der1 for degradation (an overview is given in Table 18).

5. BIBLIOGRAPHY

1. Powers, E. T., Morimoto, R. I., Dillin, A., Kelly, J. W. & Balch, W. E. Biological and chemical approaches to diseases of proteostasis deficiency. *Annu Rev Biochem* **78**, 959–991 (2009).
2. Labbadia, J. & Morimoto, R. I. The biology of proteostasis in aging and disease. *Annu Rev Biochem* **84**, 435–464 (2015).
3. Walker, L. C. Proteopathic strains and the heterogeneity of neurodegenerative diseases. *Annu Rev Genet* **50**, 329–346 (2016).
4. Qi, L., Tsai, B. & Arvan, P. New insights into the physiological role of endoplasmic reticulum-associated degradation. *Trends Cell Biol* **27**, 430–440 (2017).
5. Guerriero, C. J. & Brodsky, J. L. The delicate balance between secreted protein folding and endoplasmic reticulum-associated degradation in human physiology. *Physiol Rev* **92**, 537–576 (2012).
6. Berner, N., Reutter, K.-R. & Wolf, D. H. Protein quality control of the endoplasmic reticulum and ubiquitin–proteasome-triggered degradation of aberrant proteins: Yeast pioneers the path. *Annual Review of Biochemistry* **87**, 751–782 (2018).
7. Amm, I., Sommer, T. & Wolf, D. H. Protein quality control and elimination of protein waste: The role of the ubiquitin-proteasome system. *Biochimica et Biophysica Acta - Molecular Cell Research* **1843**, 182–196 (2014).
8. Wolf, D. H. & Menssen, R. Mechanisms of cell regulation – proteolysis, the big surprise. *FEBS Letters* **592**, 2515–2524 (2018).
9. Kachroo, A. H. *et al.* Evolution. Systematic humanization of yeast genes reveals conserved functions and genetic modularity. *Science* **348**, 921–925 (2015).
10. Chen, Y. *et al.* SPD-a web-based secreted protein database. *Nucleic Acids Res* **33**, D169-73 (2005).
11. Choi, J. *et al.* Fungal Secretome Database: Integrated platform for annotation of fungal secretomes. *BMC Genomics* **11**, (2010).
12. Wallin, E. & Heijne, G. Von. Genome-wide analysis of integral membrane proteins from eubacterial, archaean, and eukaryotic organisms. *Protein Science* **7**, 1029–1038 (2008).
13. Zimmermann, R., Eyrisch, S., Ahmad, M. & Helms, V. Protein translocation across the ER membrane. *Biochimica et Biophysica Acta - Biomembranes* **1808**,

912–924 (2011).

14. Gogala, M. *et al.* Structures of the Sec61 complex engaged in nascent peptide translocation or membrane insertion. *Nature* **506**, 107–110 (2014).
15. Finke, K. *et al.* A second trimeric complex containing homologs of the Sec61p complex functions in protein transport across the ER membrane of S. cerevisiae. *The EMBO Journal* **15**, 1482–1494 (1996).
16. Aviram, N. & Schuldiner, M. Targeting and translocation of proteins to the endoplasmic reticulum at a glance. *Journal of Cell Science* **130**, 4079–4085 (2017).
17. Simon, S. M., Peskin, C. S. & Oster, G. F. What drives the translocation of proteins? *Proceedings of the National Academy of Sciences of the United States of America* **89**, 3770–3774 (1992).
18. Matlack, K. E. S., Misselwitz, B., Plath, K. & Rapoport, T. A. BIP acts as a molecular ratchet during posttranslational transport of prepro-α factor across the ER membrane. *Cell* **97**, 553–564 (1999).
19. Simons, J. F., Ferro-Novick, S., Rose, M. D. & Helenius, A. BiP/Kar2p serves as a molecular chaperone during carboxypeptidase Y folding in yeast. *Journal of Cell Biology* **130**, 41–49 (1995).
20. Blobel, G. & Dobberstein, B. Transfer of proteins across membranes I . Presence of proteolytically processed and Unprocessed nascent immunoglobulin light chains on membrane-bound ribosomes of murine myeloma. **67**, 835–851 (1975).
21. Weihofen, A., Binns, K., Lemberg, M. K., Ashman, K. & Martoglio, B. Identification of signal peptide peptidase, a presenilin-type aspartic protease. *Science* **296**, 2215–2218 (2002).
22. Appenzeller-Herzog, C. & Ellgaard, L. The human PDI family: versatility packed into a single fold. *Biochim Biophys Acta* **1783**, 535–548 (2008).
23. Xu, C. & Ng, D. T. Glycosylation-directed quality control of protein folding. *Nat Rev Mol Cell Biol* **16**, 742–752 (2015).
24. Helenius, A. & Aebi, M. Roles of N-linked glycans in the endoplasmic reticulum. *Annu Rev Biochem* **73**, 1019–1049 (2004).
25. Aebi, M., Bernasconi, R., Clerc, S. & Molinari, M. N-glycan structures: recognition and processing in the ER. *Trends Biochem Sci* **35**, 74–82 (2010).
26. Xu, C. & Ng, D. T. W. O-mannosylation: The other glycan player of ER quality

control. *Seminars in cell & developmental biology* **41**, 129–134 (2015).

27. Xu, C., Wang, S., Thibault, G. & Ng, D. T. Futile protein folding cycles in the ER are terminated by the unfolded protein O-mannosylation pathway. *Science* **340**, 978–981 (2013).
28. Kelleher, D. J. & Gilmore, R. An evolving view of the eukaryotic oligosaccharyltransferase. *Glycobiology* **16**, 47–62 (2006).
29. Xu, X., Kanbara, K., Azakami, H. & Kato, A. Expression and characterization of Saccharomyces cerevisiae Cne1p, a calnexin homologue. *J Biochem* **135**, 615–618 (2004).
30. Jakob, C. A., Burda, P., Roth, J. & Aebi, M. Degradation of misfolded endoplasmic reticulum glycoproteins in Saccharomyces cerevisiae is determined by a specific oligosaccharide structure. *J Cell Biol* **142**, 1223–1233 (1998).
31. Knop, M., Hauser, N. & Wolf, D. H. N-Glycosylation affects endoplasmic reticulum degradation of a mutated derivative of carboxypeptidase yscY in yeast. *Yeast* **12**, 1229–1238 (1996).
32. Gauss, R., Kanehara, K., Carvalho, P., Ng, D. T. & Aebi, M. A complex of Pdi1p and the mannosidase Htm1p initiates clearance of unfolded glycoproteins from the endoplasmic reticulum. *Mol Cell* **42**, 782–793 (2011).
33. Clerc, S. *et al.* Htm1 protein generates the N-glycan signal for glycoprotein degradation in the endoplasmic reticulum. *J Cell Biol* **184**, 159–172 (2009).
34. Quan, E. M. *et al.* Defining the glycan destruction signal for endoplasmic reticulum-associated degradation. *Mol Cell* **32**, 870–877 (2008).
35. Sakoh-Nakatogawa, M., Nishikawa, S. & Endo, T. Roles of protein-disulfide isomerase-mediated disulfide bond formation of yeast Mnl1p in endoplasmic reticulum-associated degradation. *J Biol Chem* **284**, 11815–11825 (2009).
36. Gillece, P., Luz, J. M., Lennarz, W. J., de La Cruz, F. J. & Romisch, K. Export of a cysteine-free misfolded secretory protein from the endoplasmic reticulum for degradation requires interaction with protein disulfide isomerase. *J Cell Biol* **147**, 1443–1456 (1999).
37. Nakatsukasa, K., Nishikawa, S., Hosokawa, N., Nagata, K. & Endo, T. Mnl1p, an α-mannosidase-like protein in yeast Saccharomyces cerevisiae , is required for endoplasmic reticulum-associated degradation of glycoproteins. *Journal of*

Biological Chemistry **276**, 8635–8638 (2001).

38. Jakob, C. A. *et al.* Htm1p, a mannosidase-like protein, is involved in glycoprotein degradation in yeast. *EMBO Rep* **2**, 423–430 (2001).
39. Gnann, A., Riordan, J. R. & Wolf, D. H. Cystic fibrosis transmembrane conductance regulator degradation depends on the lectins Htm1p/EDEM and the Cdc48 protein complex in yeast. *Mol Biol Cell* **15**, 4125–4135 (2004).
40. Sun, Z. & Brodsky, J. L. The degradation pathway of a model misfolded protein is determined by aggregation propensity. *Molecular Biology of the Cell* **29**, 1422–1434 (2018).
41. Vashist, S. & Ng, D. T. W. Misfolded proteins are sorted by a sequential checkpoint mechanism of ER quality control. *Journal of Cell Biology* **165**, 41–52 (2004).
42. Carvalho, P., Goder, V. & Rapoport, T. A. Distinct ubiquitin-ligase complexes define convergent pathways for the degradation of ER proteins. *Cell* **126**, 361–373 (2006).
43. Hiller, M. M., Finger, A., Schweiger, M. & Wolf, D. H. ER degradation of a misfolded luminal protein by the cytosolic ubiquitin-proteasome pathway. *Science* **273**, 1725–1728 (1996).
44. Hochstrasser, M. Ubiquitination and protein turnover. in *LANDMARK PAPERS IN YEAST BIOLOGY* (eds. Linder, P., Shore, D. & Hall, M. N.) 267–284 (Cold Spring Harbor Laboratory Press, 2006).
45. Buschhorn, B. A., Kostova, Z., Medicherla, B. & Wolf, D. H. A genome-wide screen identifies Yos9p as essential for ER-associated degradation of glycoproteins. *FEBS Lett* **577**, 422–426 (2004).
46. Bhamidipati, A., Denic, V., Quan, E. M. & Weissman, J. S. Exploration of the topological requirements of ERAD identifies Yos9p as a lectin sensor of misfolded glycoproteins in the ER lumen. *Mol Cell* **19**, 741–751 (2005).
47. Kim, W., Spear, E. D. & Ng, D. T. Yos9p detects and targets misfolded glycoproteins for ER-associated degradation. *Mol Cell* **19**, 753–764 (2005).
48. Szathmary, R., Bielmann, R., Nita-Lazar, M., Burda, P. & Jakob, C. A. Yos9 protein is essential for degradation of misfolded glycoproteins and may function as lectin in ERAD. *Mol Cell* **19**, 765–775 (2005).
49. Plemper, R. K., Bohmler, S., Bordallo, J., Sommer, T. & Wolf, D. H. Mutant

analysis links the translocon and BiP to retrograde protein transport for ER degradation. *Nature* **388**, 891–895 (1997).

50. Brodsky, J. L. *et al.* The requirement for molecular chaperones during endoplasmic reticulum-associated protein degradation demonstrates that protein export and import are mechanistically distinct. *J Biol Chem* **274**, 3453–3460 (1999).
51. Nishikawa, S. I., Fewell, S. W., Kato, Y., Brodsky, J. L. & Endo, T. Molecular chaperones in the yeast endoplasmic reticulum maintain the solubility of proteins for retrotranslocation and degradation. *J Cell Biol* **153**, 1061–1070 (2001).
52. Hampton, R. Y., Gardner, R. G. & Rine, J. Role of 26S proteasome and HRD genes in the degradation of 3-hydroxy-3-methylglutaryl-CoA reductase, an integral endoplasmic reticulum membrane protein. *Mol Biol Cell* **7**, 2029–2044 (1996).
53. Plemper, R. K. *et al.* Genetic interactions of Hrd3p and Der3p/Hrd1p with Sec61p suggest a retro-translocation complex mediating protein transport for ER degradation. *J Cell Sci* **112**, 4123–4134 (1999).
54. Gardner, R. G. *et al.* Endoplasmic reticulum degradation requires lumen to cytosol signaling. Transmembrane control of Hrd1p by Hrd3p. *J Cell Biol* **151**, 69–82 (2000).
55. Mehnert, M. *et al.* The interplay of Hrd3 and the molecular chaperone system ensures efficient degradation of malfolded secretory proteins. *Mol Biol Cell* **26**, 185–194 (2015).
56. Denic, V., Quan, E. M. & Weissman, J. S. A luminal surveillance complex that selects misfolded glycoproteins for ER-associated degradation. *Cell* **126**, 349–359 (2006).
57. Gauss, R., Jarosch, E., Sommer, T. & Hirsch, C. A complex of Yos9p and the HRD ligase integrates endoplasmic reticulum quality control into the degradation machinery. *Nat Cell Biol* **8**, 849–854 (2006).
58. Kanehara, K., Xie, W. & Ng, D. T. Modularity of the Hrd1 ERAD complex underlies its diverse client range. *J Cell Biol* **188**, 707–716 (2010).
59. Schoebel, S. *et al.* Cryo-EM structure of the protein-conducting ERAD channel Hrd1 in complex with Hrd3. *Nature* **548**, 352–355 (2017).
60. Horn, S. C. *et al.* Usa1 functions as a scaffold of the HRD-ubiquitin ligase. *Mol*

Cell **36**, 782–793 (2009).

61. Mehnert, M., Sommer, T. & Jarosch, E. Der1 promotes movement of misfolded proteins through the endoplasmic reticulum membrane. *Nat Cell Biol* **16**, 77–86 (2014).
62. Knop, M., Finger, A., Braun, T., Hellmuth, K. & Wolf, D. H. Der1, a novel protein specifically required for endoplasmic reticulum degradation in yeast. *The EMBO journal* **15**, 753–63 (1996).
63. Hampton, R. Y. & Sommer, T. Finding the will and the way of ERAD substrate retrotranslocation. *Curr Opin Cell Biol* **24**, 460–466 (2012).
64. Zhao, G. & London, E. An amino acid “transmembrane tendency” scale that approaches the theoretical limit to accuracy for prediction of transmembrane helices: Relationship to biological hydrophobicity. *Protein Science* **15**, 1987–2001 (2006).
65. Sato, B. K., Schulz, D., Do, P. H. & Hampton, R. Y. Misfolded membrane proteins are specifically recognized by the transmembrane domain of the Hrd1p ubiquitin ligase. *Molecular Cell* **34**, 212–222 (2009).
66. Habeck, G., Ebner, F. A., Shimada-Kreft, H. & Kreft, S. G. The yeast ERAD-C ubiquitin ligase Doa10 recognizes an intramembrane degron. *Journal of Cell Biology* **209**, 261–273 (2015).
67. Khmelinskii, A. *et al.* Protein quality control at the inner nuclear membrane. *Nature* **516**, 410–413 (2014).
68. Foresti, O., Rodriguez-Vaello, V., Funaya, C. & Carvalho, P. Quality control of inner nuclear membrane proteins by the Asi complex. *Science* **346**, 751–755 (2014).
69. Ravid, T., Kreft, S. G. & Hochstrasser, M. Membrane and soluble substrates of the Doa10 ubiquitin ligase are degraded by distinct pathways. *EMBO J* **25**, 533–543 (2006).
70. Finley, D., Ulrich, H. D., Sommer, T. & Kaiser, P. The ubiquitin-proteasome system of Saccharomyces cerevisiae. *Genetics* **192**, 319–360 (2012).
71. Ruggiano, A., Foresti, O. & Carvalho, P. ER-associated degradation: Protein quality control and beyond. *Journal of Cell Biology* **204**, 869–879 (2014).
72. Zattas, D., Berk, J. M., Kreft, S. G. & Hochstrasser, M. A conserved C-terminal element in the yeast Doa10 and human MARCH6 ubiquitin ligases required for

selective substrate degradation. *Journal of Biological Chemistry* **291**, 12105–12118 (2016).

73. Shiber, A., Breuer, W., Brandeis, M. & Ravid, T. Ubiquitin conjugation triggers misfolded protein sequestration into quality control foci when Hsp70 chaperone levels are limiting. *Mol Biol Cell* **24**, 2076–2087 (2013).
74. Metzger, M. B., Maurer, M. J., Dancy, B. M. & Michaelis, S. Degradation of a cytosolic protein requires endoplasmic reticulum-associated degradation machinery. *Journal of Biological Chemistry* **283**, 32302–32316 (2008).
75. Furth, N. *et al.* Exposure of bipartite hydrophobic signal triggers nuclear quality control of Ndc10 at the endoplasmic reticulum/nuclear envelope. *Molecular Biology of the Cell* **22**, 4726–4739 (2011).
76. Han, S., Liu, Y. & Chang, A. Cytoplasmic Hsp70 promotes ubiquitination for endoplasmic reticulum-associated degradation of a misfolded mutant of the yeast plasma membrane ATPase, PMA1. *J Biol Chem* **282**, 26140–26149 (2007).
77. Alfassy, O. S., Cohen, I., Reiss, Y., Tirosh, B. & Ravid, T. Placing a disrupted degradation motif at the C-terminus of proteasome substrates attenuates degradation without impairing ubiquitylation. *Journal of Biological Chemistry* **288**, 12645–12653 (2013).
78. Romisch, K. A case for Sec61 channel involvement in ERAD. *Trends Biochem Sci* **42**, 171–179 (2017).
79. Schlenstedt, G., Gudmundsson, G. H., Boman, H. G. & Zimmermann, R. A large presecretory protein translocates both cotranslationally, using signal recognition particle and ribosome, and post-translationally, without these ribonucleoparticles, when synthesized in the presence of mammalian microsomes. *Journal of Biological Chemistry* **265**, 13960–13968 (1990).
80. Wiertz, E. J. *et al.* The human cytomegalovirus US11 gene product dislocates MHC class I heavy chains from the endoplasmic reticulum to the cytosol. *Cell* **84**, 769–779 (1996).
81. Wiertz, E. J. H. J. *et al.* To the proteasome for destruction. **384**, 636–638 (1996).
82. Gillece, P., Pilon, M. & Römisch, K. The protein translocation channel mediates glycopeptide export across the endoplasmic reticulum membrane. *Proceedings of the National Academy of Sciences of the United States of America* **97**, 4609–

4614 (2000).

83. Kaiser, M. L. & Römisch, K. Proteasome 19S RP binding to the Sec61 channel plays a key role in ERAD. *PLoS ONE* **10**, 1–19 (2015).
84. Tretter, T. *et al.* ERAD and protein import defects in a sec61 mutant lacking ER-lumenal loop 7. *BMC Cell Biol* **14**, 56 (2013).
85. Schäfer, A. & Wolf, D. H. Sec61p is part of the endoplasmic reticulum-associated degradation machinery. *EMBO Journal* **28**, 2874–2884 (2009).
86. Stolz, A., Schweizer, R. S., Schafer, A. & Wolf, D. H. Dfm1 forms distinct complexes with Cdc48 and the ER ubiquitin ligases and is required for ERAD. *Traffic* **11**, 1363–1369 (2010).
87. Rubenstein, E. M., Kreft, S. G., Greenblatt, W., Swanson, R. & Hochstrasser, M. Aberrant substrate engagement of the ER translocon triggers degradation by the Hrd1 ubiquitin ligase. *Journal of Cell Biology* **197**, 761–773 (2012).
88. Ng, W., Sergeyenko, T., Zeng, N., Brown, J. D. & Römisch, K. Characterization of the proteasome interaction with the Sec61 channel in the endoplasmic reticulum. *Journal of Cell Science* **120**, 682–691 (2007).
89. Werner, E. D., Brodsky, J. L. & McCracken, A. A. Proteasome-dependent endoplasmic reticulum-associated protein degradation: An unconventional route to a familiar fate. *Proc Natl Acad Sci U S A* **93**, 13797–13801 (1996).
90. Pilon, M., Schekman, R. & Romisch, K. Sec61p mediates export of a misfolded secretory protein from the endoplasmic reticulum to the cytosol for degradation. *EMBO J* **16**, 4540–4548 (1997).
91. Garza, R. M., Sato, B. K. & Hampton, R. Y. In vitro analysis of Hrd1p-mediated retrotranslocation of its multispanning membrane substrate 3-hydroxy-3-methylglutaryl (HMG)-CoA reductase. *Journal of Biological Chemistry* **284**, 14710–14722 (2009).
92. Wahlman, J. *et al.* Real-time fluorescence detection of ERAD substrate retrotranslocation in a mammalian in vitro system. *Cell* **129**, 943–955 (2007).
93. Walter, J., Urban, J., Volkwein, C. & Sommer, T. Sec61p-independent degradation of the tail-anchored ER membrane protein Ubc6p. *EMBO J* **20**, 3124–3131 (2001).
94. Deak, P. M. & Wolf, D. H. Membrane topology and function of Der3/Hrd1p as a ubiquitin-protein ligase (E3) involved in endoplasmic reticulum degradation. *J*

Biol Chem **276**, 10663–10669 (2001).

95. Carvalho, P., Stanley, A. M. & Rapoport, T. A. Retrotranslocation of a misfolded luminal ER protein by the ubiquitin-ligase Hrd1p. *Cell* **143**, 579–591 (2010).
96. Stein, A., Ruggiano, A., Carvalho, P. & Rapoport, T. a. Key steps in ERAD of luminal ER proteins reconstituted with purified components. *Cell* **158**, 1375–88 (2014).
97. Baldridge, R. D. & Rapoport, T. A. Autoubiquitination of the Hrd1 ligase triggers protein retrotranslocation in ERAD. *Cell* **166**, 394–407 (2016).
98. Berg, B. Van Den *et al.* X-ray structure of a protein-conducting channel. **427**, 34–44 (2004).
99. Voorhees, R. M., Fernández, I. S., Scheres, S. H. W. & Hegde, R. S. Structure of the mammalian ribosome-Sec61 complex to 3.4 Å resolution. *Cell* **157**, 1632–1643 (2014).
100. Kumazaki, K. *et al.* Structural basis of Sec-independent membrane protein insertion by YidC. *Nature* **509**, 516–519 (2014).
101. Dalbey, R. E. & Kuhn, A. Membrane insertases are present in all three domains of life. *Structure* **23**, 1559–1560 (2015).
102. Wu, X. & Rapoport, T. A. Mechanistic insights into ER-associated protein degradation. *Current Opinion in Cell Biology* **53**, 22–28 (2018).
103. Braun, S., Matuschewski, K., Rape, M., Thoms, S. & Jentsch, S. Role of the ubiquitin-selective CDC48(UFD1/NPL4) chaperone (segregase) in ERAD of OLE1 and other substrates. *EMBO J* **21**, 615–621 (2002).
104. Meyer, H. H., Shorter, J. G., Seemann, J., Pappin, D. & Warren, G. A complex of mammalian Ufd1 and Npl4 links the AAA-ATPase, p97, to ubiquitin and nuclear transport pathways. *EMBO Journal* **19**, 2181–2192 (2000).
105. Ye, Y., Meyer, H. H. & Rapoport, T. A. The AAA ATPase Cdc48/p97 and its partners transport proteins from the ER into the cytosol. *Nature* **414**, 652–656 (2001).
106. Neal, S. *et al.* The Dfm1 derlin is required for ERAD retrotranslocation of integral membrane proteins. *Molecular Cell* **69**, 306–320 (2018).
107. Goder, V., Carvalho, P. & Rapoport, T. A. The ER-associated degradation component Der1p and its homolog Dfm1p are contained in complexes with distinct cofactors of the ATPase Cdc48p. *FEBS Lett* **582**, 1575–1580 (2008).

108. Sato, B. K. & Hampton, R. Y. Yeast Derlin Dfm1 interacts with Cdc48 and functions in ER homeostasis. *Yeast* **23**, 1053–1064 (2006).
109. Kreft, S. G., Wang, L. & Hochstrasser, M. Membrane topology of the yeast endoplasmic reticulum-localized ubiquitin ligase Doa10 and comparison with its human ortholog TEB4 (MARCH-VI). *J Biol Chem* **281**, 4646–4653 (2006).
110. Bernasconi, R. *et al.* Cyclosporine A-sensitive, cyclophilin B-dependent endoplasmic reticulum-associated degradation. *PLoS ONE* **5**, 1–7 (2010).
111. Hirayama, H., Seino, J., Kitajima, T., Jigami, Y. & Suzuki, T. Free oligosaccharides to monitor glycoprotein endoplasmic reticulum-associated degradation in Saccharomyces cerevisiae. *Journal of Biological Chemistry* **285**, 12390–12404 (2010).
112. Ushioda, R. *et al.* ERdj5 is required as a disulfide reductase for degradation of misfolded proteins in the ER. *Science* **321**, 569–572 (2008).
113. Ploegh, H. L. A lipid-based model for the creation of an escape hatch from the endoplasmic reticulum. *Nature* **448**, 435–438 (2007).
114. Olzmann, J. A. & Kopito, R. R. Lipid droplet formation is dispensable for endoplasmic reticulum-associated degradation. *Journal of Biological Chemistry* **286**, 27872–27874 (2011).
115. Vijay-kumar, S., Bugg, C. E. & Cook, W. J. Structure of ubiquitin refined at 1.8 Å resolution. *Journal of Molecular Biology* **194**, 531–544 (1987).
116. Shimizu, Y., Okuda-Shimizu, Y. & Hendershot, L. M. Ubiquitylation of an ERAD substrate occurs on multiple types of amino acids. *Mol Cell* **40**, 917–926 (2010).
117. Ciechanover, A. & Stanhill, A. The complexity of recognition of ubiquitinated substrates by the 26S proteasome. *Biochim Biophys Acta* **1843**, 86–96 (2014).
118. Boutet, S. C., Disatnik, M.-H., Chan, L. S., Iori, K. & Rando, T. A. Regulation of Pax3 by proteasomal degradation of monoubiquitinated protein in skeletal muscle progenitors. *Cell* **130**, 349–62 (2007).
119. Thrower, J. S., Hoffman, L., Rechsteiner, M. & Pickart, C. M. Recognition of the polyubiquitin proteolytic signal. *The EMBO journal* **19**, 94–102 (2000).
120. Chau, V. *et al.* A multiubiquitin chain is confined to specific lysine in a targeted short-lived protein. *Science (New York, N.Y.)* **243**, 1576–83 (1989).
121. Hershko, A. & Ciechanover, A. The ubiquitin system. *Annual Review of Biochemistry* **67**, 425–479 (1998).

122. Hershko, A. & Heller, H. Occurrence of a polyubiquitin structure in ubiquitin-protein conjugates. *Biochemical and Biophysical Research Communications* **128**, 1079–1086 (1985).
123. Phillips, A. H. & Corn, J. E. Using protein motion to read, write, and erase ubiquitin signals. *Journal of Biological Chemistry* **290**, 26437–26444 (2015).
124. Peng, J. *et al.* A proteomics approach to understanding protein ubiquitination. *Nature Biotechnology* **21**, 921–926 (2003).
125. Xu, P. *et al.* Quantitative proteomics reveals the function of unconventional ubiquitin chains in proteasomal degradation. *Cell* **137**, 133–45 (2009).
126. Cunningham, C. N. *et al.* USP30 and parkin homeostatically regulate atypical ubiquitin chains on mitochondria. *Nature cell biology* **17**, 160–9 (2015).
127. Ordureau, A. *et al.* Quantitative proteomics reveal a feedforward mechanism for mitochondrial PARKIN translocation and ubiquitin chain synthesis. *Molecular Cell* **56**, 360–375 (2014).
128. Williamson, A. *et al.* Identification of a physiological E2 module for the human anaphase-promoting complex. *Proceedings of the National Academy of Sciences* **106**, 18213–18218 (2009).
129. Bremm, A., Moniz, S., Mader, J., Rocha, S. & Komander, D. Cezanne (OTUD 7B) regulates HIF -1α homeostasis in a proteasome-independent manner. *EMBO reports* **15**, 1268–1277 (2014).
130. Iwai, K., Fujita, H. & Sasaki, Y. Linear ubiquitin chains: NF-κB signalling, cell death and beyond. *Nature Reviews Molecular Cell Biology* **15**, 503–508 (2014).
131. Hofmann, R. M. & Pickart, C. M. Noncanonical MMS2-encoded ubiquitin-conjugating enzyme functions in assembly of novel polyubiquitin chains for DNA repair. *Cell* **96**, 645–653 (1999).
132. Qiu, J. *et al.* Ubiquitination independent of E1 and E2 enzymes by bacterial effectors. *Nature* **533**, (2016).
133. Johnson, E. S. & Blobel, G. Ubc9p is the conjugating enzyme for the Ubiquitin-like protein Smt3p. *Journal of Biological Chemistry* **272**, 26799–26802 (1997).
134. Liakopoulos, D., Doenges, G., Matuschewski, K. & Jentsch, S. A novel protein modification pathway related to the ubiquitin system. *The EMBO Journal* **17**, 2208–2214 (1998).
135. Williamson, A. *et al.* Regulation of ubiquitin chain initiation to control the timing

of substrate degradation. *Molecular Cell* **42**, 744–757 (2011).

136. Wu, K., Kovacev, J. & Pan, Z. Q. Priming and extending: A UbcH5/Cdc34 E2 handoff mechanism for polyubiquitination on a SCF substrate. *Molecular Cell* **37**, 784–796 (2010).
137. Jin, L., Williamson, A., Banerjee, S., Philipp, I. & Rape, M. Mechanism of ubiquitin-chain formation by the human anaphase-promoting complex. *Cell* **133**, 653–665 (2008).
138. Kirkpatrick, D. S. *et al.* Quantitative analysis of in vitro ubiquitinated cyclin B1 reveals complex chain topology. *Nature Cell Biology* **8**, 700–710 (2006).
139. Weber, A. *et al.* Sequential poly-ubiquitylation by specialized conjugating enzymes expands the versatility of a quality control ubiquitin ligase. *Molecular Cell* **63**, 827–839 (2016).
140. Komander, D. & Rape, M. The ubiquitin code. *Annu Rev Biochem* **81**, 203–229 (2012).
141. Ye, Y. & Rape, M. Building ubiquitin chains: E2 enzymes at work. *Nat Rev Mol Cell Biol* **10**, 755–764 (2009).
142. Scheffner, M., Nuber, U. & Huibregtse, J. M. Protein ubiquitination involving an E1–E2–E3 enzyme ubiquitin thioester cascade. *Nature* **373**, 81–83 (1995).
143. Huang, L. *et al.* Structure of an E6AP-UbcH7 complex: Insights into ubiquitination by the E2-E3 enzyme cascade. *Science* **286**, 1321–1326 (1999).
144. Spratt, D. E., Walden, H. & Shaw, G. S. RBR E3 ubiquitin ligases: new structures, new insights, new questions. *Biochemical Journal* **458**, 421–437 (2014).
145. Smit, J. J., Sixma, T. K., Irp, H. & Ring, I. RBR E3 -ligases at work. *EMBO reports* **15**, 142–155 (2014).
146. Bordallo, J., Plemper, R. K., Finger, A. & Wolf, D. H. Der3p/Hrd1p is required for endoplasmic reticulum-associated degradation of misfolded lumenal and integral membrane proteins. *Molecular biology of the cell* **9**, 209–222 (1998).
147. Hitt, R. & Wolf, D. H. Der1p, a protein required for degradation of malfolded soluble proteins of the endoplasmic reticulum: Topology and Der1-like proteins. *FEMS Yeast Res* **4**, 721–729 (2004).
148. Bordallo, J. & Wolf, D. H. A RING-H2 finger motif is essential for the function of Der3/Hrd1 in endoplasmic reticulum associated protein degradation in the yeast

Saccharomyces cerevisiae. *FEBS Lett* **448**, 244–248 (1999).

149. Bays, N. W., Gardner, R. G., Seelig, L. P., Joazeiro, C. A. & Hampton, R. Y. Hrd1p/Der3p is a membrane-anchored ubiquitin ligase required for ER-associated degradation. *Nat Cell Biol* **3**, 24–29 (2001).
150. Wilhovsky, S., Gardner, R. & Hampton, R. HRD gene dependence of endoplasmic reticulum-associated degradation. *Mol Biol Cell* **11**, 1697–1708 (2000).
151. Biederer, T., Volkwein, C. & Sommer, T. Role of Cue1p in ubiquitination and degradation at the ER surface. *Science* **278**, 1806–1809 (1997).
152. von Delbruck, M. *et al.* The CUE domain of Cue1 aligns growing ubiquitin chains with Ubc7 for rapid elongation. *Mol Cell* **62**, 918–928 (2016).
153. Bagola, K. *et al.* Ubiquitin binding by a CUE domain regulates ubiquitin chain formation by ERAD E3 ligases. *Mol Cell* **50**, 528–539 (2013).
154. Friedlander, R., Jarosch, E., Urban, J., Volkwein, C. & Sommer, T. A regulatory link between ER-associated protein degradation and the unfolded-protein response. *Nat Cell Biol* **2**, 379–384 (2000).
155. Deng, M. & Hochstrasser, M. Spatially regulated ubiquitin ligation by an ER/nuclear membrane ligase. *Nature* **443**, 827–831 (2006).
156. Meinema, A. C., Poolman, B. & Veenhoff, L. M. The transport of integral membrane proteins across the nuclear pore complex. *Nucleus* **3**, 322–329 (2012).
157. Boban, M., Pantazopoulou, M., Schick, A., Ljungdahl, P. O. & Foisner, R. A nuclear ubiquitin-proteasome pathway targets the inner nuclear membrane protein Asi2 for degradation. *Journal of Cell Science* **127**, 3603–3613 (2014).
158. Huyer, G. *et al.* Distinct machinery is required in Saccharomyces cerevisiae for the endoplasmic reticulum-associated degradation of a multispanning membrane protein and a soluble luminal protein. *J Biol Chem* **279**, 38369–38378 (2004).
159. Stolz, A., Besser, S., Hottmann, H. & Wolf, D. H. Previously unknown role for the ubiquitin ligase Ubr1 in endoplasmic reticulum-associated protein degradation. *Proc Natl Acad Sci U S A* **110**, 15271–15276 (2013).
160. Stolz, A., Hilt, W., Buchberger, A. & Wolf, D. H. Cdc48: A power machine in protein degradation. *Trends Biochem Sci* **36**, 515–523 (2011).

161. Ye, Y., Tang, W. K., Zhang, T. & Xia, D. A mighty “protein extractor” of the cell: Structure and function of the p97/CDC48 ATPase. *Frontiers in Molecular Biosciences* **4**, 1–20 (2017).
162. Buchberger, A., Schindelin, H. & Hanzelmann, P. Control of p97 function by cofactor binding. *FEBS Lett* **589**, 2578–2589 (2015).
163. Bodnar, N. & Rapoport, T. Toward an understanding of the Cdc48/p97 ATPase. *F1000Research* **6**, 1318 (2017).
164. Wolf, D. H. & Stolz, A. The Cdc48 machine in endoplasmic reticulum associated protein degradation. *Biochim Biophys Acta* **1823**, 117–124 (2012).
165. Barbin, L., Eisele, F., Santt, O. & Wolf, D. H. The Cdc48-Ufd1-Npl4 complex is central in ubiquitin-proteasome triggered catabolite degradation of fructose-1,6-bisphosphatase. *Biochemical and Biophysical Research Communications* **394**, 335–341 (2010).
166. Braun, R. J. & Zischka, H. Mechanisms of Cdc48/VCP-mediated cell death - from yeast apoptosis to human disease. *Biochimica et Biophysica Acta - Molecular Cell Research* **1783**, 1418–1435 (2008).
167. Meyer, H. & Popp, O. Role(s) of Cdc48/p97 in mitosis. *Biochemical Society Transactions* **36**, 126–130 (2008).
168. Deichsel, A., Mouysset, J. & Hoppe, T. The ubiquitin-selective chaperone CDC-48/p97, a new player in DNA replication. *Cell cycle (Georgetown, Tex.)* **8**, 185–90 (2009).
169. Wilcox, A. J. & Laney, J. D. A ubiquitin-selective AAA-ATPase mediates transcriptional switching by remodelling a repressor-promoter DNA complex. *Nature Cell Biology* **11**, 1481–1486 (2009).
170. Verma, R., Oania, R., Fang, R., Smith, G. T. & Deshaies, R. J. Cdc48/p97 mediates UV-dependent turnover of RNA Pol II. *Molecular Cell* **41**, 82–92 (2011).
171. Neuber, O., Jarosch, E., Volkwein, C., Walter, J. & Sommer, T. Ubx2 links the Cdc48 complex to ER-associated protein degradation. *Nat Cell Biol* **7**, 993–998 (2005).
172. Schuberth, C. & Buchberger, A. Membrane-bound Ubx2 recruits Cdc48 to ubiquitin ligases and their substrates to ensure efficient ER-associated protein degradation. *Nat Cell Biol* **7**, 999–1006 (2005).
173. DeLaBarre, B. & Brunger, A. T. Nucleotide dependent motion and mechanism

of action of p97/VCP. *Journal of molecular biology* **347**, 437–52 (2005).

174. Schuller, J. M., Beck, F., Lössl, P., Heck, A. J. R. & Förster, F. Nucleotide-dependent conformational changes of the AAA+ ATPase p97 revisited. *FEBS Letters* **590**, 595–604 (2016).
175. Blythe, E. E., Olson, K. C., Chau, V. & Deshaies, R. J. Ubiquitin- and ATP-dependent unfoldase activity of P97/VCP•NPLOC4•UFD1L is enhanced by a mutation that causes multisystem proteinopathy. *Proceedings of the National Academy of Sciences of the United States of America* **114**, E4380–E4388 (2017).
176. Bodnar, N. O. & Rapoport, T. A. Molecular mechanism of substrate processing by the Cdc48 ATPase complex. *Cell* **169**, 722-735 e9 (2017).
177. Bebeacua, C. *et al.* Distinct conformations of the protein complex p97-Ufd1-Npl4 revealed by electron cryomicroscopy. *Proceedings of the National Academy of Sciences of the United States of America* **109**, 1098–103 (2012).
178. Bruderer, R. M., Brasseur, C. & Meyer, H. H. The AAA ATPase p97/VCP interacts with its alternative co-factors, Ufd1-Npl4 and p47, through a common bipartite binding mechanism. *Journal of Biological Chemistry* **279**, 49609–49616 (2004).
179. Hänzelmann, P. & Schindelin, H. Characterization of an additional binding surface on the p97 N-terminal domain involved in bipartite cofactor interactions. *Structure (London, England : 1993)* **24**, 140–147 (2016).
180. Banerjee, S. *et al.* 2.3 Å resolution cryo-EM structure of human p97 and mechanism of allosteric inhibition. *Science (New York, N.Y.)* **351**, 871–5 (2016).
181. Tang, W. K. *et al.* A novel ATP-dependent conformation in p97 N–D1 fragment revealed by crystal structures of disease-related mutants. *The EMBO Journal* **29**, 2217–2229 (2010).
182. Bodnar, N. O. *et al.* Structure of the Cdc48 ATPase with its ubiquitin-binding cofactor Ufd1–Npl4. *Nature Structural and Molecular Biology* **25**, 616–622 (2018).
183. Kim, S. J. *et al.* Structural basis for ovarian tumor domain-containing protein 1 (OTU1) binding to p97/valosin-containing protein (VCP). *The Journal of biological chemistry* **289**, 12264–74 (2014).
184. Burton, R. E. Effects of protein stability and structure on substrate processing by

the ClpXP unfolding and degradation machine. *The EMBO Journal* **20**, 3092–3100 (2001).

185. Liu, C.-W., Corboy, M. J., DeMartino, G. N. & Thomas, P. J. Endoproteolytic activity of the proteasome. *Science (New York, N.Y.)* **299**, 408 (2003).
186. Lee, C., Prakash, S. & Matouschek, A. Concurrent translocation of multiple polypeptide chains through the proteasomal degradation channel. *Journal of Biological Chemistry* **277**, 34760–34765 (2002).
187. Alberts, S. M., Sonntag, C., Schafer, A. & Wolf, D. H. Ubx4 modulates cdc48 activity and influences degradation of misfolded proteins of the endoplasmic reticulum. *J Biol Chem* **284**, 16082–16089 (2009).
188. Tran, J. R., Tomsic, L. R. & Brodsky, J. L. A Cdc48p-associated factor modulates endoplasmic reticulum-associated degradation, cell stress, and ubiquitinated protein homeostasis. *The Journal of biological chemistry* **286**, 5744–55 (2011).
189. Raasi, S. & Wolf, D. H. Ubiquitin receptors and ERAD: A network of pathways to the proteasome. *Semin Cell Dev Biol* **18**, 780–791 (2007).
190. Bays, N. W., Wilhovsky, S. K., Goradia, A., Hodgkiss-Harlow, K. & Hampton, R. Y. HRD4/NPL4 is required for the proteasomal processing of ubiquitinated ER proteins. *Mol Biol Cell* **12**, 4114–4128 (2001).
191. Jarosch, E. *et al.* Protein dislocation from the ER requires polyubiquitination and the AAA-ATPase Cdc48. *Nat Cell Biol* **4**, 134–139 (2002).
192. Rabinovich, E., Kerem, A., Frohlich, K. U., Diamant, N. & Bar-Nun, S. AAA-ATPase p97/Cdc48p, a cytosolic chaperone required for endoplasmic reticulum-associated protein degradation. *Mol Cell Biol* **22**, 626–634 (2002).
193. Richly, H. *et al.* A series of ubiquitin binding factors connects CDC48/p97 to substrate multiubiquitylation and proteasomal targeting. *Cell* **120**, 73–84 (2005).
194. Kohlmann, S., Schafer, A. & Wolf, D. H. Ubiquitin ligase Hul5 is required for fragment-specific substrate degradation in endoplasmic reticulum-associated degradation. *J Biol Chem* **283**, 16374–16383 (2008).
195. Neal, S. E., Mak, R., Bennett, E. J. & Hampton, R. A “retrochaperone” function for Cdc48: The Cdc48 complex is required for retrotranslocated ERAD-M substrate solubility. *Journal of Biological Chemistry* **292**, 3112–3128 (2017).
196. Taxis, C. *et al.* Use of modular substrates demonstrates mechanistic diversity and reveals differences in chaperone requirement of ERAD. *Journal of Biological*

Chemistry **278**, 35903–35913 (2003).

197. Medicherla, B., Kostova, Z., Schaefer, A. & Wolf, D. H. A genomic screen identifies Dsk2p and Rad23p as essential components of ER-associated degradation. *EMBO Rep* **5**, 692–697 (2004).
198. Wolf, D. H. & Hilt, W. The proteasome: a proteolytic nanomachine of cell regulation and waste disposal. *Biochim Biophys Acta* **1695**, 19–31 (2004).
199. Tomko Jr., R. J. & Hochstrasser, M. Molecular architecture and assembly of the eukaryotic proteasome. *Annu Rev Biochem* **82**, 415–445 (2013).
200. Kish-Trier, E. & Hill, C. P. Structural biology of the proteasome. *Annu Rev Biophys* **42**, 29–49 (2013).
201. Finley, D., Chen, X. & Walters, K. J. Gates, channels, and switches: Elements of the proteasome machine. *Trends in Biochemical Sciences* **41**, 77–93 (2016).
202. Bard, J. A. M. *et al.* Structure and function of the 26S proteasome. *Annual review of biochemistry* **87**, 697–724 (2018).
203. Glickman, M. H. *et al.* A subcomplex of the proteasome regulatory particle required for ubiquitin-conjugate degradation and related to the COP9-signalosome and eIF3. *Cell* **94**, 615–623 (1998).
204. Saeki, Y. & Tanaka, K. Assembly and function of the proteasome. in *Methods in molecular biology (Clifton, N.J.)* (eds. Dohmen, J. R. & Scheffner, M.) **832**, 315–337 (2012).
205. van Nocker, S. *et al.* The multiubiquitin-chain-binding protein Mcb1 is a component of the 26S proteasome in Saccharomyces cerevisiae and plays a nonessential, substrate-specific role in protein turnover. *Molecular and Cellular Biology* **16**, 6020–6028 (1996).
206. Deveraux, Q., Ustrell, V., Pickart, C. & Rechsteiner, M. A 26 S protease subunit that binds ubiquitin conjugates. *The Journal of biological chemistry* **269**, 7059–61 (1994).
207. Shi, Y. *et al.* Rpn1 provides adjacent receptor sites for substrate binding and deubiquitination by the proteasome. *Science* **351**, (2016).
208. He, J. *et al.* The structure of the 26S proteasome subunit Rpn2 reveals its PC repeat domain as a closed toroid of two concentric α-helical rings. *Structure* **20**, 513–521 (2012).
209. Husnjak, K. *et al.* Proteasome subunit Rpn13 is a novel ubiquitin receptor.

Nature **453**, 481–488 (2008).

210. Chen, X. *et al.* Structures of Rpn1 T1:Rad23 and hRpn13:hPLIC2 reveal distinct binding mechanisms between substrate receptors and shuttle factors of the proteasome. *Structure* **24**, 1257–1270 (2016).
211. Martin, A., Baker, T. A. & Sauer, R. T. Pore loops of the AAA+ ClpX machine grip substrates to drive translocation and unfolding. *Nature Structural and Molecular Biology* **15**, 1147–1151 (2008).
212. Maillard, R. A. *et al.* ClpX(P) generates mechanical force to unfold and translocate its protein substrates. *Cell* **145**, 459–469 (2011).
213. Aubin-Tam, M. E., Olivares, A. O., Sauer, R. T., Baker, T. A. & Lang, M. J. Single-molecule protein unfolding and translocation by an ATP-fueled proteolytic machine. *Cell* **145**, 257–267 (2011).
214. Beckwith, R., Estrin, E., Worden, E. J. & Martin, A. Reconstitution of the 26S proteasome reveals functional asymmetries in its AAA+ unfoldase. *Nature Structural & Molecular Biology* **20**, 1164–1172 (2013).
215. Erales, J., Hoyt, M. A., Troll, F. & Coffino, P. Functional asymmetries of proteasome translocase pore. *Journal of Biological Chemistry* **287**, 18535–18543 (2012).
216. de Poot, S. A. H., Tian, G. & Finley, D. Meddling with fate: The proteasomal deubiquitinating enzymes. *Journal of Molecular Biology* **429**, 3525–3545 (2017).
217. Verma, R. *et al.* Role of Rpn11 metalloprotease in deubiquitination and degradation by the 26S proteasome. *Science* **298**, 611–615 (2002).
218. Yao, T. & Cohen, R. E. A cryptic protease couples deubiquitination and degradation by the proteasome. Nature 419, 403–407. Molecular. *Nature* **419**, 406–407 (2002).
219. Groll, M. *et al.* Structure of 20S proteasome from yeast at 2.4 Å resolution. *Nature* **386**, 463–471 (1997).
220. Chen, P. & Hochstrasser, M. Autocatalytic subunit processing couples active site formation in the 20S proteasome to completion of assembly. *Cell* **86**, 961–972 (1996).
221. Arendt, C. S. & Hochstrasser, M. Identification of the yeast 20S proteasome catalytic centers and subunit interactions required for active-site formation. *Proceedings of the National Academy of Sciences of the United States of*

America **94**, 7156–7161 (1997).

222. Fort, P., Kajava, A. V., Delsuc, F. & Coux, O. Evolution of proteasome regulators in Eukaryotes. *Genome Biology and Evolution* **7**, 1363–1379 (2015).
223. Finger, A., Knop, M. & Wolf, D. H. Analysis of two mutated vacuolar proteins reveals a degradation pathway in the endoplasmic reticulum or a related compartment of yeast. *Eur J Biochem* **218**, 565–574 (1993).
224. Benitez, E. M., Stolz, A. & Wolf, D. H. Yos9, a control protein for misfolded glycosylated and non-glycosylated proteins in ERAD. *FEBS Lett* **585**, 3015–3019 (2011).
225. Jaenicke, L. A., Brendebach, H., Selbach, M. & Hirsch, C. Yos9p assists in the degradation of certain nonglycosylated proteins from the endoplasmic reticulum. *Mol Biol Cell* **22**, 2937–2945 (2011).
226. Goder, V. & Melero, A. Protein O-mannosyltransferases participate in ER protein quality control. *J Cell Sci* **124**, 144–153 (2011).
227. Vashistha, N., Neal, S. E., Singh, A., Carroll, S. M. & Hampton, R. Y. Direct and essential function for Hrd3 in ER-associated degradation. *Proc Natl Acad Sci U S A* **113**, 5934–5939 (2016).
228. Fu, L. & Sztul, E. Traffic-independent function of the Sar1p/COPII machinery in proteasomal sorting of the cystic fibrosis transmembrane conductance regulator. *Journal of Cell Biology* **160**, 157–163 (2003).
229. Nakatsukasa, K., Huyer, G., Michaelis, S. & Brodsky, J. L. Dissecting the ER-associated degradation of a misfolded polytopic membrane protein. *Cell* **132**, 101–112 (2008).
230. Vashist, S. *et al.* Distinct retrieval and retention mechanisms are required for the quality control of endoplasmic reticulum protein folding. *The Journal of cell biology* **155**, 355–368 (2001).
231. Schafer, A. & Wolf, D. H. Yeast genomics in the elucidation of endoplasmic reticulum (ER) quality control and associated protein degradation (ERQD). *Methods Enzymol* **399**, 459–468 (2005).
232. Besser, S. Die Endoplasmatisches Retikulum assoziierte Degradation (ERAD) eines fehlgefalteten Membran verankerten Proteins mit variierender zytoplasmatischer Domäne und die Erkennung eines neuen ERAD-Weges. (Universität Stuttgart, 2011).

233. Hanahan, D. *Techniques for transformation of E. coli*. **1.**, (1985).
234. Wilcox, C. A., Redding, K., Wright, R. & Fuller, R. S. Mutation of a tyrosine localization signal in the cytosolic tail of yeast Kex2 protease disrupts Golgi retention and results in default transport to the vacuole. *Molecular Biology of the Cell* **3**, 1353–1371 (1992).
235. Plemper, R. K., Deak, P. M., Otto, R. T. & Wolf, D. H. Re-entering the translocon from the lumenal side of the endoplasmic reticulum. Studies on mutated carboxypeptidase yscY species. *FEBS Lett* **443**, 241–245 (1999).
236. Sikorski, R. S. & Hieter, P. A system of shuttle vectors and yeast host strains designed for efficient manipulation of DNA in Saccharomyces cerevisiae. *Genetics Society of America* **122**, 19–27 (1989).
237. Gueldener, U., Heinisch, J., Koehler, G. J., Voss, D. & Hegemann, J. H. A second set of loxP marker cassettes for Cre-mediated multiple gene knockouts in budding yeast. *Nucleic Acids Research* **30**, 23e (2002).
238. Norell, D. Untersuchungen zum Mechanismus der Proteinqualitätskontrolle im zellulären Zytoplasma. (Universität Stuttgart, 2011).
239. Mandlmeir, D. Bedeutung der Transmembrandomäne eines fehlgefalteten Carboxypeptidase Y- Fusionsproteins im ER-assoziierten Proteindegradationsprozess (ERAD). (Universität Stuttgart, 2017).
240. Inoue, H., Nojima, H. & Okayma, H. High efficiency transformation of Escherichia coli with plasmids. *Gene* **96**, 23–28 (1990).
241. Sambrook, J. & Russell, D. W. The Inoue method for preparation and transformation of competent E.coli: “ultra-competent” cells. in *Molecular Cloning: a laboratory manual* 1.112-1.115 (Cold Spring Harbor Laboratory Press, 2001).
242. Guldener, U., Heck, S., Fielder, T., Beinhauer, J. & Hegemann, J. H. A new efficient gene disruption cassette for repeated use in budding yeast. *Nucleic Acids Research* **24**, 2519–2524 (1996).
243. Laemmli, U. K. Cleavage of structural proteins during the assembly of the head of bacteriophage T4. *Nature* **227**, 680–685 (1970).
244. Schägger, H. Tricine-SDS-PAGE. *Nature Protocols* **1**, 16–23 (2006).
245. Woolford, C. A. *et al.* The PEP4 gene encodes an aspartyl protease implicated in the posttranslational regulation of Saccharomyces cerevisiae vacuolar hydrolases. *Molecular and Cellular Biology* **6**, 2500–2510 (1986).

246. Geng, F. & Tansey, W. P. Polyubiquitylation of histone H2B. *Molecular Biology of the Cell* **19**, 3616–3624 (2008).
247. Satyanarayana, T., Umbarger, H. E. & Lindegren, G. Biosynthesis of branched-chain amino acids in yeast: correlation of biochemical blocks and genetic lesions in leucine auxotrophs. *Journal of Bacteriology* **96**, 2012–2017 (1968).
248. Kohlmann, S. Die HECT-Ligase Hul5, eine neue Komponente der ER-assoziierten Proteindegradatoin. (Universität Stuttgart, 2007).
249. Tsien, R. Y. The green fluorescent protein. *Annual review of biochemistry* **67**, 509–44 (1998).
250. Fisher, A. C. & DeLisa, M. P. Laboratory evolution of fast-folding green fluorescent protein using secretory pathway quality control. *PLoS ONE* **3**, 1–7 (2008).
251. Greenblatt, E. J., Olzmann, J. A. & Kopito, R. R. Derlin-1 is a rhomboid pseudoprotease required for the dislocation of mutant alpha-1 antitrypsin from the endoplasmic reticulum. *Nat Struct Mol Biol* **18**, 1147–1152 (2011).
252. Spear, E. D. & Ng, D. T. W. Stress tolerance of misfolded carboxypeptidase Y requires maintenance of protein trafficking and degradative pathways. *Molecular biology of the cell* **14**, 2617–3063 (2003).
253. Lodder, A. L., Lee, T. K. & Ballester, R. Characterization of the Wsc1 protein, a putative receptor in the stress response of Saccharomyces cerevisiae. *Genetics* **152**, 1487–1499 (1999).
254. Hershko, A., Heller, H., Elias, S. & Ciechanover, A. Components of ubiquitin-protein ligase system. *The Journal of Biological Chemistry* **258**, 8206–8214 (1983).
255. McDowell, G. S. & Philpott, A. *New insights into the role of ubiquitylation of proteins*. *International Review of Cell and Molecular Biology* **325**, (Elsevier Inc., 2016).
256. Reid, B. G. & Flynn, G. C. Chromophore formation in green fluorescent protein. *Biochemistry* **36**, 6786–6791 (1997).
257. Hirsch, C., Gauss, R., Horn, S. C., Neuber, O. & Sommer, T. The ubiquitylation machinery of the endoplasmic reticulum. *Nature* **458**, 453–460 (2009).
258. Cohen, I., Wiener, R., Reiss, Y. & Ravid, T. Distinct activation of an E2 ubiquitin-conjugating enzyme by its cognate E3 ligases. *Proceedings of the National*

Academy of Sciences of the United States of America **112**, E625–E632 (2015).

259. Stoll, K. E., Brzovic, P. S., Davis, T. N. & Klevit, R. E. The Essential Ubc4/Ubc5 Function in Yeast Is HECT E3-dependent, and RING E3-dependent Pathways Require Only Monoubiquitin Transfer by Ubc4. *Journal of Biological Chemistry* **286**, 15165–15170 (2011).
260. Wiebel, F. F. & Kunau, W. H. The Pas2 protein essential for peroxisome biogenesis is related to ubiquitin-conjugating enzymes. *Nature* **359**, 73–6 (1992).
261. Kragt, A., Voorn-Brouwer, T., van den Berg, M. & Distel, B. The Saccharomyces cerevisiae peroxisomal import receptor Pex5p is monoubiquitinated in wild type cells. *Journal of Biological Chemistry* **280**, 7867–7874 (2005).
262. Scheffer, J., Hasenjäger, S. & Taxis, C. Degradation of integral membrane proteins modified with the photosensitive degron module requires the cytosolic endoplasmic reticulum-associated degradation pathway. *Molecular Biology of the Cell* **30**, 2558–2570 (2019).
263. Neal, S., Duttke, S. H. & Hampton, R. Y. *Assays for protein retrotranslocation in ERAD*. *Methods in Enzymology* **619**, (Elsevier Inc., 2019).
264. Cymer, F. & Schneider, D. Oligomerization of polytopic α-helical membrane proteins: causes and consequences. *Biological Chemistry* **393**, 1215–1230 (2012).
265. Houck, S. A. & Cyr, D. M. Mechanisms for quality control of misfolded transmembrane proteins. *Biochimica et Biophysica Acta (BBA) - Biomembranes* **1818**, 1108–1114 (2012).
266. Ng, D. P., Poulsen, B. E. & Deber, C. M. Membrane protein misassembly in disease. *Biochimica et biophysica acta* **1818**, 1115–22 (2012).
267. Hara, T. *et al.* Rer1 and calnexin regulate endoplasmic reticulum retention of a peripheral myelin protein 22 mutant that causes type 1A Charcot-Marie-Tooth disease. *Scientific Reports* **4**, 6992 (2015).
268. Li, Q. *et al.* Transmembrane segments prevent surface expression of sodium channel Nav1.8 and promote calnexin-dependent channel degradation. *Journal of Biological Chemistry* **285**, 32977–32987 (2010).
269. Swanton, E., High, S. & Woodman, P. Role of calnexin in the glycan-independent quality control of proteolipid protein. *The EMBO journal* **22**, 2948–58 (2003).
270. Totani, K., Ihara, Y., Tsujimoto, T., Matsuo, I. & Ito, Y. The recognition motif of

the glycoprotein-folding sensor enzyme UDP-Glc:glycoprotein glucosyltransferase. *Biochemistry* **48**, 2933–40 (2009).

271. Fleig, L. *et al.* Ubiquitin-dependent intramembrane rhomboid protease promotes ERAD of membrane proteins. *Molecular cell* **47**, 558–69 (2012).
272. Merulla, J., Soldà, T. & Molinari, M. A novel UGGT1 and p97-dependent checkpoint for native ectodomains with ionizable intramembrane residue. *Molecular biology of the cell* **26**, 1532–42 (2015).
273. Kaether, C. *et al.* Endoplasmic reticulum retention of the gamma-secretase complex component Pen2 by Rer1. *EMBO reports* **8**, 743–8 (2007).
274. Valkova, C. *et al.* Sorting receptor Rer1 controls surface expression of muscle acetylcholine receptors by ER retention of unassembled alpha-subunits. *Proceedings of the National Academy of Sciences of the United States of America* **108**, 621–5 (2011).
275. Sato, K., Sato, M. & Nakano, A. Rer1p, a retrieval receptor for ER membrane proteins, recognizes transmembrane domains in multiple modes. *Molecular biology of the cell* **14**, 3605–16 (2003).
276. Chu, C. Y. *et al.* Degradation mechanism of a Golgi-retained distal renal tubular acidosis mutant of the kidney anion exchanger 1 in renal cells. *American journal of physiology. Cell physiology* **307**, C296-307 (2014).
277. Roxrud, I., Raiborg, C., Gilfillan, G. D., Strømme, P. & Stenmark, H. Dual degradation mechanisms ensure disposal of NHE6 mutant protein associated with neurological disease. *Experimental cell research* **315**, 3014–27 (2009).
278. Briant, K., Johnson, N. & Swanton, E. Transmembrane domain quality control systems operate at the endoplasmic reticulum and Golgi apparatus. *PloS one* **12**, e0173924 (2017).
279. Spasic, D. *et al.* Rer1p competes with APH-1 for binding to nicastrin and regulates gamma-secretase complex assembly in the early secretory pathway. *The Journal of cell biology* **176**, 629–40 (2007).
280. Shao, S. & Hegde, R. S. Membrane Protein Insertion at the Endoplasmic Reticulum. *Annual Review of Cell and Developmental Biology* **27**, 25–56 (2011).
281. Reggiori, F. & Pelham, H. R. B. A transmembrane ubiquitin ligase required to sort membrane proteins into multivesicular bodies. *Nature cell biology* **4**, 117–23 (2002).

282. Valdez-Taubas, J. & Pelham, H. Swf1-dependent palmitoylation of the SNARE Tlg1 prevents its ubiquitination and degradation. *The EMBO journal* **24**, 2524–32 (2005).
283. Hettema, E. H., Valdez-Taubas, J. & Pelham, H. R. B. Bsd2 binds the ubiquitin ligase Rsp5 and mediates the ubiquitination of transmembrane proteins. *The EMBO Journal* **23**, 1279–1288 (2004).
284. Travers, K. J. *et al.* Functional and genomic analyses reveal an essential coordination between the unfolded protein response and ER-associated degradation. *Cell* **101**, 249–258 (2000).
285. Hetz, C. & Papa, F. R. The unfolded protein response and cell fate control. *Molecular Cell* **69**, 169–181 (2018).
286. Zattas, D., Adle, D. J., Rubenstein, E. M. & Hochstrasser, M. N-terminal acetylation of the yeast Derlin Der1 is essential for Hrd1 ubiquitin-ligase activity toward luminal ER substrates. *Molecular biology of the cell* **24**, 890–900 (2013).
287. Rodrigo-Brenni, M. C. & Morgan, D. O. Sequential E2s drive polyubiquitin chain assembly on APC targets. *Cell* **130**, 127–139 (2007).
288. Eisele, F. ERAD of membrane attached misfolded CPY (CPY*): Importance of the cytosolic tail. (Universität Stuttgart, 2005).
289. Colbeau, A., Nachbaur, J. & Vignais, P. M. Enzymac characterization and lipid composition of rat liver subcellular membranes. *BBA - Biomembranes* **249**, 462–492 (1971).
290. Geelen, M. J. H. The use of digitonin-permeabilized mammalian cells for measuring enzyme activities in the course of studies on lipid metabolism. *Analytical Biochemistry* **347**, 1–9 (2005).
291. Thines-Sempoux D., Amar-Costesec A., Beaufay H., B. J. The association of cholesterol, 5'-nucleotidase, and alkaline phosphodiesterase I with a distinct group of microsomal particles. *J Cell Biol* **43**, 189–192 (1969).
292. Briant, K., Koay, Y. H., Otsuka, Y. & Swanton, E. ERAD of proteins containing aberrant transmembrane domains requires ubiquitylation of cytoplasmic lysine residues. *Journal of Cell Science* **128**, 4112–4125 (2015).
293. Bonifacino, J. S., Suzuki, C. K. & Klausner, R. D. A peptide sequence confers retention and rapid degradation in the endoplasmic reticulum. *Science* **247**, 79–82 (1990).

294. Bonifacino, J. S., Cosson, P., Shah, N. & Klausner, R. D. Role of potentially charged transmembrane residues in targeting proteins for retention and degradation within the endoplasmic reticulum. *The EMBO Journal* **10**, 2783–2793 (1991).
295. Ishikura, S., Weissman, A. M. & Bonifacino, J. S. Serine residues in the cytosolic tail of the T-cell antigen receptor alpha-chain mediate ubiquitination and endoplasmic reticulum-associated degradation of the unassembled protein. *Journal of Biological Chemistry* **285**, 23916–23924 (2010).
296. Cauvi, D. M., Tian, X., Von Loehneysen, K. & Robertson, M. W. Transport of the IgE receptor α-chain is controlled by a multicomponent intracellular retention signal. *Journal of Biological Chemistry* **281**, 10448–10460 (2006).
297. Fayadat, L. & Kopito, R. R. Recognition of a single transmembrane degron by sequential quality control checkpoints. *Molecular Biology of the Cell* **14**, 1268–1278 (2003).
298. Williams, G. T., Venkitaraman, A. R., Gilmore, D. J. & Neuberger, M. S. The sequence of the μ transmembrane segment determines the tissue specificity of the transport of immunoglobulin M to the cell surface. *Journal of Experimental Medicine* **171**, 947–952 (1990).
299. Feige, M. J. & Hendershot, L. M. Quality control of integral membrane proteins by assembly-dependent membrane integration. *Molecular Cell* **51**, 297–309 (2013).
300. Shin, J., Lee, S. & Strominger, J. L. Translocation of TCRα chains into the lumen of the endoplasmic reticulum and their degradation. *Science* **259**, 1901–1904 (1993).

SUPPLEMENTAL INFORMATION

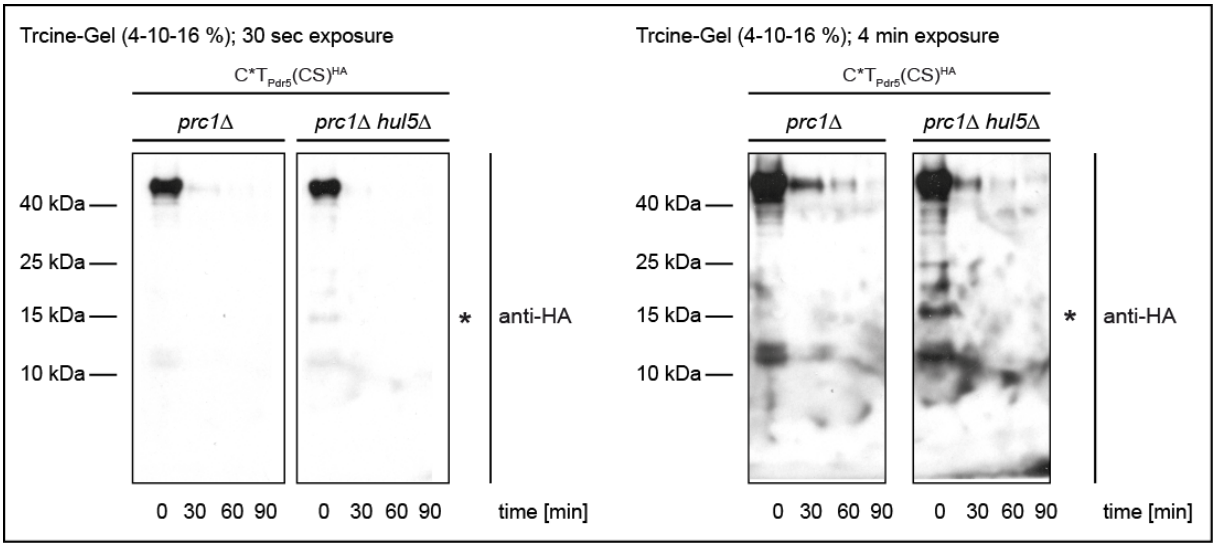

Figure S1: Distinct intermediates occur during the degradation of C*T$_{Pdr5}$(CS)^{HA}.

Cycloheximide-chase analysis of C*T$_{Pdr5}$(CS)^{HA} degradation was performed in *prc1*Δ and *prc1*Δ*hul5*Δ cells.

Samples were taken every 30 min after cycloheximide addition. Proteins were separated in gel electrophoresis using a 4-10-16% Tricin-gel. C*T$_{Pdr5}$(CS)^{HA} was detected by immunoblotting using CPY antibody and HA antibody. Dfm1 was used as loading control. For comparison exposure of 30 sec (left side) and 4 minutes (right side) were shown.

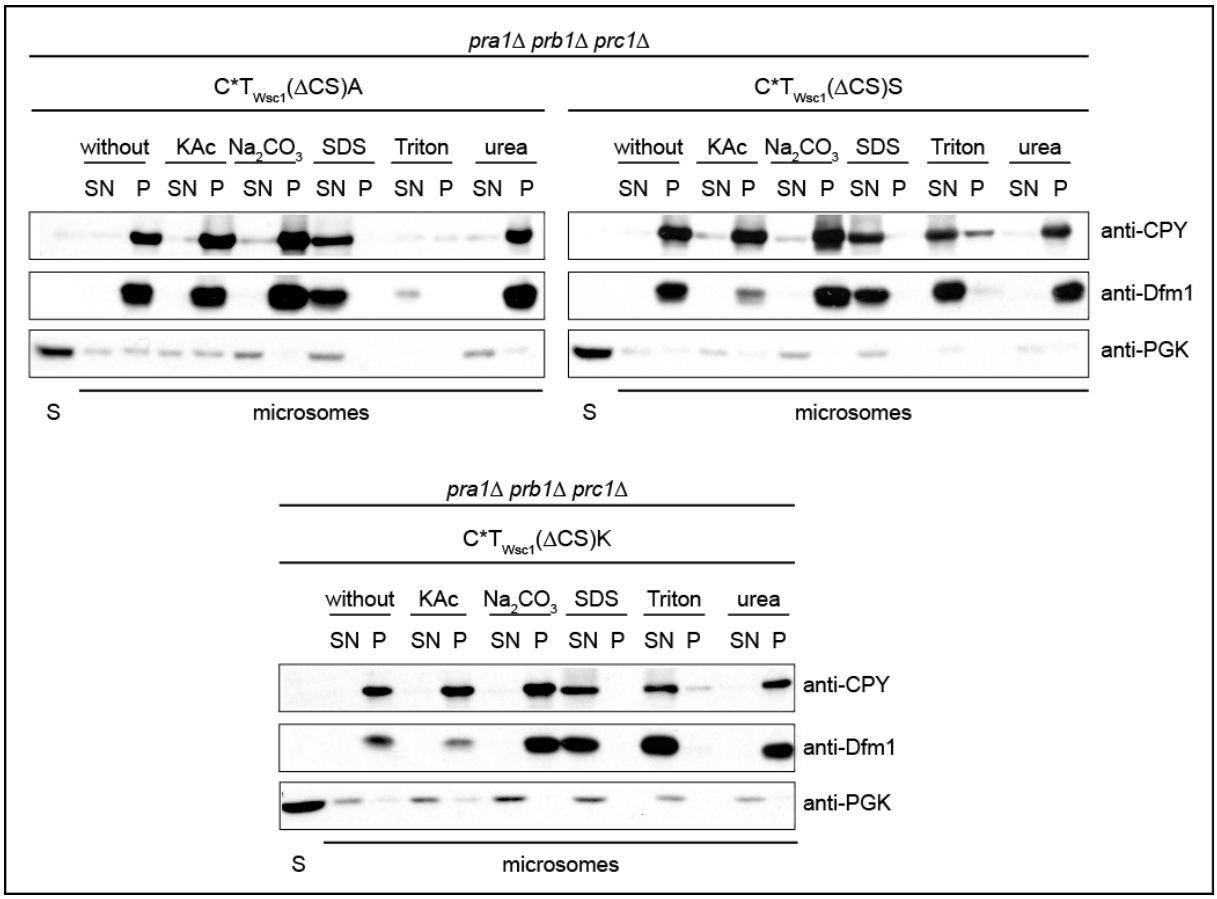

Figure S2: C*T$_{Wsc1}$(ΔCS)A, C*T$_{Wsc1}$(ΔCS)S and C*T$_{Wsc1}$(ΔCS)K are integral membrane proteins.

Microsomes and supernatant 1 (S) were separated from lysate of *pra1Δprb1Δprc1Δ* cells expressing C*T$_{Wsc1}$(ΔCS) derivatives (as indicated). Microsomes were treated only with buffer (without) or buffer containing either 1 M potassium acetate (KAc) or 0.1 M sodium carbonate (Na_2CO_3) or 1% (w/v) SDS (SDS) or 1% (v/v) Triton X-100 (Triton) or 2.5 M urea (urea), followed by centrifugation. Receiving supernatant 2 (SN) and pellet (P), which were analyzed by immunoblotting. C*T$_{Wsc1}$ derivatives were detected using CPY antibody. The integral ER membrane protein Dfm1 was visualized using Dfm1 antibody. As control for separating supernatant 1 (S) and microsomes, the soluble cytosolic protein PGK was detected using PGK antibody.

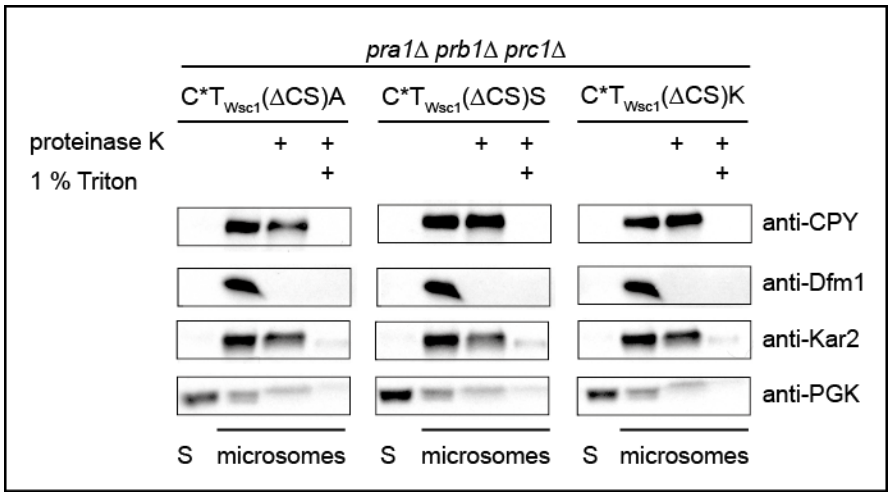

Figure S3: C*T$_{Wsc1}$(ΔCS)A, C*T$_{Wsc1}$(ΔCS)S and C*T$_{Wsc1}$(ΔCS)K are membrane proteins with the N-terminal CPY* domain in the ER lumen and a C-terminal tail (CS) in the cytosol.

Microsomes and supernatant (S) were separated from lysate of *pra1Δprb1Δprc1Δ* cells, expressing C*T$_{Wsc1}$(ΔCS) derivatives (as indicated). Microsomes were treated only with buffer or buffer containing either proteinase K (0.5 mg/ml) or proteinase K (0.5 mg/ml) and 1% (v/v) Triton X-100. Digestion was stopped by adding 110 mM PMSF. C*T$_{Wsc1}$ derivatives were analyzed by immunoblotting, using CPY antibody. The ER membrane protein Dfm1 was visualized using Dfm1 antibody. Kar2, as a control for ER lumenal soluble proteins, was analyzed using Kar2 antibody. As a control for separating supernatant 1 (S) and microsomes, the soluble cytosolic protein PGK was detected using PGK antibody.

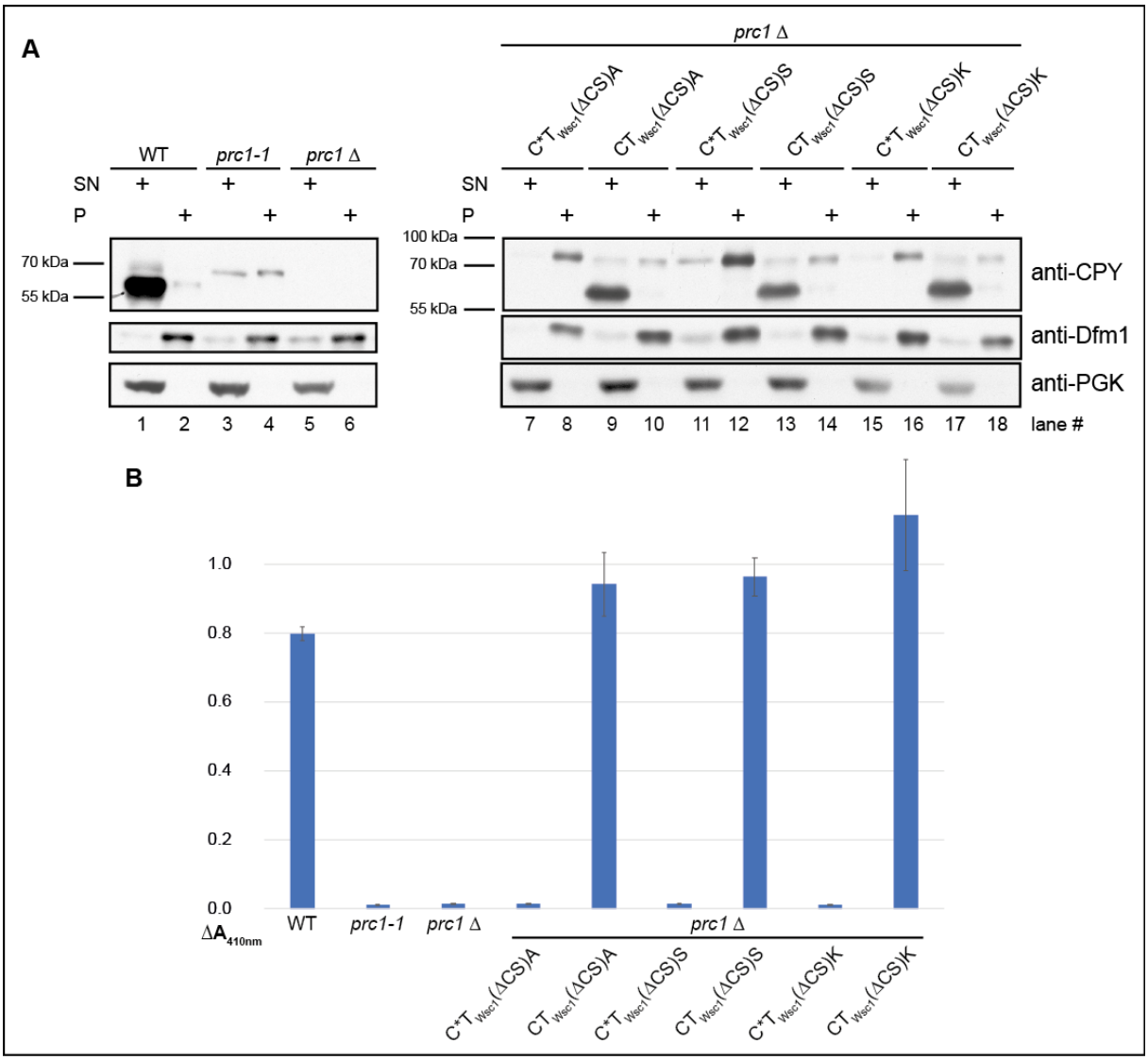

Figure S4: ER lumenal CPY* moiety of C*T$_{Wsc1}$(ΔCS)A, C*T$_{Wsc1}$(ΔCS)S and C*T$_{Wsc1}$(ΔCS)K is required for retention in the ER

A: Localization of the carboxypeptidase Y (CPY) and its derivatives (WT, endogenous CPY; *prc1-1*, endogenous CPY*; *prc1*Δ, lacking endogenous CPY) was determined in cells expressing the indicated variants. Pellet (P) and supernatant (SN) were separated from lysate and analyze by immunoblotting. CPY variants were detected using CPY antibody. The integral ER membrane protein Dfm1 was visualized using Dfm1 antibody. As control for separating pellet and supernatant, the soluble cytosolic protein PGK was detected using PGK antibody.
B: Cells were incubated for 12 h with BTpNA and absorbance was measured at 410 nm (ΔA_{410nm}). The quantification represents the data of five independent experiments. Error bars indicate the respective standard error of the mean (SEM). *P < 0.05, unpaired two-sample *t*-test relative to the control (WT).

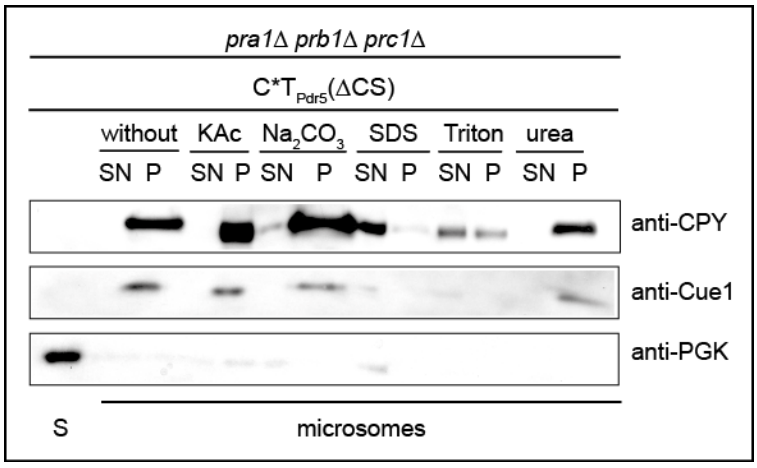

Figure S5: C*T$_{Pdr5}$(ΔCS) is an integral membrane protein.

Microsomes and supernatant 1 (S) were separated from lysate of *pra1Δprb1Δprc1Δ* cells expressing C*T$_{Pdr5}$(ΔCS). Microsomes were treated only with buffer (without) or buffer containing either 1 M potassium acetate (KAc) or 0.1 M sodium carbonate (Na_2CO_3) or 1% (w/v) SDS (SDS) or 1% (v/v) Triton X-100 (Triton) or 2.5 M urea (urea), followed by centrifugation. Receiving supernatant 2 (SN) and pellet (P), which were analyzed by immunoblotting. C*T$_{Pdr5}$(ΔCS) was detected using CPY antibody. The integral ER membrane protein Cue1 was visualized using Cue1 antibody. As control for separating supernatant 1 (S) and microsomes, the soluble cytosolic protein PGK was detected using PGK antibody.

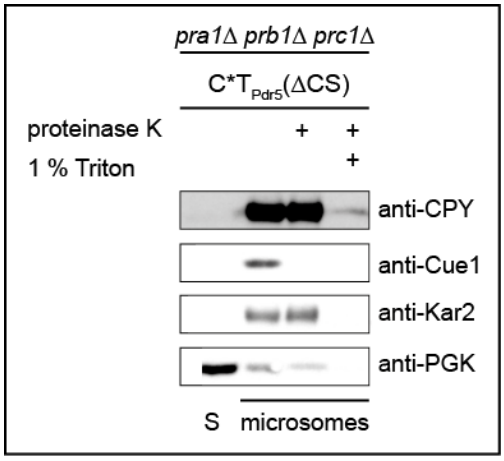

Figure S6: C*T$_{Pdr5}$(ΔCS) is a membrane protein with the N-terminal CPY* domain in the ER lumen and a C-terminal tail (CS) in the cytosol.

Microsomes and supernatant (S) were separated from lysate of *pra1Δprb1Δprc1Δ* cells expressing C*T$_{Pdr5}$(ΔCS). Microsomes were treated only with buffer or buffer containing either proteinase K (0.5 mg/ml) or proteinase K (0.5 mg/ml) and 1% (v/v) Triton X-100. Digestion was stopped by adding 110 mM PMSF. C*T$_{Pdr5}$(ΔCS) is analyzed by immunoblotting using CPY antibody. The ER membrane protein Cue1 was visualized using Cue1 antibody. Kar2, as a control for ER lumenal soluble proteins, was analyzed using Kar2 antibody. As a control for separating supernatant (S) and microsomes, the soluble cytosolic protein PGK was detected using PGK antibody.

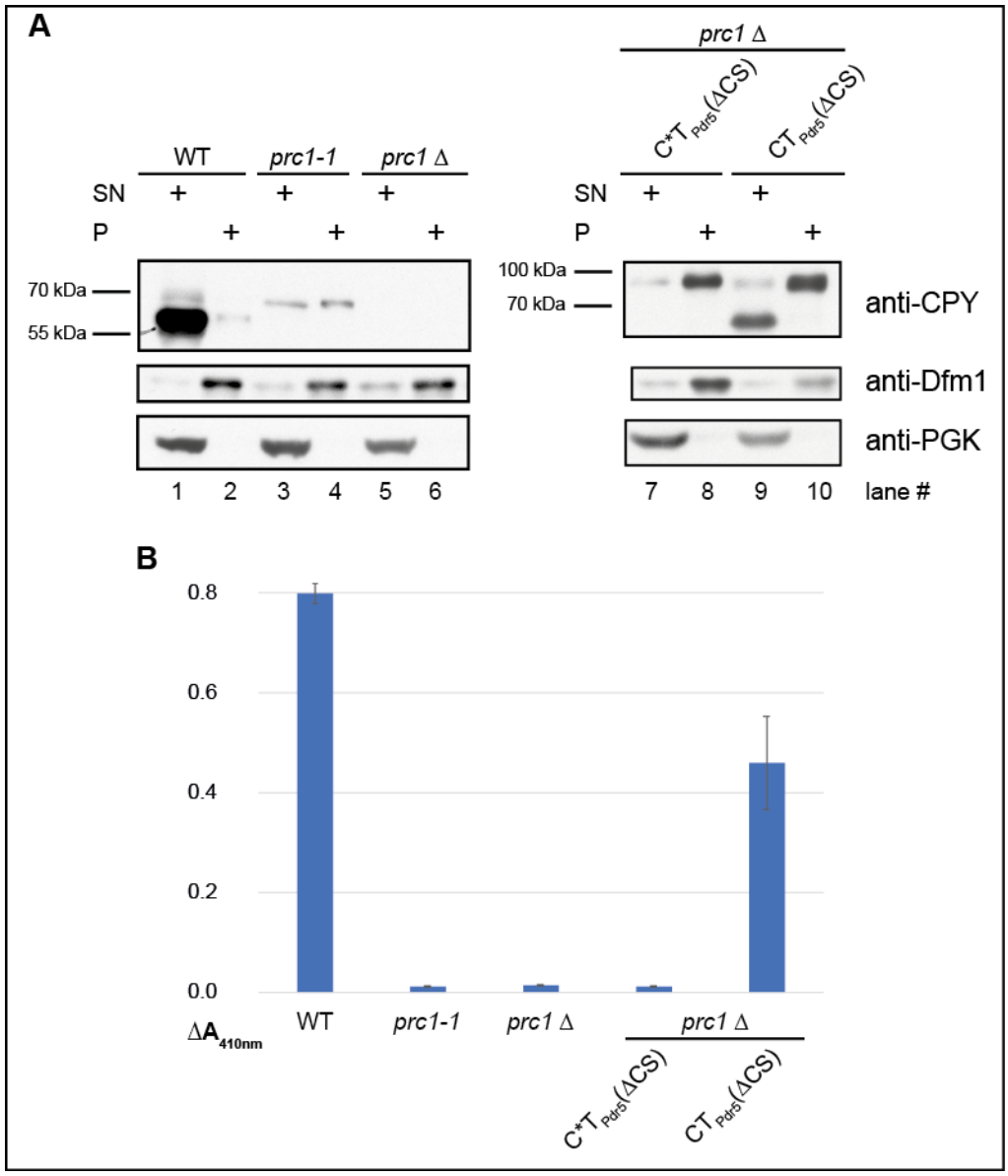

Figure S7: ER lumenal CPY* moiety of C*T$_{Pdr5}$(ΔCS) is required for retention in the ER

A: Localization of the carboxypeptidase Y (CPY) and its derivatives (WT, endogenous CPY; *prc1-1*, endogenous CPY*; *prc1*Δ, lacking endogenous CPY) was determined in cells expressing the indicated variants. Pellet (P) and supernatant (SN) were separated from lysate and analyze by immunoblotting. CPY variants were detected using CPY antibody. The integral ER membrane protein Dfm1 was visualized using Dfm1 antibody. As control for separating pellet and supernatant, the soluble cytosolic protein PGK was detected using PGK antibody.
B: Cells were incubated for 12 h with BTpNA and absorbance was measured at 410 nm (ΔA_{410nm}). The quantification represents the data of five independent experiments. Error bars indicate the respective standard error of the mean (SEM). *P < 0.05, unpaired two-sample *t*-test relative to the control (WT).

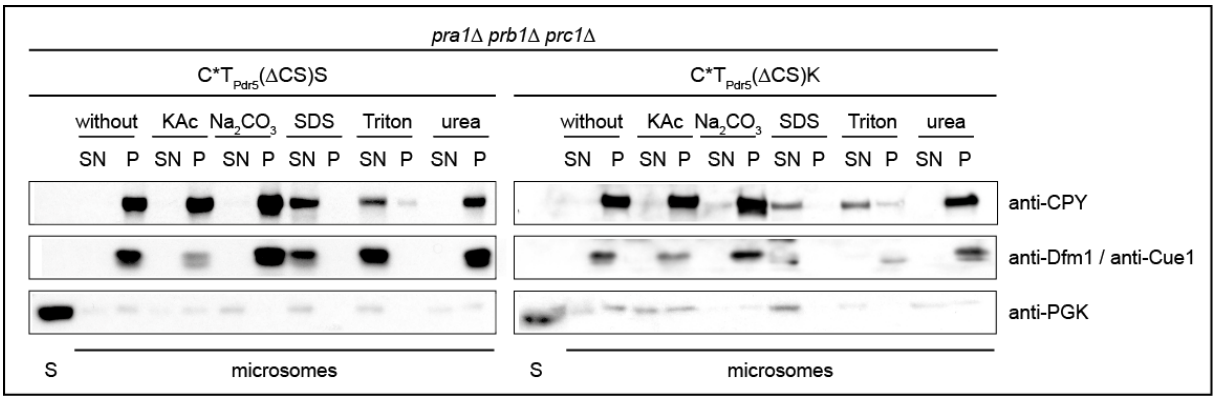

Figure S8: C*T$_{Pdr5}$(ΔCS)S and C*T$_{Pdr5}$(ΔCS)K are integral membrane proteins.

Microsomes and supernatant 1 (S) were separated from lysate of *pra1Δprb1Δprc1Δ* cells expressing C*T$_{Pdr5}$(ΔCS) derivatives (as indicated). Microsomes were treated only with buffer (without) or buffer containing either 1 M potassium acetate (KAc) or 0.1 M sodium carbonate (Na_2CO_3) or 1% (w/v) SDS (SDS) or 1% (v/v) Triton X-100 (Triton) or 2.5 M urea (urea), followed by centrifugation. Receiving supernatant 2 (SN) and pellet (P), which were analyzed by immunoblotting. C*T$_{Pdr5}$(ΔCS) derivatives were detected using CPY antibody. The integral ER membrane proteins Dfm1 and Cue1 were visualized using Dfm1 or Cue1 antibody. As control for separating supernatant 1 (S) and microsomes, the soluble cytosolic protein PGK was detected using PGK antibody.

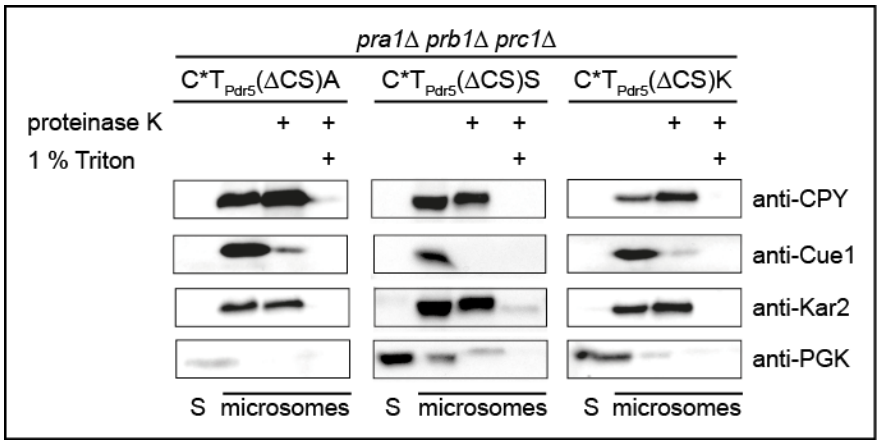

Figure S9: C*T$_{Pdr5}$(ΔCS)A, C*T$_{Pdr5}$(ΔCS)S and C*T$_{Pdr5}$(ΔCS)K are membrane proteins with the N-terminal CPY* domain in the ER lumen and a C-terminal tail (CS) in the cytosol.

Microsomes and supernatant (S) were separated from lysate of *pra1Δprb1Δprc1Δ* cells expressing C*T$_{Pdr5}$(ΔCS) derivatives (as indicated). Microsomes were treated only with buffer or buffer containing either proteinase K (0.5 mg/ml) or proteinase K (0.5 mg/ml) and 1% (v/v) Triton X-100. Digestion was stopped by adding 110 mM PMSF. C*T$_{Pdr5}$ derivatives were analyzed by immunoblotting using CPY antibody. The ER membrane protein Cue1 was visualized using Cue1 antibody. Kar2, as a control for ER lumenal soluble proteins, was analyzed using Kar2 antibody. As a control for separating supernatant (S) and microsomes, the soluble cytosolic protein PGK was detected using PGK antibody.

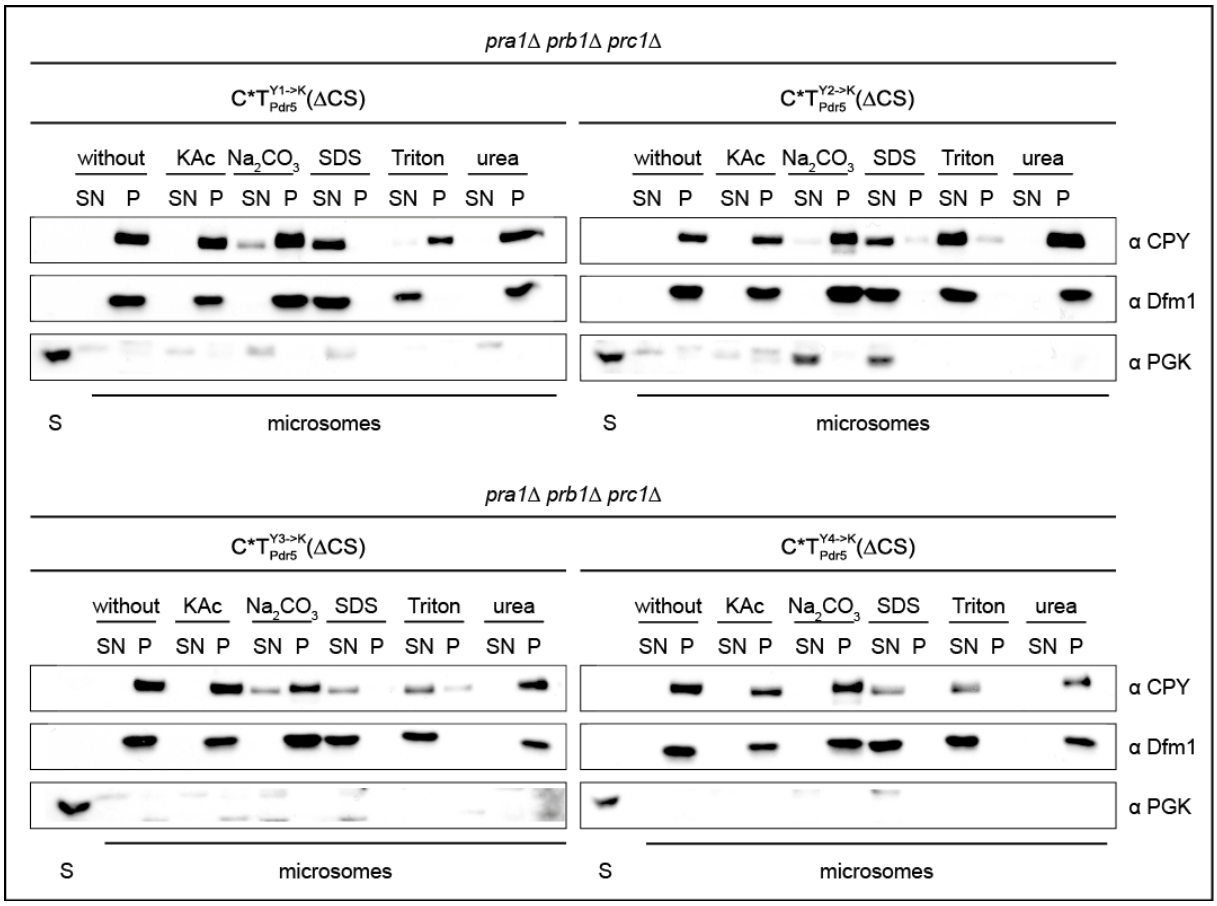

Figure S10: $C^{*}T_{Pdr5}^{Y1\rightarrow K}$ (ΔCS); $C^{*}T_{Pdr5}^{Y2\rightarrow K}$ (ΔCS); $C^{*}T_{Pdr5}^{Y3\rightarrow K}$ (ΔCS) and $C^{*}T_{Pdr5}^{Y4\rightarrow K}$ (ΔCS) are integral membrane proteins.

Microsomes and supernatant 1 (S) were separated from lysate of *pra1Δprb1Δprc1Δ* cells expressing $C^{*}T_{Pdr5}$(ΔCS) derivatives (as indicated). Microsomes were treated only with buffer (without) or buffer containing either 1 M potassium acetate (KAc) or 0.1 M sodium carbonate (Na_2CO_3) or 1% (w/v) SDS (SDS) or 1% (v/v) Triton X-100 (Triton) or 2.5 M urea (urea), followed by centrifugation. Receiving supernatant 2 (SN) and pellet (P), which were analyzed by immunoblotting. $C^{*}T_{Pdr5}$(ΔCS) derivatives were detected using CPY antibody. The integral ER membrane protein Dfm1 was visualized using Dfm1 antibody. As control for separating supernatant 1 (S) and microsomes, the soluble cytosolic protein PGK was detected using PGK antibody.

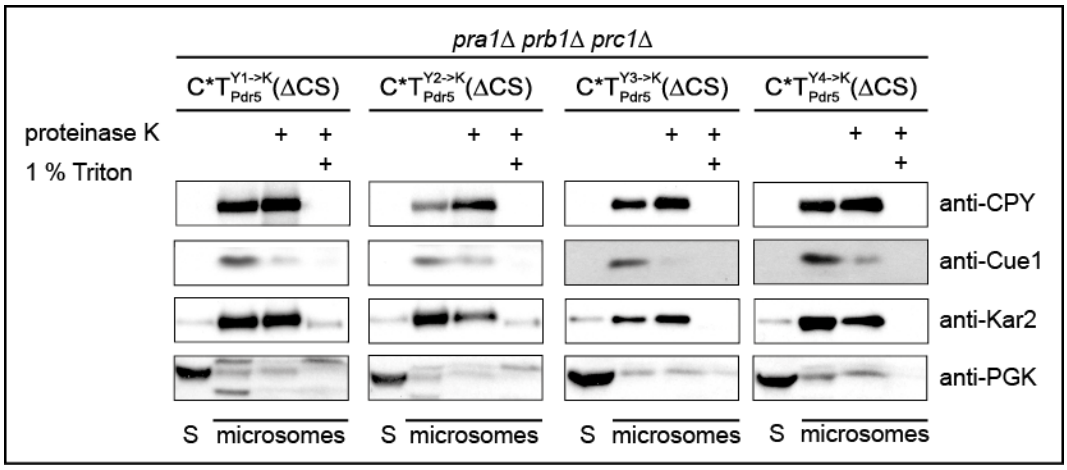

Figure S11: $C^{*}T^{Y1\rightarrow K}_{Pdr5}$ (ΔCS); $C^{*}T^{Y2\rightarrow K}_{Pdr5}$ (ΔCS); $C^{*}T^{Y3\rightarrow K}_{Pdr5}$ (ΔCS) and $C^{*}T^{Y4\rightarrow K}_{Pdr5}$ (ΔCS) are membrane proteins with the N-terminal CPY* domain in the ER lumen and a C-terminal tail (CS) in the cytosol.

Microsomes and supernatant (S) were separated from lysate of *pra1Δprb1Δprc1Δ* cells expressing $C^{*}T_{Pdr5}$(ΔCS) derivatives (as indicated). Microsomes were treated only with buffer or buffer containing either proteinase K (0.5 mg/ml) or proteinase K (0.5 mg/ml) and 1% (v/v) Triton X-100. Digestion was stopped by adding 110 mM PMSF. $C^{*}T_{Pdr5}$(ΔCS) derivatives were analyzed by immunoblotting using CPY antibody. The ER membrane protein Cue1 was visualized using Cue1 antibody. Kar2, as a control for ER lumenal soluble proteins, was analyzed using Kar2 antibody. As a control for separating supernatant (S) and microsomes, the soluble cytosolic protein PGK was detected using PGK antibody.

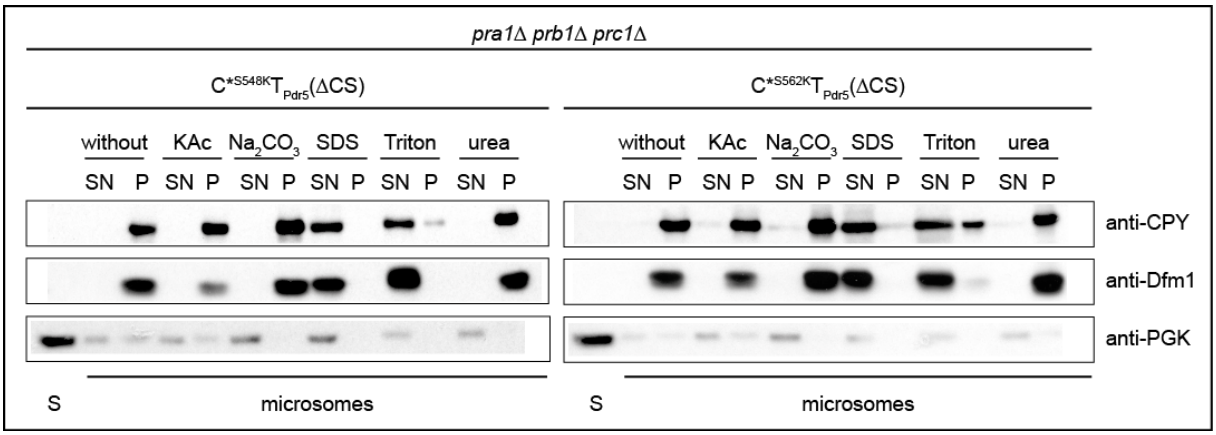

Figure S12: $C^{*S548K}T_{Pdr5}$(ΔCS) and $C^{*S562K}T_{Pdr5}$(ΔCS) are integral membrane proteins.

Microsomes and supernatant 1 (S) were separated from lysate of *pra1Δprb1Δprc1Δ* cells expressing $C^{*}T_{Pdr5}$(ΔCS) derivatives (as indicated). Microsomes were treated only with buffer (without) or buffer containing either 1 M potassium acetate (KAc) or 0.1 M sodium carbonate (Na_2CO_3) or 1% (w/v) SDS (SDS) or 1% (v/v) Triton X-100 (Triton) or 2.5 M urea (urea), followed by centrifugation. Receiving supernatant 2 (SN) and pellet (P), which were analyzed by immunoblotting. $C^{*}T_{Pdr5}$(ΔCS) derivatives were detected using CPY antibody. The integral ER membrane protein Dfm1 was visualized using Dfm1 antibody. As control for separating supernatant 1 (S) and microsomes, the soluble cytosolic protein PGK was detected using PGK antibody.

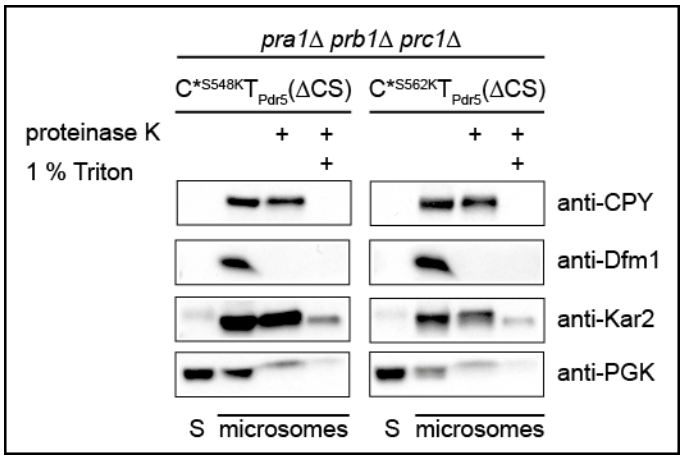

Figure S13: C*S548KTPdr5(ΔCS) and C*S562KTPdr5(ΔCS) are membrane proteins with the N-terminal CPY* domain in the ER lumen and a C-terminal tail (CS) in the cytosol.

Microsomes and supernatant (S) were separated from lysate of *pra1Δprb1Δprc1Δ* cells expressing C*TPdr5(ΔCS) derivatives (as indicated). Microsomes were treated only with buffer or buffer containing either proteinase K (0.5 mg/ml) or proteinase K (0.5 mg/ml) and 1% (v/v) Triton X-100. Digestion was stopped by adding 110 mM PMSF. C*TPdr5(ΔCS) derivatives were analyzed by immunoblotting using CPY antibody. The ER membrane protein Dfm1 was visualized using Dfm1 antibody. Kar2, as a control for ER lumenal soluble proteins, was analyzed using Kar2 antibody. As a control for separating supernatant (S) and microsomes, the soluble cytosolic protein PGK was detected using PGK antibody.

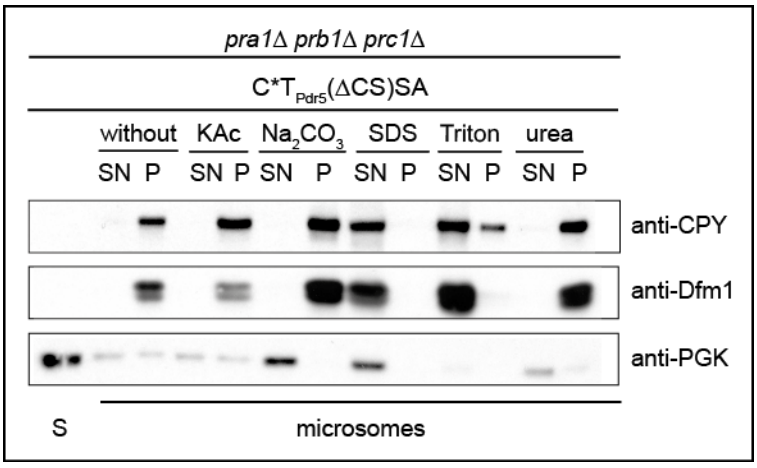

Figure S14: C*TPdr5(ΔCS)SA is an integral membrane protein.

Microsomes and supernatant 1 (S) were separated from lysate of *pra1Δprb1Δprc1Δ* cells expressing C*TPdr5(ΔCS)SA. Microsomes were treated only with buffer (without) or buffer containing either 1 M potassium acetate (KAc) or 0.1 M sodium carbonate (Na_2CO_3) or 1% (w/v) SDS (SDS) or 1% (v/v) Triton X-100 (Triton) or 2.5 M urea (urea), followed by centrifugation. Receiving supernatant 2 (SN) and pellet (P), which were analyzed by immunoblotting. C* TPdr5(ΔCS)SA was detected using CPY antibody. The integral ER membrane protein Dfm1 was visualized using Dfm1 antibody. As control for separating supernatant 1 (S) and microsomes, the soluble cytosolic protein PGK was detected using PGK antibody.

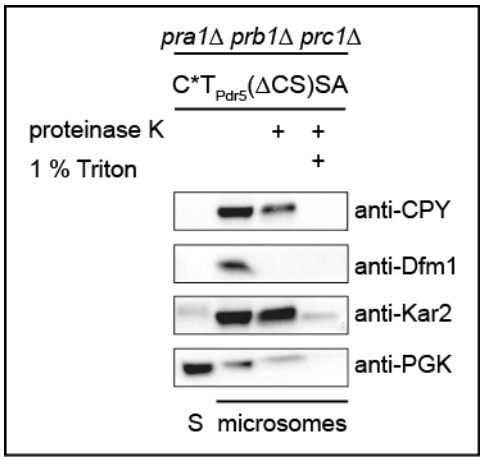

Figure S15: C*T$_{Pdr5}$(ΔCS)SA is a membrane protein with the N-terminal CPY* domain in the ER lumen and a C-terminal tail (CS) in the cytosol.

Microsomes and supernatant (S) were separated from lysate of *pra1Δprb1Δprc1Δ* cells expressing C*T$_{Pdr5}$(ΔCS)SA. Microsomes were treated only with buffer or buffer containing either proteinase K (0.5 mg/ml) or proteinase K (0.5 mg/ml) and 1% (v/v) Triton X-100. Digestion was stopped by adding 110 mM PMSF. C*T$_{Pdr5}$(ΔCS)SA was analyzed by immunoblotting using CPY antibody. The ER membrane protein Dfm1 was visualized using Dfm1 antibody. Kar2, as a control for ER lumenal soluble proteins, was analyzed using Kar2 antibody. As a control for separating supernatant (S) and microsomes, the soluble cytosolic protein PGK was detected using PGK antibody.

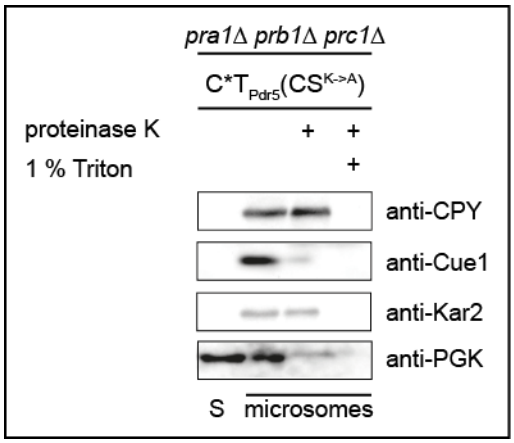

Figure S16: C*T$_{Pdr5}$(CS$^{K->A}$) is a membrane protein with the N-terminal CPY* domain in the ER lumen and a C-terminal tail (CS) in the cytosol.

Microsomes and supernatant (S) were separated from lysate of *pra1Δprb1Δprc1Δ* cells expressing C*T$_{Pdr5}$(CS$^{K->A}$). Microsomes were treated only with buffer or buffer containing either proteinase K (0.5 mg/ml) or proteinase K (0.5 mg/ml) and 1% (v/v) Triton X-100. Digestion was stopped by adding 110 mM PMSF. C*T$_{Pdr5}$(CS$^{K->A}$) was analyzed by immunoblotting using CPY antibody. The ER membrane protein Cue1 was visualized using Cue1 antibody. Kar2, as a control for ER lumenal soluble proteins, was analyzed using Kar2 antibody. As a control for separating supernatant (S) and microsomes, the soluble cytosolic protein PGK was detected using PGK antibody.

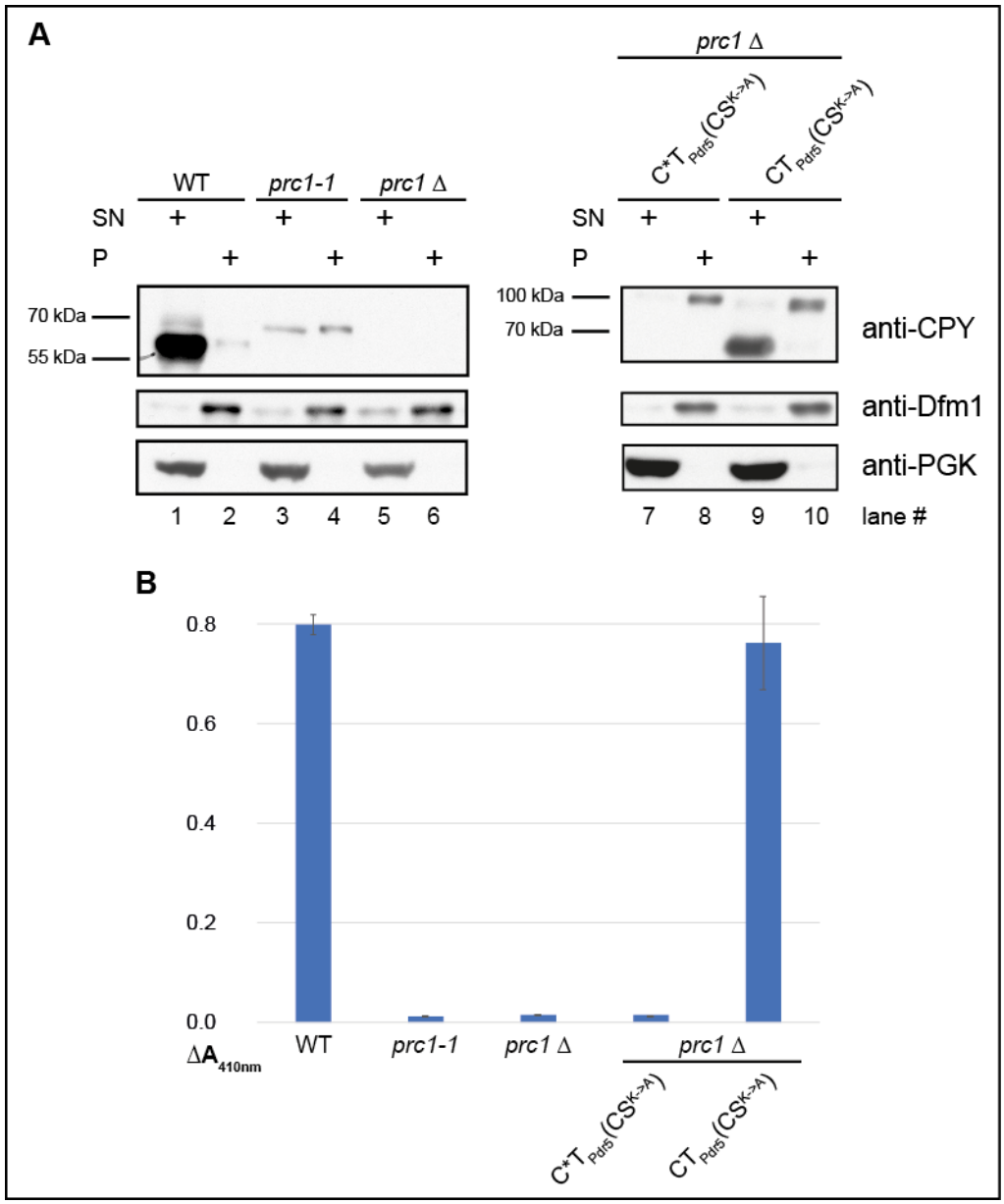

Figure S17: ER lumenal CPY* moiety of C*T$_{Pdr5}$(CS$^{K->A}$) is required for retention in the ER

A: Localization of the carboxypeptidase Y (CPY) and its derivatives (WT, endogenous CPY; *prc1-1*, endogenous CPY*; *prc1*Δ, lacking endogenous CPY) was determined in cells expressing the indicated variants. Pellet (P) and supernatant (SN) were separated from lysate and analyze by immunoblotting. CPY variants were detected using CPY antibody. The integral ER membrane protein Dfm1 was visualized using Dfm1 antibody. As control for separating pellet and supernatant, the soluble cytosolic protein PGK was detected using PGK antibody.
B: Cells were incubated for 12 h with BTpNA and absorbance was measured at 410 nm (ΔA_{410nm}). The quantification represents the data of five independent experiments. Error bars indicate the respective standard error of the mean (SEM). *P < 0.05, unpaired two-sample *t*-test relative to the control (WT).

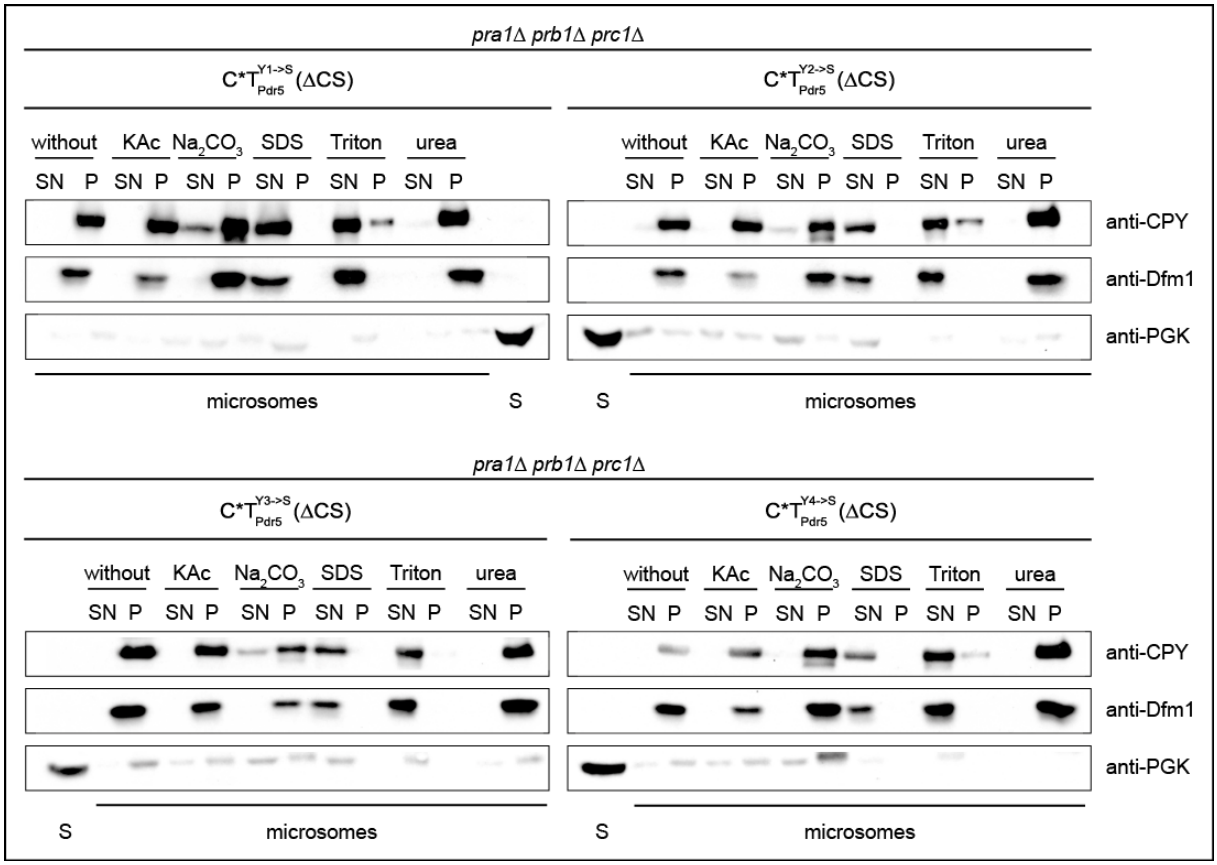

Figure S18: $C^{*}T^{Y1\rightarrow S}_{Pdr5}$ (ΔCS); $C^{*}T^{Y2\rightarrow S}_{Pdr5}$ (ΔCS); $C^{*}T^{Y3\rightarrow S}_{Pdr5}$ (ΔCS) and $C^{*}T^{Y4\rightarrow S}_{Pdr5}$ (ΔCS) are integral membrane proteins.

Microsomes and supernatant 1 (S) were separated from lysate of *pra1Δprb1Δprc1Δ* cells expressing $C^{*}T_{Pdr5}$(ΔCS) derivatives (as indicated). Microsomes were treated only with buffer (without) or buffer containing either 1 M potassium acetate (KAc) or 0.1 M sodium carbonate (Na_2CO_3) or 1% (w/v) SDS (SDS) or 1% (v/v) Triton X-100 (Triton) or 2.5 M urea (urea), followed by centrifugation. Receiving supernatant 2 (SN) and pellet (P), which were analyzed by immunoblotting. $C^{*}T_{Pdr5}$(ΔCS) derivatives were detected using CPY antibody. The integral ER membrane protein Dfm1 was visualized using Dfm1 antibody. As control for separating supernatant 1 (S) and microsomes, the soluble cytosolic protein PGK was detected using PGK antibody

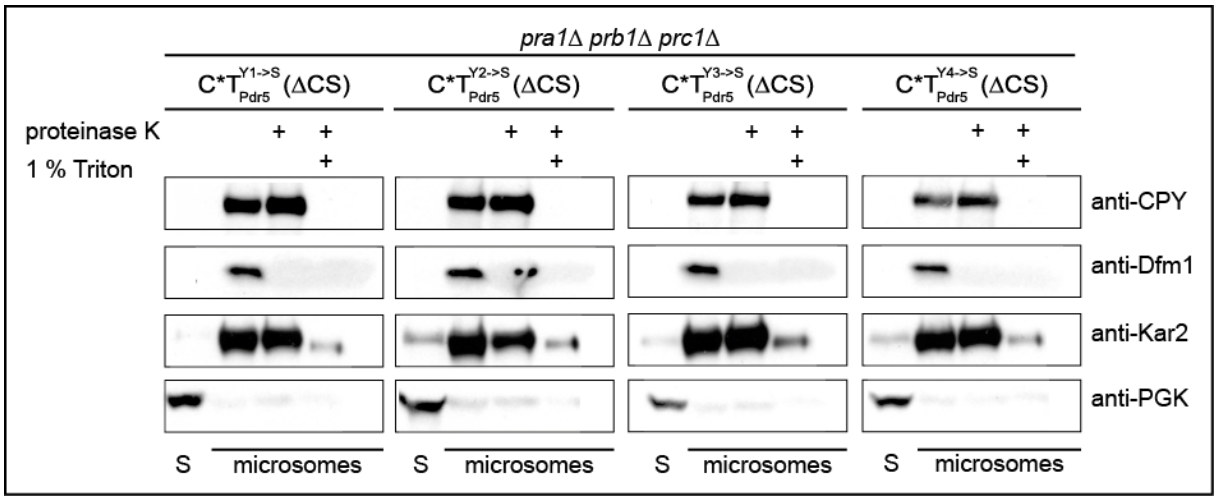

Figure S19: $C^{*}T_{Pdr5}^{Y1\rightarrow S}$ (ΔCS); $C^{*}T_{Pdr5}^{Y2\rightarrow S}$ (ΔCS); $C^{*}T_{Pdr5}^{Y3\rightarrow S}$ (ΔCS) and $C^{*}T_{Pdr5}^{Y4\rightarrow S}$ (ΔCS) are membrane proteins with the N-terminal CPY* domain in the ER lumen and a C-terminal tail (CS) in the cytosol.

Microsomes and supernatant (S) were separated from lysate of *pra1Δprb1Δprc1Δ* cells expressing $C^{*}T_{Pdr5}$(ΔCS) derivatives (as indicated). Microsomes were treated only with buffer or buffer containing either proteinase K (0.5 mg/ml) or proteinase K (0.5 mg/ml) and 1% (v/v) Triton X-100. Digestion was stopped by adding 110 mM PMSF. $C^{*}T_{Pdr5}$(ΔCS) derivatives were analyzed by immunoblotting using CPY antibody. The ER membrane protein Dfm1 was visualized using Dfm1 antibody. Kar2, as a control for ER lumenal soluble proteins, was analyzed using Kar2 antibody. As a control for separating supernatant (S) and microsomes, the soluble cytosolic protein PGK was detected using PGK antibody.

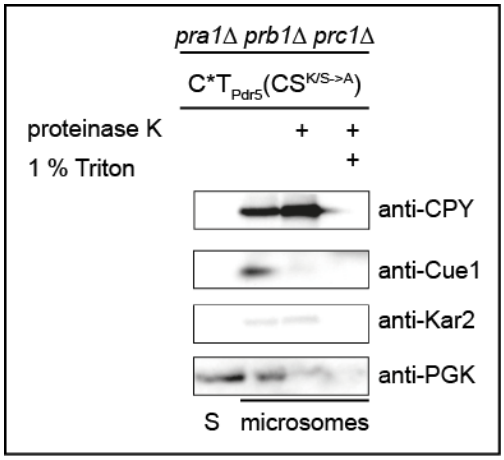

Figure S20: $C^{*}T_{Pdr5}(CS^{K/S\rightarrow A})$ is a membrane protein with the N-terminal CPY* domain in the ER lumen and a C-terminal tail (CS) in the cytosol.

Microsomes and supernatant (S) were separated from lysate of *pra1Δprb1Δprc1Δ* cells expressing $C^{*}T_{Pdr5}(CS^{K/S\rightarrow A})$. Microsomes were treated only with buffer or buffer containing either proteinase K (0.5 mg/ml) or proteinase K (0.5 mg/ml) and 1% (v/v) Triton X-100. Digestion was stopped by adding 110 mM PMSF. $C^{*}T_{Pdr5}(CS^{K/S\rightarrow A})$ was analyzed by immunoblotting using CPY antibody. The ER membrane protein Cue1 was visualized using Cue1 antibody. Kar2, as a control for ER lumenal soluble proteins, was analyzed using Kar2 antibody. As a control for separating supernatant (S) and microsomes, the soluble cytosolic protein PGK was detected using PGK antibody.

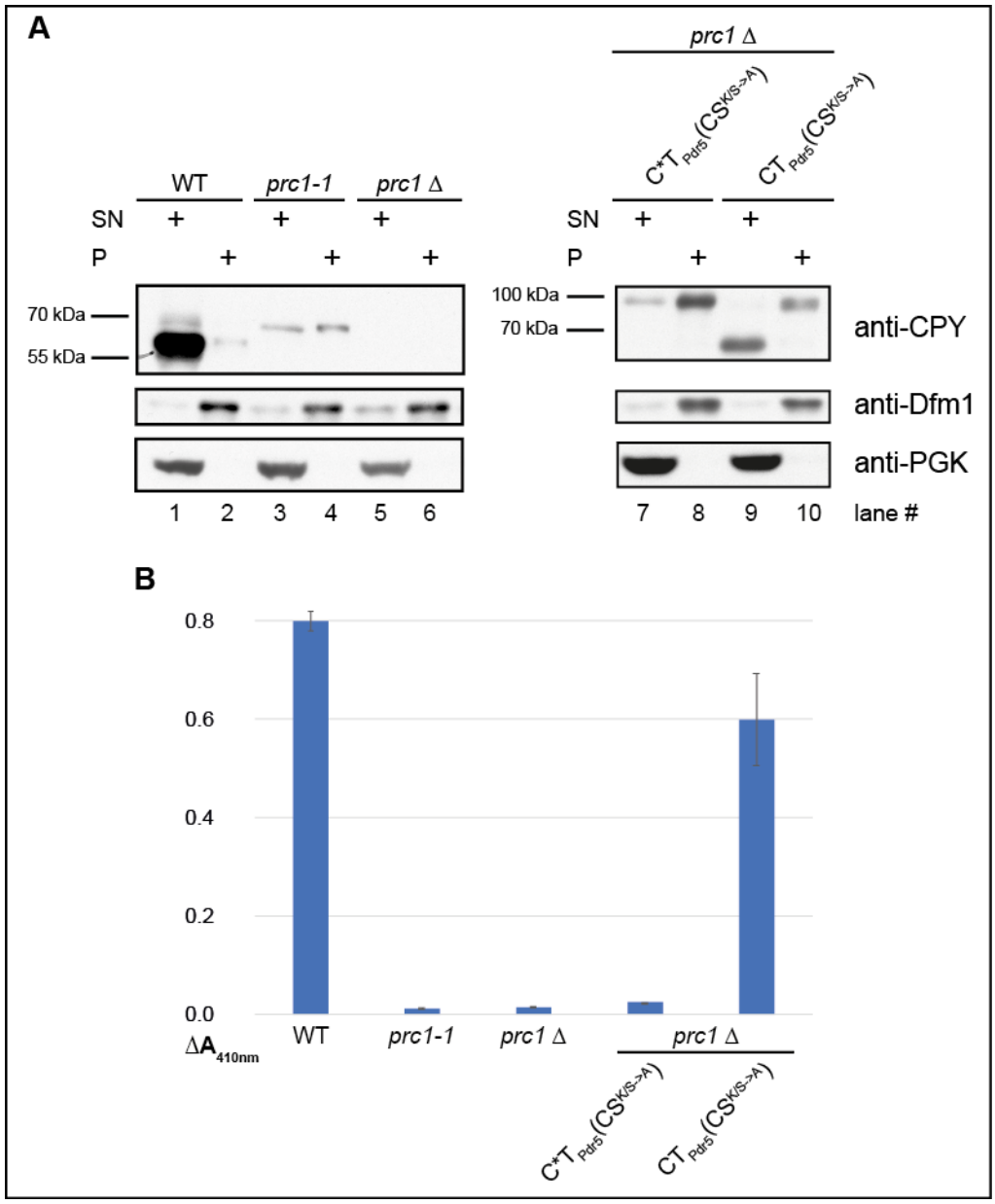

Figure S21: ER lumenal CPY* moiety of C*T$_{Pdr5}$(CS$^{K/S->A}$) is required for retention in the ER

A: Localization of the carboxypeptidase Y (CPY) and its derivatives (WT, endogenous CPY; *prc1-1*, endogenous CPY*; *prc1*Δ, lacking endogenous CPY) was determined in cells expressing the indicated variants. Pellet (P) and supernatant (SN) were separated from lysate and analyze by immunoblotting. CPY variants were detected using CPY antibody. The integral ER membrane protein Dfm1 was visualized using Dfm1 antibody. As control for separating pellet and supernatant, the soluble cytosolic protein PGK was detected using PGK antibody.
B: Cells were incubated for 12 h with BTpNA and absorbance was measured at 410 nm (ΔA_{410nm}). The quantification represents the data of five independent experiments. Error bars indicate the respective standard error of the mean (SEM). *P < 0.05, unpaired two-sample *t*-test relative to the control (WT).

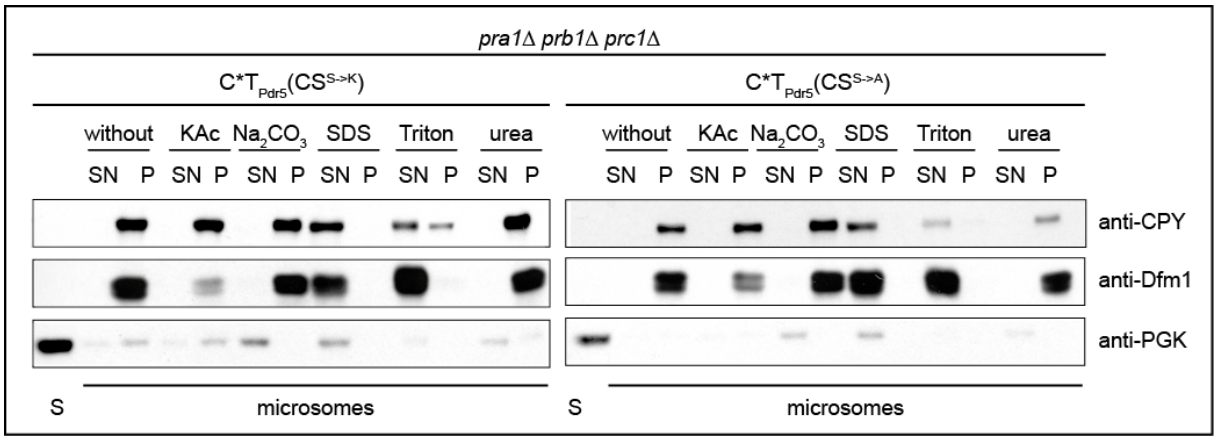

Figure S22: C*T$_{Pdr5}$(CS$^{S->K}$) and C*T$_{Pdr5}$(CS$^{S->A}$) are integral membrane proteins.

Microsomes and supernatant 1 (S) were separated from lysate of *pra1Δprb1Δprc1Δ* cells expressing C*T$_{Pdr5}$(CS) derivatives (as indicated). Microsomes were treated with only buffer (without) or buffer containing either 1 M potassium acetate (KAc) or 0.1 M sodium carbonate (Na_2CO_3) or 1% (w/v) SDS (SDS) or 1% (v/v) Triton X-100 (Triton) or 2.5 M urea (urea), followed by centrifugation. Receiving supernatant 2 (SN) and pellet (P), which were analyzed by immunoblotting. C*T$_{Pdr5}$(CS) derivatives were detected using CPY antibody. The integral ER membrane protein Dfm1 was visualized using Dfm1 antibody. As control for separating supernatant 1 (S) and microsomes, the soluble cytosolic protein PGK was detected using PGK antibody.

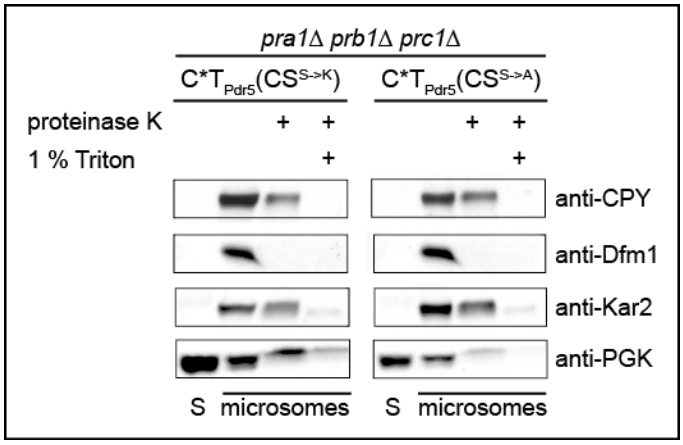

Figure S23: C*T$_{Pdr5}$(CS$^{S->K}$) and C*T$_{Pdr5}$(CS$^{S->A}$) are membrane proteins with the N-terminal CPY* domain in the ER lumen and a C-terminal tail (CS) in the cytosol.

Microsomes and supernatant (S) were separated from lysate of *pra1Δprb1Δprc1Δ* cells expressing either C*T$_{Pdr5}$(CS$^{S->K}$) or C*T$_{Pdr5}$(CS$^{S->A}$). Microsomes were treated only with buffer or buffer containing either proteinase K (0.5 mg/ml) or proteinase K (0.5 mg/ml) and 1% (v/v) Triton X-100. Digestion was stopped by adding 110 mM PMSF. C*T$_{Pdr5}$(CS) derivatives were analyzed by immunoblotting using CPY antibody. The ER membrane protein Dfm1 was visualized using Dfm1 antibody. Kar2, as a control for ER lumenal soluble proteins, was analyzed using Kar2 antibody. As a control for separating supernatant (S) and microsomes, the soluble cytosolic protein PGK was detected using PGK antibody.

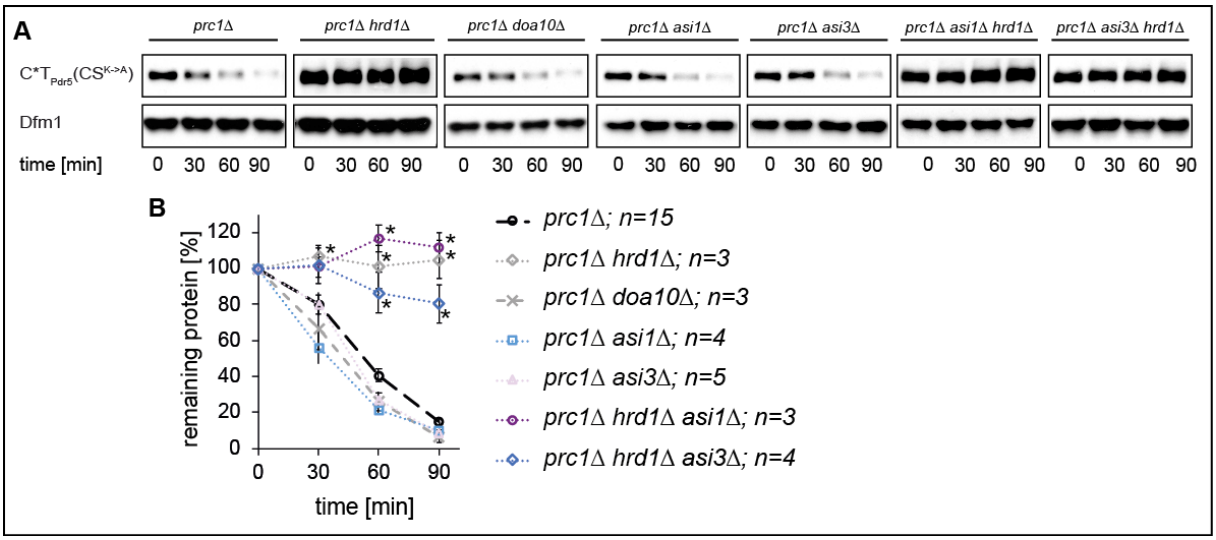

Figure S24: Hrd1 seems to be the only ubiquitin ligase required for degradation of C*T$_{Pdr5}$(CS$^{K->A}$).

A: Cycloheximide-chase analysis of C*T$_{Pdr5}$(CS$^{K->A}$) degradation was performed in *prc1Δ; prc1Δhrd1Δ; prc1Δdoa10Δ; prc1Δasi1Δ; prc1Δasi3Δ; prc1Δhrd1Δasi1Δ* and *prc1Δhrd1Δasi3Δ* cells. Samples were taken every 30 min after cycloheximide addition (t=0 min) and C*T$_{Pdr5}$(CS$^{K->A}$) was detected by immunoblotting using CPY antibody. Dfm1 was used as loading control.
B: The quantification represents the data of up to 15 independent experiments. Error bars indicate the respective standard error of the mean (SEM). *P < 0.05, unpaired two-sample *t*-test relative to the control (*prc1Δ*).

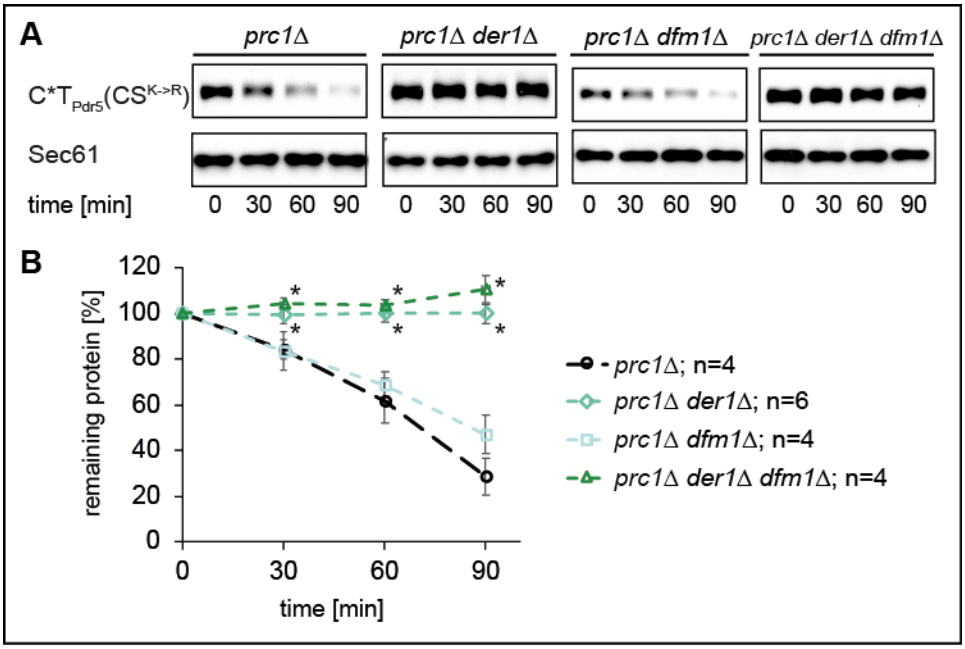

Figure S25: Der1 is indispensible for C*T$_{Pdr5}$(CS$^{K->R}$) degradation but its homolog Dfm1 is not required.

A: Cycloheximide-chase analysis of C*T$_{Pdr5}$(CS$^{K->R}$) degradation was performed in *prc1Δ; prc1Δder1Δ; prc1Δdfm1Δ and prc1Δder1Δdfm1Δ* cells.
Samples were taken every 30 min after cycloheximide addition (t=0 min) and C*T$_{Pdr5}$(CS$^{K->R}$) was detected by immunoblotting using CPY antibody. Sec61 was used as loading control.
B: The quantification represents the data of up to 6 independent experiments. Error bars indicate the respective standard error of the mean (SEM). *P < 0.05, unpaired two-sample *t*-test relative to the control (*prc1Δ*).

ACKNOWLEDGMENTS

There were so many people, who gave me support during my PhD. My thanks go to all of them.

I want to thank Prof. Dr. Dieter H. Wolf for supervising my PhD thesis. I appreciate that he gave me a lot of freedom to develop my ideas and interests in research.

I also want to thank Prof. Dr. Albert Jeltsch for the opportunity to work on his institute and for the open door in case I had any questions.

A great thank-you to Dr. Ruth Menssen-Franz, if I had any scientific but also private issues you were the first who had an open door.

In the last six years I had the chance to meet so many wonderful lab mates like Dr. Ingo Amm, Dr. Frederik Eisele, Karl-Richard Reutter, Anja Reutter, Dr. Maren Schumacher, Dr. Andrea Dietz, Dorothea Mandlmeir, Nadine Frey. I hope there will be always an open restaurant, where we can come together.

I am thankful that I could meet so many other great people during my time in the institute. Thank you all for the friendly working atmosphere, for the productive exchanges of views and profound discussions.

I wish to thank Elisabeth Tosta and PD Dr. Hans Rudolph, who showed me how to deal even with unpleasant situations.

Finally, a special thanks goes to my family, especially to my beloved husband Bernd, for your infinite support and love.

CURRICULUM VITAE

Personal data

Name:	Nicole Zabel
Address:	Keilbergstrasse 22
	71032 Böblingen
Date of birth:	April 1th, 1988
E-mail:	nicole.berner1@gmx.net

Education

Doctoral student in the group of Prof. Dr. Dieter H. Wolf at the Institut für Biochemie und Technische Biochemie; Universität Stuttgart; March 2014 - January 2020
Master thesis at the Institut für Biochemie; Universität Stuttgart; October 2012 - May 2013
Student of biochemistry; Master of Science degree; Technische Universität München; München; - 2013
Student of biochemistry; Bachelor of Science degree; Technische Universität München; München; - 2010
A-Levels (Abitur); Max-Planck-Gymniasium; Böblingen - 2007

Publications

Berner, N., Reutter, K.-R. & Wolf, D. H. Protein quality control of the endoplasmic reticulum and ubiquitin–proteasome-triggered degradation of aberrant proteins: Yeast pioneers the path. *Annual Review of Biochemistry* **87**, 751–782 (2018).

EIDESSTATTLICHE ERKLÄRUNG

Hiermit versichere ich, dass ich diese Arbeit selbst verfasst und dabei keine anderen als die angegebenen Quellen und Hilfsmittel verwendet habe.

Böblingen, 03. August 2021

Nicole Zabel geb. Berner